UNIVERSITY OF LEICESTER

Graduate School

Occurrence and roles of two integrative and conjugative elements in *Klebsiella pneumoniae*

Thesis submitted for the degree of

Doctor of Philosophy

at the University of Leicester

by

Robeena Farzand (M. Phil)

Department of Infection, Immunity, and Inflammation

University of Leicester

October 2017

Abstract

The genome of *Klebsiella pneumoniae* HS11286 carries two integrative and conjugative elements (ICEs), ICEKpnHS-1 and ICEKpnHS-2; the former belongs to the ICEKp1 family and the latter was unexplored. This study was designed to further characterise the two ICEs, and investigate their prevalence in local clinical *K. pneumoniae* isolates. Sequence analysis showed that ICEKpnHS-2 belonged to the subfamily of PAPI elements with XerC-like integrases and PCR screening revealed that ICEKpnHS-1 associated elements were more (30%) prevalent in local isolates compared to ICEKpnHS-2 (12.5%).

Contributions of these elements to cell physiology, virulence and antibiotic resistance were investigated. Deletion of ICEKpnHS-1 reduced siderophore secretion and growth, particularly in iron restricted conditions. The ΔICEKpnHS-1 strain also showed reduced resistance to various antibiotics, especially those known to be affected by the ATP binding cassette (ABC) and major facilitator superfamily (MFS) exporters. Assays in *Galleria mellonella* provided preliminary evidence that deletion of ICEKpnHS-2 reduced the virulence of *K. pneumoniae* HS11286.

Type IV secretion systems (T4SS) are major component modules of ICEs responsible for conjugative transfer of nucleoprotein complexes. Observed reduction of conjugative transfer of one of the ICEs following deletion of the other led us to study interactions between the two distinct T4SSs encoded on the ICEs in HS11286. A marker plasmid containing *oriT* of ICEKpnHS-1 (P-oriT1) was constructed and deletion of ICEKpnHS-2 was shown to produce a six–fold reduction in trans-conjugants. Deletion of the *mobB* (ICEKpnHS-1) orthologue in ICEKpnHS-2 (*mob*-2) and *traI* (relaxase of ICEKpnHS-2) both produced similar defects in transconjugants frequencies that could be complemented *in-trans*. The ATPase Mob-1 was bioinformatically shown to lack a Walker B and it was speculated that Mob-2 might compensate for this. Accordingly, point mutations in Walker motifs of *mob-2* provided evidence supporting this complementary function in energy transduction contributing significantly to the crosstalk between the two non-homologous ICEs. Data on frequency of transfer of the native chromosomal ICEKpnHS-1 and its effects on the phenotypes of an *E. coli* were also shown. However, ICEKpnHS-2 self-conjugation was not detected.

Acknowledgement

First, I would like to thank **ALLAH** for without Him, I wouldn't be here.

Secondly, I would like to express my sincere gratitude to my supervisor, Prof Mike Barer for his constant support and motivation. It would never have been possible for me to take this work to completion without his incredible support and encouragement. I would also like to thank my second supervisor Dr Helen O'Hare, with her assistance I have achieved many of the objectives I set out to do at the beginning of my journey.

I would like to thank the Commonwealth Scholarship Commission UK for offering the fund for this study. Without their financial support, this research would not have been possible.

I am also very grateful to my very first supervisor Dr Kumar Rajakumar for giving me the opportunity to undertake this study, and has taught me so much academically. My sincere thanks goes to my progress review panel members, Dr Galina Mukamolova and Dr Primrose Freestone, for providing me with critical feedback and assist me throughout my PhD.

Furthermore, I am very grateful to have been a part of lab212 and lab136, and give thanks to all past and present members. Especially many thanks to Dr Eva Horvath-Papp, Dr Nutan Sapkota, Ros Abdul Aziz, and Dr Zaaima Al Jabri for working together, for stimulating discussions, and for all the fun we have in my first two years of PhD. I would also like to thank Dr Marialuisa Crosatti for helping me in the early stages of my study.

My sincere thanks also go to Dr Caroline, Dr Natalie Garton, Irina Elliott, Malgorzata Grazyna, and Dr Kairabi Sadhu Haldar who were always on hand to help with any issues and who warmly welcomed me into lab136. I also give thanks to Dr Natalie Lazar Adler, for many discussions about biofilm assay.

I would like to thanks all my dear friends, Enass Al-Mkhadhree, Mashael Alruways, Wafaa Khalaf, and Azain for their support, motivational talks and continuous

encouragement. I am thankful to all people in III Department (especially CTS services), who have been involved in this research and helped me to fulfil this project.

I would like to express my deepest thanks to my parents especially my father Farzand Ali, for all the inspiration, support and good education. My thanks also go to my siblings, especially my brothers Amir Hussain and Zaheer Abbas for their belief in me and care during every stage of my life. Special thanks to my parent in-laws, especially Syed Shah Saqalain and Syed Badshah Hussain for showing me love and support throughout my PhD journey. I would also like to thanks my brother in-law Syed Iqtedar Hanif and Syed Mosa Mustajab for their support through the emotional ups and downs, right from the beginning of my studies.

This PhD would not have been possible without my husband Syed Naseem Abbas, who shows me love and support throughout my PhD journey, I would like to express my deepest thanks to him for trying to understand the complex genetics of my research and always try to add his opinions. My love and thanks also go to my kids, Syed Nauym Abbas and Syeda Hu-Elia who are just about the best children a mum could hope for; happy, loving and fun to be with me.

Finally I would like to pay special thanks to Sayed Mujahid Hussain for his support and belief in me during my studies.

I would like to dedicate this work to my Husband

“SYED NASEEM ABBAS”

and to my lovely kids

“SYED NAUYM ABBAS” and “SYEDA HU-ELIA”

List of Abbreviation

ABC	ATP-binding cassette
AB	Antibiotic
ATP	Adenosine triphosphate
Att site	Attachment site
ApE	A plasmid editor
A+T	Adenine + Thymine
Blast	Basic Local Alignment Tool
bp	Base pair
CFU	Colony forming unit
CRKP	Carbapenem-resistant *Klebsiella pneumoniae*
DNA	Deoxyribose nucleic acid
dNTP	Deoxy-ribonucleotide triphosphate
DR	Direct repeat
dsDNA	Double stranded DNA
DF	Downstream flank
Dtr	DNA transfer
ddH_2O	Deionised distilled water
ESBL	extended-spectrum beta-lactamases
FIC	Filamentation Induced by Cyclic-AMP
FRT	Flippase Recognition Target
g	Gram
g	Gravity
GC	Guanine and Cytosine
GI	Genomic island
HGT	Horizontal gene transfer
his	Histidine
HPI	High pathogenicity island
ICE	Integrative and conjugative element
int	Integrase

IR	Inverted repeat
IS	Insertion sequences
IPTG:	Isopropyl-β-D-thiogalactopyranoside
Kb	Kilo base
KEGG	Kyoto Encyclopaedia of Genes and Genomes
Kp	*Klebsiella pneumoniae*
LA	Luria Bertani agar
LB	Luria Bertani broth
LGT	Lateral gene transfer
M	Molar
MCP	methyl-accepting chemotaxis protein
MFS	major facilitator super family
Mpf	Mating pair formation
MGE	Mobile genetic element
MLSA	Multi-locus sequence analysis
MCS	Multiple Cloning Site
mM	Millimolar
NCBI	National Centre for Biotechnology Information
NEB	New England Bio lab
OD	Optical Density
OD_{600}	OD at absorbance of 600nm
ORF	Open reading frame
oriT	Origin of transfer
P	Level of significance
Pfam	Protein families
PFGI	*Pseudomonas fluorescens* genomic island
PLA	pyogenic liver abscesses
PAI	Pathogenicity island
PCR	Polymerase Chain Reaction
PBS	Phosphate buffered saline
RF	Robeena Farzand

RDF	recombination directionality factor
REI	Resistance island
RNA	Ribose nucleic acid
ssDNA	Single stranded DNA
ST	Sequence type
SOC	Super optimal broth with Catabolite repression
SOE	Splice overlap extension
SFU	Specific function undefined
T4SS	Type four secretion system
T4CP	Type four coupling protein
T6SS	Type six secretion system
tRNA	Transfer RNA
UF	Upstream flank
v/v	Volume to volume
VGT	Vertical gene transfer
w/v	Weight to volume
Ybt	Yersiniabactin
^{o} C	Degree Celsius
λ	Lambda
µl	Microliter
µg	Microgram
µM	Micro Molar

List of Figures

List of Tables

Table of Contents

Contribution to this work

This work was initiated in the lab of Dr Kumar Rajakumar, who left the University in early 2015 and reflects a program of study initiated by him. As noted in section 1.16 some work had been started on this project. Moreover, a study concern with virulence was initiated in parallel by Dr Mohammad Al Madadha. The experiment described in section 4.3.10 were in equal collaboration between both parties.

Chapter 1 Introduction

1.1 General Introduction

This study is concerned with the genetic and functional analysis of two mobile genetic elements (MGEs) in *Klebsiella pneumoniae*. New genetic material appears in bacteria either by internal mutation, or from external sources such as horizontal gene transfer (HGT) (Wozniak and Waldor, 2010). The acquisition and spread of resistance-associated and/or virulence-associated genes, as well as the wider evolution of bacteria, is strongly associated with certain types of MGE (Partridge, 2011, Frost et al., 2005) including plasmids, insertion sequences (ISs), transposons, integrons and associated gene cassettes, prophages, integrative and conjugative elements (ICEs) and genomic islands (GIs). ICEs are the particular focus of this study.

Increases in the levels of multiple antibiotic resistance associated with *Klebsiella pneumoniae* poses a major emerging global problem. Carbapenem-resistant *Klebsiella pneumoniae* (CRKP) isolates are often associated with severe infections with few treatment options and represent a serious threat to health. *Klebsiella pneumoniae* strains that produce carbapenemase and extended-spectrum beta-lactamases (ESBLs) are often associated with the CRPK clones of sequence type (ST) 258 or 15 (Arnold et al., 2011, Wyres and Holt, 2016). *Klebsiella pneumoniae* strain HS11286 studied here belongs to ST11, which is a major carbapenemase producing clone closely related to ST258 (Liu et al., 2012).

Thus the importance of *Klebsiella pneumoniae,* hereinafter referred to as *K. pneumoniae*, as a pathogen, its significance as a reservoir and means of disseminating antimicrobial resistance and the abundance of MGEs that the study strain hosts provided ample incentive for this investigation. The basic features of MGEs and their significance are outlined below.

1.2 Horizontal gene transfer

Microorganisms inherit genetic information via two major mechanisms; vertical gene transfer (VGT) that involves the parent to offspring relationship (Metcalf et al., 2014), and horizontal gene transfer (HGT also known as lateral gene transfer) in which DNA is transferred between different organisms. (Soucy et al., 2015).

HGT in microorganisms was first documented in 1947 (Tatum and Lederberg, 1947). The methods of HGT detection were improved after speculating on its potential role in the adaptation of plants (Went, 1971). Advances in the field of detection revealed the relationship between HGT and genetic variations of viral, prokaryotic and eukaryotic organisms. To maintain itself, the transferred genetic material needs to provide advantage to the recipient (Soucy et al., 2015). Generally, most of the transferred genes between close relatives have neutral effects in recipients (Gogarten and Townsend, 2005a). A widely accepted assumption about HGT is that the transfer broadly follows the rule of "First Do Not Harm". According to this, the transferred genes successfully integrate themselves in the recipient genome and give very low expression that functions at the periphery of metabolism (Park and Zhang, 2012). However, this neutral acquisition can later provide novel combinations of genetic material that play an important role in the evolution of organisms. The transferred DNA is usually retained by the recipient if it produces a beneficial phenotype. However, where the effect is neutral, provides no specific benefits or is deleterious, the encoding genes are likely to be lost over period of time (Soucy et al., 2015).

Based on its effects on bacterial evolution, HGT has been referred to as the "madness of gene transfer" because it can produce rapid gene turnover leading to extensive genome differences among closely related bacterial populations (Polz et al., 2013). Isolates that have recent common genetic origin can have many unique genes (Shapiro et al., 2012). Comparisons of hundreds of sequenced genomes shows that ~20% (on average) of genes have been acquired by HGT (Popa et al., 2011). These extensive genome differences make it difficult for the estimation of the total gene pool even for the highly related microbes (Tettelin et al., 2008, Mira et al., 2010).

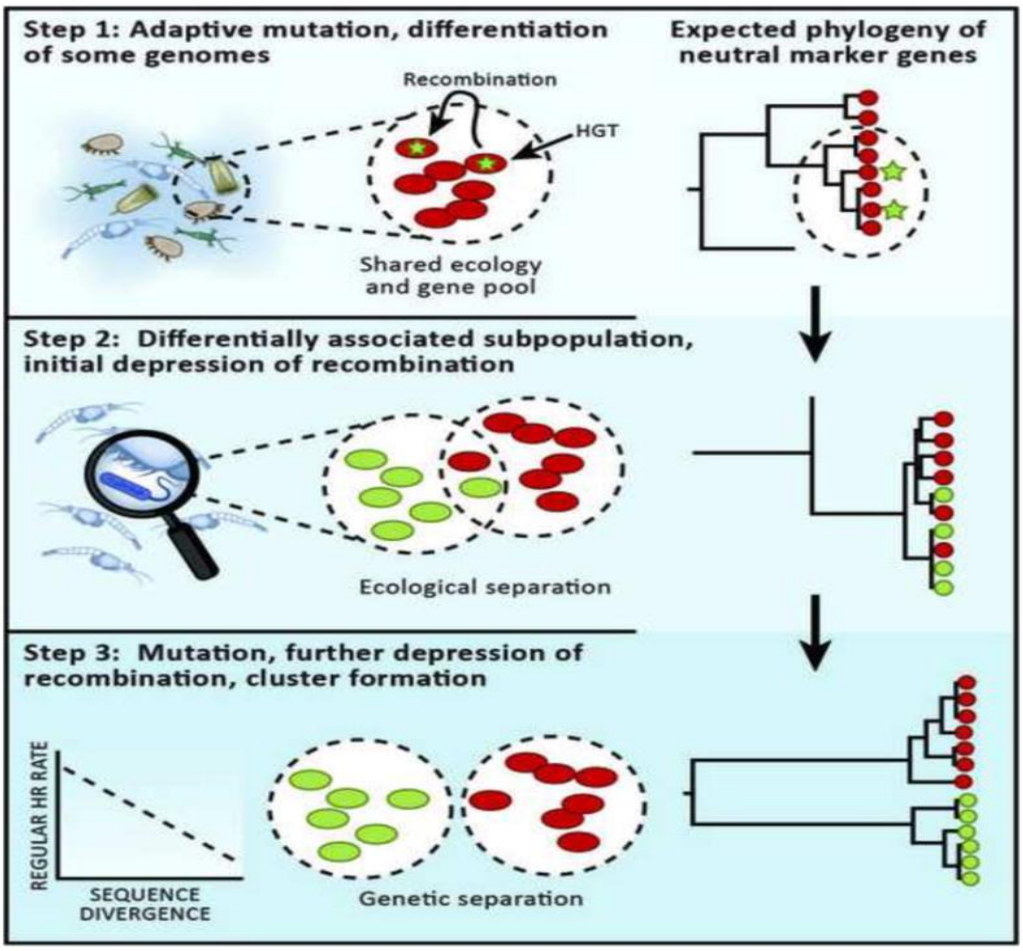

Figure 1-1 Model of genotypic clusters formation caused by HGT and ecological niches.

Step 1: Addresses the acquisition of genetic material (green star) via recombination, in a phylogenetic tree, the gene was neutral at this stage and the population remains homogeneous. Step 2: represents the role of the surrounding environmental conditions in the separation of two populations (red and green). The novel population (green) is starting to occupy a niche separate from the ancestor. The phylogeny still appears because the recombination is not evident in neutral marker genes. Finally, Step 3: Differences accumulate with in each population, because of decrease in recombination rate due to sequence divergence that decreases the gene flow between nascent populations. At this point, phylogenetic tree shows genetic clusters, which are consistent with ecological differentiation (Polz et al., 2013).

HGT depends on both sequence similarities and environmental conditions resulting in geno- and pheno-typically clustered microbes (Polz et al., 2013). The wide availability of genome sequence data overcomes the previous difficulty of appropriate phylogenetic clustering of microbes (Polz et al., 2013) (Rosselló-Mora and Amann, 2001). Figure 1-1 shows a recent model of genotypic cluster formation (Shapiro et al., 2012, Polz et al., 2013).

1.3 Mechanisms of HGT

Conjugation, transformation and transduction are the three well recognised mechanisms of HGT. Conjugative transfer of DNA requires direct physical contact between donor and recipient cells, the transfer takes place via a conjugation pilus. Formerly, conjugation was thought restricted to bacteria but the transfer of *Agrobacterium* spp. DNA into plant cells showed that cross Domain HGT was also possible (Norman et al., 2009, Kyndt et al., 2015).

Transformation is the uptake of exogenous genetic material from the environment and has been reported in both Bacteria and Archaea (Johnston et al., 2014, Chimileski et al., 2014). Bacteriophage mediated transduction involves incorporation of exogenous DNA into the phage genome and transfer to a new bacterial cell. Transduction can be generalised or specialised based on the incorporated genetic material (Soucy et al., 2015). The present study is concentrated on conjugative mechanisms associated with integrative and conjugative elements (ICEs).

1.4 Methods for HGT detection

Detection of HGT depends on differences between the inferred sequence homology-based genealogy of the element interrogated and that of the host genome (Williams et al., 2011). Multiple housekeeping or conserved function genes (e.g. ribosomal proteins) are used to construct the host reference genealogy tree (Soucy et al., 2015).

Multi-locus sequence analysis (MLSA) has been recently documented to be useful for the determination of prokaryotic phylogeny. The method avoids conflicts resulting from HGT of one or more of the genes. The method can also be applied to a larger number of genes in order to study the phylogenetic conflicts between reference and test species (Colston et al., 2014, Delamuta et al., 2012, Gogarten and Townsend, 2005b).

Quantitative description of bacterial HGT is challenging because DNA transfers usually take place between highly related organisms and it is hard to distinguish the genetic differences between host and recipient genomes (Williams et al., 2012, Andam and Gogarten, 2011, Polz et al., 2013). Direction of transfer is another difficulty in HGT detection that is usually overcome by extensive analysis of the branching patterns of various genes within the reference species (Soucy et al., 2015). Gene loss after

duplication can raise further difficulties in determining the frequency of HGT. It is generally hoped that availability of more genome sequences will help to resolve these issues and also help to identify independent or spontaneous gene loss (Gogarten and Townsend, 2005b). Finally, codon usage may also provide significant information related to HGT detection (Langille et al., 2010).

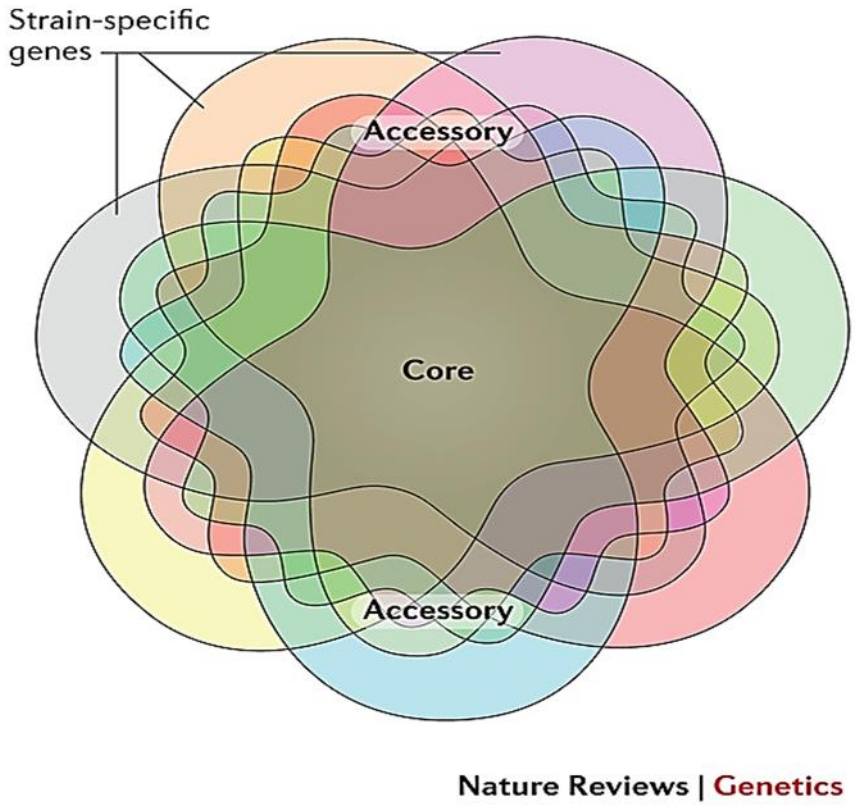

Figure 1-2 Pan-genome

After Soucy et al. (2015), based data from the following; (Edwards, 2004, Morris et al., 2012, Lobkovsky et al., 2014, Lapierre and Gogarten, 2009, Puigbò et al., 2014).

The genome of each prokaryotic species has been described in several ways: Pan-genome "The set of all genes present in a taxon", Accessory genome "The set of genes that are present only in one or a few members of taxon", and Core genome "The set of genes present in every member of taxon" (Hamburger, 2005, Morris et al., 2012, Puigbò et al., 2014). Therefore, a part from pan-genome is represented in the genome of each individual (Figure 1-2).

In prokaryotes, comparisons of genomes have identified a wide range of variations even among highly related organisms, (Soucy et al., 2015). Lukjancenko et al. (2010) has analysed genomes of 61 *Escherichia coli* strains and identified that only 6% of the gene families present were shared by all genomes. Thus the pan-genome provides a better description of the set of genes that occur in the entire group.

1.5 HGT and evolution

HGT contributes to the new features in a bacterial population that may be shared with other populations. Acquisition of selective advantageous genes are usually promoted by these self-splicing genetic elements (Smillie et al., 2011). One of the best examples of this is the dissemination of antibiotic resistance genes is via conjugative plasmids and MGEs (Rankin et al., 2011).

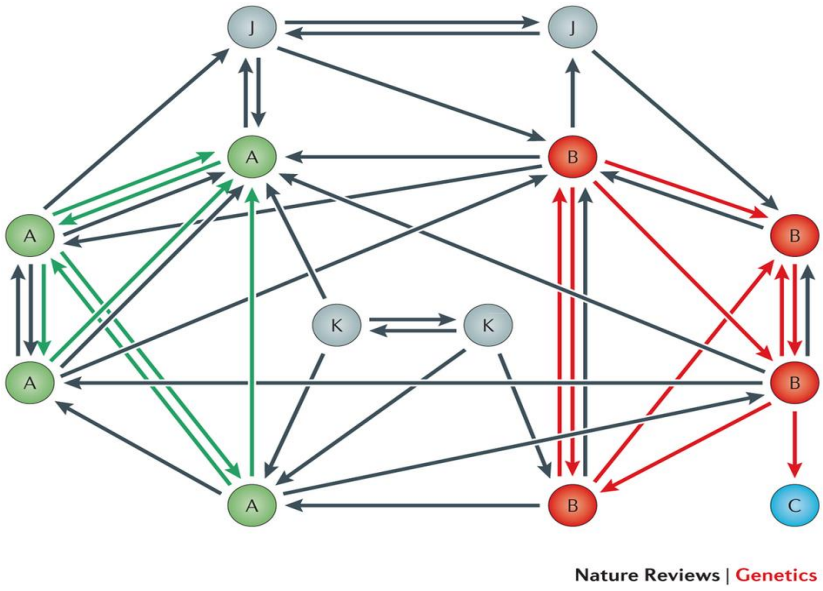

Figure 1-3 Structured exchange community.

A and B represent microbes occupying two distinct niches whereas K and J indicates related species occupying different niches. Genes associated with niche adaptation are mostly exchanged between members of the same niche (green and red arrows), but they might also be shared with recent niche invaders (blue circle; C), accelerating the adaptation of the invader to a new habitat. Gray arrows represents the genes that are freely exchanged between members of different niches. Adapted from (Soucy et al., 2015)

The compositional similarities between the genomes enable homologous recombination and supports mobility of genes (Skippington and Ragan, 2012). This may facilitate migration to new ecological niches (Papke and Gogarten, 2012) as shown in Figure 1-3..

1.6 Genomic islands

Genomic islands (GIs) belong to a major group of mobile genetic elements (MGEs). The term GI was adapted from 'Pathogenicity islands' (Hacker et al., 1990). These were first identified in uropathogenic *E. coli*, and were described as virulence associated horizontally acquired self-splicing DNA fragments. GIs can belong both to closely or distinctly related hosts. Furthermore, GIs appear to be the products of combinations involving many different MGEs (Juhas et al., 2009a, Juhas et al., 2007b, Vernikos and Parkhill, 2008a). Based on their mosaic nature Mathee et al. (2008) have named these MGEs as region of genome flexibility.

1.6.1 Structure of GIs

GIs are generally large DNA fragments ranging from 10–200kb, and when <10kb they are known as genomic islets (Hacker and Kaper, 2000, Dobrindt et al., 2004, Gal-Mor and Finlay, 2006) and they are site-specific for their integration. Vernikos & Parkhill (2008) stated that ~75% of the total known GIs are integrated at the 3´ end of various transfer RNA (*tRNA*) genes.

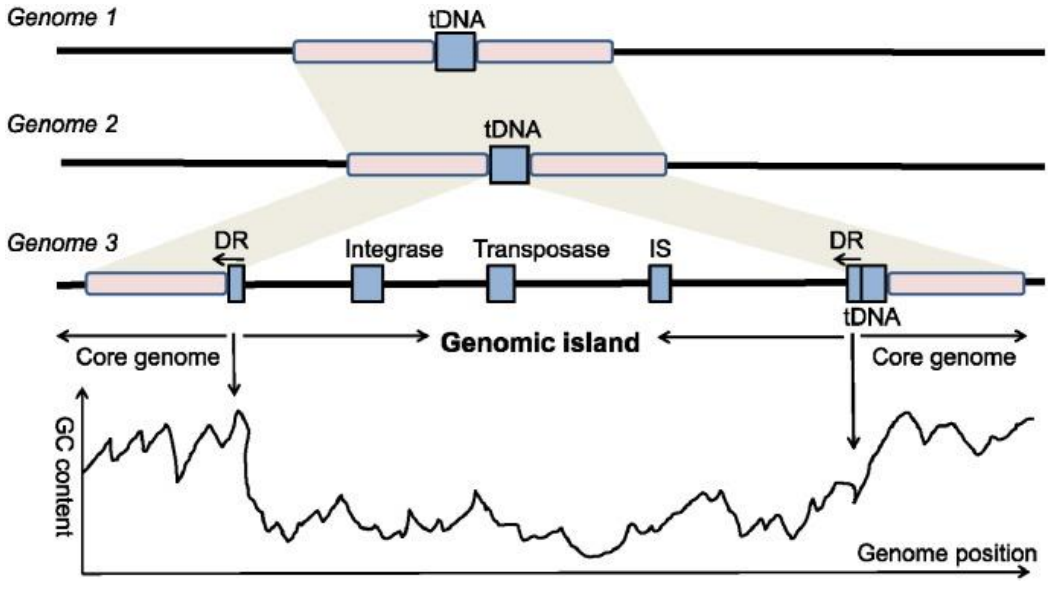

Figure 1-4 Schematic representation of GIs and their associated features.

GIs usually have atypical compositional characteristics compared to the core genome; this often includes a different GC content, insertion sequences (ISs) and transposase (Lu and Leong, 2016) and other mobility associated genes such as integrases (Juhas et al.,

2009b, Schmidt and Hensel, 2004). GIs are often flanked by short direct repeats (DRs) (Figure 1-4), which act as integrase recognition sites. DRs are most likely artefacts generated from integration/excision events. The repeats are similar to the *attL (3´-end)* and *attR (5´-end)* sites that flank prophages after their genomic insertion (Bachman et al., 2011). GI integration is generally mediated by homologous recombination between the DRs present both in genome and MGE (Pavlovic et al., 2004). However, not every GI includes all of these features; as a result GIs are considered as a superfamily of MGEs with core and variable characteristics (Vernikos and Parkhill, 2008b).

GIs harbour set of accessory genes known as cargo genes that encode various functions. As described earlier, laterally acquired genes usually confer advantageous traits resulting in increased host fitness in specific environmental niches (Hacker and Kaper, 2000, Dobrindt et al., 2004, Gal-Mor and Finlay, 2006). Depending on their gene complement, GIs can be classified according to their encoded functions into pathogenicity islands (PAIs), resistance islands (REIs) and metabolic islands and so on (Lu and Leong, 2016). However, this classification can be troublesome as GIs often code for more than one of these functions or they may include genes with no clear function. Thus, islands without virulence-associated genes are often just referred to as GIs (Dobrindt and Hacker, 2001). In addition, GIs can be further classified in to subgroups based on their mobility: some GIs are not mobile and some are mobile and can transfer further. The later include transposons, prophages and integrative and conjugative elements (Juhas et al., 2009b).

1.6.2 Recognition of GIs is a challenge

Potential GIs can be recognised by computational methods in the first instance and this approach is generally essential for a novel island. Input of annotated genome sequences from related organisms is generally required. Prediction of GIs has two major challenges, the extremely variable content of GIs and a lack of standardised GI datasets (reviewed by Lu and Leong, 2016).

Variation in content and functions encoded, together with the mosaic nature of GIs, increases the difficulty in their recognition (Vernikos, 2008). Multiple HGT events from different origins and genomic rearrangements leading to loss and gain of genes complicate sequence data interpretation (Dobrindt et al., 2004). This diversity reduces

the effectiveness of GI recognition methods; for example selection of too few features may result in missing many GIs that naturally lack those features. The lack of benchmark datasets defining GIs provides another challenge in recognition of new islands but several databases such as PAIDB (Yoon et al., 2007), ICEberg (Bi et al., 2012) and Islander (Mantri and Williams, 2004) are now providing useful resources. All these databases provide information on methods of prediction. However, insufficient datasets could embed problems during recognition and identification. Figure 1-5 shows a computational framework for the prediction of GIs.

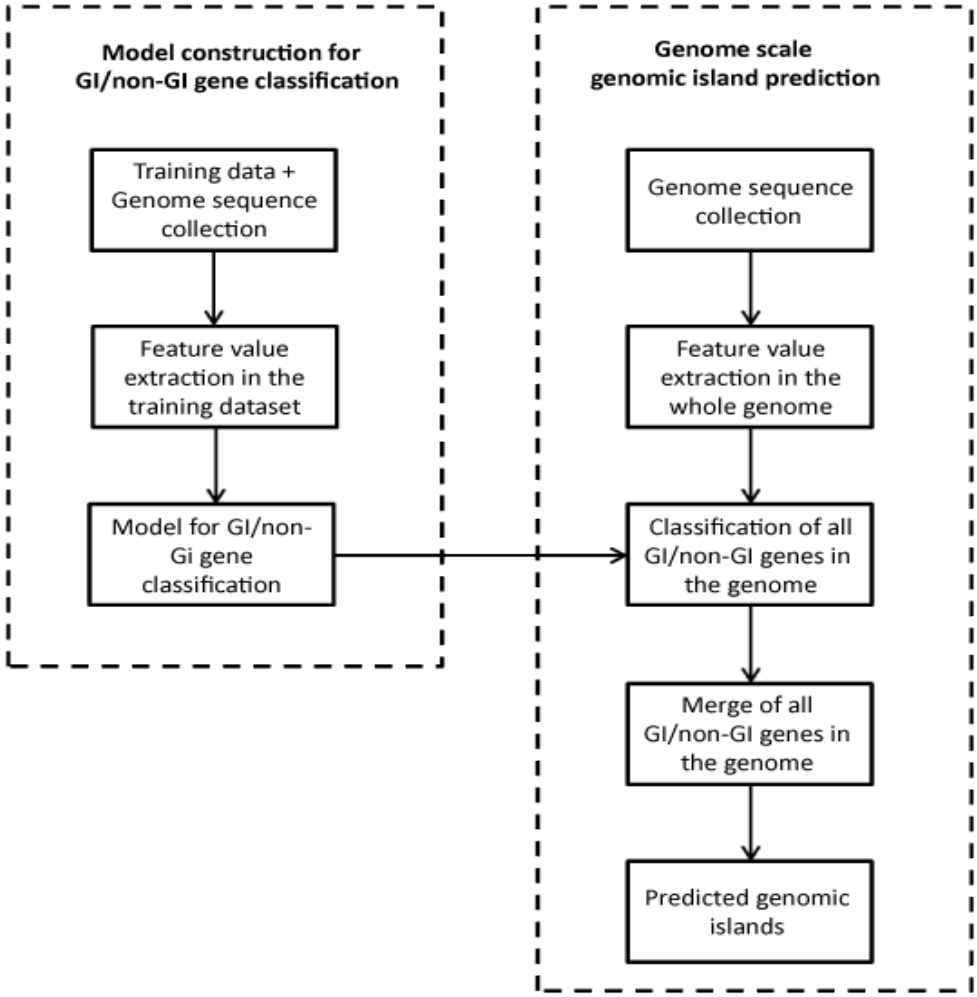

Figure 1-5 Computational framework for the prediction of GIs on genome scale. Adapted from (Han Wang, 2014).

1.7 General types of MGEs/GIs

Single mobile elements may possibly have features of more than one type of element and the majority of these elements are not self-mobilising. The major classes of

MGEs/GIs are listed below (Curcio and Derbyshire, 2003, Siguier et al., 2014, Soucy et al., 2015):

Transposable elements are capable of moving to different DNA sites based on site selectivity. Mobility of some elements is based on a "cut and paste" method, in which they excise from the original site and insert into a new position. Some elements transpose through a "copy and paste" method in which a replicative mechanism is used to create a new copy at a new site.

Integrative bacteriophages are mobile between cells and integrate into the host genome

Conjugative plasmids are mobile and generally replicate independently of the host chromosome.

ICEs mobilise via conjugation.

1.8 ICEs

ICEs are self-mobile and encode their own conjugative machineries and systems of regulation and maintenance (Salyers et al., 1995, Burrus and Waldor, 2004).

ICEs are generally maintained because they integrate thereby replicating and partitioning with the host chromosome (Carraro and Burrus, 2015). Mobilisation of ICEs involves excision and formation of an extrachromosomal circular intermediate that acts as a substrate for conjugative transfer (Johnson and Grossman, 2015, Carraro and Burrus, 2015). Similar to other GIs, ICEs also have mosaic and modular structures (Wozniak and Waldor, 2010); including three distinct modules: i) integration and excision, ii) conjugation, and iii) regulation (Figure 1-6).

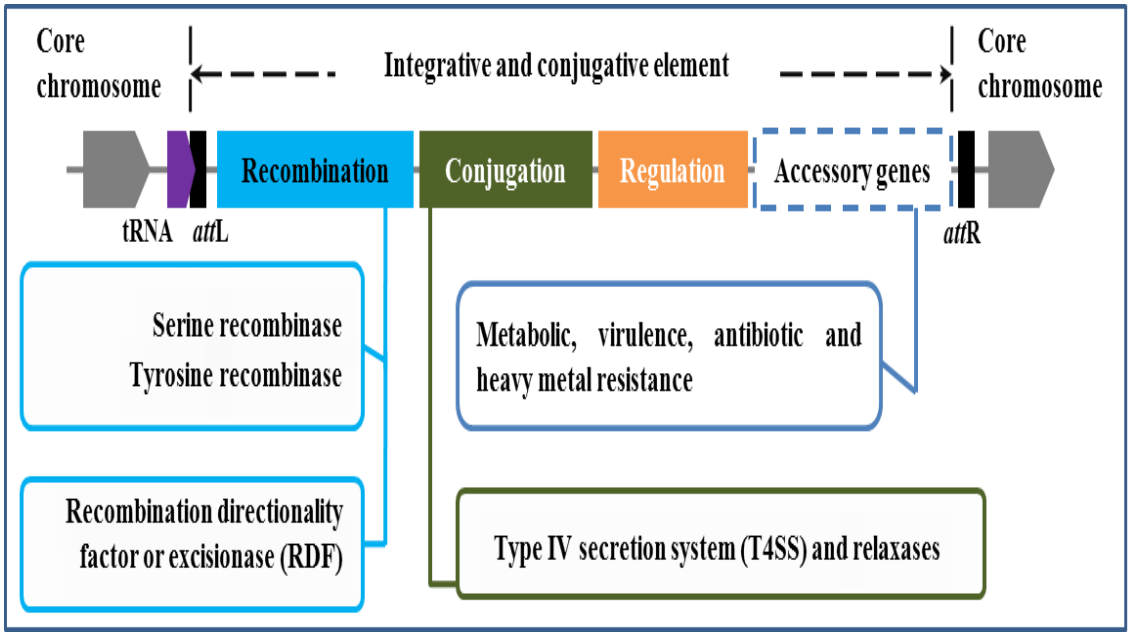

Figure 1-6 Schematic representation of an ICE.
Different modules including recombination (integration/excision), conjugation, and accessory genes are represented. Black rectangles indicate the ICE flanking repeats (*attL* and *attR*). Serine and tyrosine recombinases are the integrase responsible for integration/excision of an ICE.

ICEs range from ~20 kb to >500kb and contain functional modules from a variety of sources (Wozniak et al., 2009, Wozniak and Waldor, 2010, Toussaint and Merlin, 2002, Osborn and Böltner, 2002, Mohd et al., 2004, Johnson and Grossman, 2015)

1.9 ICE mobilisation cycle

The mobilisation cycle of ICE consists of the following stages (Figure 1-7):

1. Excision from host genome
2. Conjugative Transfer
3. Integration in both donor and recipient genome
4. Maintenance/regulation

Briefly, the ICE excises and forms a non-replicative extrachromosomal circular intermediate and genes encoding the mating pore are expressed. Proteins that recognise the origin of transfer (*oriT*), process the DNA transfer via conjugation (sections 1.9.1-1.9.4).

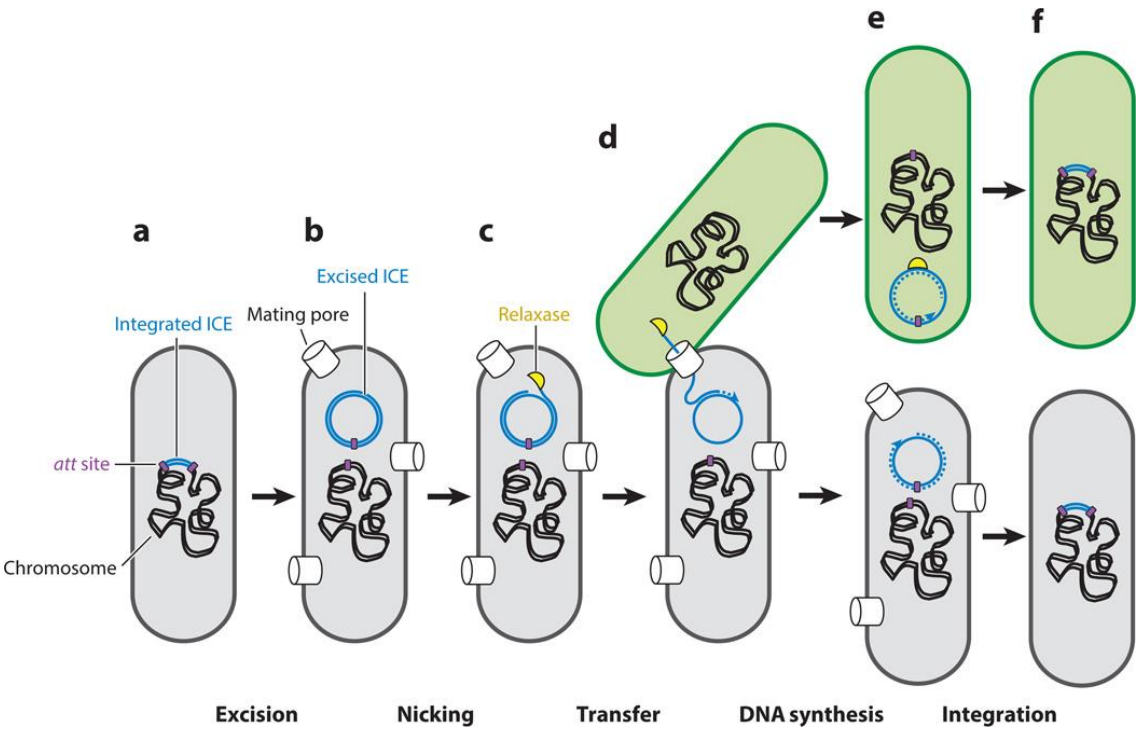

Figure 1-7 The ICE life cycle.

(*a*) The ICE is integrated in the host chromosome. (*b*) Expression of specific genes induce ICE excision and formation of dsDNA circular plasmid. (*c*) The relaxase creates nick in one strand of the ICE and covalently attaches to the 5´ end of the nicked DNA (T-DNA) (*d)* In the presence of recipient cell, the conjugation machinery transports the T-DNA. (*e*) In the recipient cell, the relaxase ligates the 5´ and 3´ ends of the DNA to form a covalently closed ssDNA circle. The complementary DNA strand is synthesized to generate a dsDNA circle for integration into the host genome. In donor, the remaining DNA strand likely serves as the template for rolling-circle replication, generating a dsDNA circle. (*f)* The circular dsDNA ICE integrates into both host and recipient chromosome. Taken from(Johnson and Grossman, 2015).

1.9.1 Excision of ICE

Excision is mediated by an ICE-encoded integrase (Carraro and Burrus, 2015) and recombination directionality factors (RDF) (also known as Xis), promote excision and inhibit integration (Hirano et al., 2011, Lewis and Hatfull, 2001). Although RDF do not initiate excision, nonetheless their absence reduces this around 1000 fold (Wozniak and Waldor, 2010). RDFs have only been detected in a few well-characterised ICEs. These proteins bind adjacent to the integrase binding sites (Connolly et al., 2002) and favour increased excision; any mutations in them reduce the excision frequency (e.g. ICE *Tn*916, (Hinerfeld and Churchward, 2001, Connolly et al., 2002).

The mechanism of excision of these elements is variable and high rates of excision do not necessarily increase transfer rates. This suggests that excision is not always the limiting step for mobilisation. Environmental conditions also affect excision. Sometimes

ICEs excise imprecisely and acquire their flanking regions (Campbell, 2007), this is more common in ICEs that have unrestricted integration sites, e.g. *Tn*916 (Johnson and Grossman, 2015).

1.9.2 Mobilisation of ICEs

ICEs encodes Type 4 secretion systems (T4SSs) which provides conjugation machinery for mobilisation. The DNA transfer involves the following steps:

1.9.2.1 DNA processing:

Extrachromosomal ICEs are processed before their conjugal transfer. Most ICEs are processed by the same mechanisms as plasmids indicating that proteins have similar behaviour for both plasmid and ICE (Wozniak and Waldor, 2010). The process initiates when relaxase identifies and nicks *oriT* (Lank, 1995). The relaxase remains bound to the nick and interacts with the conjugation/type four coupling protein (T4CP); this facilitates the transfer of the nucleoprotein complex to the secretion channel (Hamilton et al., 2000, Llosa et al., 2002). *OriT* is usually identified by the presence of direct and inverted repeats in A+T rich sequences (Lee and Grossman, 2007, Wozniak and Waldor, 2010). *oriT* is usually located adjacent to the gene encoding relaxase (Lee and Grossman, 2007). However, in some ICEs the relaxase and *oriT* sequences are located far apart from each other, e.g. in ICE SXT, relaxase (*traI*) and its cognate *oriT* are separated by 40kb (Ceccarelli et al., 2008).

1.9.2.2 Replication

Excised ICEs and conjugative plasmids exist as covalently closed circles of dsDNA and are processed before mobilisation. Conjugative plasmids pass through three phases; replication, partitioning and conjugation (Lawley et al., 2002). Plasmid vegetative replication occurs with every generation so that plasmid copy number is maintained. ICEs are primarily considered non-replicative outside the replication associated with conjugation, thus their copy number does not usually increase in the host (Wozniak and Waldor, 2010, Johnson and Grossman, 2015). The maintenance of ICEs relies mainly on their integration and replication along with a replicon of their host in a prophage-like manner (Carraro and Burrus, 2015).

Plasmid vegetative replication is initiated at the origin of replication (*oriV*), usually by plasmid-encoded replication proteins (Lawley et al., 2002). Conjugative DNA replication is a distinct process initiated at *oriT*. In this mode of replication one strand of the replicated molecule is retained in the donor cell, while the second strand is transferred to the recipient cell in the 5´ to 3´ direction(Zechner et al., 2000). ICE replication is unidirectional from *oriT* (Lee et al., 2010, Thomas et al., 2013). However, some ICEs have replicative forms. For example, in *E. coli* the SXT element is associated with the *attP* site in its unintegrated form and the abundance of this site is slightly higher than that of its chromosomal associated site, *attB*, indicating more copies of extrachromosomal SXT (Burrus and Waldor, 2003). Similarly, Lee et al. (2010) showed that ICEBs1 can replicate autonomously having two to fivefold more unintegrated forms under inducing conditions. The mechanism of conjugative replication of ICE is shown in Figure 1-8.

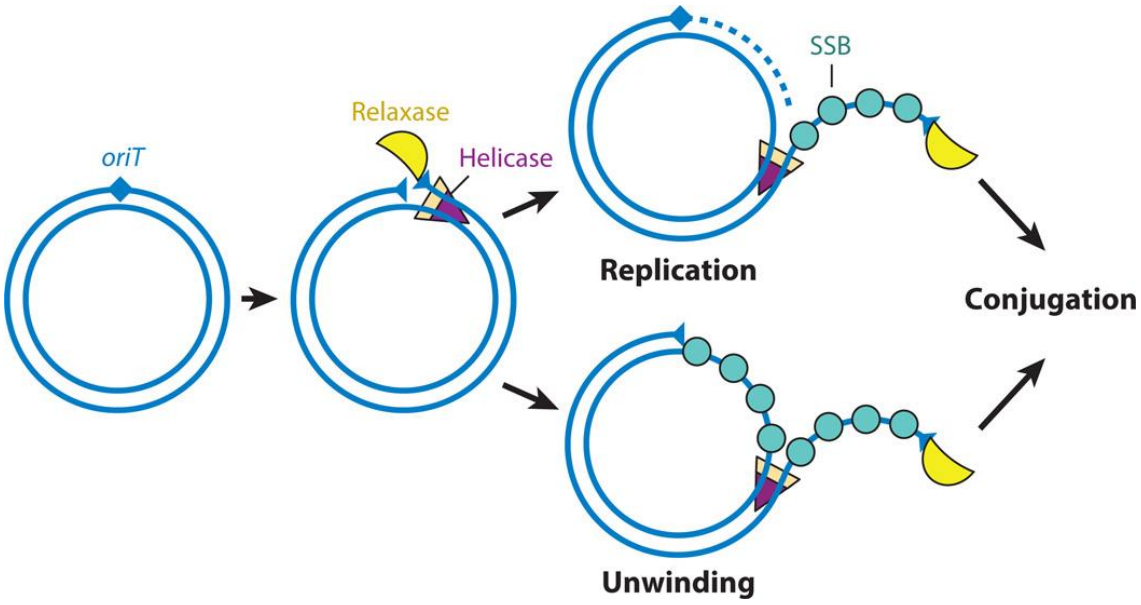

Figure 1-8 Conjugative replication of ICEs during conjugation.

Conjugative replication resembles rolling-circle replication. The ICE is shown as double blue lines. Relaxase recognizes and nicks its cognate *oriT,* binding to the 5´ end. Helicase (purple triangle) unwinds the DNA with the help of single-strand binding protein (turquoise circle).

1.9.2.3 DNA secretion system

The ICE T4SSs are a complex of proteins that produce a membrane spanning channel including and extracellular pilus (Christie et al., 2005). These systems are used for both exchange of DNA and export of protein (Cascales and Christie, 2003). See section 1.11.

1.9.3 Integration of ICEs

Integrase is sometimes sufficient for both integration and excision of the element. However, additional factors are involved. Regulation of *int* expression is one of the key determinants that controls ICE transmission (reviewed by Wozniak and Waldor, 2010).

Most ICEs contain an integrase belonging to the tyrosine recombinase family (Johnson and Grossman, 2015). The phage λ integrase is one of these; it utilises topoisomerase activity to promote site-specific recombination between similar sequences. Integrase similarities allow different ICEs to integrate by similar mechanisms (Hochhut and Waldor, 1999, Beaber et al., 2002). A few ICE integrases belong to the serine/DDE recombinase family (Brochet et al., 2009, Dordet Frisoni et al., 2013, Guérillot et al., 2014). The functional consequences are the same but, the serine recombinases catalyse a slightly different reaction (Rajeev et al., 2009, Grindley et al., 2006) that generates variation in the integration sites.

Generally, ICE target a single *attB* site in the host genome that is identical or nearly identical to the *attI* site in the circularised ICE1. When *attB* is absent alternative sites may be targeted but integration efficiency is lower (Burrus and Waldor, 2003, Lee and Grossman, 2007, Menard and Grossman, 2013). The phenomenon of integration at alternative sites is well explained in several elements e.g. C*Tn*DOT and *Tn*916 (Cheng et al., 2000, Roberts and Mullany, 2009). Moreover, ICEs carrying serine recombinases are typically associated with non-specific integration (Brochet et al., 2009, Guérillot et al., 2014).

Other ICE associated integrases include P4-like integrases of ICEclc^{B13} (Ravatn et al., 1998b) and ICEMlSym^{R7A} (Ramsay et al., 2006), the XerC/XerD family integrase of PAPI-1 and ICEHin1056 (Mohd et al., 2004, Qiu et al., 2006). The exchange of integration modules between MGEs potentially creates new ICE with modified insertion site and new host ranges.

1.9.4 ICE regulation/maintenance

The genes for excision and conjugation are not constitutively expressed. Majority of ICES appear to excise in relatively small subpopulation of cells (Minoia et al., 2008, Johnson and Grossman, 2015). The signals for ICE activation and selective pressures for their

maintenance are not universally conserved although some common features are shared.

1.9.4.1 Selective pressure and ICE activation

Gene expression under most circumstances create a metabolic burden to the host (Johnson and Grossman, 2015), which constitutes a selection pressure favouring loss of activated ICEs (Auchtung et al., 2005, Ramsay et al., 2006). ICE activation can also be directly detrimental to host for specific reasons. As in the case of Gram-negative conjugation system, expression of conjugative pili make the host susceptible to phages (Johnson and Grossman, 2015).

1.9.4.2 ICE inducing signals

There are some common signals that activate various ICEs, for example, the *recA*-dependent SOS-response (Auchtung et al., 2005, Beaber et al., 2004, Bellanger et al., 2007), secretion of signalling molecules from the recipient (Sitkiewicz et al., 2011), and growth phase (e.g. ICEclc activated in stationary phase by sigma factor RpoS (Miyazaki et al., 2012, Kamenšek et al., 2010, Pennington and Rosenberg, 2007). .

1.10 Classification of ICEs

Expansion of full genome sequence databases has led to the identification and characterisation of many ICEs. However, their classification still needs development because many remain still unclassified.

The current classification of ICEs is based on the homology of their integrase genes and the synteny of their coding sequences (Burrus et al., 2002). In comparative genomics, ICEberg (http://db_mml.sjtu.edu.cn/ICEberg) is a web-based resource reflecting previously identified ICEs (Bi et al., 2012). Based on the features described above, 344 out of 428 ICEs are categorised into 28 distinct families. ICEberg does not classify 84 ICEs due to their possession of unique integrases and other structural components(Bi et al., 2012).

The present study is focused on an unclassified ICE present in *Klebsiella pneumoniae* HS11286. .

1.11 T4SSs

Bacteria utilise specialised secretion systems for the transfer of macromolecules across their cell envelopes; these are grouped into six major classes, known as I, II, III, IV, V and VI (Thanassi and Hultgren, 2000, Henderson et al., 2004, Mougous et al., 2006). Recently, type VII secretion system has been described as the major secretion system in mycobacteria (Costa et al., 2015). As noted above T4SSs are associated with bacterial conjugation and transfer of both nucleoprotein complexes and protein effectors (Lawley et al., 2003, Christie et al., 2005).

1.12 Mechanisms of T4SSs

T4SSs are composed of multiple subunits spanning in the cell envelope with a surface pilus (Lawley et al., 2003, Christie et al., 2005). The overall process of conjugation appears to be mechanistically conserved in nearly all systems. The processing proteins (Dtr) are required for DNA transfer and replication and include relaxase together with accessory factors that identify and bind to the *oriT* forming a complex known as the relaxosome (Chen et al., 2005, Draper et al., 2005, Garcillán-Barcia et al., 2007).

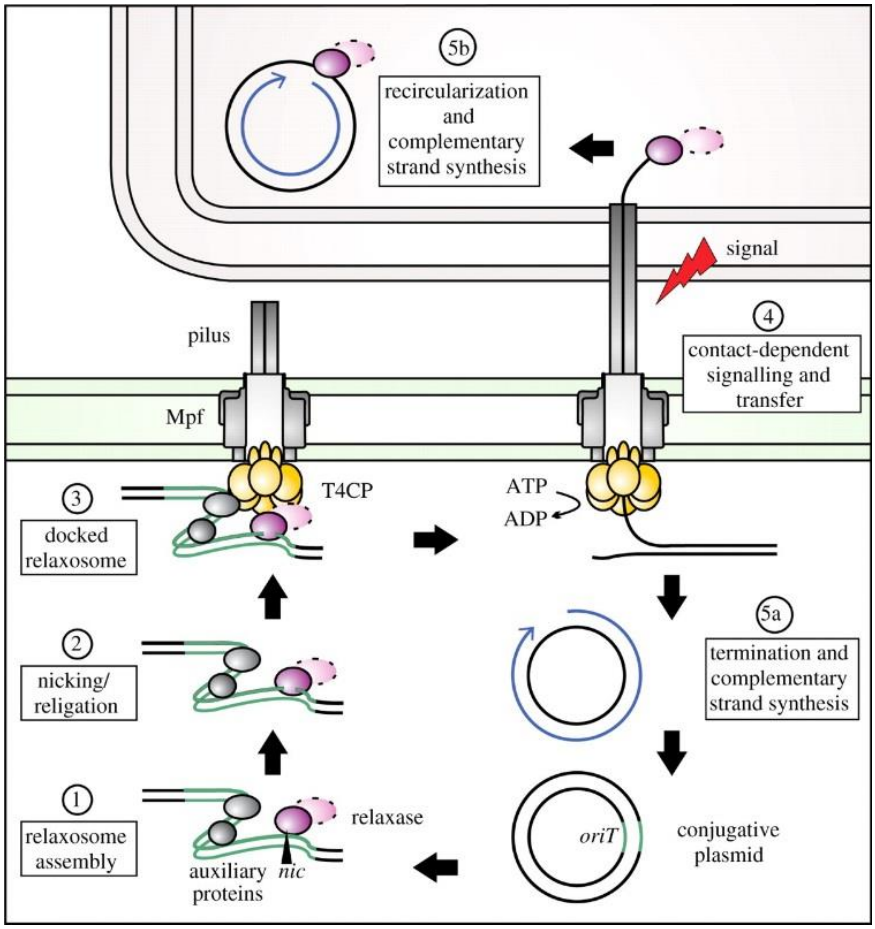

Figure 1-9 General mechanism of conjugative DNA transfer via T4 secretion channel.
Conjugative plasmids carry an *oriT* and express proteins for pili, the envelope spanning T4 channel (Mpf), a T4CP (yellow), the secretion initiation complex (relaxosome), and secretion substrate and DNA nicking relaxase (pink). Dotted oval indicates bifunctional relaxases that are fused to a helicase to facilitate conjugative DNA processing. The complementary plasmid strand remains circular throughout.
(Zechner et al., 2012)

.

ICEs are engaged with the transfer channel by the interactions between the relaxosome and coupling proteins (T4CPs). These proteins interact with the secretion machinery comprising, the complex multi subunit matting pair formation (Mpf) proteins (Christie, 2004, Gomis-Ruth et al., 2004, Lawley et al., 2003). In Gram-negatives, the Mpfs also promote attachment of the donor to the target cells (Christie and Cascales, 2005, Lawley et al., 2003), see Figure 1-9.

1.13 Different types of T4SSs

1.13.1 T4SSs-A

T4SS-A resembles the standard VirB/VirD4 system of *Agrobacterium tumefaciens*. This system is encoded by the *virB* operon (~10 kb), which consists of 11 adjacent genes

(*virB1-virB11*) and one separate, *virD4*. VirB1 is a lytic transglycosylase that digests the peptidoglycan to allow space for assembly of the secretion channel. VirB2 and VirB5 are pilus components, B4 and B11 comprise the ATPase that provides energy to the machinery. B3, B6, B7, B8, B9 and B10 are associated with the transmembrane channel (Figure 1-10). VirD4 is the T4CP and contributes an additional ATPase to the system (Christie et al., 2005, Backert and Meyer, 2006).

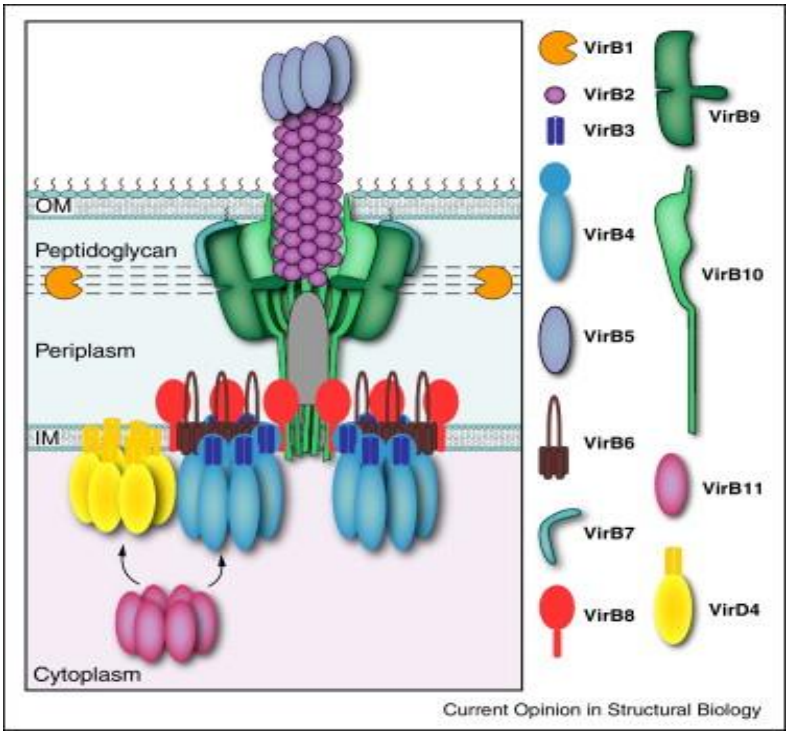

Figure 1-10 Schematics of T4SS-A.
(Trokter et al., 2014).

Various other T4SSs are identified that share common features with the VirB/VirD4 system. A few have the complete set of genes in an operon, while others are chimeras involving some unrelated genes and VirB/VirD4 (Christie et al., 2005).(e.g. the T4SS encoded by the cag PAI of *Helicobacter pylori* (Buhrdorf et al., 2003, Andrzejewska et al., 2006)). The VirB/VirD4 related systems also play an important role in bacterial pathogenesis (Schmid et al., 2004) by translocating various virulence associated effector proteins (Backert and Meyer, 2006). Verma and Burns (2007) showed that during first stage of infection, the pertussis toxin first interacts with the partially assembled T4SS in the periplasm leading to assembly and secretion of toxin into the extracellular environment. .

1.13.2 GIs-associated T4SSs

A novel family of T4SS has been identified on ICEHin1056 in *Haemophilus influenzae* and this has distinctive features compared to other T4SSs; the element has been found in various related MGEs from multiple bacterial strains *(Juhas et al., 2008).* Based on its strong association with GIs, this family was named GI-associated T4SS (Juhas et al., 2007a). The system involves 24 open reading frames that are proposed to form the secretion channel for conjugative transfer of DNA (Juhas et al., 2008).

1.14 Why it is important to study *Klebsiella pneumoniae*?

1.14.1 Taxonomy and ecology

Klebsiella are rod shaped, Gram-negative, facultative anaerobic, non-motile, encapsulated bacteria belonging to the family *Enterobacteriaceae.* The genus *Klebsiella* has been classified into eight distinct species (Brisse et al., 2006): including *K. pneumoniae*, *K. oxytoca*, *K. planticola, K. ornithinolytica, K. terrigena, K. mobilis, K. granulomatis, and K. variicola*.

K. pneumoniae strains are further classified into three subspecies: *pneumoniae*, *ozaenae* and *rhinoscleromatis* (Rosenblueth et al., 2004, Capitani et al., 2006). Genomic and phenotypic studies on virulent strains have shown that the sub-species ozaenae and rhinoscleromatis are descendants of *K. pneumoniae* and are referred as virulent sub-clones of *K. pneumoniae* (Brisse et al., 2009). *Klebsiella* are widely spread in the environment and can be isolated from water, soil, plants, industrial waste, and food (Fouts et al., 2008, Podschun et al., 2001).

1.14.2 Infections and Epidemiology

Klebsiella spp. are pathogenic for both animals and humans. They cause serious infections in horses, dogs, guinea pigs, birds and monkeys (Fox and Rohovsky, 1975, Glickman, 1981, Kinkler Jr et al., 1976, Wilson, 1994). A high prevalence of multiple *Klebsiella* species has been noted in water, soil and rumen samples suggesting their transmission by the faecal-oral route (Zadoks et al., 2011).

K. pneumoniae is found in the human commensal microbiota of the gastrointestinal and nasopharyngeal tracts. About 29-35% of individuals carrying *Klebsiella* spp. in their stool

and 3-4% in their throat, and carriage may more frequent in hospitalised patients (Davis and Matsen, 1974).

K. pneumoniae is an important cause of pyogenic liver abscesses (PLA) (Carpenter, 1990). Related to hepatobiliary dysfunction. Since the 1990s *K. pneumoniae* has appeared as a prominent PLA-causing agent in eastern-Asia (Peters and Craig, 2001, Rahimian et al., 2004). The infection may disseminate to cause complications such as endopthalmitis and meningitis (Thomsen et al., 2007, Ko et al., 2002). Several cases of *K. pneumoniae* associated PLAs and meningitis have been reported in Europe, Canada and USA (Giobbia et al., 2003, Karama et al., 2008, Nadasy et al., 2007, Sobirk et al., 2010).

K. pneumoniae is also a cause of community acquired pneumonia and is prominent in various parts of the world. In Japan and Malaysia between 15 and 40% of pneumoniae (particularly the elderly) have been estimated to be caused by *K. pneumoniae* (Podschun and Ullmann, 1998, Qureshi, 2016). The incidence of *K. pneumoniae* infections varies in different parts of the world but according to Qureshi (2016), mortality can be ~50% and is higher in alcoholics and when associated with bacteraemia.

Klebsiella infections are also important in immunocompromised hosts and feature as important causes of nosocomial infections. Infection risk increases with the use of intravascular devices and urinary catheters (Podschun and Ullmann, 1998) and with other underlying conditions such as diabetes mellitus or chronic cardiac, renal or pulmonary problems (Marchaim et al., 2008, Meatherall et al., 2009). Epidemics of *K. pneumoniae* infections highly resistant to antibiotics have been described in neonatal units (Cordero et al., 2004, Damjanova et al., 2007, Randrianirina et al., 2009).

Paterson et al. (2003) reported that the majority of the *Klebsiella* spp. isolated from clinical samples harbour at least two beta lactamase genes. Members of the *Klebsiella* species are rapidly acquiring resistance to many previously effective agents including aminoglycosides, fluoroquinolones, tetracycline, chloramphenicol and sulfamethoxazole. Various precautions have been documented to reduce the spread of *Klebsiella* infections in hospitals. For example, environmental hygiene, maintenance and cleaning of medical equipment and, most importantly, good hand washing practice.

1.14.3 *K. pneumoniae* genome structure

K. pneumoniae genomes are ~5.5 Mbp and encode ~5500 genes (Wyres and Holt, 2016). Whole-genome comparisons of hundreds of isolates indicate that the core genome of *K. pneumoniae* includes fewer than 2000 genes (Bialek-Davenet et al., 2014, Holt et al., 2015). The additional 3500 'accessory' genes are drawn from a pool of more than 30,000 genes (Holt et al., 2015). This high rate of acquisition of accessory genes indicates that *K. pneumoniae* has an open pan genome (Medini et al., 2005).

Holt et al. (2015) categorised *K. pneumoniae* accessory genes into functional groups and assessed their frequencies: carbohydrate metabolism (19%), membrane transport (13%), exopolysaccharide production (capsule) (11%), iron metabolism (2%), drug, heavy metal and stress resistance (1%) and several other accessory genes of unknown functions (~56%). Although evidence shows the presence of discrete sets of accessory genes in multiple phylogenetic lineages, each lineage includes sufficiently diverse sets to enable their differentiation (Holt et al., 2015). Thus various *K. pneumoniae* strains are noticeably different in their metabolic activities enabling adaptation to a broad range of habitats.

1.15 Variations in the genetic complement of *K. pneumoniae* strains.

Exchange of accessory genes within the *K. pneumoniae* population, contributes to the evolution of *K. pneumoniae* strains (Holt et al., 2015, Ramirez et al., 2014, Löhr et al., 2015). Recently, ~50% of sequenced *K. pneumoniae* isolates from dairy cows with mastitis showed presence of a plasmid-encoded lactose utilisation operon. A plasmid-encoded siderophore system was associated with strains isolated from human cases of bacteraemia and other invasive infections (Holt et al., 2015, Paczosa and Mecsas, 2016).

Conjugative plasmids are associated with the rapid spread of antimicrobial resistance. For example, pLVPK (219 kb), first identified in *K. pneumoniae* CG43 (Chen et al., 2004), appears to encode for heavy metal resistance (copper, silver, lead and tellurite) and iron acquisition. It also harbours regulatory genes for capsule synthesis (*rmpA* and *rmpA2*) that interact with capsule expression (Cheng et al., 2010). Wu et al. (2009) documented the presence of a similar plasmid in the hyper-virulent strain NTUH-K2044.

The presence of the 41.7kb conjugative-transmissible plasmid pMET1 in *K. pneumoniae* indicates cross species HGT incidence in view of similarity to the pCRY plasmid of *Yersinia pestis* (Figure 1-11). pMET1 encodes a conjugation-associated type IV secretion system in addition to multiple antibiotic resistance genes including bla*TEM*-1 and bla*OXA*-9 (Soler et al., 2008); these genes were also found on *Tn*1331.2 (11.0kb transposon). These genes confer resistance to several aminoglycosides and β-lactams, including ampicillin, amikacin, kanamycin, streptomycin and tobramycin (Soler et al., 2008, Tolmasky et al., 1988).

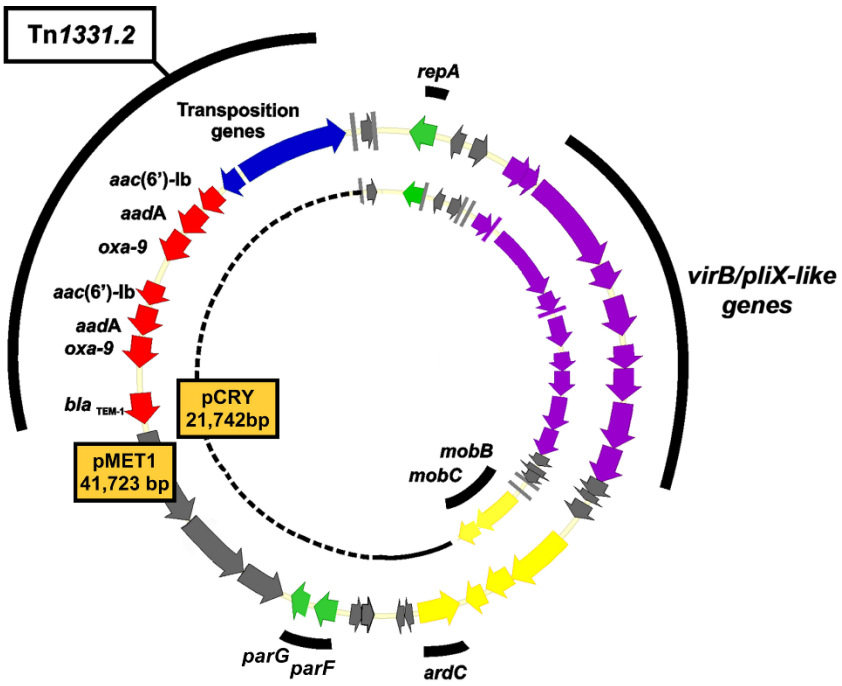

Figure 1-11 Genetic map of pMET1 and comparison to plasmid pCRY.
The genetic maps of pMET1 and pCRY are compared showing the homologous regions. Homologous genes are shown with same colors. Yellow: mobilization; green: replication and partition; red: antibiotic resistance; purple: virB/pilX-like; blue: transposition; grey: unknown. Since pCRY is smaller than pMET1, to represent it in circular form a dotted line was added to fill the gap. Taken from (Bistué et al., 2008)

The presence of various resistance encoding integrons in different *K. pneumoniae* strains also support the occurrence of HGT events as integrons are themselves non-mobile and are usually transferred with MGEs (Dropa et al., 2010, Correia et al., 2003). Bacteriophages also have important roles in generating genome diversity as comparative analysis of sequenced genomes identifies numerous prophages in multiple

K. pneumoniae strains. For example there are, two prophages (36.3 kb and 48.6 kb) in *Kp*342, five in MGH78578 (from 11.0 kb to 58.3 kb) and one in NTUH-K2044 (23.9 kb) (Fouts et al., 2008, Wu et al., 2009). Dissemination of ICEs has also contributed to *K. pneumoniae* evolution with ICE*Kp1 (*~76 kb) the first identified ICE in *K. pneumoniae* NTUH-K2044 (See below 1.13.5).

1.15.1 Genomic Islands in *K. pneumoniae*

Eight tRNA genes including (*thr5, arg6, asn33, asn34, pheV, met56, leu82* and *tmRNA*) were found to be hotspots for insertion of strain specific GIs in *K. pneumoniae* strains (Zhang et al., 2011, Chen et al., 2010, Aartsen, 2008, Ou et al., 2007).

The importance of *pheV-tRNA* loci has been investigated and 95 out of 101 strains showed likely insertions within *pheV tRNA* (Aartsen, 2008, Chen et al., 2010). KpGI-1 (3.6 kb) was the first identified GI at *pheV* locus of two *K. pneumoniae* strains (KR116 and KR164: isolated at the Leicester Royal Infirmary, UK) (Aartsen, 2008). It was more common in sputum isolates compared to strains isolated from urine, blood, wound or bile, whereas KpGI-2 (6.4kb) was common in urine isolates (Chen et al., 2010). The GIs found in different *K. pneumoniae* strains are summarised in Table 1-1.

Several *non-tRNA* loci in *K. pneumoniae* NTUH-K2044 were shown to harbour strain-specific DNA. Ma et al. identified a 20kb DNA fragment that encodes an iron uptake system (*kfuABC*) and a phosphoenolpyruvate phosphotransferase system (*PTS*) (Ma et al., 2005). Comparison between the MGH78578, *Kp*342 and NTUH-K2044 genomes showed that these strains share 54.7% of their recognised genes (Zhang et al., 2011). Interestingly, a 13kb citrate fermentation encoding locus was found upstream of the dihydrodipicolinate synthase (*dapB*) gene in MGH78578 and *Kp*342 but absent from NTUH-K2044. *In-vitro* studies showed that this locus improved growth of host strains in the citrate-rich but oxygen deprived conditions of the urinary tract (Chen et al., 2009).

Table 1-1 Summary of GIs found in various *K. pneumoniae* strains.

GIs	Strain	Size (kb)	Locus	Possible function	Sources[a]
KpGI-1	KR116	3.6	*pheV*	Unknown, but over-represented in sputum isolates	1,2
KpGI-2	HS04160	6.4	*pheV*	Role in growth regulation & possible role in pathogenesis	2
KpGI-3	MGH78578	12.6	*pheV*	Unknown, but possible role in surface adhesion and colonization	1,2
KpGI-4	KR173		*pheV*	Unknown	1
mGI_Kp20093	Kp20093	15.4	*tmRNA*	Unknown	3
tmGI_Kp10011	Kp10011	17.5	*tmRNA*	Unknown	3
tmGI_Kp49790	Kp49790	12.7	*tmRNA*	Unknown	3
tmGI_Kp44	Kp44	9.0	*tmRNA*	Unknown	3
tmGI_Kp63	Kp63	12.0	*tmRNA*	Unknown	3
HPI	RK75	~40.0	*asnT*	Iron acquisition via yersiniabactin; virulence factor in murine respiratory tract infections	4,5
pks	KpCF1	54.0	*asn*	Synthesis of colibactin, which can induce double-stranded DNA breaks and death in eukaryotic cells	6
kfu/PTS	NTUH-K2044	20.0	non-tRNA	Iron acquisition; virulence factor in murine infection model	7
allS island	NTUH-K2044	21.7	non-tRNA	Allantoin metabolism; mutation in allS increased LD50 10 to 100-fold.	8
Citrate fermentation locus	MGH78578	13.0	non-tRNA	Improved ability to grow in the presence of citrate	9

a= (Aartsen, 2008)[1], (Chen et al., 2010)[2], (Zhang et al., 2011)[3], (Bachman et al., 2011)[4], (Koczura and Kaznowski, 2003)[5], (Putze et al., 2009)[6], (Ma et al., 2005)[7], (Chou et al., 2004)[8], (Chen et al., 2009)[9]

Lin et al. (2008) demonstrated the mobilisation cycle of ICEKp-1 in *K. pneumoniae* NTUH-K2044. It was able to exist both in a circular and a chromosomally-integrated form within the *asn-tRNA site* (Lin et al., 2008, Wu et al., 2009). The central region of ICEKp-1 shows similarities to the plasmid pLVPK with the 5´ end carrying genes similar to the yersiniabactin siderophore system of the high pathogenicity island (HPI) of *Y. pestis*. ICEKp-1 also encodes its own T4SS that is a homologue of T4SS-A (section 1.13.1). The prevalence of ICE*Kp1* was significantly higher in strains isolated from patients suffering

with PLA (Lin et al., 2008). In conclusion, the presence of GIs and GI-like regions highlight their potential contributions to strain specific phenotypes in *K. pneumoniae* strains.

1.16 Why *K. pneumoniae* HS11286 was selected for this study

K. pneumoniae HS11286 was isolated from a sputum specimen in 2011 at Huashan Hospital, Shanghai, China. The genome was sequenced by Liu, Dr Kumar Rajakumar and colleagues and revealed seven circular replicons including one ~5.3 Mbp chromosome and six plasmids. The chromosome encodes 87 *tRNAs*, 5,316 proteins, 1 tmRNA and 8 copies of ribosomal RNA. Of the six plasmids (pKPHS1-6), 1-3 are large and 4-6 are small with unknown functions (Table 1-2)(Liu et al., 2012).

Dr Rajakumar and colleagues analysed the genome against *K. pneumoniae* strains MGH78578, NTUH-K2044, *Kp*342 and KCTC2242 using GenomeSubtractor (Shao et al., 2010) and detected seven prophage regions..

Table 1-2 Plasmid of *K. pneumoniae*HS11286.

Plasmid	Size (bp)	G+C content (%)	Putative Function
pKPHS1	122,799	49.50	*CTX-M-14* extended-spectrum beta lactamase
pKPHS2	111,195	53.30	*blaTEM-1 ,blaKPC-2*
pKPHS3	105,974	52.50	Resistance genes *tetG, cat, sul1*, *dfra12*, aac(3)-Ia, and aph
pKPHS4	3,751	52.20	unknown
pKPHS5	3,353	42.80	unknown
pKPHS6	1,308	47.90	unknown

Together with Chinese colleagues the Rajakumar's lab recently explored the landscape of the mobile genome in *K. pneumoniae* HS11286 with a focus on antibiotic resistance. Sixteen resistance genes were identified on the large plasmids, 14 of which were found to be variously associated with *Tn*1721, *Tn*3, *Tn*5393, In2, ISCR2 and ISCR3 derived elements (Bi et al., 2015). Comparative bioinformatic analysis against multiple clinical and environmental *K. pneumoniae* strains had revealed that HS11286 possesses an extremely flexible genome (Zhang et al., 2011).

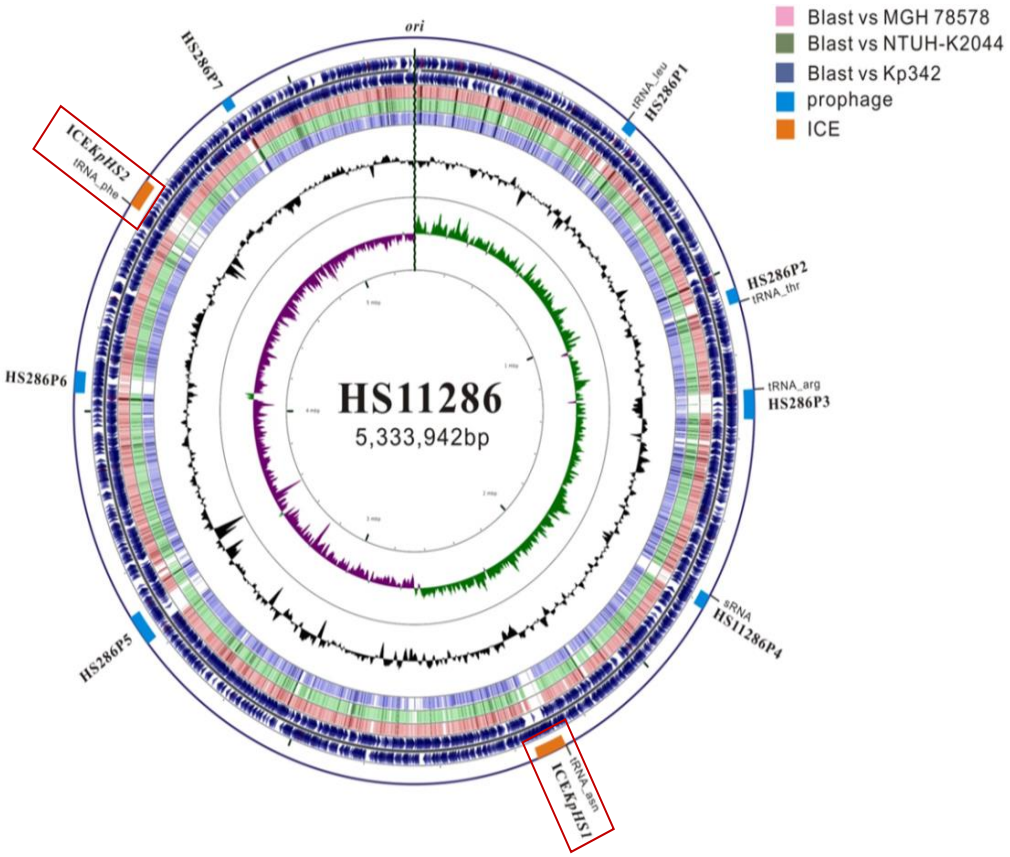

Figure 1-12 Schematic representation of *K. pneumoniae* HS11286 chromosomal genome.

A parallel study in the Rajakumar's lab focussed on the functional analysis of Fic-Domain-bearing proteins (Roy and Cherfils, 2015) in HS11286. These proteins include secreted bacterial toxins and the local studies revealed that the T4SS present on ICEKpnHS11286-1 had this function (Al-Madadha, 2017). Additional local studies identified T6SSs at three different loci (T6SS-1-3) in this strain, amongst which system 1 and 3 were intact and functional for their virulence associated features, whereas T6SS-2 was truncated and inactive (unpublished).

The HS11286 chromosome also harbours two novel ICEs (ICE*Kp*nHS11286-1: 62 kb and ICE*Kp*nHS11286-2: 56 kb) (Figure 1-12). ICE*Kp*nHS11286-1 was putatively characterised as ICEKp-1-associated element, however, no experimental data was provided (Bi et al., 2013). Moreover, ICE*Kp*nHS11286-2 remained essentially unexplored. Thus more insight into these elements was clearly desirable and the present project was initiated.

This study used *K. pneumoniae* HS11286 ΔMDRΔKPCΔCPS designated as WT, which lack *blaKPC* (carbapenems resistance) on plasmid pKPHS2, a multidrug resistance island on

plasmid pKPHS3 and *cps* cluster responsible for capsule formation whereas parent strain (ΔMDRΔKPC) (section 6.3.2) was capsulated (Table 1-3).

1.17 Overall aim and Objectives

The aim of the present study is to build on work established in the former Rajakumar lab at Leicester University and to further characterize two ICEs of an extensively studied *K. pneumoniae* strain (HS11286) with a view to further understanding their contributions to HGT, cell physiology, virulence and antibiotic resistance.

The elements studied and abbreviations used in the text are summarised in Table 1-3.

Table 1-3 Key related to this study.

Previously used Name/Abbreviations	Abbreviation in this thesis
ICEKp-1 family	ICEKP-1
ICEKp-1 of *Kp* NTUH-K2044	ICEKp1
ICEKpnHS11286-1 of *K. pneumoniae* HS11286	ICE-1
ICEKpnHS11286-2 of *K. pneumoniae* HS11286	ICE-2
K. pneumoniae HS11286 ΔMDRΔKPCΔCPS	WT
K. pneumoniae HS11286 ΔMDRΔKPC	Parent strain

The specific objectives were:

1. To characterise and annotate uncharacterised contents of ICE-1 and ICE-2 of *K. pneumoniae* HS11286 and to study their prevalence in 40 local clinical isolates.
2. To investigate the contribution of ICE-1 and ICE-2 on the phenotypes of *K. pneumoniae* HS11286 including: Growth characteristics; Biofilm formation; Antibiotic resistance; and Contribution to virulence.
3. To study the mobilisation cycle of ICE-1 and its effects on recipient phenotypic biology.
4. To study mobilisation cycle of ICE-2. To investigate whether or not ICE-1 and ICE-2 have functional interactions during conjugative transfer of DNA.

Chapter 2 Materials and Methods

2.1 Bacterial strains and plasmids

K. pneumoniae strains were obtained from two major sources; 40 strains were obtained from Leicester Royal Infirmary (LRI) Hospital, isolated from clinical samples (Table 2-1) whereas, *K. pneumoniae* HS11286 was kindly provided by Dr Hong-Yu Ou (Tianjin University of Science and Technology, China). All bacterial strains in each case were stored at -20/-80^{o}C in BHI broth with 30% glycerol. Strains were routinely recovered by growing at 37^{o}C using LB or LA, unless otherwise specified. Appropriate antibiotics (when applicable) were used during the recovery or growth. Details of all the bacterial strains used and constructed in this study are summarised in Table 2-2. Plasmid used and constructed are listed in Table 2-3.

Table 2-1 Summary of 42 local *K. pneumoniae* strains obtained from LRI.

K. pneumoniae isolates[a]	Time of collection	Source	Reference
KR2170	(Feb 2009 to June 2010)	Sputum	LAB 212 Archive
KR2171		Ascites Fluid	
KR2172		Peritoneal Dialysis Fluid	
KR2173		Dialysis Catheter	
KR2174		Peritoneal Dialysis Fluid	
KR2175		Peritoneal Dialysis Fluid	
KR2176		Peritoneal Dialysis Fluid	
KR2177		Ascites Fluid	
KR2178		Biliary Fluid	
KR2179		Ascites Fluid	
KR2180		Sputum	
KR2181		Ascites Fluid	
KR2201		Blood Culture	
KR2202		Blood Culture	
KR2203		Blood Culture	
KR2204		Cerebrospinal Fluid	
KR2205		Ascites Fluid	
KR2206		Blood Culture	
KR2207		Cerebrospinal Fluid	
KR3152	(Jun 2011 - Dec 2011)	Blood Culture	
KR3153		Blood Culture	
KR3154		Blood Culture	
KR3155		Blood Culture	
KR3156		Blood Culture	
KR3157		Blood Culture	
KR3158		Blood Culture	
KR3159		Blood Culture	
KR3160		Blood Culture	
KR3161		Blood Culture	
KR3162		Blood Culture	
KR3163		Blood Culture	
KR3164		Blood Culture	
KR3165		Blood Culture	
KR3166		Blood Culture	
KR3167		Blood Culture	
KR3168		Blood Culture	
KR3169		Blood Culture	
KR3170		Blood Culture	
KR3171		Blood Culture	
KR3172		Blood Culture	
KR2170		Blood Culture	
KR2171		Blood Culture	

a: KR stands for Kumar Rajakumar

Table 2-2 Summary of bacterial strain used and constructed.

Bacterial strain	Description	Resistance[a]	Reference
K. pneumoniae MGH78578	Fully sequenced strain Isolated in Washington University from a sputum sample		Lab 212 Archive
K. pneumoniae NTUH-K2044	Fully sequenced strain		Lab 212 Archive
K. pneumoniae HS11286	Fully sequenced strain with multi-drug resistance isolated from human sputum in Shanghai, China	Amp 100μg/ml	Lab212 Archive[85]
K. pneumoniae HS11286 ΔKPCΔMDR	A mutant constructed with in-frame deletion of *blaKPC* (carbapenems resistance) on plasmid pKPHS2 and a multidrug resistance island on plasmid pKPHS3 between-KPHS_p300510 and KPHS_p300880 gene (gene IDs).	Amp 100μg/ml	Lab 212 Archive (Dr Dexi Bi)
K. pneumoniae HS11286 ΔMDRΔKPCΔCPS	*K. pneumoniae* HS11286 ΔKPCΔMDR with an additional inframe deletion of the genes responsible for the production of the capsular polysaccharides (Genes in cluster between gene *galF-ugd)* for easier manipulation	Amp 100μg/ml	Lab 212 (Yingzhou Xie)
K. pneumoniae HS11286 ΔKPCΔMDRΔT6SS1ΔT6SS3	A mutant constructed with an inframe deletion of both clusters (1 and 3) that contain type 6 secretion system components	Amp 100μg/ml	Lab 212 (David Ngmenterebo)
K. pneumoniae HS11286 *ΔMDRΔKPCΔCPSΔICE1*	HS11286 ΔMDR ΔKPC ΔCPS strain used to construct an inframe deletion of ICE1 genes ID designation (ICEKpnHS11286-1)[85]	Amp 100μg/ml	This study
K. pneumoniae HS11286 *ΔMDR ΔKPC ΔCPS Δmob1*	HS11286 ΔMDR ΔKPC ΔCPS strain used to construct an inframe deletion of *mob1* gene only in the element ICE1	Amp 100μg/ml	This study
K. pneumoniae HS11286 ΔMDRΔKPCΔcpsΔirp2::hph	ICE-1 was tagged on *irp2*	Hyg 100μg/ml	Lab 212 (Yingzhou Xie)
K. pneumoniae HS11286 *ΔMDRΔKPCΔcpsΔICE2*	HS11286 *ΔMDRΔKPCΔcpsΔICE2* strain used to construct an inframe deletion of ICE2 element (ICE 2 has the gene ID designation (ICEKpnHS11286-2)[85])	Amp 100μg/ml	This study
K. pneumoniae HS11286 ΔMDRΔKPCΔcpsΔKPHS44780::hph	ICE-2 was tagged on *orf8*	Hyg 100μg/ml	Lab 212 (Yingzhou Xie)

K. pneumoniae HS11286 *ΔMDRΔKPCΔCPS Δmob2*	HS11286 ΔMDR ΔKPC ΔCPS strain used to construct an inframe deletion of *mob2* gene only in the element ICE2	Amp 100µg/ml	This study
K. pneumoniae HS11286 ΔMDRΔKPCΔcpsΔtraI	HS11286 ΔMDR ΔKPC ΔCPS strain used to construct an inframe deletion of *traI* gene only in the element ICE2	Amp 100µg/ml	This study
K. pneumoniae HS11286 ΔMDRΔKPCΔcpsΔvirB(1-2)ΔvirB(4-6)::hph	HS11286 ΔMDR ΔKPC ΔCPS strain used to construct an inframe deletion of genes responsible for the cylindrical part of the Type 4 Secretion system on ICE1 conjugative element virB(1-2)ΔvirB(4-6), this is a marked mutant	Hyg 100µg/ml	Lab 212 (Yingzhou Xie)
K. pneumoniae HS11286 ΔMDRΔKPCΔcpsΔICE1ΔICE2	HS11286 ΔMDRΔKPCΔCPS strain used to construct an inframe deletion of both ICE1 and ICE2	Amp 100µg/ml	This study
K. pneumoniae HS11286 ΔKPCΔMDR ΔT6SS1	Mutant was constructed of complete genes cluster of T6SS-1	Amp 100µg/ml	Lab 212 (David Ngmenterebo)
K. pneumoniae HS11286 ΔKPCΔMDR ΔT6SS3	Mutant was constructed of complete genes cluster of T6SS-3	Amp 100µg/ml	Lab 212 (David Ngmenterebo)
K. pneumoniae HS11286 ΔMDRΔKPCΔT6SS-1Δcps::hph	*K. pneumoniae HS11286* ΔKPCΔMDR ΔT6SS1 strain was used to construct an inframe deletion of genes in cluster between gene *galF-ugd* (model strain for conjugation experiment)	Hyg 100µg/ml	This study
K. pneumoniae HS11286 ΔMDRΔKPCΔcpsΔInt2a::hph	HS11286 ΔMDRΔKPCΔCPS strain was used to performed inframe deletion of integrase(a) gene in ICE2 (excision assay)	Hyg 100µg/ml	This study
K. pneumoniae HS11286 ΔMDRΔKPCΔcpsΔInt2b::hph	HS11286 ΔMDRΔKPCΔCPS strain was used to performed inframe deletion of integrase(b) gene in ICE2 (excision assay)	Hyg 100µg/ml	This study
E. coli DH5α	Bacterial host used for cloning procedure		Promega
E. coli HB101	Bacterial strain used as a recipient in conjugation assays	Strep 50µg/ml	Lab 212
E. coli-pACYCoriT-1		C 30 µg/ml	This study
K. pneumoniae HS11286 ΔKPCΔMDR-pACYC-*oriT*1	Mutant was transformed with ICE-1 marker plasmid for conjugation assay.	C 30 µg/ml	This study
K. pneumoniae HS11286 ΔMDRΔKPCΔcps – pACYC-*oriT*1	-[b]	C 30 µg/ml	This study

K. pneumoniae HS11286 *ΔMDRΔKPCΔCPSΔICE1* –pACYC-*oriT*1	-	C 30 µg/ml	This study
K. pneumoniae HS11286 *ΔMDRΔKPCΔcpsΔICE2* –pACYC-*oriT*1	-	C 30 µg/ml	This study
K. pneumoniae HS11286 ΔMDRΔKPCΔcpsΔICE1ΔICE2-pACYCoriT1	-	C 30 µg/ml	This study
K. pneumoniae HS11286 *ΔMDRΔKPCΔCPSΔmob1-pACYCoriT1*	-	C 30 µg/ml	This study
K. pneumoniae HS11286 *ΔMDRΔKPCΔCPSΔmob2-pACYCoriT1*	-	C 30 µg/ml	This study
K. pneumoniae HS11286 ΔMDRΔKPCΔcpsΔvirB(1-2)ΔvirB(4-6)::hph-pACYC*oriT*1	-	Hyg 100µg/ml 7 C 30 µg/ml	This study
K. pneumoniae HS11286 ΔMDRΔKPCΔcpsΔirp2::hph-pACYCoriT1	-	Hyg 100µg/ml & C 30 µg/ml	This study
K. pneumoniae HS11286 ΔMDRΔKPCΔcpsΔKPHS44780::hph-pACYCoriT1	-	Hyg 100µg/ml &C 30 µg/ml	This study
K. pneumoniae HS11286 ΔMDRΔKPCΔcpsΔtraI-pACYCoriT1	-	C 30 µg/ml	This study
K. pneumoniae HS11286 ΔKPCΔMDR ΔT6SS1-pACYC*oriT*1	-	C 30 µg/ml	This study
K. pneumoniae HS11286 ΔKPCΔMDR ΔT6SS3-pACYCoriT1	-	C 30 µg/ml	This study
K. pneumoniae HS11286 ΔKPCΔMDRΔT6SS1ΔT6SS3-pACYC*oriT*1	-	C 30 µg/ml	This study
K. pneumoniae HS11286 ΔMDRΔKPCΔT6SS-1Δcps::hph-pACYCoriT1	-	Hyg 100µg/ml & C 30 µg/ml	This study
K. pneumoniae HS11286 ΔMDRΔKPCΔcpsΔInt2b::hph-pACYCoriT1	-	Hyg 100µg/ml & C 30µg/ml	This study

a= Amp (Ampicillin), Apra (Apramycin), Hyg (Hygromycin), C (Chloramphenicol), Strep (Streptomycin); b= Mutant was transformed with ICE-1 marker plasmid for conjugation assay.

Table 2-3 Summary of plasmids used and constructed.

Plasmids	Descriptions	Resistance	Reference
pACYC184	Used for construction of ICE1 marker plasmids for conjugation assay	C 30µg/ml	Lab 212
pACYC-*oriT*1	Used for mobilization assay	C 30µg/ml	This study
pACYC-*oriT*956	Used for determination of minimal region of *oriT* of *ICE-1*	C 30µg/ml	This study
pACYC-*oriT*568	Used for determination of minimal region of *oriT* of *ICE-1*	C 30µg/ml	This study
pACYC-*oriT*525	Used for determination of minimal region of *oriT* of *ICE-1*	C 30µg/ml	This study
pACYC-*oriT*525	Used for determination of minimal region of *oriT* of *ICE-1*	C 30µg/ml	This study
pACYC-*oriT*648	Used for determination of minimal region of *oriT* of *ICE-1*	C 30µg/ml	This study
pACYC-*oriT*608	Containing *hph* cassette flanked by FRT sequences	C 30µg/ml	This study
P_{Ybt}	The *ybtSXQPA* operon of ICE1 was cloned into pACYC184 for complementation experiment	C 30µg/ml	This study
RFTool-1	A plasmid was constructed for the complementation experiment of conjugation assay. The plasmid consisted an origin of replication (bHROR) of pFLP2-Apra that was cloned with backbone of pWSK29-Apra.	Apra 30µg/ml	This study
RFT-mob2	*mob2* of ICE-2 was cloned in the RFTool-1 under the control of IPTG inducible promoter	Apra 30µg/ml	This study
RFT-traI	*traI* of ICE-2 was cloned in the RFTool-1 under the control of IPTG inducible promoter	Apra 30µg/ml	This study
RFT- $mb^{K199E507}$	Point mutated *mob2* of ICE2 was cloned in RFTool-1 under the control of IPTG inducible promoter	Apra 30µg/ml	This study
pJTAG-Hyg	Containing *hph* cassette flanked by FRT sequences	Hyg 100µg/ml	Lab 212
pKOBEG-Apra	Temperature sensitive plasmid (grow at 30°C) possesses the genes for lambda red recombination.	Apra 30µg/ml	Lab 212
pFLP2-Apra	Plasmid coding for the Flippase gene for converting knockout mutants to marker less mutants by excising DNA flanked by the FRT site introduced on each flank (used to construct different versions).	Apra 30µg/ml	Lab 212
pWSK29-Apra	A plasmid previously used for protein expression in *K. pneumoniae,* Apramycin gene cassette added. selection with Apramycin at 30ug/ml.	Apra 30µg/ml	Lab 212

2.2 DNA manipulation techniques

2.2.1 DNA extraction

Genomic DNA extraction was achieved from overnight culture (containing 2 x10^9 Cfu/ml) using Archive DNA Cell/Tissue Kit (5Prime). Briefly, 500µl of overnight culture were treated with detergent buffer. The lysed cells were treated with proteinase K and RNAse at 37^{o}C for 30 min. The supernatant was collected after centrifugation (15000×*g* for 10 min). The DNA was precipitated and washed using 100% isopropanol and 70% ethanol, respectively. After air drying the DNA pellet was dissolved in ultra-pure DNAse free water.

Plasmid DNA was extracted using GenElute Plasmid Miniprep (Sigma-Aldrich) as per manufacturer's instruction. The amount of culture and the time points were depended on the nature of the experiments.

DNA extraction from the agarose gel including products of polymerase chain reactions (PCR) and plasmid digest were achieved using GenElute gel extraction Kit (Sigma Aldrich) as per the manufacturer's instructions.

2.2.2 DNA quantification

DNA was quantified using Nanodrop 2000 (Thermo Fisher scientific) spectrophotometer using DNA elution buffer/PCR graded water as blank.

2.2.3 DNA amplification methods

2.2.3.1 Primer designed

Oligonucleotide for PCR reactions were designed using following tools; Primer3 (http://insilico.ehu.es/primer3/), ApE and primer designing tool-NCBI. For ICEs screening the primers were designed using *K. pneumoniae* NTUH-K2044 and HS11286 as a reference templates. The designed primers were synthesised by Sigma-Aldrich. Primers were dissolved in ultra-pure DNAse free water at 10pmol/µl and stored at -20^{o}C.

2.2.3.2 In-silico PCR

The specificities and utilities of primers were confirmed by in *silico* PCR analysis using the freely available web based tool (http://insilico.ehu.es/PCR/). The size of the in-silico PCR fragments were used to calculate the extension time.

2.2.3.3 Standard PCR method

Standard PCR was performed using either GoTaq polymerase (Promega) or GoTaq® G2 DNA polymerase (Promega). The PCR reaction components were assembled as a master mixture as per manufacturer's instruction. The deoxynucleotide triphosphates (dNTPs) (Bioline UK) were always prepared in PCR grade water at 10mM each. High fidelity DNA polymerase such as KOD hot start polymerase (Merck-Milipore) was used for cloning and mutagenesis work. The representative cycling conditions for each enzyme is shown in Table 2-4. Cycling conditions were based on predicted PCR product size and the primers melting temperature (Tm).

Table 2-4 PCR cycling conditions.

Steps	GoTaq DNA Polymerase	KOD Hot Start DNA Polymerase
Denaturation	95 °C for 30 sec	95 °C for 30 sec
Annealing	(Lowest Tm) °C for 30 sec	(Lowest Tm) °C
Extension	72°C , 1min/kb	70°C, 20 sec/kb

2.2.3.4 Colony PCR

A single bacterial colony was suspended in 30µl of ddH_2O and heated at 100 °C for ~10 min. Cells were pelleted at 14000 × *g* for 2 min (~5-6 min for mucoid cells) and 1µl (2µl for the detection of low copy number plasmids) of the supernatant was used as template for PCR reactions.

2.2.3.5 Splice overlap extension PCR

Splice overlap extension PCR (SOE-PCR) was used to create composite PCR products to facilitate mutation in gene/genes by homologous recombination (Heckman, Pease 2007). This technically simple and potent method allows DNA strands hybridization to one another at specific junctions, forming an overlap. Extension of this overlap by DNA polymerase yields a recombinant molecule. Mutant alleles consisted of an upstream homologous flank (UF), an antibiotic resistance cassette (hygromycin) and a downstream homologous flank (DF), spliced together in the manner depicted in Figure 2-1. For successful recombination the flanking region were kept at ~ 400-500bp in size, and they were amplified using genomic DNA from the parent strain.

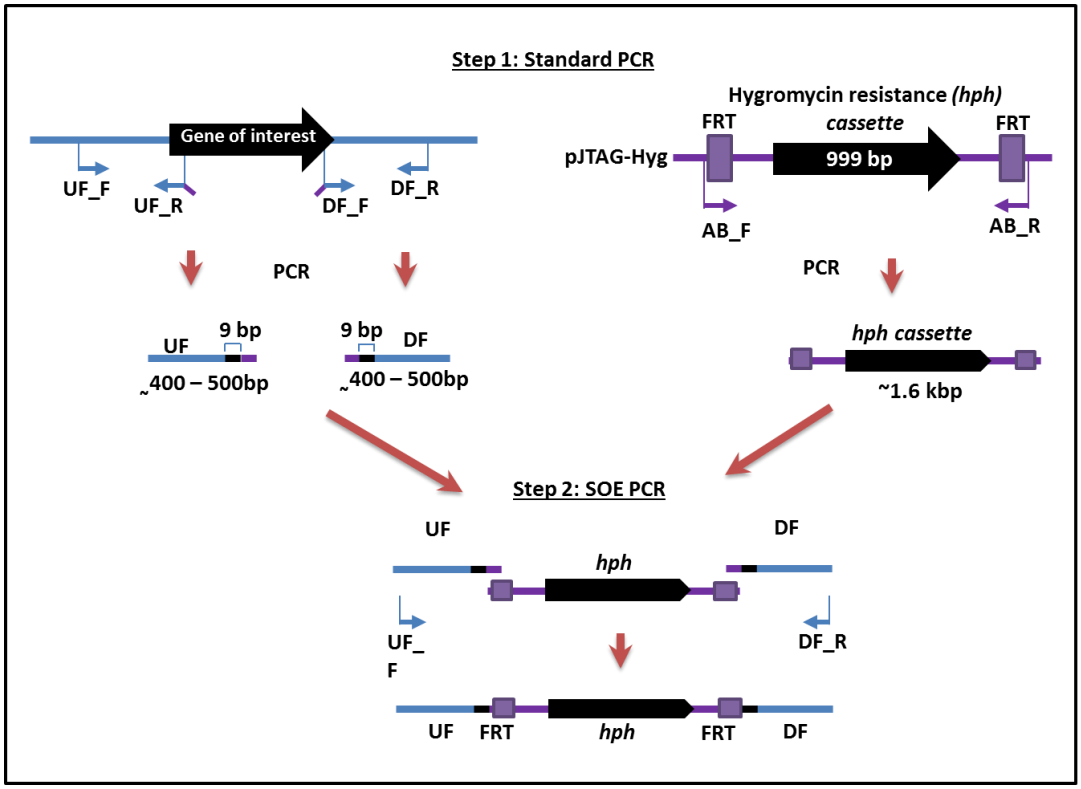

Figure 2-1 Schematics of SOE PCR.
Step 1: The left hand and right hand flanks around a gene of interest are amplified by PCR, using primers with overhangs containing regions that are homologous to the antibiotic resistance gene used (homologous regions in primers shown in purple for the left and right hand. UF and DF represent upstream and downstream flanking regions of the gene of interest. FRT indicates the flippase recognition target sequences. Step 2: The final stage of the SOE PCR involves annealing of the three amplicons from step 1, to produce the full mutant allele, which is then amplified using UF-F and DF-R primers.

Primer pairs UF-F/UF-R, DF-F/DF-R, and AB-F/AB-R were used separately to amplify PCR fragments (Figure 2-1). All fragments were gel purified (section 2.2.1). Primers UF-R and DF-F were designed so that their ends contained ~20bp sequence complementary to the *hph* fragment primers AB-F and AB-R, respectively. This added an overhang to PCR products which when mixed (Table 2-5), denatured and annealed in the SOE-PCR, the complementary fragment ends annealed, producing a spliced product where the two fragments have been merged.

Table 2-5 SOE PCR reaction mixture setup.

Master mixture for SOE PCR	Volume (ul) for 1 reaction
10 × Buffer for KOD Hot Start DNA polymerase (× 1)	5
dNTPs (0.2 mM each)	5
25 mM MgSO4 (1.5 mM)	3
Splicing fragment A (UF) (50 to 60 ng)	as required
Splicing fragment B (DF) (50 to 60 ng)	as required
Splicing fragment C (antibiotic cassette) (50 to 60 ng)	as required
Forward primer (added after 15 cycles)	1.5
Reverse primer (added after 15 cycles)	1.5
KOD Hot Start DNA polymerase (1U)	1
Ultra-pure nuclease free water	to the final volume of 50 ul

The PCR generated amplicons were mixed in an equimolar ratio in a single PCR reaction and the cyclic conditions were adjusted in two phases (Table 2-6). In order to facilitate the annealing of overlapping regions (20bp) and formation of a single spliced fragment, primers were not added in the initial 15 cycles of the first phase. The primers UF-F and DF-R were added in the second phase (35 cycles) to amplify the spliced fragment (Figure 2-2, Table 2-6).

Table 2-6 Conditions used for SOE PCR.

Steps	Number of cycles	Temperature °C	Time
Activation of KOD polymerase	1	95	2min
Annealing of overlapping regions of fragment A, B and C (without primers)			
Denaturation	15	95	20sec
Annealing		Lowest Tm of the overlapping region	10sec
Extension		70	10-25sec/kb of DNA
Amplification of spliced fragment			
Initial denaturation	1	95	20sec
Denaturation	35	95	20sec
Annealing		Lowest Tm of the primer pair used	10sec
Extension		70	10-25sec/kb of DNA
Final extension	1	70	5-10 min
Final hold	1	15	∞

2.2.4 DNA visualisation by agarose gel electrophoresis

Visualization of DNA fragments was routinely performed in agarose gels (Bio Line). The gel was prepared by dissolving 0.8g of agarose in 100ml of TAE buffer, which was later supplemented with 5µl of ethidium bromide (10 mg/ml stock) in 100ml of gel. 1X concentration of 6X loading dye (Thermo Fisher Scientific) was always added to the samples before loading. Samples were run alongside a DNA ladders; either Quick-Load 2-log DNA Ladder (0.1-10 kb) or GeneRuler^{TM} (Thermo Scientific) was used. Finally, the bands were visualized using a gel documenting system (Bio Rad) and images recorded.

2.3 General methods of recombination and mutant construction

2.3.1 Preparation of electro-competent cells

The procedure for preparation of electro-competent cells was adapted from Dower et al. (1988). Briefly, a single colony was inoculated into 5ml of LB for overnight growth at 37^{o}C with shaking at 200 rpm. The overnight culture was diluted at a ratio of 1:100 (overnight culture: fresh LB) and allowed to grow an OD_{600} of 0.4 – 0.5 (~4 hr). The culture was cooled to 4 ^{o}C by placing on ice for 20 min. The cells were harvested by centrifugation (3000 × *g*, 15 min, and 4^{o}C) and gently washed three times with successively smaller volumes of ice cold 10 % (v/v) glycerol. The final pellet of the cells were suspended in a small volume of ice cold 10 % (v/v) glycerol equal to 1/100th of the initial culture volume. The competent cells were dispensed as 50µl aliquots in pre-chilled 1.5 ml micro-centrifuge tubes and were stored at -80 ^{o}C.

2.3.2 Electroporation

Competent cells were retrieved from -80^{o}C storage and were thawed on ice for 20 min. In parallel, the required DNA was also placed on the ice. The concentration of DNA during electroporation was adjusted according to the nature of the experiment. The DNA and competent cells were mixed gently. The mixture was transferred to the 0.2cm electroporation cuvette (GeneFlow) and electro transformation was completed in the Bio-Rad Gene Pulser system (Bio-Rad) at the following settings: 25 kV/cm, 25 µF and 200 Ω. Immediately after transformation, 950µl of SOC (2.1.3) was added and cells were incubated at 37 ^{o}C for 1 hour before being diluted and plated on appropriate plates. SOC was used as it provided all necessary components for the growth of bacteria that undergo

the stressful electroporation conditions. This method was employed both for the preparation of electrocompetent *E. coli* and *K. pneumoniae.*

2.3.3 Restriction enzyme digestion of DNA

Restriction digestion enzymes were obtained from Promega, NEB and Roche. All the digestions were carried out according to the manufacturer's protocols. Final reaction volume and length of time of digestion was adjusted according to the total mass of DNA and choice of enzyme. The enzymatic reaction was always stopped by heat inactivation as per manufacturer's instructions.

2.3.4 Ligation of DNA

Ligation reactions were performed in a final volume of 10µl containing 3U of T4 DNA ligase (Promega) and 1 - 2µl of 2× ligation buffer. The reaction was incubated overnight at 4 ^{o}C, and subsequently transformed into *E. coli.*

2.4 Other methods

2.4.1 Cell counting

Cell densities were determined by measuring OD600 while culture-ability was assessed by colony forming units (Cfu) counts.

2.4.2 Growth curves

Briefly, single a colony was inoculated into 5ml LB and grown (37^{o}C at 200rpm) until late exponential phase (OD_{600} 0.8). The OD_{600} of culture was then normalized to 0.08 and 150µl aliquots added to wells of a Bioscreen microplate which was then loaded into a Bioscreen plate reader-incubator run with continuous shaking at 37 ^{o}C for 24 hr. The machine was set to measure the optical density at 600nm every 15 or 60 min. Each growth curve experiment was repeated three times. Cfu counting was performed where stated. The data was collected and analysed using GraphPad Prism version 7.0.

In addition, analysis of growth fitness of cells carrying various constructed plasmids were also examined by growth curve analysis. Inducers such as IPTG were added where required.

2.4.3 Conjugation by filter mating

A filter mating method was used for conjugative delivery of ICE-1 marker plasmids from *K. pneumoniae* strains into the recipient strain (*E. coli* HB101) (Lin et al., 2008). A single colony from overnight plate cultures of both donor and recipient were inoculated into separate 5ml of LB with antibiotic selection (30µg/ml chloramphenicol for *K. pneumoniae* bearing ICE-1 marker plasmid and 50µg/ml streptomycin for *E. coli* HB101) and grown overnight. A 1:100 dilution of both cultures were then inoculated into 5 ml fresh LB and grown to exponential phase (~4 hr for *K. pneumoniae* and ~4.5 hr for *E. coli*). The cells in 1 ml of each culture were then harvested by centrifugation (8000 x *g* for 5 min) and before mixing, the pellets were washed twice with PBS to remove remaining antibiotic and re-suspended in 200µl of phosphate buffer saline (PBS). Cfu/ml counts were optimised for donor and recipient by trial and error and 10:1 donor: recipient ratio was found to be satisfactory for mixing.

The mixed bacterial suspension was then spotted onto the centre of 0.22µm pore size membrane filter (Thermo Fisher) placed on LA. The spot was allowed to dry and the preparation incubated overnight at 37 ^{o}C. The filter paper was washed in 1ml PBS to detach the bacterial cells. The transconjugants were selected on LA supplemented with both chloramphenicol and streptomycin, or as otherwise stated, from the neat suspension. Serial dilutions up to 10^{-6} were performed for the donor and recipient Cfu/ml counts. Plates were incubated overnight at 37^{o}C. The efficiency of transconjugation was calculated using following formulas.

$$\text{Efficiency of transconjugation} = \frac{\text{nTransconjugants}}{nRecipient\ Recovered}\left(\frac{\text{Cfu}}{\text{ml}}\right)$$

$$\%\text{Efficiency of transconjugation} = \frac{\text{nTransconjugants}}{nRecipient\ Recovered}\left(\frac{\text{Cfu}}{\text{ml}}\right) \times 100$$

PCR was used to confirm presence of the ICE-1 marker plasmid using plasmid-specific primers and also recipient were confirmed to be *E. coli* by using primers specific to *E. coli* genome.

2.5 Bioinformatic methods

2.5.1 Bioinformatics tools

Bioinformatics tools used in this study are in listed in Table 2-7.

Table 2-7 List of bioinformatic tools used in this study.

Name	Function	Reference
BLASTn	Searches DNA databases for similar DNA sequences	(Altschul et al., 1997)
BLASTp	Search protein databases for similar sequences	(Altschul et al., 1997)
COBALT	computes a multiple protein sequence alignment using conserved domain and local sequence similarity information	(Papadopoulos and Agarwala, 2007)
STRING	Performed protein-protein interactions	
PHYRE2	Automatic fold recognition server for predicting the structure and/or function of protein sequence	(http://string-db.org/)
RAST	Used for putative annotation of unknown gene	(Aziz et al., 2008)
ORF Finder	Identifies open reading frames (**ORFs)** using the standard or alternative genetic codes	(https://www.ncbi.nlm.nih.gov/orffinder/)
Pfam	It is database of protein families that includes their annotations and multiple sequence alignments generated using hidden Markov models.	(Finn et al., 2014)
BPROM	Identifies the bacterial promoter regions and transcription initiation sites.	(http://linux1.softberry.com/berry.html)
Clustal-Omega	Multiple sequence Alignment tool	(Larkin et al., 2007)
Primer-BLAST	A tool for finding specific primers to the PCR template	(Altschul et al., 1997)
ICEberg	web-based resource for integrative and conjugative elements found in Bacteria	(Bi et al., 2012)
SecReT4	Type IV Secretion system Resource	(Bi et al., 2013)
NEB-Cutter	Online tool to identify enzyme restriction sites in nucleotide sequences	(Vincze, 2003)
In-silico PCR	Online program to perform in-silico PCR	(Bikandi et al., 2004)
Primer3 plus	Primer design	(Steve Rozen and Skaletsky, 2000)
OligoCalc	Oligonucleotide analysis	(Kibbe, 2007)
ApE	used for assembly of sequencing traces, virtual digests, sequence annotation, and schematic sequence representation	biologylabs.utah.edu/jorgensen/wayned/ape

2.5.2 Plasmid maps and in-silico construction of DNA fragments

Plasmid and genome maps were visualized and constructed using Snapgene, APE, and pDRAW32.

2.6 Media, reagents and solutions

All media and reagents were obtained from Sigma and Thermo-Fisher unless otherwise stated.

2.6.1 Brain Heart Infusion (BHI) broth plus 30 % glycerol

47 g of brain heart infusion broth powder (Oxoid) was dissolved in a final volume of 1 litre of deionised distilled water (ddH_2O) containing 30 % (v/v) glycerol. Media was autoclaved before use. This medium was used for storage of bacterial stocks at -20 and -80°C.

2.6.2 Luria Bertani (LB) and Agar (LA)

Luria Bertani is one of the standard liquid (LB) and solid growth (LA) medium for bacterial growth. LB was prepared by dissolving 4 g of tryptone, 2 g of yeast extract and 2 g of NaCl in ddH_2O to a final volume of 400 ml. Whereas, LA was prepared as for LB with 1.5 % (w/v) of agar, it was always autoclaved at 121^oC for 15 min.

2.6.3 Super optimal broth with Catabolite repression (SOC)

SOC was prepared by dissolving 5 g of tryptone, 2.5 g of yeast extract and 5 g of NaCl into 200 ml of ddH_2O. After autoclaving, 50 µl of 2 M $MgCl_2$ (filter sterilized) and 200 µl of 1M glucose (filter sterilized) were added to 1 ml of medium. SOC was used for non-selective growth of bacteria post-transformation.

2.6.4 Tris-acetate-EDTA (TAE) buffer (PH 8.3)

2 M Tris-HCl

2 M Acetic acid

50 mM EDTA

2.6.5 Normal Saline

9 g NaCl (154 mM final; 0.9% w/v)

Distilled water to 1 litre. Filter sterilised/autoclaved

2.6.6 Trace Metal Mix

Composition /per litre (sterile solution) to make 1000X

H_3BO_3 2860mg

$MnCl_2 \times 4H_2O$ (1810mg)

$ZnSO_4 \times 7H_2O$ (222mg)

$Na_2MoO_4 \times 2H_2O$ (390mg)

$CuSO_4 \times 5H_2O$ (79mg)

$Co(NO_3)_2 \times 6H_2O$ (49mg)

1 ml of Trace metal mix was added to M9 minimal medium.

Chapter 3 Characterisation and Occurrence of ICEs in *K. pneumoniae* HS11286

3.1 Introduction

Genomic diversity of bacteria is affected by changes in uniformity of the coding and noncoding regions of bacterial genome. A major cause of this diversity is the acquisition of mobile genetic elements (MGEs), such as plasmids, transposons, and GIs (Arber., 2000, Roy, 1999). Comparative mapping and sequence analysis within species has revealed an abundance and variety of genomic islands acquired by HGT in many species of *Proteobacteria* (Hacker and Kaper, 2000, Hacker., 2000). MGEs can be variable in size ranging from 10- to 200-kb; they may contain genes or clusters of genes related to virulence, antibiotic resistance or niche adaptation. Previous research has documented that ICEs are self-mobilisable DNA fragments as well as being represented in diverse Gram-positive and Gram-negative bacteria (Burrus et al., 2002, Burrus and Waldor, 2004, Lin et al., 2008, Wozniak and Waldor, 2010). Given the focus here on *K. pneumoniae*, as a background to the current project, ICEberg databases and published literature (until 2013) were explored for the information about ICEs present in *Enterobacteriaceae*; these are summarised in Table 3-1. The majority of documented ICEs are generated by site-specific recombination at 3´ends of tRNA-encoding genes and are marked by directly repeated sequences at both ends (Kelly, 2002, Baar et al., 2003, Tuanyok et al., 2008).

The core genome of *K. pneumoniae* is interrupted by multiple MGEs (Zhang et al., 2011). These authors identified eight tRNA gene loci serving as insertion hotspots for GI insertion, nonetheless, very little is known about the prevalence of different ICEs in *K. pneumoniae* strains. The background strain for this study contains two ICEs, ICE-1 and ICE-2 (Chapter 1), integrated at the *asn-tRNA* and *phe-tRNA* sites respectively. In *K. pneumoniae* the *phe-tRNA* and *asn-tRNA* genes were always known to be the *tRNA* genes most frequently occupied by GIs (Aartsen, 2008, Chen et al., 2010). In a recent study 73% of *K. pneumoniae* strains contained at least one GI integrated in the *asn-tRNA* gene (Marcoleta et al., 2016)

Table 3-1 Summary of all different ICEs found in various bacterial species of *Enterobacteriaceae*.

Bacterial Species from diff. genus of *Enterobacteriaceae*	**ICEs**		**Size[b] (~Kbp)**	***Int*[c]**	**Insertion site**	**Possible function of cargo genes[d]**	**Reference**
	Family[a]	**Nomenclature**					
C. koseri ATCC BAA-895	ICEKP-1	ICECkoBAA-1	103	+	*tRNA-asn*	Salicylate synthesis	1
C. rodentium ICC168	NA	ICECroICC168-1	40	NI	*tRNA-leu*	U	2
*E. hormaeche*i05-545	ICEKP-1	HPI-ICEEh1	66	+	*tRNA-asn*	Pathogenicity	3
E. carotovora SCRI1043	NA	HAI2	97	NI	*tRNA-phe*	U	2
E. coli ED1a	ICEKP-1	ICEEcoED1a-1	58	+	*tRNA-asn*	Yersiniabactin^{S}	1
E. coli UMN026	ICEKP-1	ICEEcoUMN026-1	65	+	*tRNA-asn*	Yersiniabactin^{S}	1
E. coli ECOR31	ICEKP-1	ICEEc1	38	NI	*tRNA-asn*	Pathogenicity	4
E. coli BEN374	PKLC102/PAGI-1	ICEEc2	94	+	*tRNA-phe*	U	2,5
E. coli IHE3034	NA	ICEEcIHE3034-1	54	+	*tRNA-asn*	Colibactin	6
E. coli J53	SXT/R391	ICEEcoJ53	PS	NI	*prfC*	U	1
K. pneumoniae 342	NA	ICEKpn342-1	70	+	*tRNA-asn*	Putrescine^{S}, PA^{M}	7
K. pneumoniae NTUH-K2044	ICEKP-1	ICEKp-1	75	+	*tRNA-asn*	U	8,9
K. pneumoniae HS11286	ICEKP-1	ICEKpnHS11286-1	62	+	*tRNA-asn34*	U	1

K. pneumoniae HS11286	NA	ICEKpnHS11286-2	56	+	*tRNA-phe*	U	1
P. mirabilis HI4320	SXT/R391	ICEPmiUSA1	80	+	*prfC*	U	10,11
P. mirabilis HI4320	NA	ICEPm1	92	+	*tRNA-phe*	Proteus toxic agglutinin	10, 11
P. mirabilis TUM4660	SXT/R391	ICEPmiJpn1	PS	+	*prfC*	Beta lactam	13
P. mirabilis	SXT/R391	R997	85	+	*prfC*	Amp^R, $Strep^R$ $Sulf^R$	14
P. vulgaris	SXT/R391	R705	PS	+	*prfC*	Kan^R, $Mercury^R$	15
P. vulgaris	SXT/R391	R706	PS	NI	*prfC*	Kan^R, $Mercury^R$	15
D. zeae Ech1591	ICEKP-1	ICEDzeEch1591-1	53	+	*tRNA-asn*	U	1
D. dadantii Ech586	ICEKP-1	ICEDdaEch586-1	51	+	*tRNA-asn*	U	1
D. dadantii 3937	NA	ICEDda3937-1	74	+	*tRNA-asn*	U	1
P. luminescens TTO1	NA	ICEPluTTO1-1	141	NI	*tRNA-phe*	U	2
S. Typhi CT18	SPI-7	SPI-7	133	+	*tRNA-phe*	Pathogenicity	2
S. Typhi Ty2	SPI-7	ICESenTy2-1	131	+	*tRNA-phe*	U	1
S. enterica 5494-57	NA	C*Tn*scr94	126	+	*tRNA-phe*	$Sucrose^M$	16
S. bongori CEIM46082	SPI-7	ICESb1	109	+	*tRNA-phe*	U	2
S. bongori 2022/77	SPI-7	ICESb2	101	+	*tRNA-phe*	U	16
S. enterica SARC16	NA	ICESe3	104	+	*tRNA-phe*	U	16
S. enterica RKS4594	SPI-7	SPI-7RKS4594	81	NI	*tRNA-phe*	Pathogenicity	2

S. enterica 1662K	SPI-7	SPI-71662K	86	NI	*tRNA-phe*	Pathogenicity	2
S. enterica 18	NA	ICESe4	96	NI	*tRNA-phe*	U	2
Y. enterocolitica 8081	ICEYe1	YAPI(ye)	66	+	*tRNA-phe*	TA & Arsenic^{R}	2,17
Y. pseudotuberculosis IP 31758	ICEYe1	YAPI(IP31758)	64	+	*tRNA-phe*	Pathogenicity	2,18
Y. enterocolitica Y69	ICEYe1	ICEYe1	120	+	*tRNA-phe*	U	2
Y. pseudotuberculosis 32777	ICEYe1	YAPI	98	+	*tRNA-phe*	Pathogenicity	2,19

a: NA = Not assigned; **b:** PS = partially sequence; **c:** NI = not identified, *prfC* = protein releasing factor C, **d:** U = unknown, , Amp = ampicillin, Strep = streptomycin, Sulfa = sulfamethoxazole, Kan = Kanamycin, S=synthesis, R= resistance, M = metabolism, PA= polyamines, TA = toxin-antitoxin system
[1](Bi et al., 2012), [2](Seth et al., 2012), [3](Paauw et al., 2010), [4](Burrus and Waldor, 2004), [5](Roche et al., 2010), [6](Putze et al., 2009), [7](Zhang et al., 2011), [8](Wu et al., 2009, Lin et al., 2008), [10](Flannery et al., 2009, Flannery et al., 2011), [12](Mata et al., 2011), [13](Harada et al., 2010), [14](Daccord et al., 2012), [15](McGrath et al., 2005 & 2004), [16](Moreno et al., 2012), [17](Thomson et al., 2006), [18](Seth et al., 2012, Eppinger et al., 2007), [19](Collyn et al., 2004)

The ICEKP-1 associated element was first identified in uropathogenic *E. coli* strain ECOR31 (Schubert et al., 2004) and later on in *K. pneumoniae* strain NTUH-K2044 isolated from primary liver abscess (Lin et al., 2008). Both occurrences were integrated downstream of *tRNA-asn*. ICEKp-1 is divided into 3 regions: a region homologous to the High pathogenicity island (HPI) of *Yersinia pestis* (Schubert et al., 2000), a region with similarities to pLVPK plasmid of *K. pneumoniae* strain CG43 (Chen et al., 2004) and finally a region containing the genes responsible for conjugation (Lin et al., 2008).

An ICE identified in *E. coli* BEN374 classified in the PKLC102/PAGI-1 family is of particular interest (Roche et al., 2010). *Clc* was the first element recognized in this family and was detected in *Pseudomonas* sp. B13 (Reineke et al., 1982). The family includes several other elements including PAGI-1, PAGI-2, pKCL102 present in various *Pseudomonas* strains (van der Meer and Sentchilo, 2003, Klockgether et al., 2004). Subsequently, Bi and colleagues (Bi et al., 2012) classified all these elements and several other related elements into one family named PAPI. Elements from this family share a homologous set of core genes (Mohd et al., 2004) and all are integrated at the 3' end of tRNA genes (Larbig et al., 2002, van der Meer and Sentchilo, 2003). Transfer of these elements involved an integrase and a Type 4 pilus (Ravatn et al., 1998a, Ravatn et al., 1998b, Qiu et al., 2006, Juhas et al., 2007a).

3.1.1 Overall Aim

This section is focused on the characteristics and annotation of ICE-1 and ICE-2 of *K. pneumoniae* HS11286 and their prevalence in 40 local clinical isolates. The following objectives were set.

3.1.2 Objective

1. To characterise the previously uncharacterised components of both ICEs by bioinformatic analysis.
2. To classify ICE-2 into an appropriate ICEs family based on sequence homology.
3. To investigate the occurrence of these two elements in a group of 40 local isolates of *K. pneumoniae.*
4. To study the structural variation between the known ICEs and novel ICEs identified in clinical isolates.

3.2 Methods

3.2.1 Overview of bioinformatics analysis.

Several bioinformatics tools were comparative and functional analysis of both ICEs (Figure 3-1).

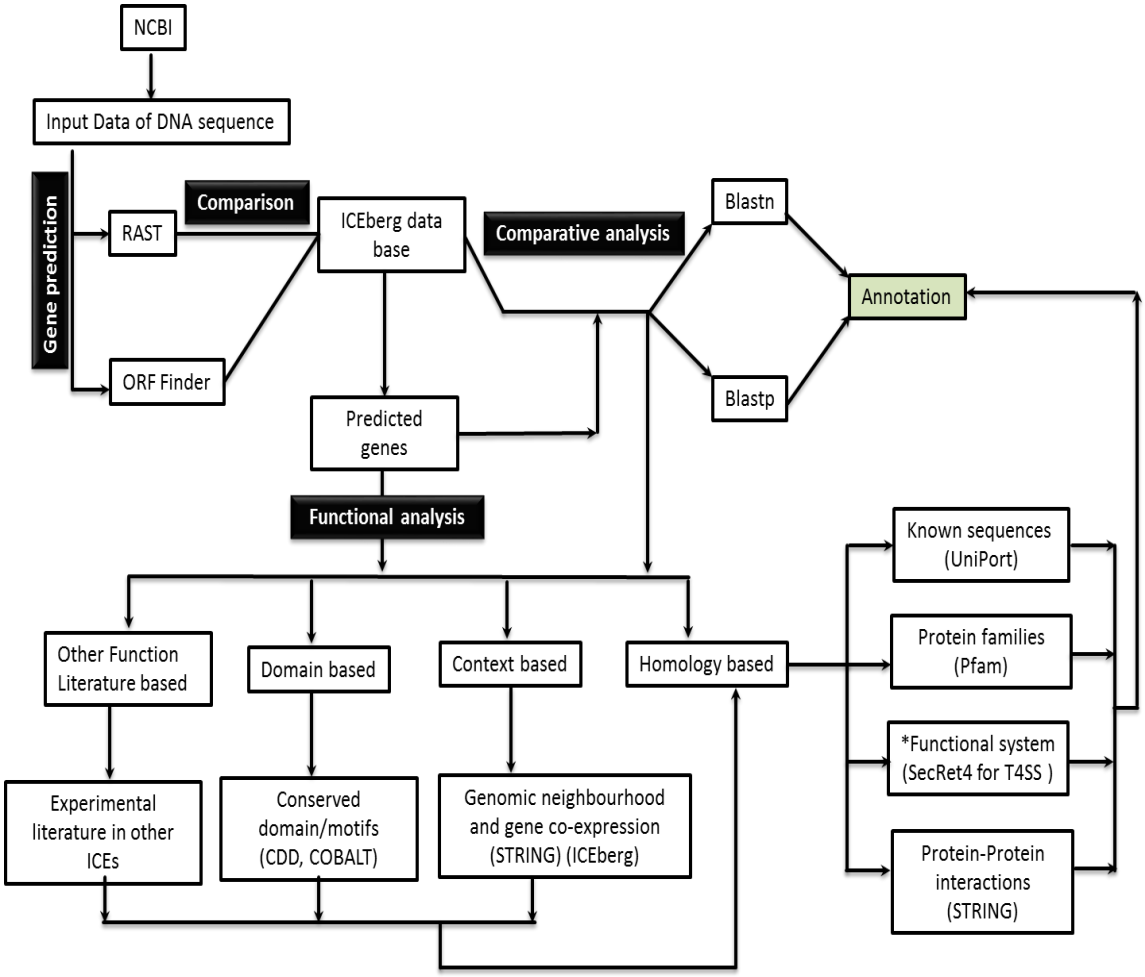

Figure 3-1 Flowchart of bioinformatics analysis.
Various bioinformatics tools were used for gene predictions, comparative and functional analysis of ICE-1 and ICE-2 content.

3.2.2 PCR analysis

Standard PCR methods are explained in section 2.2.3.3.

3.2.3 PCR for the determination of locus of insertion of ICE

3.2.3.1 Principle

The insertion of new genes in host genome was investigated using *t*RIP (*tRNA* site interrogation for pathogenicity islands, prophages and other GIs), which is a quick PCR

based screening method (Chen et al., 2010, Ou et al., 2006). *tR*IP is a PCR strategy, where negative PCR results indicates 3' located GI end in the *tRNA* gene (Figure 3-2). GIs usually carry one copy of the DR that corresponds to the sequence of the 3 terminus of the target gene. The primers **F** and **R** produce negative PCR (no amplification) results when a large integrated element is present.

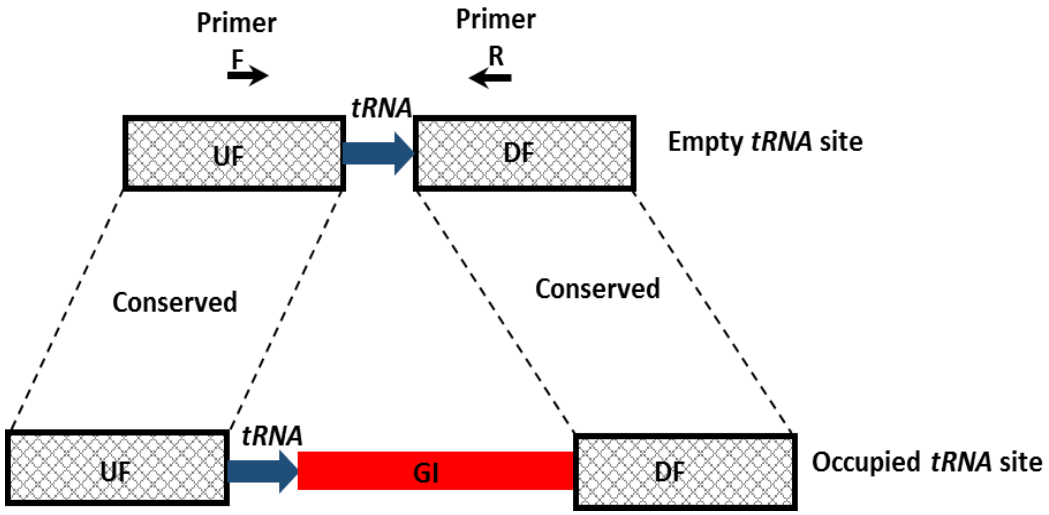

Figure 3-2 Schematics of principle of tRIP PCR.
Upstream and downstream region of the tRNA are indicated by UF and DF respectively. Red rectangle represents integration of genomic island (GI) at the 3´ end of tRNA.

3.2.3.2 Primer design for tRIP

Multiple sequence alignment of ~2kb flanking regions (upstream and downstream) of the target gene were performed using Clustal-Omega. Conserved upstream (primer F) and downstream (primer R) sequences were selected as primers pairs for each locus. The primers sequences were checked for hairpin and primer dimer formation using OligoCalc. *K. pneumoniae* strains MGH78578, HS11286 and NTUH were used as reference for primer design.

3.2.3.3 PCR cycling condition

The cycling conditions were based on primers used during screening of: Initial denaturation at 95°C for 2 min, followed by 30 cycles of denaturation at 95°C for 30 sec, annealing at T°C for 30 sec, extension at 72°C (time was depended on the length of the empty site) and final extension for 10 min at 72°C. Reference strains NTUH K2044 and HS11286 and MGH78578 were used as a control for the PCR screening.

3.2.4 PCR mapping

A total of 42 local *K. pneumoniae* strains (Table 2-1) were screened for the occurrence of ICE-1 and ICE-2 related elements using PCR. The ICE-1 and ICE-2 sequence of *K. pneumoniae* HS11286 were used as a template for PCR based mapping to understand strain to strain variation in the arrangement of these elements. Primers with overlapping regions were designed to better understand the physical linkage in these elements. Primers used for ICEs mapping are enlisted in Appendix I and II.

3.3 Results

3.3.1 Synteny of genetic context and characterisation of ICE-1

Whole genome sequencing of *K. pneumoniae* HS11286 demonstrated the presence of two ICEs (ICE-1 and ICE-2) (Liu et al., 2012). In order to investigate the synteny and conservation of ICE-1 with other reported ICEs, the nucleotide sequence of ICE-1 were compared with ICEKp1 (~76 kb; 52 % GC content)(Lin et al., 2012). These ICEs were found adjacent to the *asn* (asparagine) *tRNA* gene and were flanked by 17-bp (100 % identical) directly repeated sequences. The average GC content of the *K. pneumoniae* HS11286 chromosome was 57.5 % compared to 52.5% in the ~62kb ICE-1 fragment, evidence for acquisition of the latter by horizontal gene transfer. ICE-1 was found to be structurally similar to ICEKp1 and ICEEc1 of *E. coli* ECOR31 (Schubert et al., 2004, Lin et al., 2012). The comparison of ICE-1 with ICEKp1 in Figure 3-3 demonstrates two regions of homology in the former. The first, adjacent to the asn-tRNA gene, shows 99 % identity to the gene cluster found in ICEKp-1 of NTUH-K2044 and is closely related to the *Yersinia* high pathogenicity island (Lin et al., 2008, Lawlor et al., 2007). This view is reinforced by the 99 % of identity of this region to the operon encoding yersiniabactin and a phage-integrase in multiple *Yersinia* strains. The second region comprises a gene cluster (~16-kb) with 94% identity to its homologue in ICEKp1 and is associated with DNA mobilisation and mating pair formation in ICEKp1 and in ICEEc1 (Schubert et al., 2004, Lin et al., 2012). This region includes genes encoding a probable type IV secretion system (T4SS) related to virB1/VirD4 (Eric et al., 2013).

Apart from the two major regions of homology, 9 hypothetical (H) genes were also found scattered in ICE-1. Among 9 H genes, 3 are downstream of the HPI cluster and 6 were present at the 3´ end of the element (Figure 3-3). Based on the evidence that ICEs carry different sets of cargo genes (Wozniak and Waldor, 2010), attempts were made to characterise these hypothetical genes in ICE-1 to assess their possible role in *K. pneumoniae* HS11286 biology. Sequence analysis was performed with Blastn, Blastp and with Pfam. The results are summarised in Table 3-2. Genes downstream to HPI were highly conserved and uncharacterised in multiple species of *Enterobacteriaceae.* They were usually close to 3´-end of HPI, indicating the possible linkage to other HPI genes. Comparative analysis of KPHS_34900 and KPHS_34910 revealed their 99 and 100 %

identical to restriction endonucleases and the KPHS_34930 and KPHS_34950 showed similarities to ATPase (AAA domain protein) encoding genes.

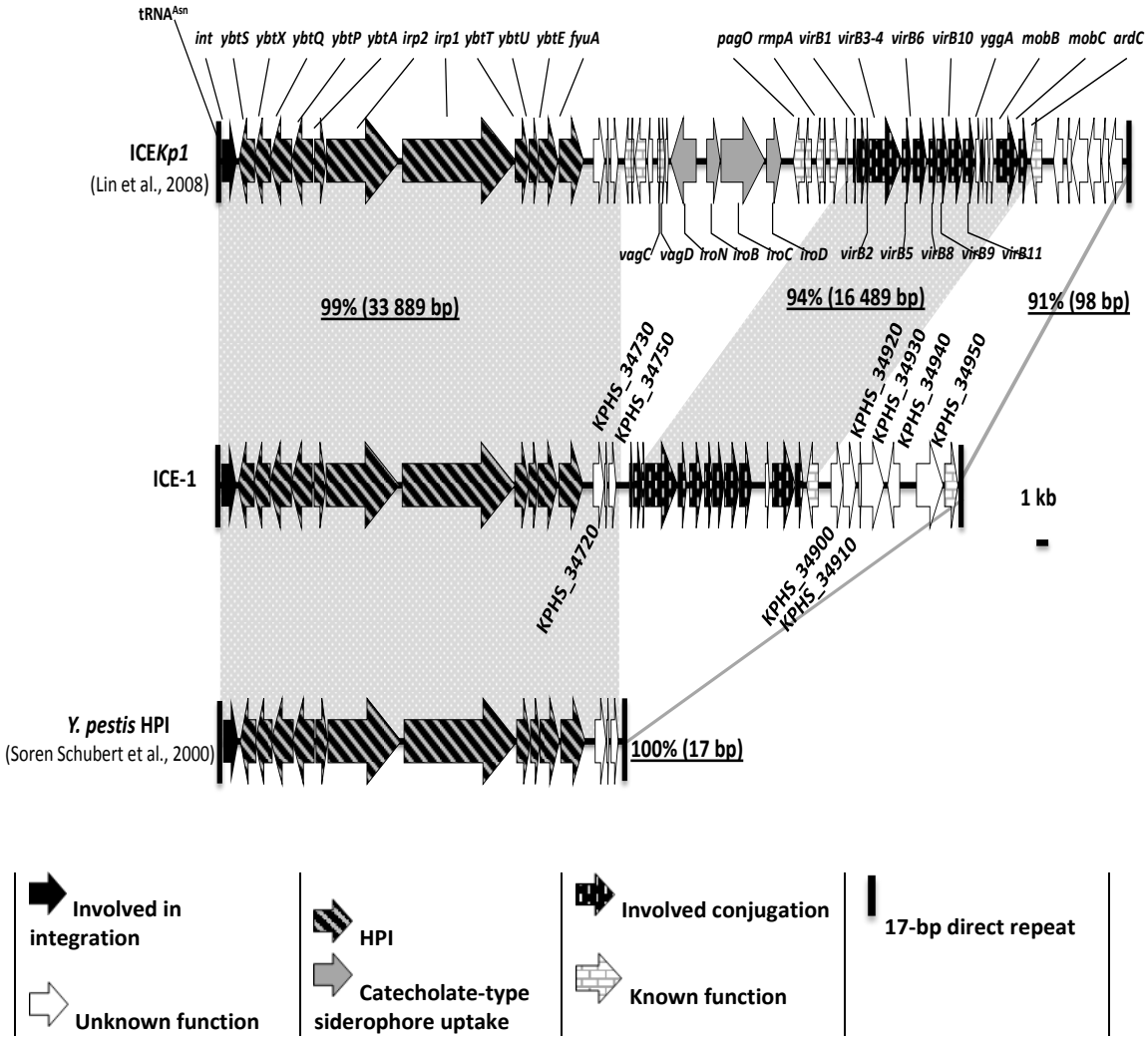

Figure 3-3 Genetic contexts of the conserved regions of ICE-1 of *K. pneumoniae* HS11286.
The syntenic regions of the ICEKp1 (AB298504), ICE1 and HPI (AF091251) of *Yersinia pestis* are indicated by grey shading (99 % of DNA sequence identity). The genes responsible for conjugation are indicated, theses share 94% identity. HPI stands for High Pathogenicity Island. The schematics are drawn to scale.

Table 3-2 Analysis of hypothetical genes in ICE-1.

No	ORFs[a] Designation	aa[b] residues	Protein GI[c]	Homologous Protein	Source	% identity of aa[d]	Accession no
1	KPHS_34720	308	364519042	Uncharacterised protein	*K. pneumoniae*	100	SAX82063.1
2	KPHS_34730	399	364519044	hypothetical protein	Multispecies *Entrobacterales*	100	WP_000937857.1
3	KPHS_34750	77	364519045	hypothetical protein	Multispecies *Entrobacterales*	100	WP_001231171.1
4	KPHS_34900	331	364519060	Restriction endonuclease	*K. pneumoniae*	99	KXA87112.1
5	KPHS_34910	362	364519061	Restriction endonuclease-1	*E. coli* UMN026	100	YP_002413022.1
6	KPHS_34920	84	364519062	Threonine transporter	*K. variicola*	98	WP_049156918.1
7	KPHS_34930	626	364519063	ATPase (DNA repair)	*E. coli* SCD2	100	ESA25964.1
8	KPHS_34940	339	364519064	DUF4917 protein	*Yersinia intermedia*	96	CRY76049.1
9	KPHS_34950	748	364519065	AAA domain protein	*E. coli* 2-156-04_S4_C1	100	KDW22106.1`

a Nucleotide position in the GenBank accession no. CP003200 sequences.

b Amino acids

c Gene identification number of query protein sequences

d Determined by BLAST-P analysis * Amino acids

3.3.2 Comparative analysis of ICE-2

The nucleotide sequence of ICE-2 (50.2 GC %) was first analysed for coding sequences using RAST and ORF finder (Aziz et al., 2008). A total of 64 CDS were identified, 3 among 64 were neglected as the coding indicates a polypeptide of less than 30 amino acids with no conserved domains. The schematics of remaining of 61 ORFs are presented in Figure 3-4 and listed in Table 3-3.

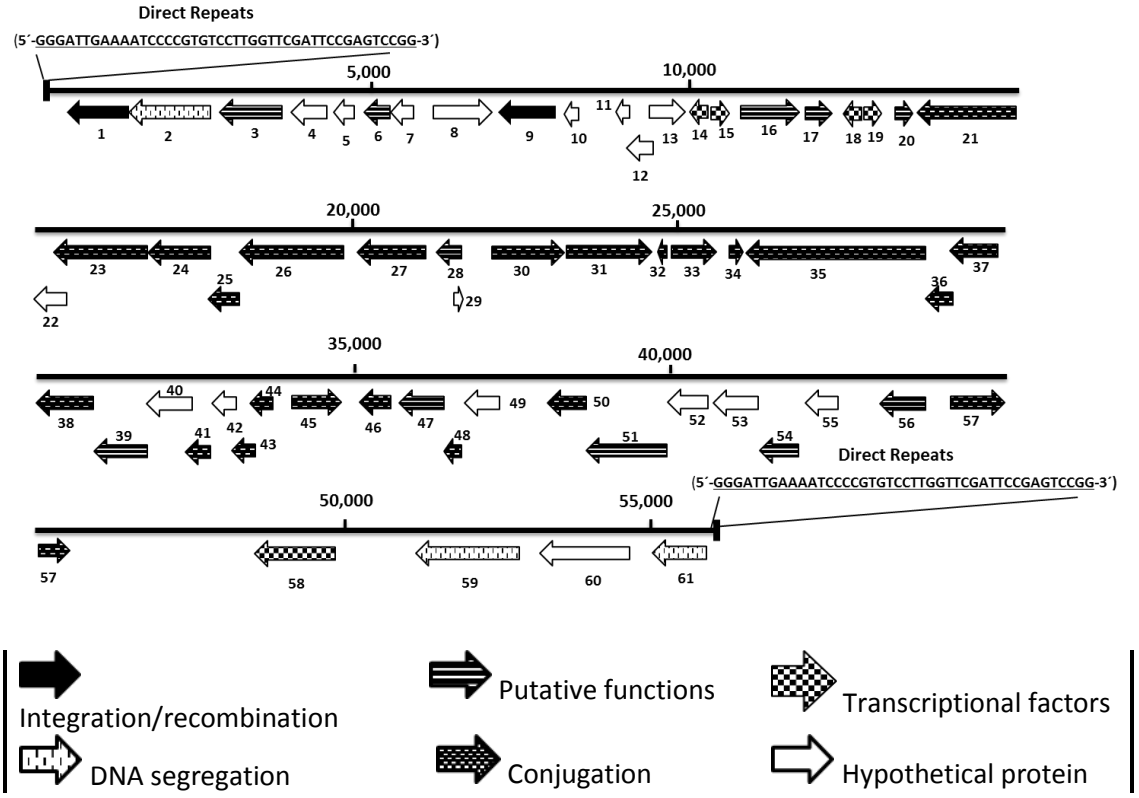

Figure 3-4 Genetic organisation of ICE-2 of *K. pneumoniae* HS11286.
Predicted open reading frames (ORFs) are shaded in similar pattern according to their putative functions. The ORFs numbers are cross reference to Table 3-3.

Amino acid sequences were used to compare the ORFs for their putative functions. ICE-2 fragment was divided in to 3 regions (Figure 3-5). 1) Integration and segregation including an integrase (ORF 1), a putative homologue of relaxase of PFGI-1 class (ORF 2), a DNA binding protein ParB (ORF 58), a putative DNA helicase (ORF 59) and chromosomal partitioning protein ParA (ORF 61). 2) DNA mobilisation via conjugation. This region showed >85% identity to the *PFGI-1* of *P. fluorescens* Pf-5 conjugation system (Mavrodi et al., 2009). 3) The remaining 28 cargo genes included 17 conserved hypothetical while the rest showed homology to proteins having some putative functions (Table 3-3).

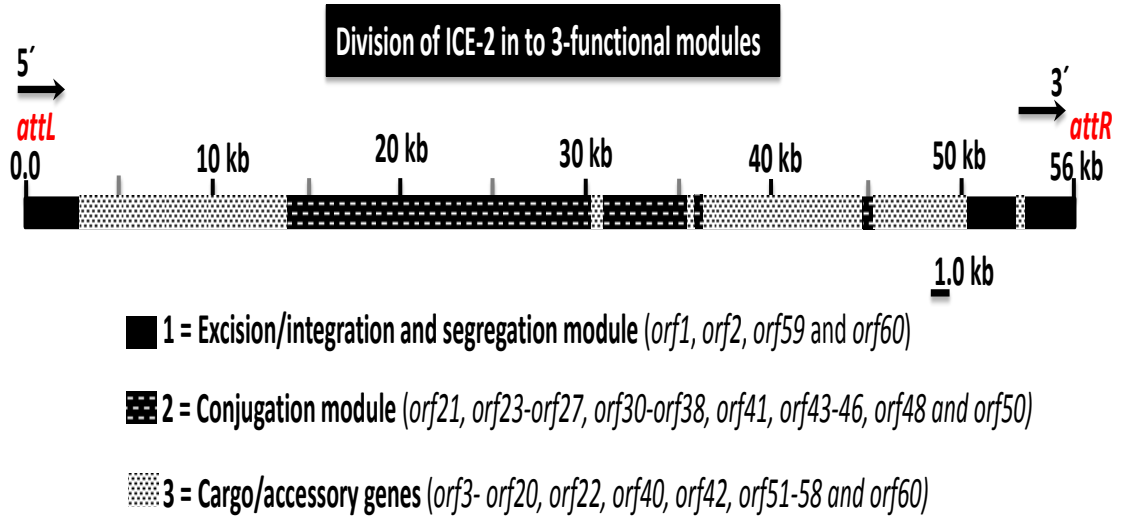

Figure 3-5 Categorisation of ICE-2 components in to various modules.
ICE-2 components were categorised into 3 regions based on their putative functions.

From the results it was clear that the majority of the backbone contents of ICE-2 resembled PFGI-1 of the *P. fluorescens* Pf-5, such as gene cluster responsible for DNA mobilisation, DNA segregation, relaxase, helicase. These shared homology and belonged to the same PFL family. Based on high level of similarities this study classified ICE-2 in PAPI family (Figure 3-6)

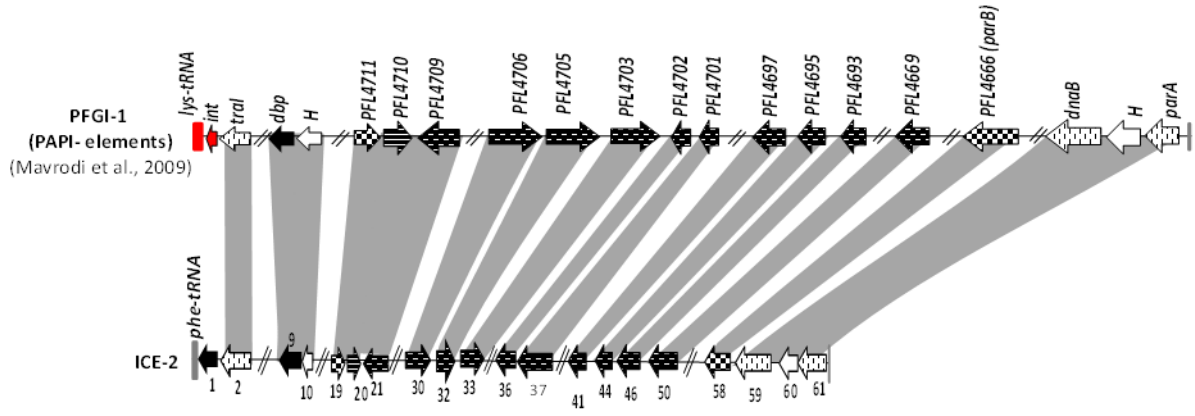

Figure 3-6 Synteny between PFGI-1 of PAPI elements and ICE-2.
The gray shading represents similarities between the two elements.

Table 3-3 In silico characterisation and summary of ORFs found in ICE-2.

ORFs[a]		Strand[b]	Aa[c] residues	Homologous Protein/Possible Function[d]	Source	% identity of aa[f]	Accession no
No	**Designation**						
1	ORF1	-	315	DNA integration/recombination	*K. pneumoniae* 30684	100	AHM77645.1
2	ORF2	-	429	Relaxase, PFGI-1 class	*K. pneumoniae* UCICRE 8	99	ESL95504.1
3	ORF3	-	327	ArdC	*K. pneumoniae*Q3	99	EKF77242.1
4	ORF4	-	202	Hypothetical	*K. pneumoniae*[e]	100	WP_004151763.1
5	ORF5	-	115	Hypothetical	*K. pneumoniae*	100	WP_004151762.1
6	ORF6	-	132	ArdB	*K. oxytoca*	98	SBL38293.1
7	ORF7	-	92	Hypothetical	*Klebsiella* spp.	99	WP_016809387.1
8	ORF8	+	317	Hypothetical	*K. pneumoniae*	100	WP_004151759.1
9	ORF9	-	297	Integrase	*K. pneumoniae K. pneumoniae*Q3	99	EKF77241.1
10	ORF10	-	92	Xre Family TF	*S. enterica*	86	GAS79470.1
11	ORF11	+	86	Ner like TF	*K. oxytoca*	93	WP_016809394.1
12	ORF12	+	307	IS903 Transposase	*Enterobacteria* phage HK022	99	AAF30382.1

13	ORF13	+	154	Cold shock protein	*K. pneumoniae* 306601	100	AHM83223.1
14	ORF14	-	81	Xre Family TF	*K. oxytoca*	96	SBL38079.1
15	ORF15	+	83	Nlp TF	*K. pneumoniae* KPNIH4	83	EJJ32891.1
16	ORF16	+	99	Hypothetical	*Klebsiella* spp.	100	EOR16801.1
17	ORF17	-	509	TraG	*K. oxytoca*	99	WP_016809399.1
18	ORF18	-	113	HP A9L51_14115	*K. pneumoniae*	95	WP_040236211.1
19	ORF19	-	473	ICE protein, PFL_4711	*K. pneumoniae* UHKPC23	100	EOR16806.1
20	ORF20	-	313	ICE protein, PFL_4710	*K. pneumoniae* UHKPC23	100	EOR16796.1
21	ORF21	-	131	ICE protein, PFL_4709 family	*K. pneumoniae* UHKPC23	100	EOR16813.1
22	ORF22	-	532	HP H207_0366	*K. pneumoniae* UHKPC40	100	EOY67835.1
23	ORF23	-	336	secA Preprotein Translocase	*K. pneumoniae* 30684	100	AHM77621.1
24	ORF24	-	143	Toxin SymE	*K. pneumoniae* VA360	100	EMI36389.1

25	ORF25	+	371	HP SK89_04460	*K. oxytoca*	99	KLY12101.1
26	ORF26	+	455	Glycosaminoglycan attachment protein	*K. pneumoniae* IS43	93	CDL12588.1
27	ORF27	-	44	Hypothetical	*Klebsiella* spp.	100	WP_004217757.1
28	ORF28	-	234	Restriction endonuclease	*K. pneumoniae* KPNIH23	100	EJK38858.1
29	ORF29	+	59	Hypothetical	*Klebsiella* spp.	100	WP_004198954.1
30	ORF30	-	924	CT ATPase, PFL_4706	*K. pneumoniae* VAKPC309	98	EOZ52981.1
31	ORF31	-	132	CT protein	*K. pneumoniae*	97	OBT34302.1
32	ORF32	-	494	TrbI-like / PFL_4705	*K. pneumoniae*	98	KTG59771.1
33	ORF33	-	281	PFL_4704/TraK	*K. pneumoniae* UHKPC23	100	EOR14930.1
34	ORF34	-	217	ICE protein, PFL_4703	*K. pneumoniae* UHKPC23	100	EOR14940.1
35	ORF35	-	123	CT region protein, TIGR03750	*K. pneumoniae* UHKPC23	100	EOR14950.1
36	ORF36	-	117	ICE membrane protein, PFL_4702	*K. pneumoniae* UHKPC23	100	EOR14954.1

37	ORF37	-	78	ICE protein, PFL_4701	*K. pneumoniae* UHKPC40	100	EOY67789.1
38	ORF38	-	105	ICE protein	*K. oxytoca*		SBL37582.1
39	ORF39	+	267	Phosphoribosyl transferase	*Y. enterocolitica*	67	CFQ34406.1
40	ORF40	+	158	Hypothetical	*Klebsiella* spp.	100	WP_004150886.1
41	ORF41	-	252	ICE membrane protein PFL_4697	*K. oxytoca*	97	SBL37526.1
42	ORF42	-	87	Conserved Hypothetical protein	*Klebsiella spp*.	93	WP_004150888.1
43	ORF43	-	699	conjugative coupling factor TraD, PFGI-1 class	*K. pneumoniae* UHKPC01	100	EOY73211.1
44	ORF44	-	170	ICE protein, PFL_4695	*K. pneumoniae* VA360	100	EMI37003.1
45	ORF45	-	189	Lytic murine trans glycosylase	*K. oxytoca*	99	SBL37436.1
46	ORF46	-	205	ICE protein, PFL_4693 family	*K. oxytoca*	98	SBL48986.1
47	ORF47	-	246	Methyl-accepting chemotaxis protein	*K. pneumoniae* IS33	100	CDK93076.1
48	ORF48	-	189	Type IV B pilus protein	*K. oxytoca*	99	SBL37378.1
49	ORF49	-	150	PF12101 family protein	*K. pneumoniae* VAKPC269	100	EOZ31404.1
50	ORF50	-	240	ICE protein, PFL_4669 family	*K. pneumoniae* UHKPC23	100	EOR14922.1

51	ORF51	+	354	TR, AbiEi antitoxin	*Klebsiella* spp.	100	WP_004150897.1
52	ORF52	+	290	Hypothetical	*Klebsiella* spp.	100	WP_004150898.1
53	ORF53	-	251	Hypothetical L478_05391	*K. pneumoniae* BIDMC 41	99	ESL15922.1
54	ORF54	-	442	WG repeat motif protein	*K. pneumoniae* UHKPC32	100	EPB38748.1
55	ORF55	+	291	Hypothetical	*Klebsiella* spp.	100	WP_004150901.1
56	ORF56	-	405	HTH / PFGI-1-like cluster	*K. pneumoniae*Kb677	100	EYB74595.1
57	ORF57	-	194	HP in PFGI-1-like cluster	*E. coli* ISC56	100	CDL57295.1
58	ORF58	-	540	Transcriptional regulator/ParB family protein	*K. oxytoca*	94	SBL37243.1
59	ORF59	-	455	Replicative DNA helicase	*K. pneumoniae* UCICRE 8	99	ESL95559.1
60	ORF60	-	128	Hypothetical	*Klebsiella* spp.	100	WP_004150906.1
61	ORF61	-	290	Chromosome-partitioning ATPase/ParA	*K. pneumoniae*	99	OBT34275.1

a: ORF number based on its position in ICE-2. **b:** Orientation of genes, **c:** Amino acids

d: ArdC = Antirestriction protein C, ArdB = Antirestriction protein B, TF = Transcriptional factor, CT = Conjugal Transfer, HTH = Helix turn helix domain

e: *K. pneumoniae* indicates that identical sequence was present in multiple strains**, f:** Determined by BLAST-P analysis.

3.3.3 Occurrence of both ICE-1 and ICE-2 in clinical isolates

3.3.3.1 Universal primers for the detection of integrase gene associated to ICEs in clinical isolates of *K. pneumoniae*

The first step was to screen for integrase genes. Therefore, nucleotide sequences of both *int* genes were blasted against other sequenced *K. pneumoniae* strains. Variation has been observed in the ICEKP-1 associated integrase genes and this informed the design of subtype-specific primers that could detect integrases from multiple *Enterobacteriaceae*. RF101 and RF102 (Appendix I) were designed (~0.24-kbp of product size) from the most conserved regions from the aligned sequences of integrase from various *Enterobacteriaceae* carrying ICEKP-1 elements (Figure 3-7). In addition, the *int-α* of ICE-2 was found to be 98 to 100 % identical that in many other *K. pneumoniae* strains. Therefore, primers RF154 and RF155 (Appendix II) were designed taking *int-α* as a reference sequence. The specificity of the primers were checked using *in silico* PCR test.

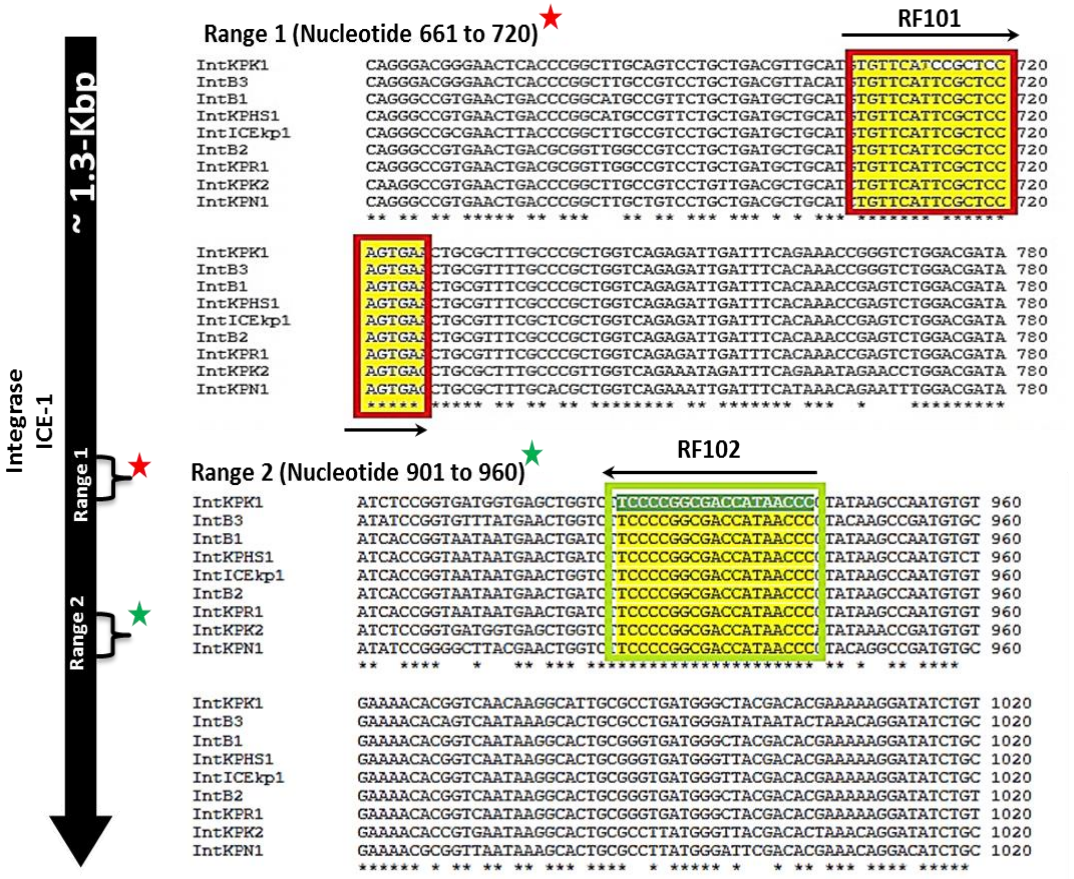

Figure 3-7 Multiple-aligned sequences of integrase genes.
To designed RF101 and RF102 for the detection of ICEKP-1 associated integrase. Integrase is drawn to the scale (0.1-kbp = 1 cm).

3.3.3.2 Occurrence of ICE-1 and ICE-2 in clinical isolates of *K. pneumoniae*

To investigate the occurrence of ICE-1 in clinical isolates, potential marker regions in this element were compared with the previously reported ICEKP-1 elements (Figure 3-8A). Based on the syntenic conservation and also considering previously published literature (Schubert et al., 2004, Lin et al., 2008, Schubert et al., 2000) i*nt, irp, fyuA* and *virB1* were selected for PCR screening of related elements. Primers for PCR screening of these marker genes were designed taking ICE-1 as a reference sequence.

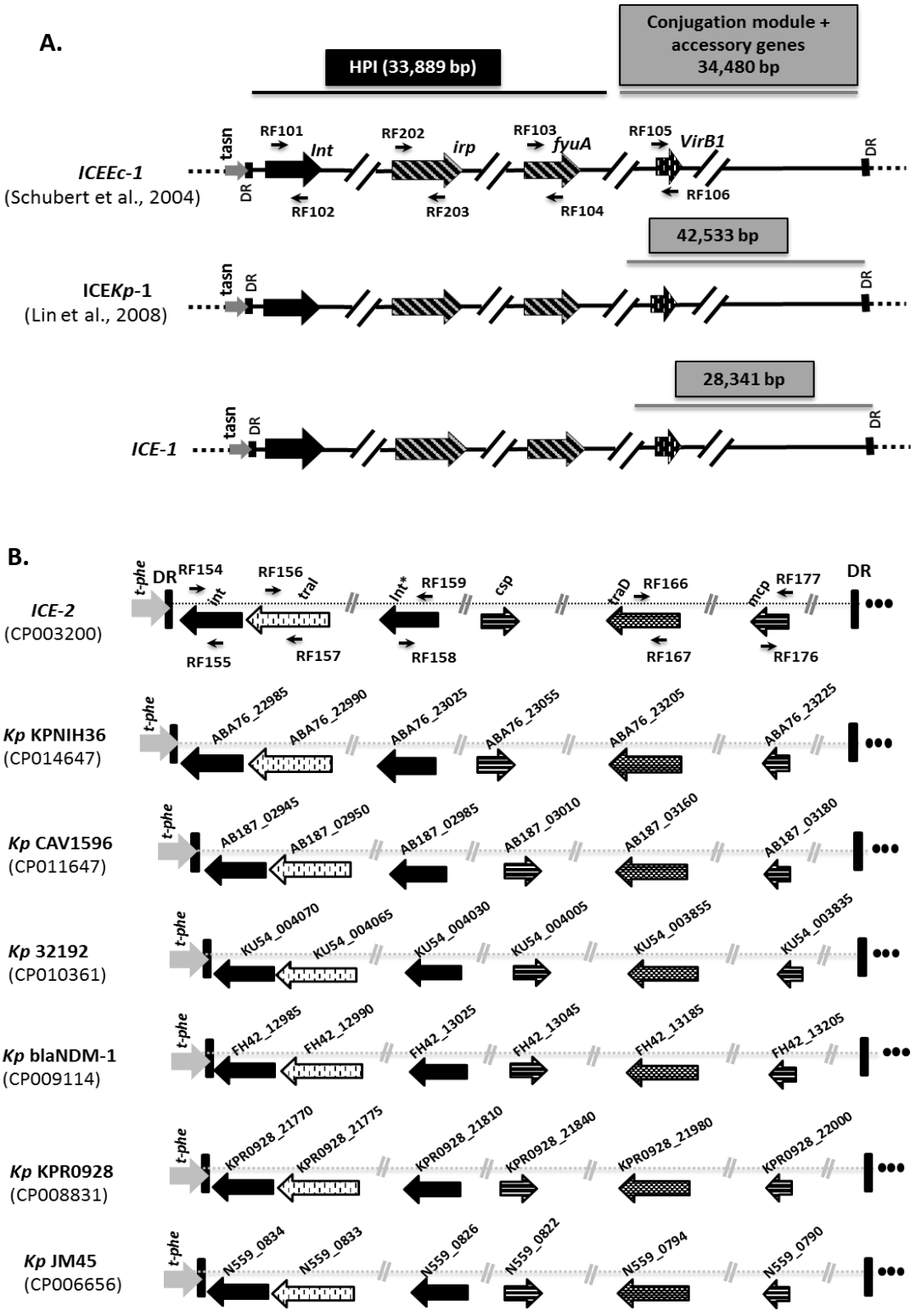

Figure 3-8 Schematics of marker regions of ICE-1 and ICE-2.

A. Composition of ICE-1. Four genes, *int* (integrase), *irp* (iron regulatory protein), *fyuA* (ferric yersiniabactin uptake) and *virB1* (T4SSs), were chosen for screening ICE-1. **B**. Comparison of ICE-2 associated elements of 6 different *K. pneumoniae* strains with strain HS11286). Small black arrows above and below the ICEs (both in A & B) represents primers used for the PCR screenings.

The presence of ICE-2 related elements has been only documented in *E. coli* BEN374 (Roche et al., 2010) but their co-occurrence with ICE-1 has not been documented in *Enterobacteriaceae*. To investigate this, comparative sequence analysis of ICE-2 was executed in multiple sequenced *K. pneumoniae* strains. Likely homologues of ICE-2 associated elements were found integrated at *phe-tRNA* sites in many strains. The newly identified ICEs were interrogated for key elements including integration/conjugation modules and DR sequences both at *attL* (left) *attR* (right) sites. Based on high homology and synteny, six strains, *K. pneumoniae* KPNIH36 (CP014647), *K. pneumoniae* CAV1596 (CP011647), *K. pneumoniae* 32192 (CP010361), *K. PNEUMONIAE* blaNDM-1 (CP009114), *K. pneumoniae* KPR0928 (CP008831) and *K. pneumoniae* JM45 (CP006656), were identified as suitable for comparison with ICE-2 based on marker regions (Figure 3-8B) including *Int-a, traI, Int-b, traD* and *mcp.* Primer design is shown in Appendix II.

A total of 40 local *K. pneumoniae* isolates were screened by PCR for the occurrence and co-occurrence of ICE-1 and ICE-2. For ICE-1, one or more of the four representative regions were amplified identical to the expected PCR fragment length from 12 (30 %) isolates; *int* was detected in all. One (KR2177) among 12 strains carried an incomplete ICE-1 marker region lacking virB1 within the conjugation system; this suggests the presence of HPI alone rather than a complete ICE. It can be seen from the results shown in Table 3-4**,** that two or more of the five marker regions were amplified by PCR from only 5 (12.5 %) isolates and only two strains (KR2207 and KR3156) were found carrying all five marker regions. These results indicate relatively infrequent occurrence of ICE-2 related elements in local *K. pneumoniae* strains. In total 17 (42.5%) isolates were found harbouring either ICE-1 or ICE-2 related elements and 23 (57 %) were negative for the representative regions. Interestingly, none of the 17 positive isolates were found carrying both ICEs (Table 3-4).

Table 3-4 Prevalence of ICE-1 and ICE-2 in local blood stream isolates of *K. pneumoniae*.

Clinical Isolates		ICE-1					ICE-2					
		int-1 (0.24-kb)	*Irp* (1.9-kb)	*fyuA* (0.35-kb)	*virB1* (0.7-kb)	$^{a}tRNA^{asn}$ (1.1-kb)	*Int-a* (0.33-kb)	*tra-I* (0.4-kb)	*Int-b* (0.35-kb)	*traD* (0.34-kb)	*mcp* (0.3-kb)	$^{c}tRNA^{phe}$ (0.67-kb)
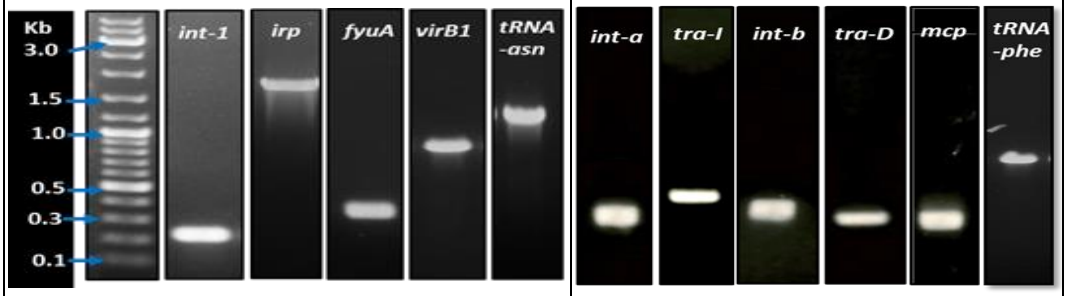												
HS11286	Control	+	+	+	+	+	+	+	+	+	+	+
NTUH-K2044	Control	+	+	+	+	+	-	-	-	-	-	-
MGH 78578	Control	-	-	-	-	-	-	-	-	-	-	-
KR2170	Isolated from blood culture	+	+	+	+	+	-	-	-	-	-	-
KR2171	Isolated from blood culture	-	-	-	-	-	-	-	-	-	-	-
KR2172	Isolated from blood culture	-	-	-	-	-	-	-	+	+		
KR2173	Isolated from blood culture	-	-	-	-	-	-	-	-	-	-	-
KR2174	Isolated from blood culture	+	+	+	+	+	-	-	+[b]	+[b]	-	-
KR2175	Isolated from blood culture	-	-	-	-	-	-	-	-	-	-	-
KR2176	Isolated from blood culture	-	-	-	-	-	-	-	-	-	-	-
KR2177	Isolated from blood culture	+	+	+	-	+	-	-	-	-	-	-
KR2178	Isolated from blood culture	-	-	-	-	-	-	-	-	-	-	-
KR2179	Isolated from blood culture	-	-	-	-	-	-	-	-	-	-	-
KR2180	Isolated from blood culture	-	-	-	-	-	-	-	-	-	-	-
KR2181	Isolated from blood culture	+	+	+	+	+	-	-	-	-	-	-
KR2201	Isolated from blood culture	+	+	+	+	+	-	-	-	-	-	-
KR2202	Isolated from blood culture	+	+	+	+	+	-	-	-	-	-	-
KR2203	Isolated from blood culture	+	+	+	+	+	-	-	-	-	-	-
KR2204	Isolated from blood culture	-	-	-	-	-	-	+	+	+	-	+
KR2205	Isolated from blood culture	-	-	-	-	-	-	-	-	-	-	-
KR2206	Isolated from blood culture	-	-	-	-	-	-	-	-	-	-	-
KR2207	Isolated from blood culture	-	-	-	-	-	+	+	+	+	+	+
KR3152	Isolated from blood culture	-	-	-	-	-	-	-	-	-	-	-
KR3153	Isolated from blood culture	+	+	+	+	+	-	-	-	-	-	-
KR3154	Isolated from blood culture	+	+	+	+	+	-	-	-	-	-	-
KR3155	Isolated from blood culture	-	-	-	-	-	-	-	-	-	-	-
KR3156	Isolated from blood culture	-	-	-	-	-	+	+	+	+	+	+
KR3157	Isolated from blood culture	-	-	-	-	-	-	-	-	-	-	-
KR3158	Isolated from blood culture	-	-	-	-	-	-	-	-	-	-	-
KR3159	Isolated from blood culture	-	-	-	-	-	-	-	-	-	-	-
KR3160	Isolated from blood culture	+	-	-	-	-	-	-	-	-	-	-
KR3161	Isolated from blood culture	-	-	-	-	-	-	-	-	-	-	-
KR3162	Isolated from blood culture	-	-	-	-	-	-	-	-	-	-	-
KR3163	Isolated from blood culture	-	-	-	-	-	-	-	-	-	-	-

KR3164		-	-	-	-	-	-	-	-	-	-	-
KR3165		-	-	-	-	-	-	-	-	-	-	-
KR3166		+	-	-	-	-	-	-	-	-	-	-
KR3167		-	-	-	-	-	-	-	-	-	-	-
KR3168		-	-	-	-	-	-	-	-	-	-	-
KR3169		-	-	-	-	-	-	-	-	-	-	-
KR3170		+	-	-	-	+	-	-	-	-	-	-
KR3171		-	-	-	-	-	-	-	-	-	-	-
KR3172		+	+	+	+	+	-	-	-	-	-	-

a: Site of integration for ICE-1, **b:** PCR amplified product was bigger than reference, **c:** Site of integration for ICE-2, PCR results represents *K. pneumoniae* HS11286.

3.3.4 Structural variation of ICE-1 and ICE-2

PCR mapping was used to further explore the identified regions. A total of 17 pairs of primers (Appendix I & II) were used to amplify different regions designated A1-Q1 covering ~62-kb of ICE-1 and 11 pairs to cover 56 kb of ICE-2 (A2 to K2). To study the physical linkage of different components of ICEs all the primers were designed with overlapping regions (Figure 3-9 & 10). It was found that 9 of 13 (*int* +ve) strains carried intact ICE-1 related elements. For ICE-2 only 2 (KR2207 and KR3156) had intact and physically linked components. Thus intact ICE-1 and ICE-2 were present in local *K. pneumoniae* isolates but none of the strains possessed both.

A.

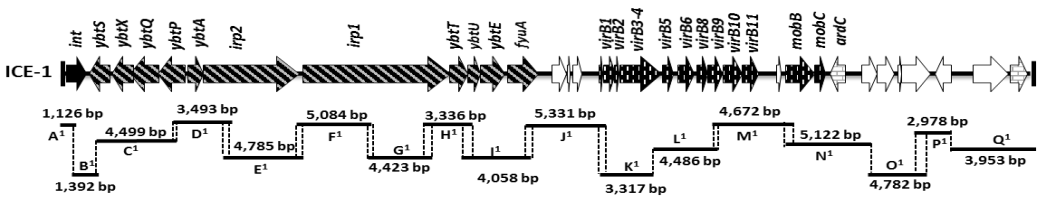

B.

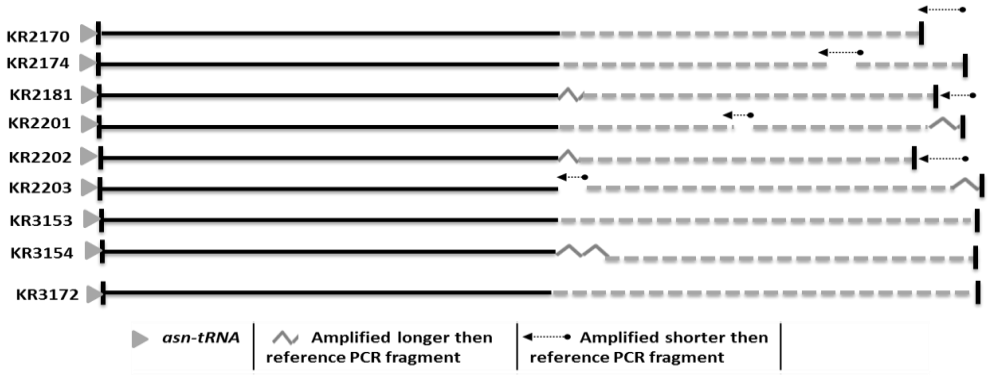

C.

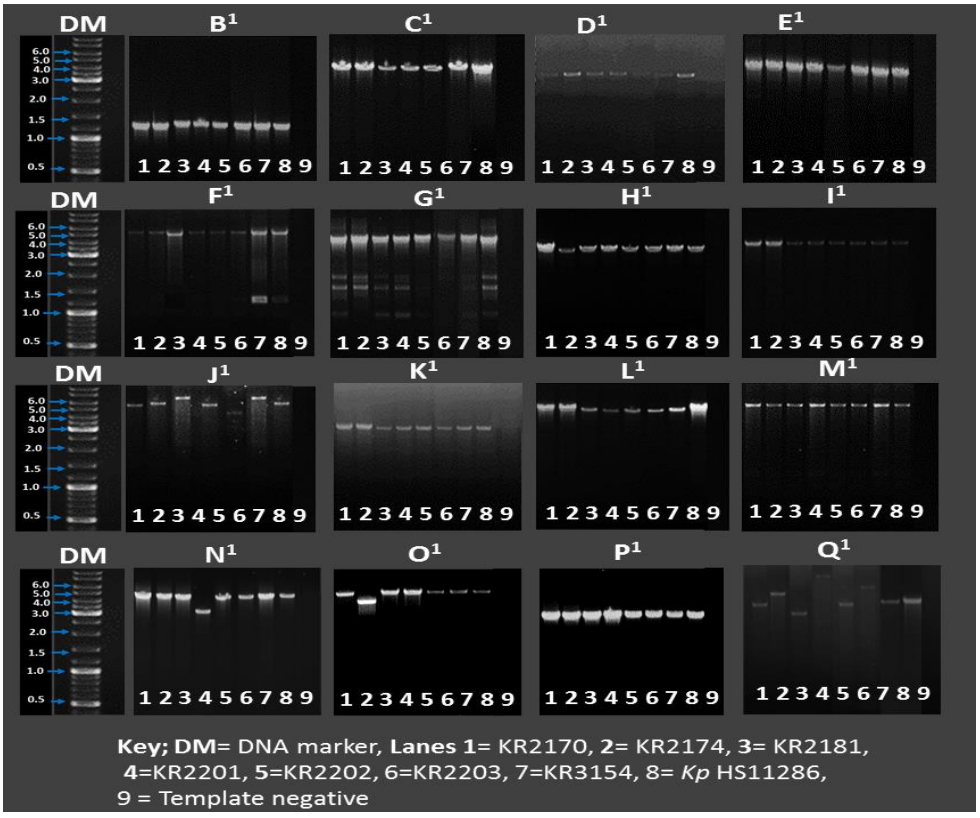

Figure 3-9 Illustrative PCR mapping of ICE-1 to investigate the intact nature of the element in local clinical isolates.

A. Schematics of primers used to amplify ICE-1 in 17 fragments, B. Map of novel ICEKP-1 elements identified in local isolates. Solid (black) lines represent HPI and the shaded (gray) lines indicate the region contained T4SS and other accessory genes. C. PCR results; results for A^1 were already confirmed in Table 3-4, KR3153 and KR3172 were not included as they had similar amplification to *K. pneumoniae* HS11286.

A.

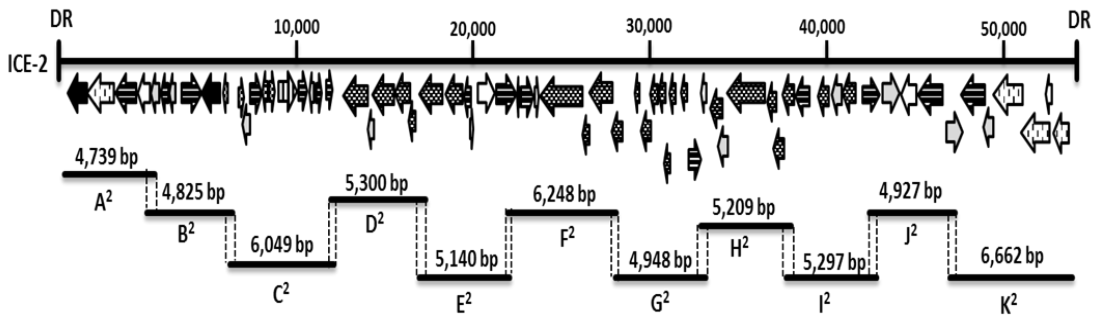

B.

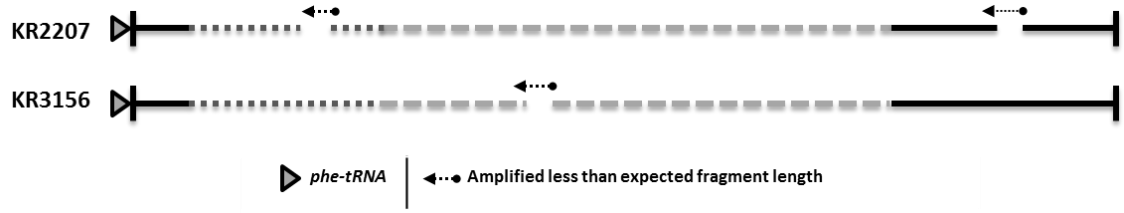

C.

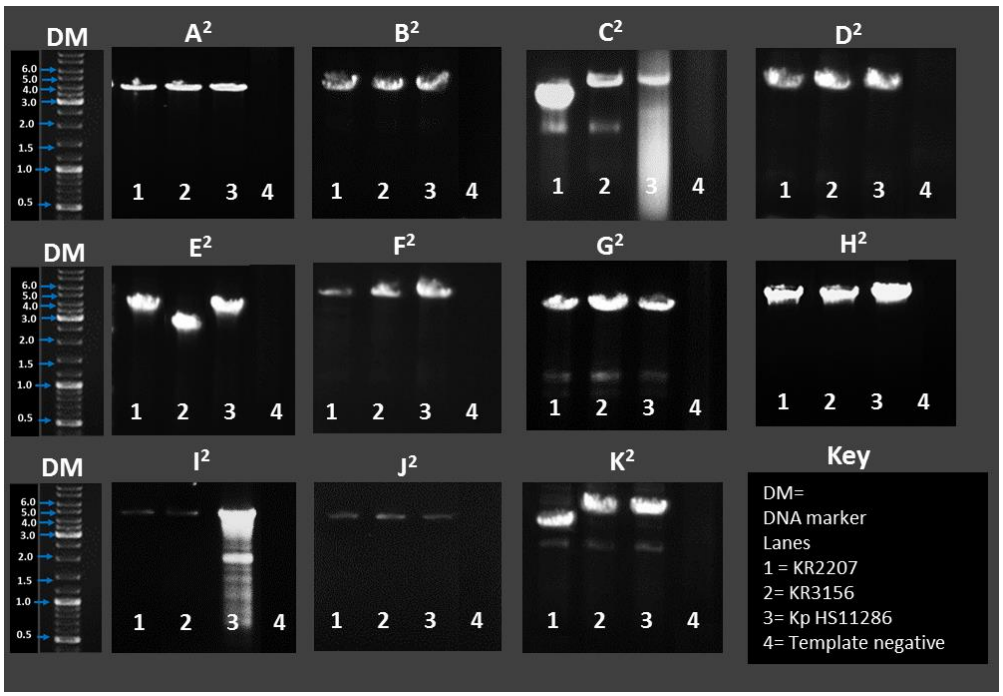

Figure 3-10 PCR mapping of ICE-2 to investigate the intact nature of the PAPI associated elements in local isolates of *K. pneumoniae*.

A. Schematics of primers used for ICE-2 mapping. **B.** Map of novel ICE-2 related elements identified in local isolates. Solid (black) lines represents the integration/excision and segregation module, dotted (black) and shaded (gray) lines indicates the presence of cargo genes and conjugation modules, respectively **C.** PCR results.

3.3.5 Chromosomal insertion sites of ICE-1 and ICE-2 in local clinical isolates

The directly repeated sequences for ICEKP-1 associated elements integration were previously identified at 3´ end of asn-tRNA in different bacterial species (Schubert et al.,

2004, Lin et al., 2008, Bi et al., 2012). Initially the *asn-tRNA* sequences were interrogated in various members of *Enterobacteriaceae,* to investigate whether the insertion of ICEKP-1 allied elements were restricted to the *asn-tRNA* for their integration. The *tRNAs* were found 100 % identical and also the 17 bp directly repeated sequences were found conserved (Figure 3-11A). Among 17 bp (5´-CCAGTCAGAGGAGC**CAA** -3´) 14 bp were within and 3 were flanking the 3' end of the *asn-tRNA* To investigate the insertion sites of ICEs in clinical isolates, primer RF204 was used with the RF102, where the former hybridised to the internal sites of the *asn-tRNA* and the latter binds complementary sites in the *int* gene. The results demonstrated linkage to *asn-tRNA* in each case (Table 3-4). Furthermore, the t*RIP*-PCR (section 3.2.3) method was used to interrogate the locus of insertion of ICE-1 related elements in these clinical isolates, as *all K. pneumoniae* possess four tRNA-*asn* at different loci and ICEKP-1 associated elements have been found at different loci (Figure 3-11B). To perform *tRIP*-PCR *K. pneumoniae* MGH78578 was used as reference strain (-ve control) as all the *asn-tRNA* loci were found empty, while NTUH-K2044 and HS11286 were used as positive control. The *asn-tRNA* locus-2 was found occupied by most newly identified ICEs, supporting their relatedness to ICE-1.

Similarly primers RF166 and RF157 (Appendix II) were used to investigate the insertion of ICE-2 related elements within *phe-tRNA.* These primer could amplified a ~0.67-kb fragment HS11286 spanning a conserved region in *phe-tRNA* and an internal region of the *int-a*. The results demonstrated the insertion of ICE-2 associated elements (KR2207 and KR3156) in *phe-tRNA* (Table 3-4). Thus these two ICEs were integrated into specific conserved regions in the *K. pneumoniae* genome in this strain set.

A.

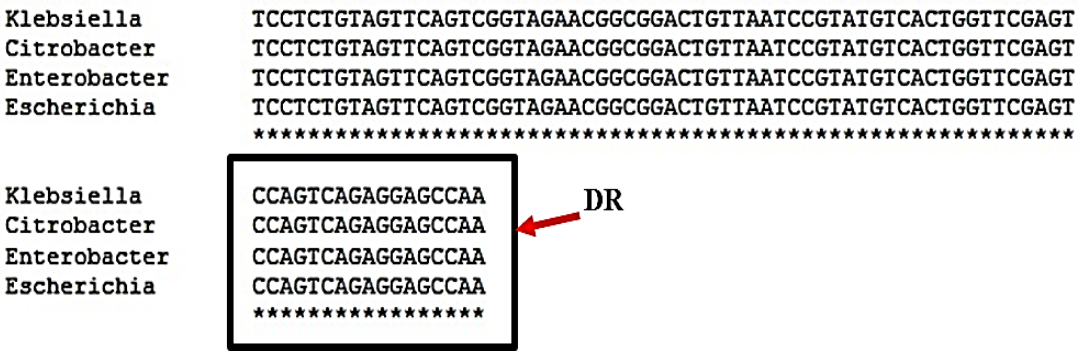

B.

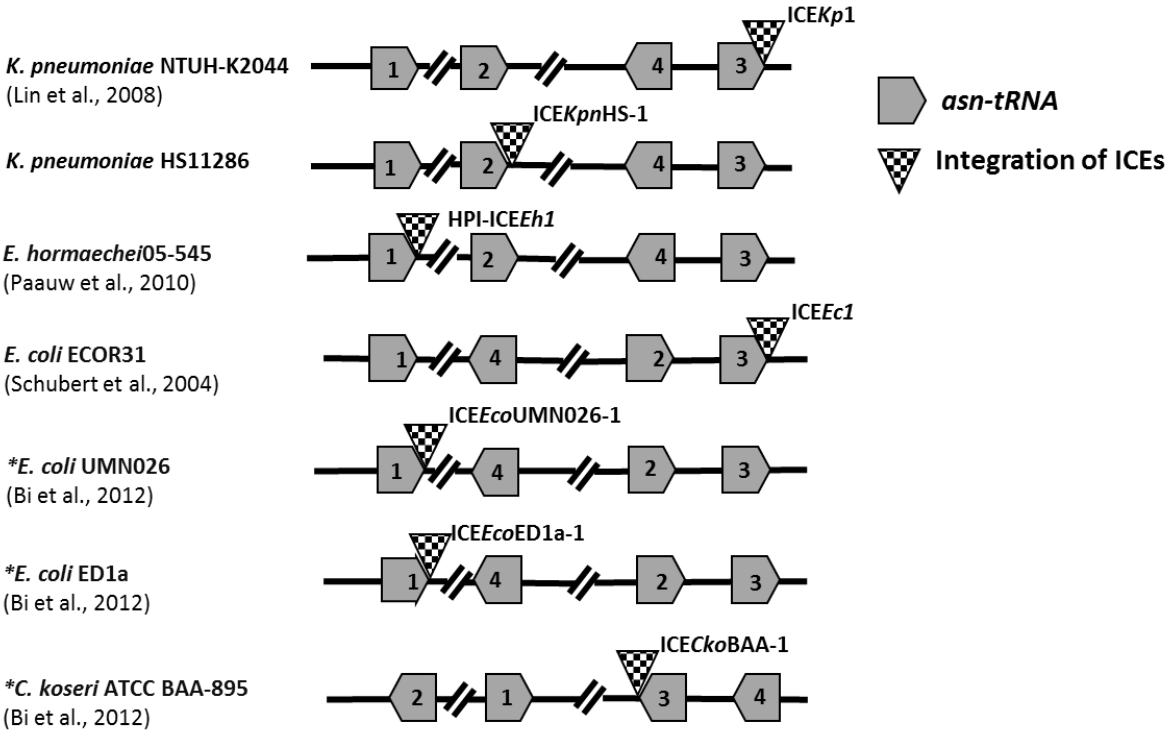

Figure 3-11 Chromosomal insertion of ICEKP-1 elements in different members of *Enterobacteriaceae*.

A. Multiple sequence alignment of *asn-tRNA* genes representing the conserved nature of 17-bp direct repeat (DR) in different species. **B**. Locus of integration of ICEs at different *asn-tRNA* loci. The proposed nomenclature for each ICEs are written with each triangle. * In-silico based from ICEberg database.

3.4 Discussion

3.4.1 Synteny of ICE-1 to the ICEKP-1 family

In this chapter the synteny of ICE-1 to ICEKP-1 is reported and reveals the presence of both common and distinct structural features of these ICEs in other members of the *Enterobacteriaceae*. An ICE belonging to ICEKP-1 was first discovered in *E. coli* ECOR31 (Schubert et al., 2004) and recently in *K. pneumoniae* NTUH-K2044 (Lin et al., 2008). All ICEKP-1 related elements described so far, were found integrated at *asn-tRNA*, contain phage-associated integrase, a gene cluster linked to the yersiniabactin siderophore system and a conjugation system (Schubert et al., 2004, Lin et al., 2008, Bi et al., 2012). The conjugal pilus appears to have originated from the R6K plasmid, while the mobilisation system resembles related elements in plasmid CloDF13 of *Enterobacter cloacae* (Cruz, 2001, Schubert et al., 2004).

Site-specific recombination is the mechanism used by ICEs to excise and integrate. The process results in the formation of identical directly repeated sequences in their flanking regions (Bellanger et al., 2011, Wozniak and Waldor, 2010). In this study ICE-1 was flanked by 17-bp of identical DR sequences, showing synteny to other ICEKP-1 elements in other hosts (Schubert et al., 2004, Lin et al., 2008, Bi et al., 2012). In addition, ICE-1 carried two ORFs KPHS_34930 and KPHS_34950 encoding AAA containing multi-domain proteins. These proteins belongs to large superfamily involved in various cellular functions including DNA repair and replication, organelle synthesis, membrane permeability and transcriptional regulation (Maurizi and Li, 2001). At the core of these functions are molecular motors; proteins (e.g. RuvB) that play a key role in homologous recombination (Snider et al., 2008), maintenance of which is critical for genome stability and DNA repair (West, 1997).

It is suggested that KPHS_34930 and KPHS_34950 are involved in DNA repair of ICE-1. However, the actual role of these putative proteins needs to be investigated further. Collectively, these findings indicate the conserved features of the ICEKP-1 backbone and their presence in various *Enterobacteriaceae*.

3.4.2 ICE-2 belongs to PAPI family

The ICEberg database (Bi et al., 2012) provides broad ranging information on 428 ICEs found in bacteria belonging from different families. At present, 80 % (344/428) of the ICEs have been classified into 28 different families based on homology of their integration module and backbone features such as T4SSs. The classification of the remaining 84 ICEs remained pending because they are poorly characterised (Bi et al., 2012); ICE-2 is one of these.

The analysis of ICE-2 at DNA and protein levels reported here indicates that ICE-2 belongs to PAPI family (Klockgether et al., 2007, Mohd et al., 2004, Roche et al., 2010, Qiu et al., 2006). Members of this family possess excision, integration and transfer capabilities (Burrus and Waldor, 2004, Klockgether et al., 2007, Seth and Croucher, 2009). Investigation of these properties for ICE- is described in Chapter 6.

Integrases play key roles in site-specific integration of ICEs (Flannery et al., 2011, Marcoleta et al., 2016, Dimopoulou et al., 2002, Wozniak and Waldor, 2010). PAPI associated ICEs have been distinguished based on the type of encoded integrase. These are classified into IntKX or IntKG groups based on the tyrosine recombinase (Roche et al., 2010); the former encodes a XerC recombinase and the latter P4-related recombinases. IntKX integrase have been associated with long flanking repeated sequence (~50bp) and the transfer of PAPI elements such as illustrated by *clc* element (Kelly, 2002, Sentchilo et al., 2003). Insertion sites include lys-*tRNA, leu-tRNA and phe-tRNA* and these have been used in classification (Roche et al., 2010).

In this study ICE-2 was flanked by 43 bp directly repeated sequences and was integrated at the *phe*-tRNA similar to ICE*Ec*-2 (Roche et al., 2010) while other PAPI elements were previously found integrated at *lys-tRNA* sites (Nancharaiah et al., 2003, Mavrodi et al., 2009, Bi et al., 2012). While the variable N-terminal DNA binding domains of integrases are considered important in determining site specificity, variations at the C-terminal of IntKX have also been considered important for the integration of PAPI elements (Roche et al., 2010).

3.4.3 Insertion sites are highly restricted

While ICE integration sites are generally close to *tRNA* genes, a few MGEs are reported at multiple sites, notably *Tn*916 and its preference for AT–rich regions (Roberts and Mullany, 2009, Mullany et al., 2012). In contrast, ICEKP-1 (Schubert et al., 2004, Lin et al., 2012, Bi et al., 2012), SXT (Bi et al., 2012, Daccord et al., 2012, Hochhut and Waldor, 1999) and ICEYe-1 (Collyn et al., 2004, Eppinger et al., 2007, Seth et al., 2012) and SPI (Moreno et al., 2012, Seth et al., 2012) elements have specific sites of integration (Table 3-1). Integration of ICEKP-1 elements into *asn-tRNA* was also found to be independent its location with the host genome (Schubert et al., 2004, Lin et al., 2008, Putze et al., 2009, Paauw et al., 2010).

Considerable importance has been attributed *phe-tRNA* as a hotspot for GI acquisition in *E. coli, Salmonella enterica*, *Yersinia pseudotuberculosis* and *K. pneumoniae* (Rumer et al., 2003, Collyn et al., 2004, Haneda et al., 2009). All *K. pneumoniae* strains carry two copies of *phe-tRNA*. In HS11286 they are located at chr.trna54 (coordinates: 4502771-4502846) and trna87 (coordinates: 405250-405325), ICE-2 is integrated into *phe-tRNa54*. Bioinformatic analysis of various sequenced *K. pneumoniae* strains (Figure 3-8B) and PCR results (Table 3-4) of local *K. pneumoniae* isolates confirms that ICE-2 related elements are highly restricted to *phe-tRNA* for their insertion. A possible explanation for their integration into *phe-tRNA* instead of *lys-tRNA* is the presence of XerC integrase that binds to the former *tRNA* (Roche et al., 2010).

3.5 Conclusions:

1. ICE-1 is highly conserved and syntenic to the ICEKP-1 elements.
2. ICE-2 belongs to subfamily of PAPI elements with XerC-like integrases.
3. ICE-2 related elements were found less disseminated in local isolates compared to ICE-1.
4. Structural components of the newly identified ICEs (ICE-1 and ICE-2 related), in clinical isolates were intact and physically linked indicating their organisational stability.

Chapter 4 Contribution of ICE-1 and ICE-2 to the phenotypes of *K. pneumoniae* and *E. coli* strains

4.1 Introduction

ICEs are usually differentiated by the specific properties they encode and these are linked to an extensive range of phenotypic characteristics such as virulence, resistance to antibiotics and heavy metals and niche adaptation (Waldor et al., 1996, Boltner et al., 2002, Whittle et al., 2002, Davies et al., 2009). Moreover, acquisition of ICEs may confer a range of complex traits e.g. host colonisation, nitrogen fixation and enhanced biofilm formation (Eliana and Frederick, 2002, He et al., 2004, Davies et al., 2009). ICEs are also associated with dissemination of antibiotic resistance determinants (Hochhut et al., 2001, Whittle et al., 2002, Mohd et al., 2004). Thus, ICEs, on the one hand, extend the survival fitness of organisms in different environments and, on the other, may enhance antibiotic resistance and virulence (Howard et al., 2000). The acquisition of GIs is not always be beneficial and may provide a genetic or metabolic burden (Niyaz et al., 2008).

Iron is a key nutrient for both humans and microorganisms. It is needed for diverse activities including DNA replication, respiration and metabolism (Cassat and Skaar, 2013). Mammals utilised high affinity iron-binding proteins (transferrin and lactoferrin) to sequester iron (Ratledge and Dover, 2000, Krewulak and Vogel, 2008) and limit the concentration of its free form; while iron is required for growth of most of pathogenic bacteria including *E. coli* and *K. pneumoniae* (Andrews et al., 2003). For growth during infection, bacteria must be able to acquire the sequestered iron from host proteins. To achieve this, members of *Enterobacteriaceae* have developed different siderophore systems; including enterobactin, aerobactin and yersiniabactin (Ybt) (Wandersman and Delepelaire, 2004). Enterobactin and aerobactin are, respectively catecholate and hydroxamate siderophore systems (Raymond et al., 2003, Mokracka et al., 2004). Ybt provides a particular focus here because this phenolate siderophore system (Perry et al., 1999) is produced by enzymes encoded on HPI and ICE-1. This system was first identified in *Yersinia* species and subsequently in multiple *Enterobacteriaceae* (Lawlor et al., 2007) including its acquisition by HGT (Bach et al., 2000, Li et al., 2005, Lin et al., 2008, Wu et al., 2009). Most *Yersinia* spp. that carry the Ybt siderophore system are associated with disseminated disease and high mortality (Scott et al., 1997, Carmen et al., 1999, Carniel, 2001). *Ybt* locus organisation, Ybt transport and its regulation in *K. pneumoniae* and *Yersinia* spp. is outlined in Figure 4-1.

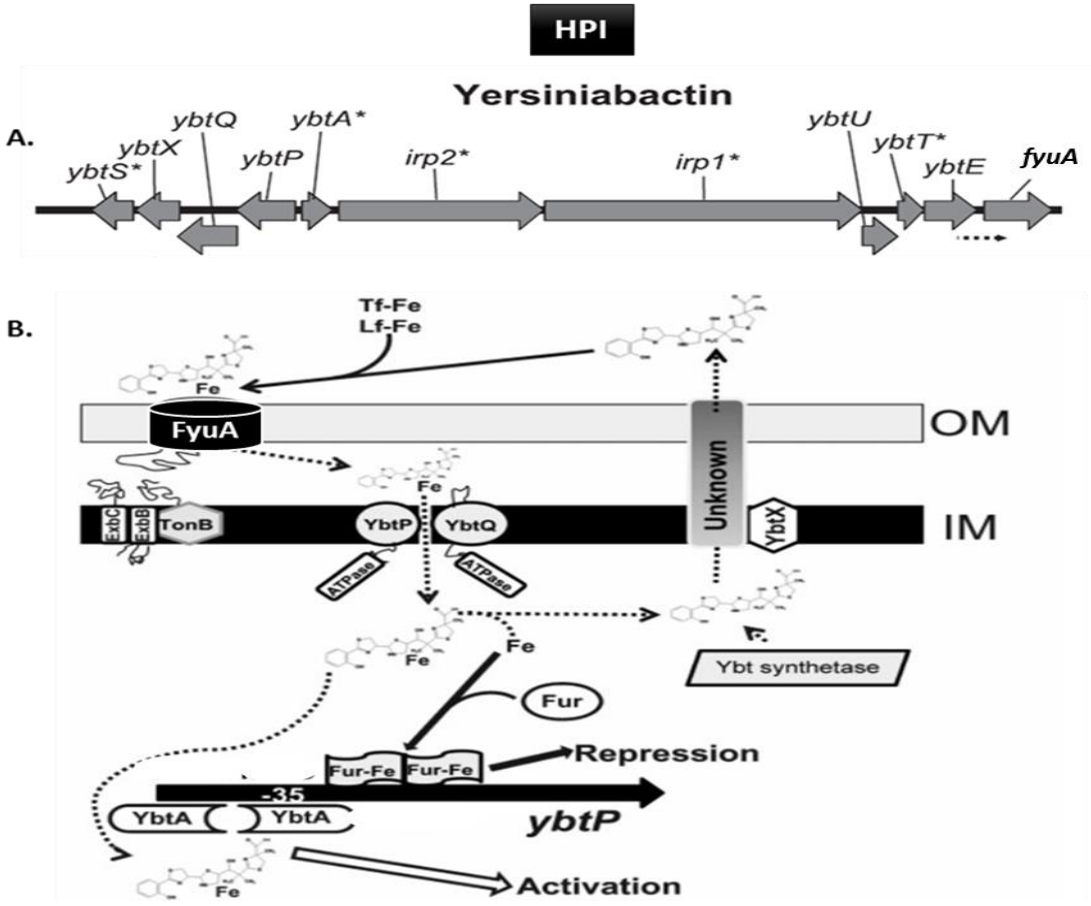

Figure 4-1 The Yersiniabactin siderophore system.
A. organisation of HPI in *K. pneumoniae* (Lawlor et al., 2007). B. model of transport and transcriptional regulation of *ybtP* (Miller et al., 2010).

In the preceding chapter, ICE-2 was classified in the PAPI family. Previously, PAPI-1 and PAPI-2 bearing *Ps. aeruginosa* strains were identified as highly virulent (He et al., 2004). To date, no detailed investigations of the role of PAPI-associated GIs in the phenotypes *Enterobacteriaceae* hosts have been reported. Therefore, it was aimed to study the role of ICE-2 in the phenotypes of *K. pneumoniae* HS11286.

In the Rajakumar's lab, PAPI-1 and PAPI-2 were recently shown to contribute to the virulence of *Ps. aeruginosa* PA14 (Harrison et al., 2010). These MGEs carry genes with limited but significant homology to genes encoding virulence factors connected to virulence in nematode and murine models of infection (Schulert et al., 2003, McMorran et al., 2003, He et al., 2004, Lee et al., 2006). Additionally, PAPI-1 elements are involved in the expression of various virulence factors including a gene cluster of type IVB pili, with *cupD1* and *cupD5*, encoding fimbrial biosynthesis (Michel and Baysse, 2002). Many homologues were found on related islands in various *Ps. aeruginosa* strains, however,

the major issue with the PAPI-1 elements is the lack of information on the encoded content as many *orfs* have not been assigned functions (Klockgether et al., 2007, Wurdemann and Tummler, 2007). Battle et al. (2008) described PAGI-5, a homologue of PAPI-1, in *Ps. aeruginosa* as playing a major role in acute murine pneumonia (Espinosa et al., 2012). In addition, PAPI-1 encoded homologues were found in strains of *Ps. aeruginosa* isolated from cystic fibrosis patients (He et al., 2004, Qiu et al., 2006, Wurdemann and Tummler, 2007).

These observations provide background to the contributions of ICEKP-1 and PAPI elements to the phenotypes of various bacteria. In this chapter, the contributions of ICE-1 and ICE-2 to the phenotype of *K. pneumoniae* HS11286 and *E. coli* are investigated.

4.1.1 Aim

To investigate the contribution of ICE-1 and ICE-2 to the phenotypes of *K. pneumoniae* HS11286 and *E. coli* HB101.

4.1.2 Objectives

1. To construct ICE deleted mutants using the Lambda Red recombination system.
2. To investigate the growth dynamics of WT and ICE mutant strains both in rich and minimal media.
3. To assess siderophore production of WT and ICE mutants.
4. To study the effect of the presence of ICEs on biofilm formation in HS11286.
5. To examine the contributions of the role of ICEs to antibiotic resistance.
6. To assess the contributions of ICEs to virulence in a *Galleria mellonella* larval infection model.
7. To study the effects of ICE-1 on siderophore production and antibiotic susceptibility in an *E. coli* recipient.

4.2 Methods

4.2.1 Knockout mutant construction

The Lambda (λ) Red recombination method was used to construct all various single and double knockout mutants of ICE-1 and ICE-2, unless and other wise stated (see Appendix VII for primers).

4.2.1.1 Lambda Red recombination

Lambda Red recombination-based allelic exchange was used to construct primary mutants in this work. This system employs three key genes from the phage λ Red operon; *bet* (β), *exo*, and *gam* (γ) (Murphy and Campellone, 2003). For efficient recombination, the Gam protein binds to the host RecBCD exonuclease complex and inhibits its exonuclease activity. The Exo protein is a 5' →3' exonuclease that facilitate the degradation of linear dsDNA molecule at the 5' end thereby generating ssDNA. Finally, the Bet protein binds to the 3' end of single stranded linear DNA generated by Exo and this supports the annealing of linear DNA to the homologous DNA in the genome. The activity of Gam ensures that the linear DNA introduced into the host is protected from the host exonuclease activity enabling the Bet and Exo proteins to assist the homologous recombination (Figure 4-2).

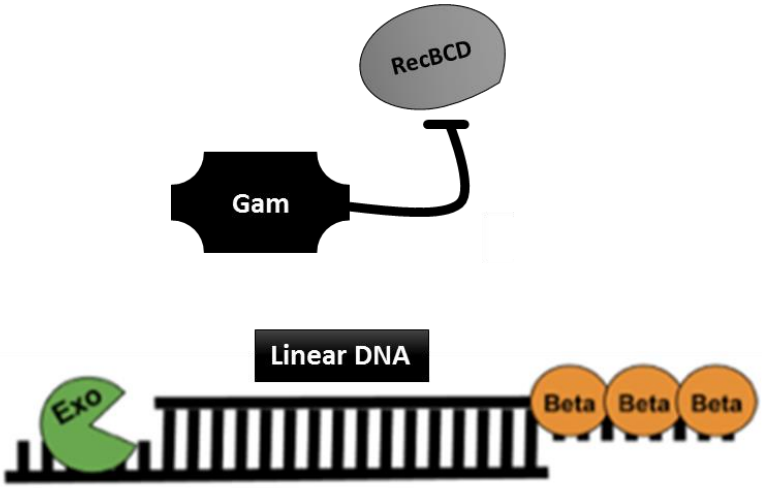

Figure 4-2 Components of Lambda Red recombination system.
The lambda red recombination system has three components 1) Exo, 2) Beta, and 3) Gam. All three are required for recombination with a dsDNA substrate. Gam prevents the endogenous RecBCD from digesting linear DNA introduced into the bacterial cells. Exo is a 5'→3' dsDNA-dependent exonuclease that degrade linear dsDNA starting from the 5'. Beta protects the ssDNA created by Exo and promotes its annealing to a complementary ssDNA target in the cell. Only Beta expression is required for recombination with an ssDNA oligo substrate.

These three genes are placed on the temperature sensitive plasmid pKOBEG-Apra under the control of the arabinose-inducible promoter PBAD (Guzman *et al.* 1995). Growing bacterial cells above 30°C causes the cell to be cured of this plasmid. The plasmid pKOBEG-Apra also contains a gene (*araC)* encoding regulatory protein AraC *that* binds to L-arabinose and facilitates the initiation of transcription from the PBAD promoter. Once transcription is initiated, the recombinase genes *bet*, *gam* and *exo* are expressed. Therefore, the presence of L-arabinose is essential for the expression of red operon.

The mutagenesis was designed in a way to cause an inframe deletion of targeted regions (from start to stop codon). The procedure started with the electro transformation linear DNA generated using the SOE-PCR method (2.2.3.5). The recombination event removed the target gene from start to stop codon and replace it with an antibiotic cassette between the homologous flanking regions (UF and DF: ~ 400-500bp) (Lesic and Rahme, 2008).

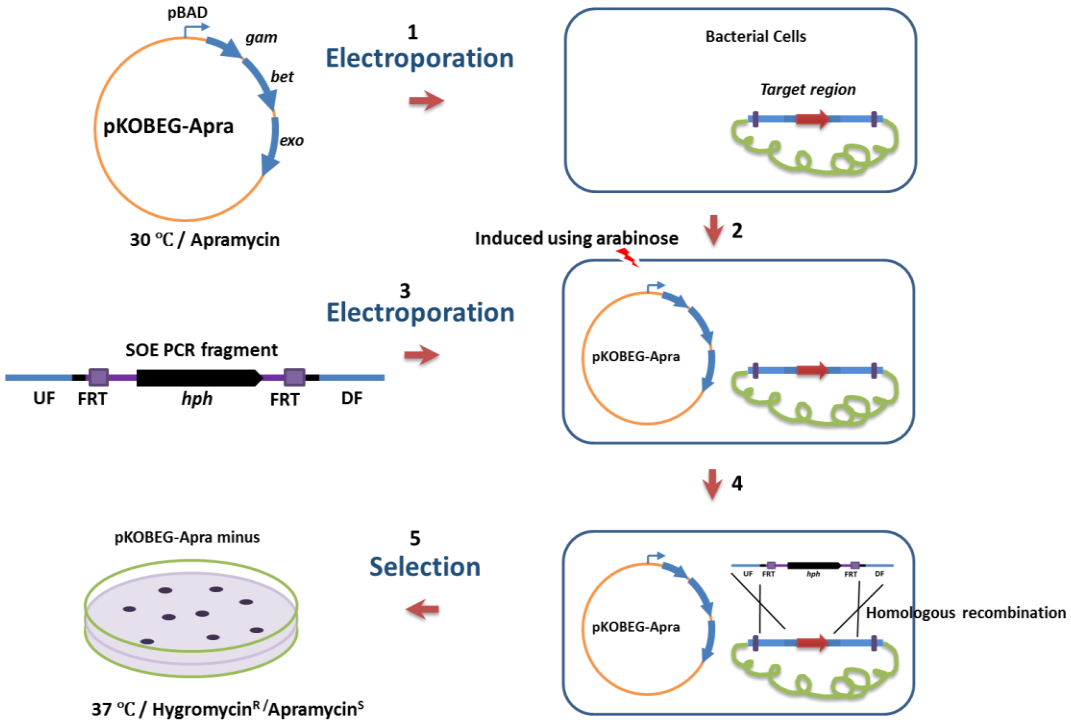

Figure 4-3 Schematics of Lambda Red recombination experiment.
The pKOBEG-Apra provided the λ phage Red-*gam, bet and exo* operon expressed under the control of the arabinose-inducible pBAD promoter. The SOE PCR fragment contained *hph* cassette and flanking regions of the target gene was electroporated in arabinose induced bacterial cells, finally the mutants were selected on medium (LB) containing hygromycin antibiotics.

Initially, pKOBEG-Apra was transformed into the target strain. Expression of the lambda red proteins was induced by growing transformed cells at 30^{o}C in LB supplemented with 30µg/ml apramycin and 0.2% L-arabinose. The presence of pKOBEG was always confirmed by PCR. Once the electrocompetent cells were prepared they were then transformed with the SOE product. The cells were recovered by growing them in SOC for 1 hour at 37^{o}C that was followed by its plating on LA supplemented with 100µg/ml of hygromycin (Figure 4-3). The mutation was confirmed using PCR with two sets of primers; one that lies outside the flanking regions on the genome and a second that lies internally in the targeted gene. For these PCRs, parent strain DNA was always used as a control. The inframe deletions were also confirmed by sequencing of amplified regions using GATC services.

4.2.2 Flippase mediated recombination

The antibiotic cassette used for the construction of various mutant strains was flanked by Flippase Recognition Target (FRT) sequences. These sequences allow a recombination event mediated by flippase, resulting in the removal of the antibiotic resistance gene.

A plasmid pFLP-2-Apra was used to supply the flippase. Target cells were transformed with pFLP-2 and grown on LA supplemented with 30µg/ml of apramycin. Knockout of the antibiotic marker cassette was confirmed by PCR and sequencing.

4.2.3 Counter selection

The pFLP-2-Apra contains sacB gene encoding the exo-enzyme levansucrase, which gives sensitivity to sucrose. Therefore, use of sucrose in the media provided a simple counter selection for the plasmid. To cure the marker-less mutant of pFLP-2-Apra; the cells were grown on LA media supplemented with 6% sucrose and the loss of pFLP-2-Apra will confirmed by PCR (Appendix VIII).

4.2.4 Plasmid construction

4.2.4.1 In-Fusion Cloning technique

The In-Fusion HD cloning kit (Takara) was used to construct the plasmid Pybt for complementation. This technique is designed for fast, directional cloning of one or more fragments of DNA into any vector. The efficeincy of this method is based on the In-

Fusion enzyme which facilitates fusion of PCR-generated DNA fragemnts effieciently and precisiely. The recombination is dependent on 15bp incorporated into primer design, which overlaps sequences present at the end of the PCR generated fragments.

4.2.4.2 Primer design

The *ybtXSPQ* operon was cloned into pACYC184 under the control of its native promoter. 15bp were added to the *ybt* operon-directed primers RF205 and RF206 (shown in red) to enable recombination (Table 4-1). These 15 bp is the complementary sequences of the primers RF207 and RF208 that were used to amplfy the vector fragment using pACYC184 as a template DNA. For good cloning effieciency, the PCR amplified fragments of both vector and inserts were purified.

Table 4-1 Primers used for the construction of P_{ybt}.

Primer Number	Primer sequence 5´ to 3´	Purpose
RF205	**ACGCAGTCAGGCAC**GGACAGTCTGGTTGTGAGG	Forward primer; used to amplify the *ybtXSPQ* operon (HPI) using *K. pneumoniae* HS11286 as a template DNA
RF206	**ATGCCTGAGGCCAGT**GTATCCGGGCCTCTGTCA	Reverse primer; used to amplify the *ybtXSPQ* operon (HPI) using *K. pneumoniae* HS11286 as a template DNA
RF207	ACTGGCCTCAGGCATTTGA	Forward primer; used to amplify vector backbone
RF208	GTGCCTGACTGCGTTAGC	Reverse primer; used to amplify vector backbone

4.2.4.3 In-Fusion Cloning

The purified PCR insert was large compared to the linearised vector, therefore for efficient cloning a 1:2 insert to vector ratio was used during the cloning step. Table 4-2 shows the reaction mixture used. The total reaction volume was adjusted to 10µl using molecular grade water then incubated for 15 min at 50°C then cooled on ice.

Table 4-2 Reaction mixture for HD-In-Fusion cloning.

Rxn Component	Cloning Rxn	Amount in µl
Purified PCR fragment	25ng	As required
Linearized vector	166ng	As required
5X In-Fusion HD Enzyme Premix	5X	2ul
Deionized Water	Upto 10µl	As required
Total	To 10µl	To 10µl

4.2.4.4 Heat shock transformation

Stellar Competent Cells (*E. coli*), provided with the kit, were used for transformation. The cells were thawed on ice and mixed gently. A total of 4µl of the reaction mixture was added and incubated on ice for 30 min. The cells were heat shocked for 45 sec at 42^{o}C and cooled on ice for 2 min. For cell recovery, the transformed cells were incubated in 500ul of SOC medium for 90 min at 37^{o}C. Finally, the cells were plated on LA suplemented with 30ug/ml of chloramphenicol. Plasmid contruction was confirmed by PCR.

4.2.5 Blue Agar chrome azurol S (CAS) siderophore diffusion assay

The CAS assay was modified from the method described by Louden et al. (2011). An overnight culture in LB was adjusted to ~0.8-1 (OD_{600}) then 10µl was spotted onto a CAS agar plate. The effects of siderophore production/secretion were observed after 24 hr incubation at 37^{o}C by measuring the halo zone around the colonies in mm.

4.2.6 2,2 dipyridyl (DIP) assay

DIP assay was used to investigate the effects of iron restriction on growth of the WT and the ICE-1 mutant. Overnight cultures (LB) were adjusted to ~0.08 (OD_{600}) in LB containing 200µM DIP. 150µl per well was transferred a Bioscreen plate was grown for 24 hour at 37^{o}C with continous shaking. The BioScreen was set to measured the optical densities at 15 min intervals. The experiment was performed three times independently with 3 three biological replicates.

4.2.7 Growth in WT culture supernatant

The ΔICE-1 strain was grown in culture supernatant (SN) obtained from the WT (late exponential phase). The mutant was grown in SN (with no fresh LB) and in 1:1 ration of fresh LB and SN. The supernantant was always filter sterlised and was used as control of cross contamiation from WT.

4.2.8 Growth assay in minimal medium (M9)

M9 was used to study the effects of nutreint limitation on growth of WT and ICE mutants. The standard M9 used for bacterial growth contained Na_2HPO_4 (6.9 g/liter), KH_2PO_4 (3 g/liter), NaCl (0.5 g/liter), NH_4Cl (1 g/liter), $CaCl_2$ (0.1 mM), $MgSO_4$ (2 mM), and gluscose (5mM) as a carbon source. M9 was modified for carbon,nitrogen, and trace elements as per requiremnets.

4.2.9 Biofilm assay

Crystal violet staining was used for the quantification of biofilm formed by WT and ICE mutant strains. Briefly, an overnight culture was normalised to ~0.8-1.0 (OD_{600}) in LB and was grown in 96-well polystyrene (NUNC) microtiter plates, each well containing 150µl of bacterial suspension. Plates were incubated statically for 24, 48 and 72 hr at 37^{o}C. The medium was removed and the wells were washed once with sterile dH2O. The biofilm was stained with 175µl of 0.1% (v/v) crytal violte dye for 15 min then washed twice with dH2O and air dried. The crystal voilet-biofilm complex was dissolved using 200µl of 95% ethanol and the absorbance measured at 595nm (BioRad Model 680 Microplate reader). The experiment was repeated for three times.

4.2.10 Antibiotic susceptibilities by disc diffusion and E-test method

Colonies from overnight LA plate cultures were picked and suspended in sterile 0.9 % NaCl. The turbidity of the suspension was adjusted to match McFarland 0.5 standard (~0.8 at OD_{600}). The suspension was spread evenly on MHB agar within 15 min of preparation using a sterile cotton swab to create a semi-confluent growth. The inoculum was allowed to dry for 10 min before applying the antibiotic discs or Etest strips then the plates were incubated at 37^{o}C for 24 hr. The plates with uneven growth were neglected. The zone of growth inhibition around the discs (BioMerieux) was measured in mm. For Etest (BioMerieux), the MIC (µg/ml) was read from the scale on the Etest strip where the symmetrical inhibition ellipse edge intercepts the strip. Antibiotics used for disc diffusion test are listed in Table 4-3.

Table 4-3 List of antibiotics used in disc diffusion test.

Antibiotics	Symbol	Concentration (mg/disc)
Trimethoprim	W	2.5
Spectinomycin	SH	10
Streptomycin	SM	10
Chloramphenicol	C	50
Tetracycline	TC	10
Minocycline	MH	30
Colistin sulphate	Co	25
Gentamicin	GM	10
Novobiocin	NO	5
Cotrimoxazol	TS	25
Sulphatriad	ST	200
Ampicillin	AMP	25

4.2.11 Virulence assay

A Galleria mellonella model of infection was used for the virulence assays. The method was modified from previous work (Harding et al., 2013, Olsen et al., 2011).

4.2.11.1 *Galleria* Preparation:

The larvae were purchased from LiveFoods UK and were kept at room temperature (25^{o}C) in the dark. The larvae were stored in plastic containers permitting air exchange and included a padding of wood shavings as a food source. Stage six larvae were selected according to size (2-3 cm) and weight (200-250 mg). At this stage the larvae can survive for around two weeks without the need for nutrients. Any larvae showing signs of inactivity (hard darkened exterior) were discarded. For each experiment, a replicate group of 15 larvae was used. The larvae were distributed into Petri dishes one day before bacterial injection.

4.2.11.2 Inoculum Preparation:

A 1:100 dilution from an overnight culture was grown for 3-4 hr. The bacteria were then pelleted by centrifugation and washed 3 times with sterile PBS then resuspended in PBS to an absorbance of 0.2 (OD_{600}). Cfu counts were determined for each inoculum.

4.2.11.3 Galleria inoculation and incubation

Injection of the larvae was done using an insulin syringe in a specialized low volume injector (capable of consistently injecting small volumes). A volume of 10µl of each sample (the undiluted 0.2 OD_{600} suspension) and the PBS control was injected into the

haemocoel via the rear left pro-leg. The larvae were incubated in plates at 37^{o}C and their mortality was assessed at 24 hour intervals over 5 days.

4.2.11.4 Observation of results

To minimize the injury, the insects were examined with a blunt object by gently flipping them onto their backs and signs of movement were checked. Live larvae are quick to flip back whereas sick larvae show dark skin pigmentation and usually die in the following days. The experiment was discarded if there were 2 deaths in any of the control groups (untouched and PBS injected).

4.2.12 Statistics

The statistical analysis in growth curves and biofilm assay was performed by multiple t-test using Holm-Sidak method and student t-test, respectively. The survival curve in killing assay was analysed by Mantel-cox test. The *p* values less than 0.05 were consisdered as statititically significant.

4.3 Results

4.3.1 Construction of mutant strains

To investigate the role of ICEs on phenotype, ΔICE-1, ΔICE-2 and ΔΔICE-1-2 (double mutant) were constructed using the Lambda Red recombination technique (section 4.2.1.1).

4.3.2 Growth dynamics of HS11286 in rich medium

Growth of the WT and ICE mutants in rich medium was studied. The WT and ΔICE-2 grew at indistinguishable rates while ΔICE-1 and ΔΔICE-1-2 showed significantly longer doubling times and lower growth yield (Figure 4-4A). The doubling times were calculated using OD_{600} readings between 60 and 180 min. Reduced growth of the mutant strains was further confirmed by Cfu counts (Figure 4-4B).

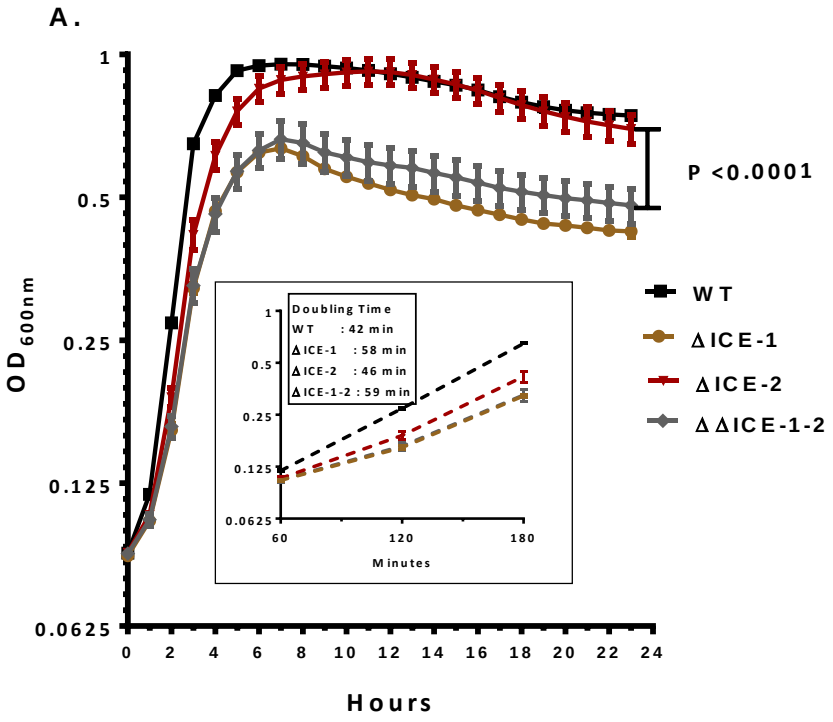

B.

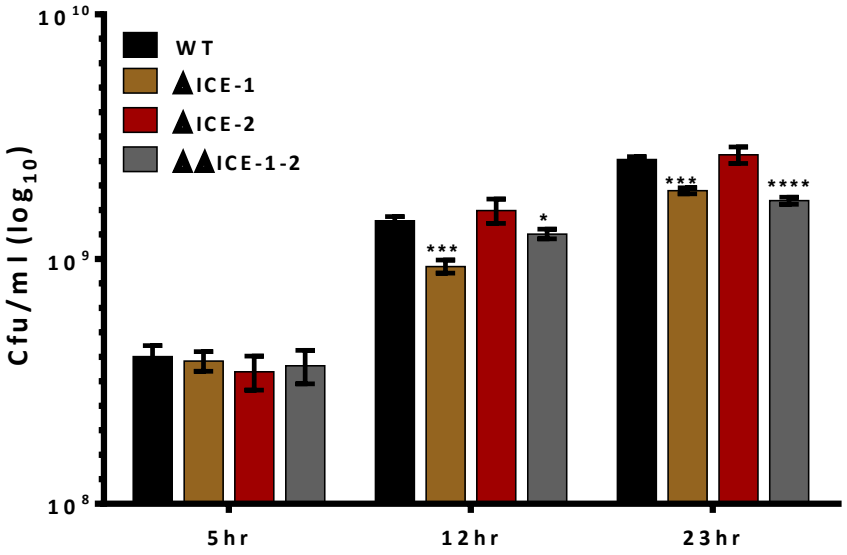

Figure 4-4 Growth dynamics of *K. pneumoniae* HS11286 and it ICE mutants in LB.
A. Optical densities **B.** Quantification of Cfu/ml at different points in the time course. The experiment was performed on 3 independent occasions. Statistical analysis was performed with multiple t-test using Holm-Sidak method. (* = P=0.02, *** = P=0.004, ****= P<0.0001) the differences are compared to the WT.

Since ICE-1 includes the yersiniabactin encoding operon (HPI), it was hypothesised that;

HPI of ICE-1 enhances growth of *K. pneumoniae* HS11286 WT in nutrient/iron limited conditions.

Hypothesis 4-1

To test this hypothesis the ΔICE-1 strain was grown in culture supernatant obtained from the WT as this should contain yersiniabactin (section 4.2.7). This did not improve the growth of the mutant strain. Thus the presnce of the siderophore in culture supernatant did not appear sufficient to enhance ΔICE-1 growth.

4.3.3 Complementation of the yersiniabactin transporter

YbtP and YbtQ, are HPI encoded proteins required for Ybt based iron uptake. Hypothesis 4-1 was further tested by complementation of the Ybt transport and regulation system (YbtP and YbtQ) in the ΔICE-1 strain. Complementing clones were made using a low copy number plasmid pACYC184 under the control the native yersiniabactin promoter (Figure 4-5).

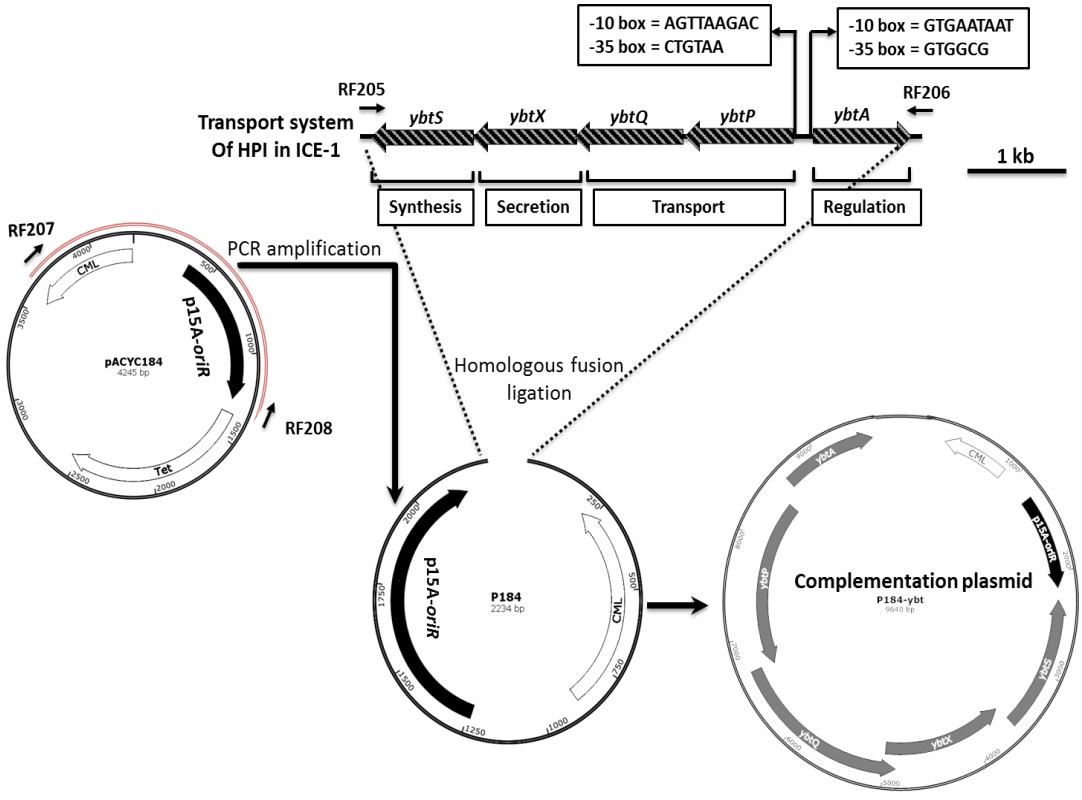

Figure 4-5 Construction of complementation plasmid P-Ybt.
The *ybtSXQPA* operon was cloned into pACYC184 using the Infusion HD cloning method (section 4.2.4).

The ΔICE-1$_{Pybt}$ strain was grown in LB and LB supplemented with WT culture supernatant. The growth yield, and the growth rate of the Pybt complemented ΔICE-1 (~30 min doubling time) was significantly remediated (P=0.0004) when grown in WT supernatant (Figure 4-6) but no change was observed in LB.

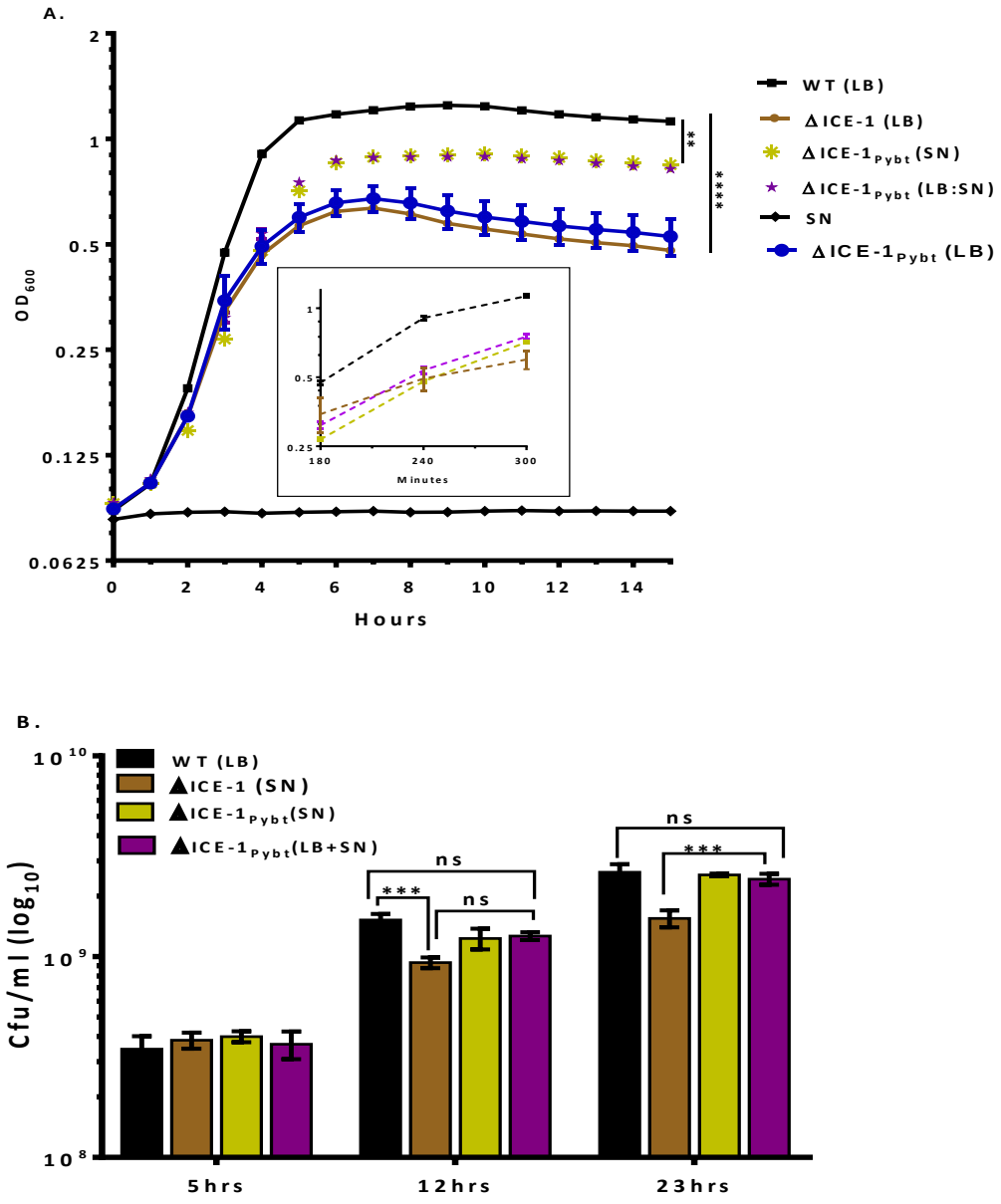

Figure 4-6 Growth dynamics of ΔICE-1 and ΔICE-1Pybt mutant strains in culture supernatant of WT.

A. Growth pattern in LB and LB supplemented with culture supernatant (SN) from WT: SN:LB was the combination of 1:1 ratio of fresh LB with WT supernatant whereas SN represents that mutant was grown only in WT supernatant. **B.** Cfu/ml counts at different time points. 4 technical replicates were assessed on three independent occasions. (**P = 0.004, ***P = 0.0004, ****P <0.0001).

4.3.4 Further evidence for siderophore involvement in ΔICE-1 strain growth defects

Hypothesis 4-1 was further investigated by assessing siderphore production in the CAS assay and growth of strains under iron limitation in the presence of 2,2-dipyridyl (DIP). Significant differences in siderophore secretion between the WT and the ΔICE-1 mutant were observed, as indicated by the reduced halo zone around ΔICE-1 strains; no obvious difference in siderophore secretion was observed in ΔICE-2 strains (Figure 4-7A). The results obtained from 2,2-dipyridyl (DIP) exposure (Figure 4-7B) reinforce the view that ICE-1 plays an important role in iron acquisition. It is noteworthy that the growth of the WT in DIP and the ΔICE-1 strain in LB were very similar.

A.

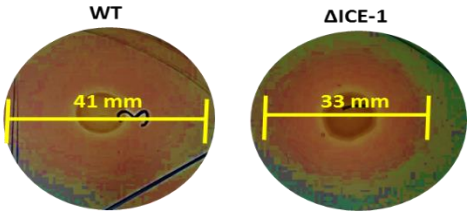

B.

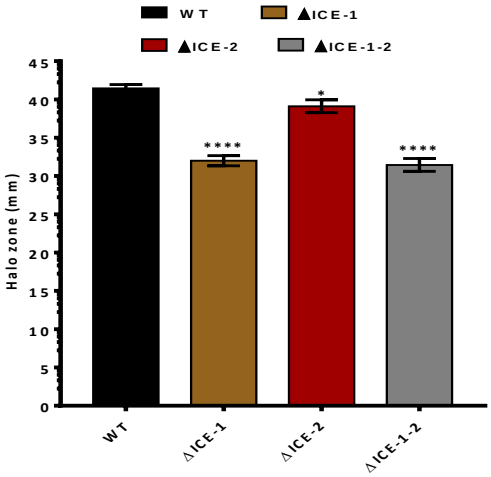

C.

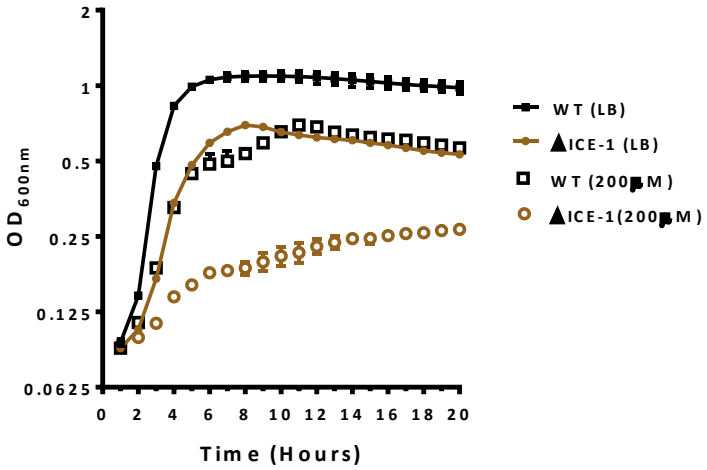

Figure 4-7 Effects of iron limited environment on the growth of ICEs mutants.
A. Siderophore production of strains assessed with the CAS assay. The halo around (measured in mm) the colonies indicates the iron chelating activity of exported siderophores (n=, *P=0.1, ****P=0.0001) **B.** Growth curve of WT and ICE-1 minus strain in LB broth supplemented with 200μM 2,2'-dipyridyl.

4.3.5 Contribution of ICEs to growth in nutrient limited media.

The WT and ICE mutants were grown in LB broth overnight then subcultured into minimal medium M9 (section 4.2.8) containing glucose and ammonium chloride (NH_4Cl) as sole carbon and nitrogen sources. Similar rates of growth were observed with the WT and ΔICE-2 strain but ΔICE-1 strain did not grow in this medium (Figure 4-8). Thus ΔICE-1 strains were impaired in M9 medium and two hypotheses were proposed:

ΔICE-1 strains cannot use glucose as a carbon/energy source. **Hypothesis 4-2**

ΔICE-1 mutants cannot use ammonium as a nitrogen source. **Hypothesis 4-3**

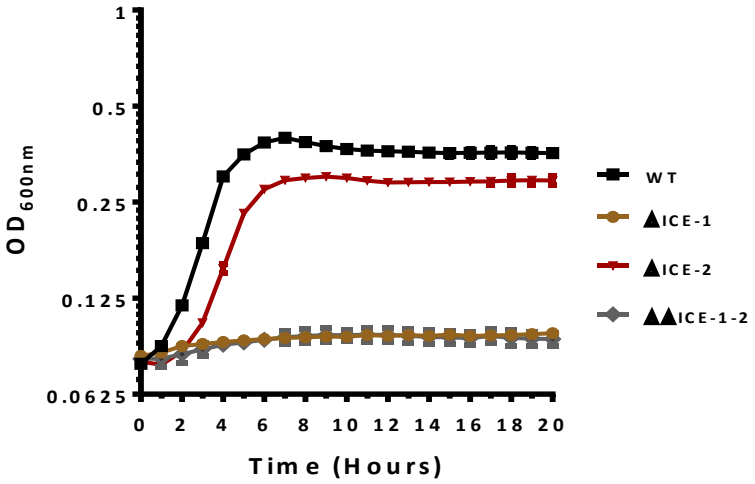

Figure 4-8 Growth of *K. pneumoniae* HS11286 and ICE mutants in defined minimal medium (M9). Glucose and ammonium chloride was used as sole carbon and nitrogen sources.

4.3.6 Effects of modifications in carbon and nitrogen sources of M9 on ICEs mutants growth

Klebsiella pneumoniae is known to ustilise both lactose (0.4%) and citrate (0.4%) and M9 was modified with these substrates as sole carbon sources to test hypothesis 4.2. Similar to $M9^{+Glu}$, the ΔICE-1 strains did not grow while growth of ΔICE-2 and WT were supported (Figure 4-9).

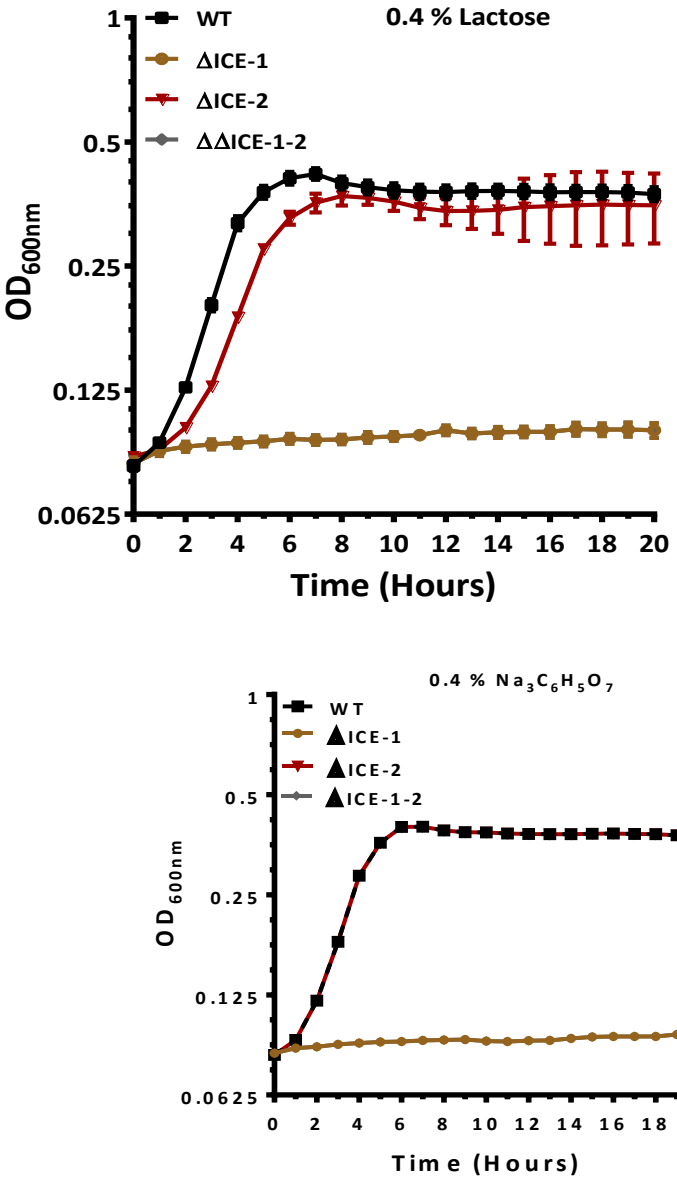

Figure 4-9 Growth pattern of WT and ICE mutants in M9 modified with different carbon sources. M9 minimal medium was modified by 0.4 % of lactose/sodium citrate ($Na_3C_6H_5O_7$). The graph represented the growth of bacteria in M9 with the modified carbon source with no glucose.

To test hypothesis 4-3, $M9^{+Glu}$ was supplemented with both organic (0.5 % Peptone, 0.5% of Casamino acids) and inorganic (0.5% KNO_3) nitrogen sources. Organic nitrogen sources in $M9^{+Glu}$ supported ΔICE-1 growth. Casamino acids and peptone producing a greater response in WT and ΔICE-2 because nitrate could be used by them but not by ΔICE-1 (Figure 4-10). The presence or absence of NH_4Cl with the casamino acids and peptone had no effect on bacterial growth (data for the media containing both NH_4Cl and other nitrogen source are not shown). Collectively these results supported

hypothesis 4-3 and suggested that ΔICE-1 strain have a defect in nitrogen assimilation or metabolism.

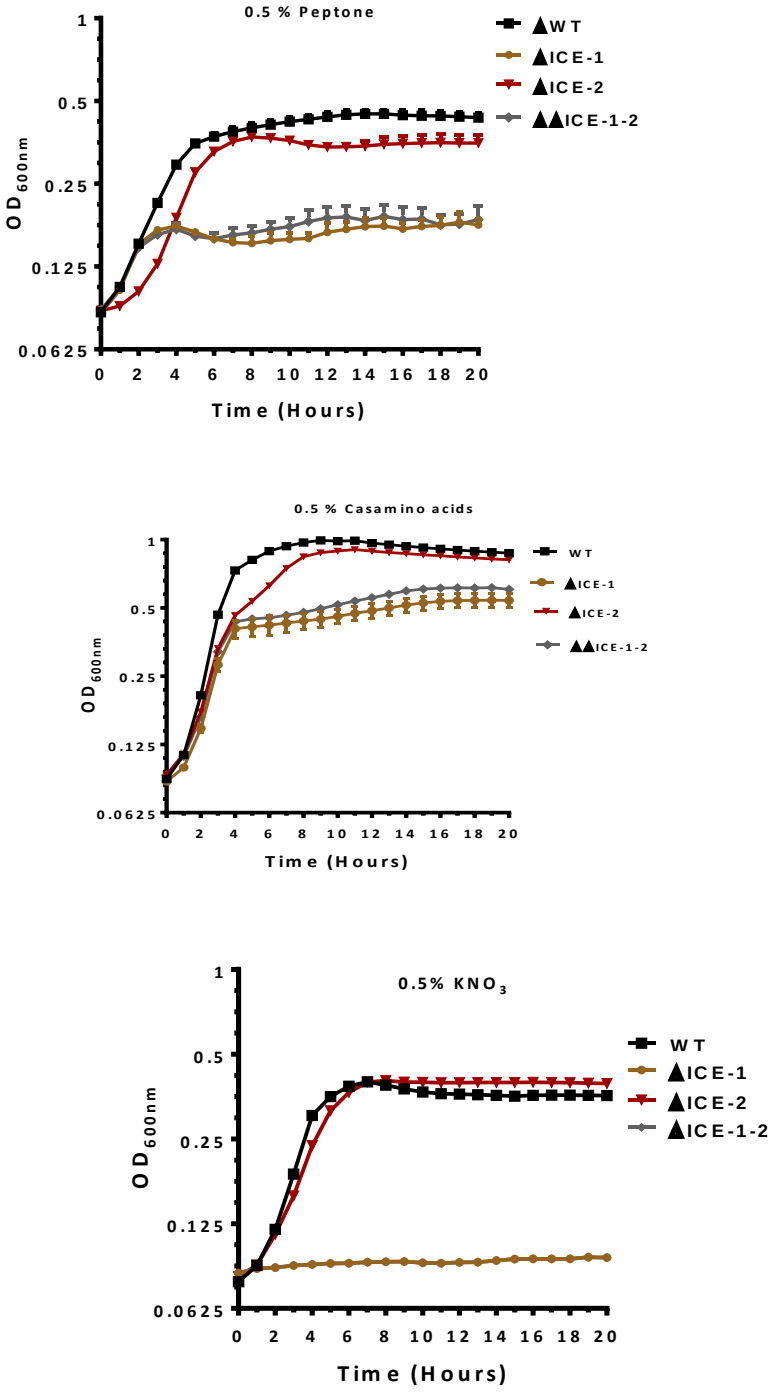

Figure 4-10 Growth of WT and ICE mutant strains in different nitrogen sources (M9+Glu). **A.** 0.5% Peptone, **B.** 0.5% Casamino acid, **C.** 0.5% KNO_3. The graphs represent the growth in media containing the modified nitrogen source only with no NH_4Cl.

4.3.7 Single amino acid studies

To detemine whether the ΔICE-1 strain was dependent on specific amino acids. Growth experiments were conducted using $M9^{+Glu}$ supplemented with 10mM of 20 different amino in the absence of NH_4Cl (Figure 4-11). Cysteine, serine and tyrosine were all associated with reduced growth of the WT. Only histidine was able to support growth of the ΔICE-1 mutant. Thus the defect in the ΔICE-1 mutant would appear to be in histidine biosynthesis.

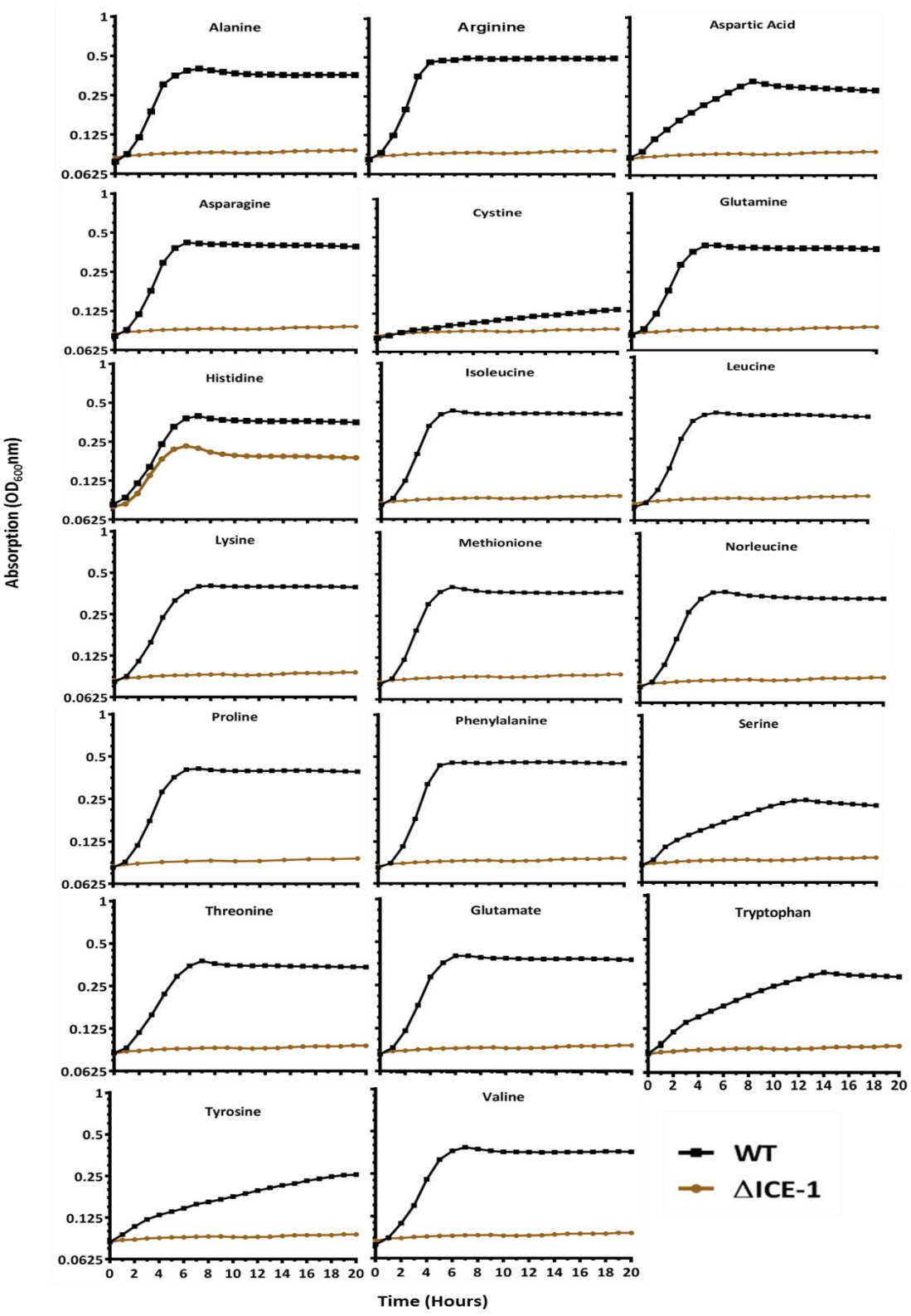

Figure 4-11 Growth responses of WT and ΔICE-1 strain in M9+Glu supplemented with different amino acids.
All various amino acids were added at 10mM concentration and growth responses were measured at OD_{600} for 24 hr. (n=3).

4.3.8 Effects of ICEs on biofilm formation *in vitro*

The HS11286 WT and ICE deletion mutants were studied for their ability to form biofilm on polystyrene *in vitro* using the crystal violet staining method (4.2.9). The double mutant showed more attachement to the surface in first 24 hr (Figure 4-12). Moreover, differences were observed in the biofilm formation of all the ICE mutants at 48 and 72 hr. Microscopic examination revealed differences in the pattern of biofilm formation witht the ICE mutants compared to the WT (Appendix XII). Overall, both ICEs appeared to be not invovled in the enhance biofilm formation.

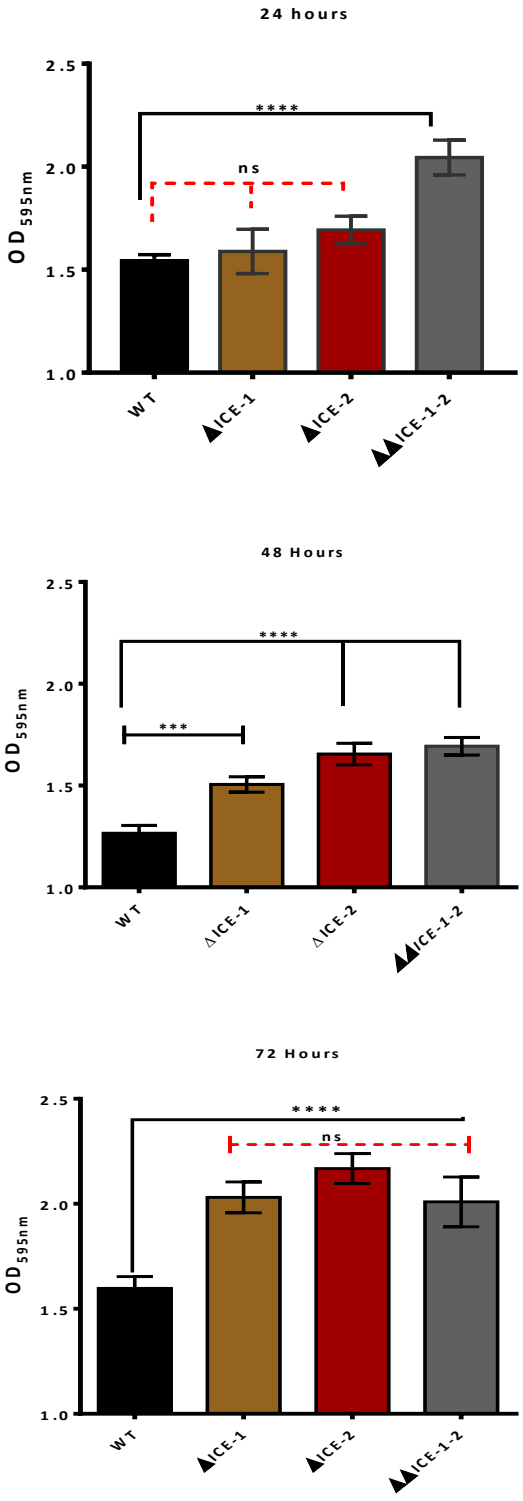

Figure 4-12 Biofilm attachment by WT and ICE mutant strains LB medium.
Crystal violet staining assay was used to quantify the initial attachment of WT and ICE mutants at different time points (24, 48 and 72 hr). The experiment was repeated three times independently with 6 replicates. (***P= 0.0002, ****P<0.0001 and ns=non-significant).

4.3.9 Effects of ICEs on antibiotic susceptibility

Disc diffusion and E-test strip methods were used to study the effects of ICE on antibiotic susceptibility. Overall, ICE-1 knockout mutants were found more susceptible against all varoius antibiotics used. Whereas, the ΔICE-2 strain only showed increased resistance to spectinomycin and streptomycin (Figure 4-13A).

The Ybt transporters encoded by HPI belong to the ABC and MFS family of transporters. This family of proteins was previoulsy demonstrated to act as as efflux pumps for various antibiotics (Lubelski et al., 2007). To explore the contribution of HPI here antibiotic susceptiblity was re-assessed in the presence of reserpine (50 µg/ml), an inhibitor for antibiotic exporters (Garvey and Piddock, 2008). Interestingly, reserpine increased the susceptibilities of the WT but did not affect the ΔICE-1 mutant strains. Furthermore, the antibiotic sensitivity pattern of ΔICE-1_{Pybt} strain with and without reserpine (Figure 4-13B) indicated that presence of HPI exporters enhanced the effect against various antibiotics**.** Finally, MICs were performed using E-test strips for selected antibiotics and the results are shown in Table 4-4. Approximately six fold reduction in MIC was observed in ICE-1 knocout strain against streptomycin, where as ~4 fold enhanced susceptibilities were observed against ceftazidime, erythromycin and rifampicin.

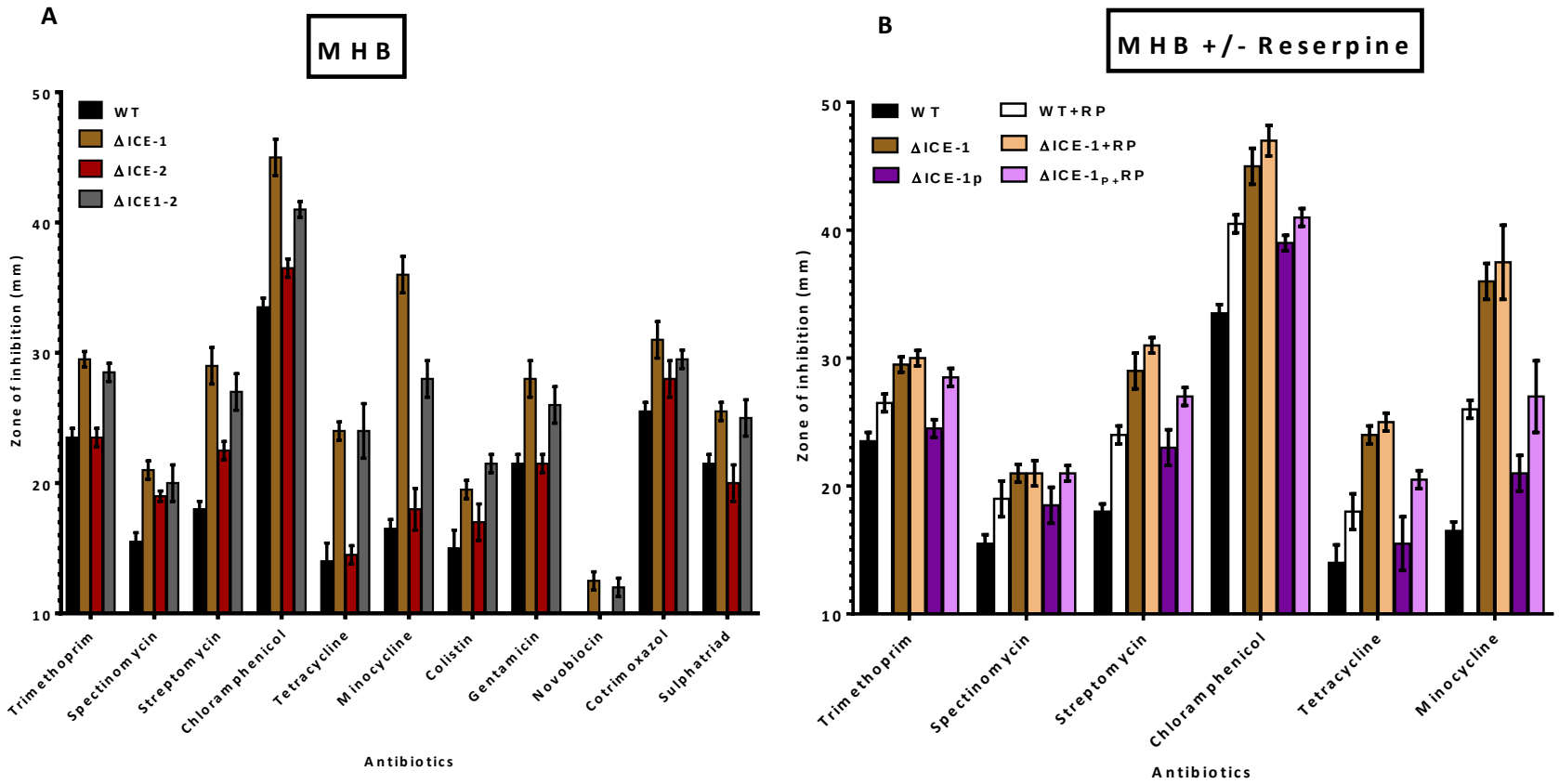

Figure 4-13 Antibiotic susceptibility of *K. pneumoniae* HS11286 and its ICE deletion mutants by disc diffusion.
A. Reserpine free MHB. B. ABC and MFS associated antibiotics were assessed with and without reserpine and the ΔICE-1P (complementing Pybt) was included to investigate contribution the Ybt transporters RP - reserpine.

Table 4-4 Minimum inhibitory concentrations (MIC) of WT and ICE mutants by E-test.

	Antibiotics[a] E-test strips (MIC ± SD)					
Strains	**Streptomycin** 0.064-1024 (µg/ml)	**Ceftazidime** 0.016-256 (µg/ml)	**Erythromycin** 0.016-256 (µg/ml)	**Tetracycline** 0.016-256 (µg/ml)	**Rifampicin** 0.002-32 (µg/ml)	**Nalidixic acid** 0.016-256 (µg/ml)
WT	2.1 ± 1.5	1.9 ± 0.2	35.6 ± 10.3	3.2 ± 1.1	11.2 ± 1.8	R[a]
ΔICE-1	0.37 ± 0.1	0.6 ± 0.1	8.7 ± 3.1	1.8 ± 0.3	2.3 ± 0.6	R
ΔICE-2	0.6 ± 0.1	0.5 ± 0.2	14.4 ± 2.2	2.3 ± 0.7	2.9 ± 1.1	R
ΔICE-1-2	0.4 ± 0.1	0.7 ± 0.1	10.8 ± 3.8	2.1 ± 0.5	2.1 ± 1.1	R

a= R (resistant)

4.3.10 Investigation of ICE-1 and ICE-2contributions to virulence in the *G. mellonella* larval killing assay

The WT bacterial load required to cause death of half (LD_{50}) of the population in each group (7-8 larvae in a group of 15 larvae) at the end of day 5 was first determined to be 20µl of an 0.8 OD_{600} (~ 5.5×10^6 Cfu). Following the determination of LD_{50} the dose that was 10 fold higher than the LD_{50} was used for the determination of surviving percentage of *G. mellonella* with WT and each of the ICE mutants using the same method. Compared to WT, the ΔICE-2 mutant appeared significantly (P= 0.008) less virulent (Figure 4-14). The ΔICE-1 and double mutants produced mortalities that were not significantly distinct from the WT. Although the presence of ICE-2 appears important for virulence in this system this effect was lost in the double mutant (Figure 4-14).

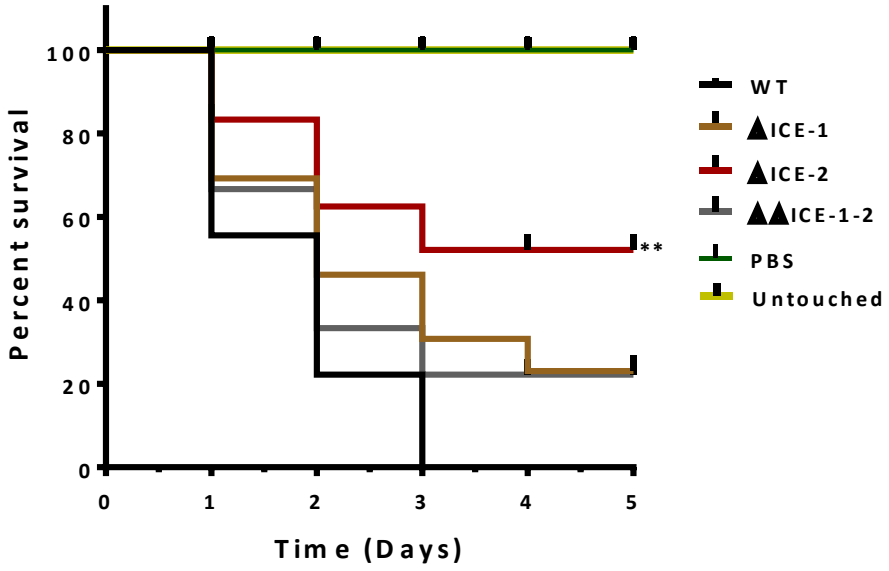

Figure 4-14 Effect of ICEs on the virulence of *K. pneumoniae* HS11286.
A group of 15 larvae were used per treatment (n=3). The mortality of *G. mellonella* was noted after every 24 hr consistently for 5 days. ** P = 0.008 calculated using one way ANOVA.

4.3.11 Phenotypic characterisation of *E. coli* carriyng ICE-1

The ICE-1 transfer to *E. coli* will be discussed in section 5.3.4. Three transconjugants were randomly selected for the growth assay, siderophore secretion and antibiotic susceptibility tests.

Both growth assays of *E. coli* and three *E. coli*$^{ICE-1}$ strains revealed no significant differences. However, significant differences were observed in siderophore secretion with significantly wider halo zone in the transconjugants (39 vs 45 mm).

To investigate whether presence of ICE-1 also affected antibiotic resistance in *E. coli*. In antibiotic disc diffusion assays, significant reductions in inhibition zones were observed in strains carrying ICE-1; the zones were increased in the presence of reserpine (Figure 4-15).

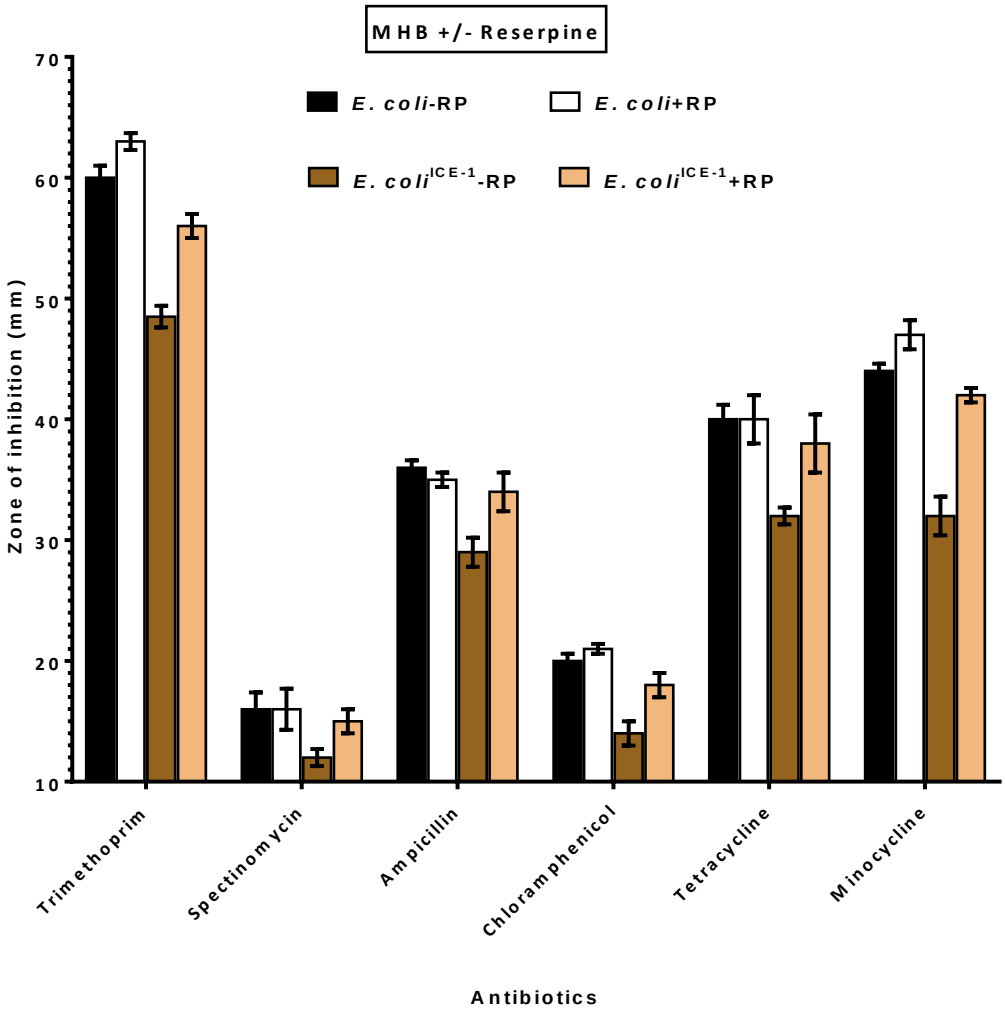

Figure 4-15 Antibiotic susceptibilities of *E. coli* HB101 against various antibiotics.
Susceptibility tests were performed on three randomly selected transconjugants (HB101^{ICE-1}); based on no significant differences among their results, the data are from one transconjugant. –RP and +RP indicates absence and presence of reserpine in the medium.

4.4 Discussion

The overall aim of this work was to investigate the contribution of ICE-1 and ICE-2 to *K. pneumoniae* phenotypes.

4.4.1 Ybt produced by HPI of ICE-1 was required for optimal growth

It was conclusively demonstrated that the ICE-1 mutant showed reduced growth both in rich and in minimal media; the defects were linked to the absence of the Ybt system encoded by HPI in ICE-1.

Due to its role in iron uptake (Schubert et al., 2000, Mokracka et al., 2004, Russo et al., 2015), Ybt has been linked to growth fitness, particularly in iron restricted conditions (Hancock et al., 2008, Paauw et al., 2009, Bachman et al., 2011). HPI has been divided into three regions. 1) Ybt biosynthesis (*irp1, irp2*, *ybtE, ybtT* and *ybtS)* (Carniel, 2001), 2) Ybt transport and 3) Ybt regulation system (Figures 4-1 & 4-5). In multiple Gram-negative bacteria, disruption of Ybt has resulted in growth defects (Smati et al., 2017, Lawlor et al., 2007, Paauw et al., 2010). For example, disruption in *irp2* impaired the growth of an *E. coli* mutant strain compared to its parent (Smati et al., 2017).

In the Ybt transport system, YtbP and YtbQ are importers while YtbX mediates the export of Ybt. In HPI, these transporters are present in a single operon (*ybtsxqp*). To avoid polar effects, the whole operon was cloned in pACYC184 under the control of its native promoter (Figure 4-5). The growth defects in the ICE-1 mutant were partially complemented by the PYbt plasmid (ΔICE-1_{Pybt}) but only in the presence of WT supernatant (Figure 4-6) which was assumed to contain Ybt.

The Ybt system requires TonB-dependent FyuA (Figure 4-1) to internalise iron (Brem et al., 2001). Interestingly, ΔICE-$1_{P\text{-}ybt}$ recovered growth even in the absence of *fyuA*, raising questions about its essentiality for iron uptake. Fetherston et al. (2010) showed similar behaviour in a *fyuA* mutant of *Y. pestis.* Thus it is speculated that an alternative TonB dependent receptor was used in this case.

A.

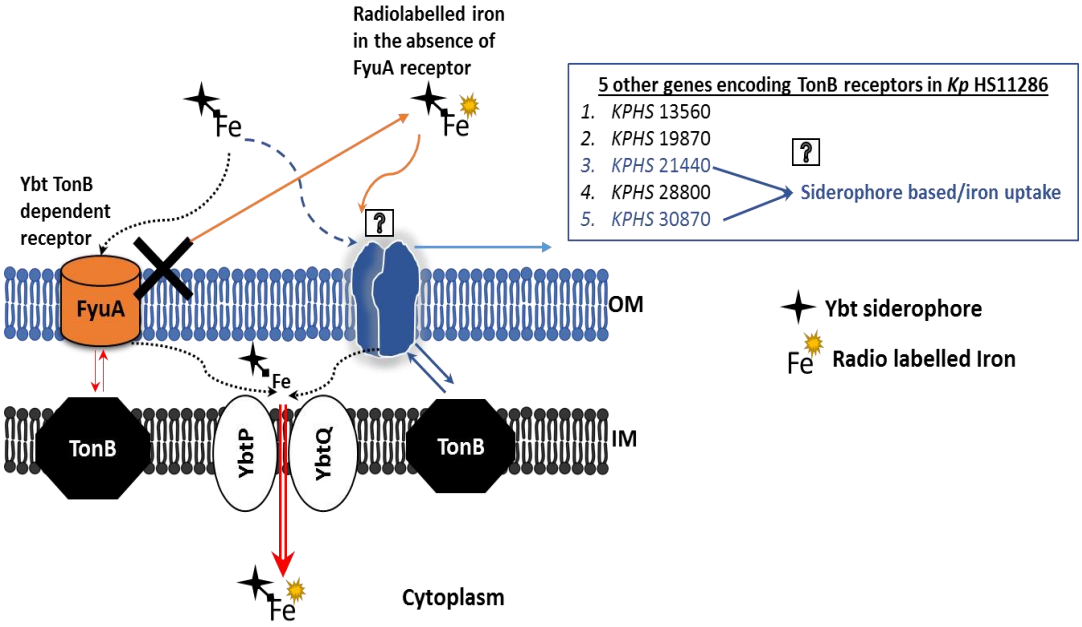

B.

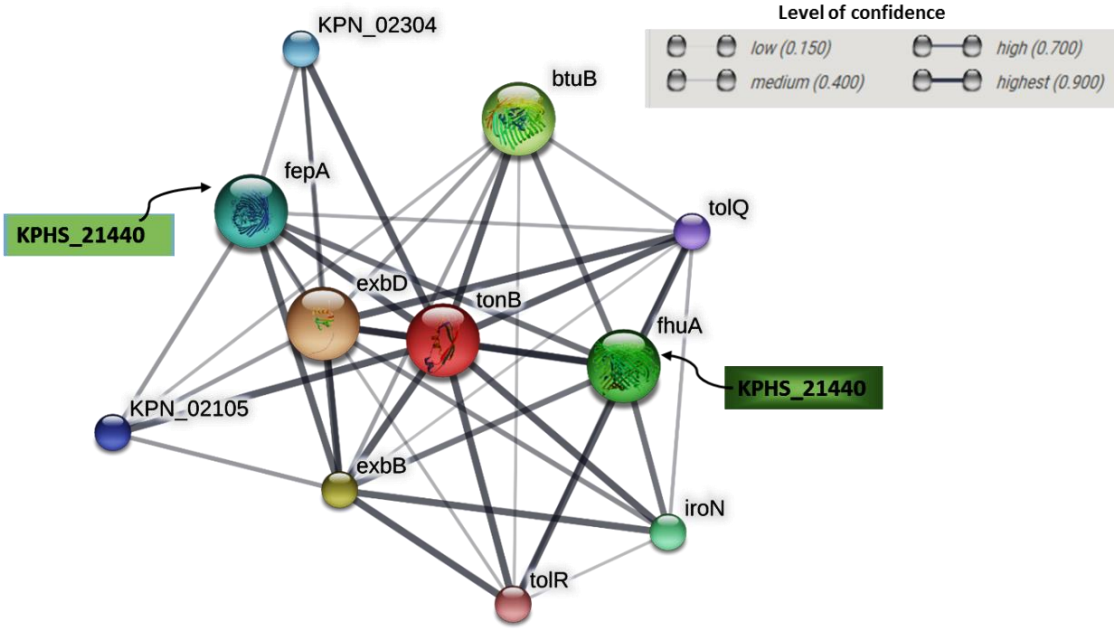

Figure 4-16 TonB dependent siderophore receptors and their interactions.
A. Schematics of Ybt based iron uptake via TonB dependent receptors. B. String analysis was performed for TonB and its interactions with other siderophore based receptors. The thickness of lines indicates the strength of interactions. The black arrows represent the homology between putative siderophore receptors of HS11286 and other well characterised receptor proteins.

Different TonB dependent siderophore receptors share similar ligand binding sites that facilitate the interactions between several iron uptake systems (Carniel, 2001). *Enterobacteriaceae* carry several TonB dependent receptors such as IroN for siderophore based iron uptake (Hsieh et al., 2008, Holden et al., 2016).

K. pneumoniae HS11286 has 6 genes encoding TonB dependent receptors including *fyuA*, among them two (*KPHS*_21440 and *KPHS*_30870) are siderophore based receptors (Figure 4-16A). BLASTp analysis of these two putative receptors showed that they belong to a family that are able to bind to siderophores of various systems. String analysis with TonB shows strong TonB-*fhuA* and TonB-*fepA* interactions, which are the siderophore-based receptors. *KPHS*_21440 and *KPHS*_30870 of *K. pneumoniae* HS11286 showed homology to these two (*fhuA* and *fepA*) well characterised siderophore receptors of *Enterobacteriaceae* (Figure 4-16B). These proposals could be further investigated by creating a *fyuA* knockout and by quantifying radiolabelled iron internalisation.

4.4.2 The Ybt system is important for *K. pneumoniae* growth in iron restricted conditions

The siderophore secretion of the ICE mutants was assessed against WT using the CAS assay. This assay is widely applied (Louden et al., 2011) and has been used extensively for siderophore detection in Gram-negative bacteria (Machuca and Milagres, 2003, Pérez-Miranda et al., 2007). The reduced level of siderophore secretion by the ΔICE-1 and ΔΔICE-1-2 strains (Figure 4-7A) was linked to the loss of the Ybt system.

The findings of siderophore secretion were extended by demonstrating its importance for growth in iron restricted conditions (Figure 4-7). Interestingly, WT (DIP) showed similar decline in growth as was shown by ΔICE-1 in LB. This finding is consistent with the interpretation that iron restriction was responsible in both cases. Similar findings were also documented by Lawlor et al. (2007), who showed slow growth of ybtS and *fyuA* mutants of *K. pneumoniae* ATCC-43816 in the presence of DIP. In addition, enhanced expression of *fyuA* was also observed under iron restriction (Lawlor et al., 2007).

4.4.3 Creation of the ICE-1 deletion was associated with histidine dependence.

Growth of WT and ICE mutant strains was compared in minimal medium, and the inability of ΔICE-1 to grow raised several questions.

An in-frame deletion of ICE-1 was confirmed by sequencing the upstream and downstream regions of the deleted fragment. In addition, sustained Cfu counts after continuous incubation for 10 days indicated that M9 had no cidal effects on the mutant strain (data not shown). Moreover, trace elements (1X) were added to the minimal medium to confirm that growth defect of ICE-1 mutant was not due to lack limitation of trace elements. However, no differences in growth defects was observed thus confirmed that inability of ICE-1 mutant strain was not associated to the limitation of trace elements in M9.

Growth recovery of ΔICE-1 in peptide and amino acid containing media indicated that the mutant strain was unable to utilise NH_4Cl as a nitrogen source. Casamino acid supplementation produced greatest improvement and this led us to investigate single amino acid sources and histidine was found to be essential (Figure 4-11).

The two initial substrates of histidine biosynthesis, PRPP (phosphoribosyl pyrophosphate) and phosphoribosyl-ATP, play a key role in the intermediate and energetic metabolism of histidine. In addition, unlike other prokaryotic operons, organisation of genes in the *his* operon is variable among different species indicating a strict requirement of this pathway for survival (Fani et al., 1998). Furthermore, histidine biosynthesis is one of the most energy-dependent metabolic pathways requiring 41ATPs per histidine molecule (Juliao et al., 2007); suggesting it's interaction to several other energy regulatory pathways.

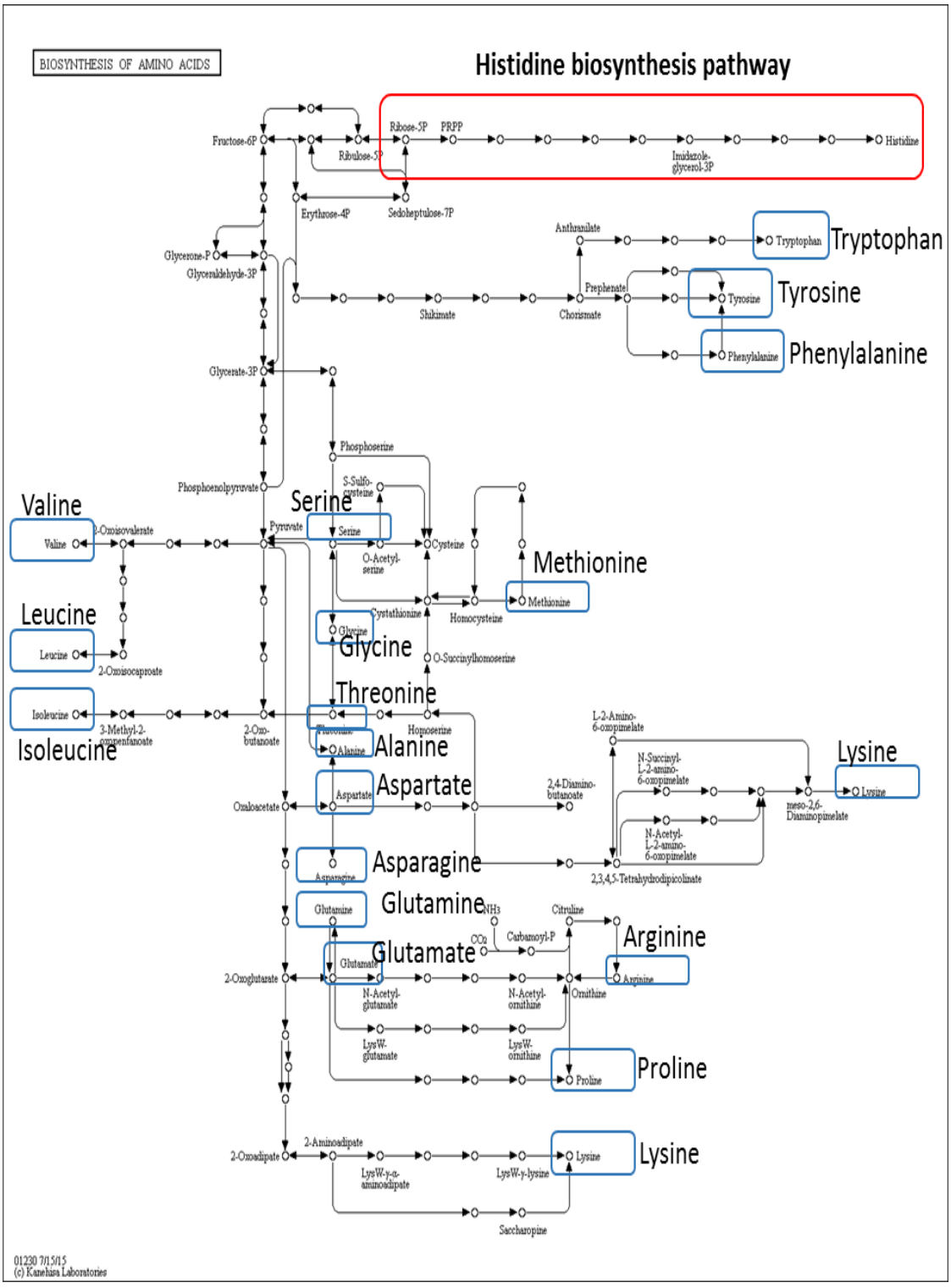

Figure 4-17 Schematics of pathways of biosynthesis of 20 amino acids.

Adapted from Kyoto Encyclopaedia of Genes and Genomes (KEGG) http://www.genome.jp/kegg-bin/show_pathway?map01230

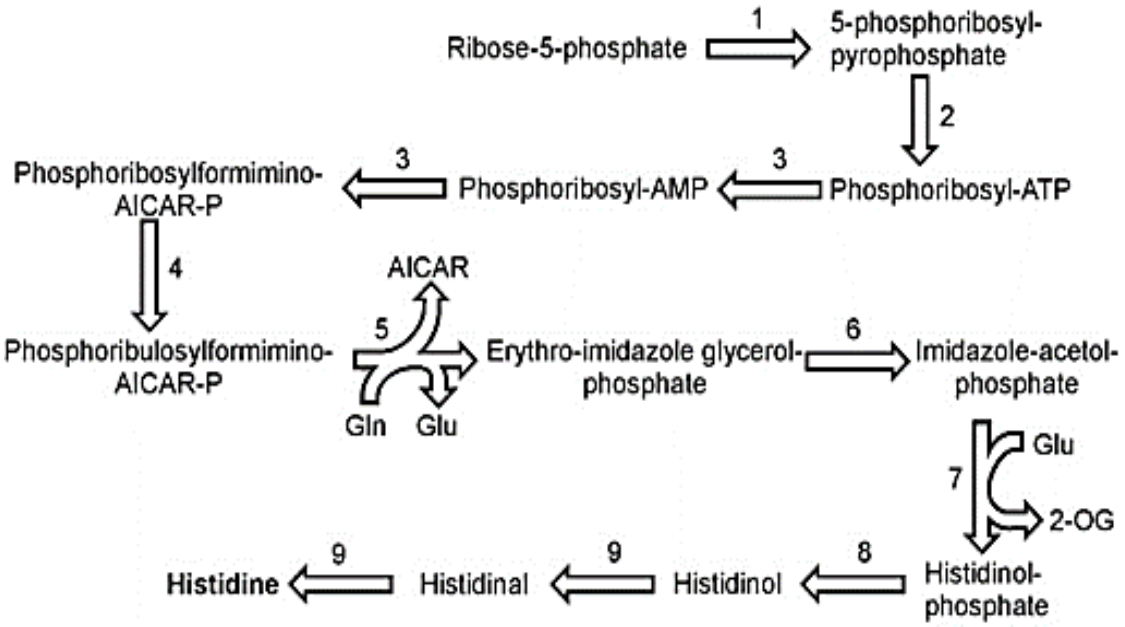

Steps	*Enzymes*
1	Ribose-phosphate diphosphokinase
2	ATP phosphoribosyltransferase
3	Phosphoribosyl-ATP pyrophosphatase
4	Phosphoribosylformiminoaicar-p isomerase
5	Imidazole glycerol phosphate synthase
6	Imidazoleglycerol-phosphate dehydratase
7	Enzyme histidinol-phosphate transaminase
8	Histidinol phosphate phosphatase
9	Histidinol dehydrogenase

Figure 4-18 Histidine biosynthesis pathway.
Adapted from (Bromke, 2013)

In *K. pneumoniae* HS11286, the histidine biosynthesis operon *hisABCDEF* (Kulis et al., 2014) lies ~39kb downstream to ICE-1. Bioinformatic analysis did not reveal any direct relationship between histidine biosynthesis and ICE-1 contents. Thus it was speculated that histidine biosynthesis might be affected due to an incidental lesion either in *his*-operon or in related other regulatory systems. Whole genome sequencing would potentially identify lesion(s) responsible for the histidine-dependent phenotype.

4.4.4 ICEs influence biofilm formation

Significant differences of biofilm formation on an abiotic surfaces were observed between WT and ICE mutant strains (Figure 4-12). This was consistent with previous observation on bacteria carrying conjugative plasmids and the contributions of these mobile elements to biofilm formation. T4SS-associated pili are the major components of the conjugative machinery involved both in cell-cell contact and in biofilm formation (Ghigo, 2001, Reisner et al., 2003, Zechner et al., 2012).

Initially it was thought that the differences in biofilm formation was only due to presence or absence of T4SS of ICE1 and ICE-2. However, a more careful analysis of previous literature revealed that there are several other factors that could have enhanced biofilm formation. *fyuA* appears to play a major role and was found to be one of the major up-regulated genes in biofilms; its disruption aborted biofilm development in *E. coli* (Hancock et al., 2008, Hancock and Klemm, 2007). Another important factor was found to be the methyl-accepting chemotaxis protein (MCP) of ICE-2, this was demonstrated to be involved in biofilm formation and biosynthesis of T4 pili in *Ps. aeruginosa* (Morgan et al., 2006, Hickman et al., 2005).

These results were extended by microscopic examination. There was agreement between findings obtained by both methods. The enhanced biofilm formation detected by crystal violet was linked to differences in the pattern of development (Appendix XII). The ΔICE-2 developed a filamentous form of biofilm and this might be due to the polar localisation of pili encoded by the T4SS-1 ICE-1 (Das and Das, 2014).

4.4.5 ICE-1 deletion enhaced antibiotic susceptibilities

K. pneumoniae HS11286 is naturally resistant to several antibiotics (Bi et al., 2015, Liu et al., 2012). ICE-1 knockout mutants showed increased susceptibility against various antibiotics.

No recognised specific antibiotic resistance determinants are present on ICE1. However, inspection of HPI transporters (YbtX, YbtQ and YbtP) revealed that YbtX is a member of the major facilitator super family (MFS), while YbtP, YbtQ are both ABC transporters. These exporters are known to be major drug efflux systems (Paulsen and Lewis, 2001, Lubelski et al., 2007, Soto, 2013).

These two systems are categorised on the basis of their transmembrane spanning regions, mode of action and the type of molecules exported (Piddock, 2006a, 2006b). ABC transporters are ATP dependent export channels, whereas the MFS are drug/H+ antiporters (Marger and Saier, 1993). The results reported here are similar to those of Srinivasan et al. (2014), who showed that disruption of the MFS system, *KpnGH,* increased the sensitivity of *K. pneumoniae* to many antibiotics and suggested that was due to loss of Ybt exporters.

Resistance to ABC/MFS related antibiotics (Figure 4-13) and its reduction in the presence of reserpine (Figure 4-13 and 4-19) adds weight to the view that Ybt exporters influenced the antibiotic susceptibilities. Bambeke et al. (2000) showed that ABC/MFS systems are responsible for extruding rifampicin, tetracycline and aminoglycosides. The E-tests showed a 6 fold reduction in MIC for erythromycin and this fits well with the findings of Poole (2005), who demonstrated that ABC-transporters are specific for expelling erythromycine in *E. coli*. Thus the role for the Ybt exporter in this context is further supported; deletion and complementation of *ybtX* would provide more definitive evidence.

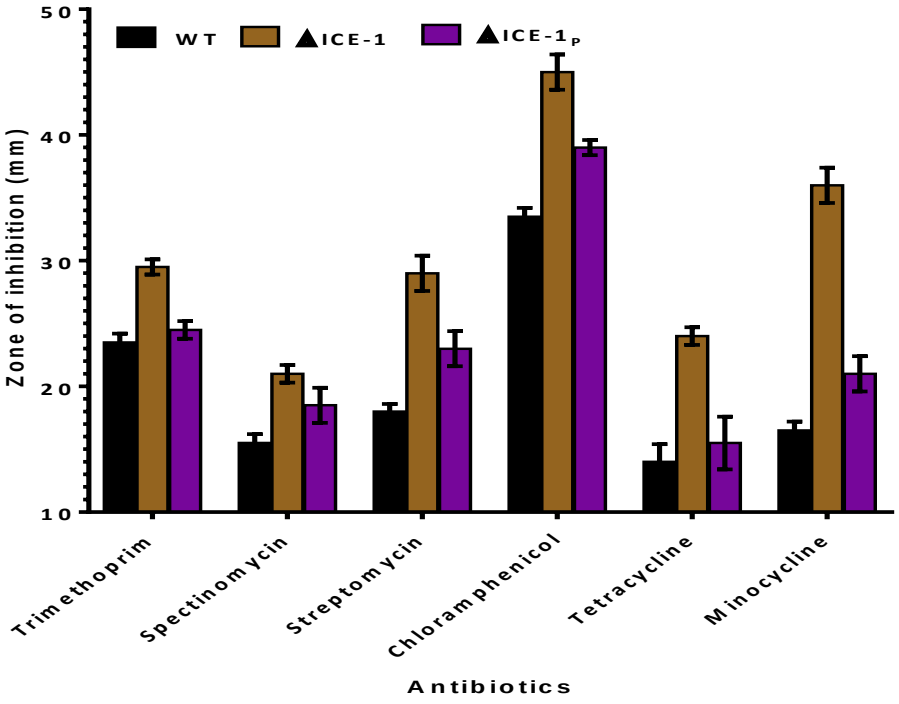

Figure 4-19 Summary of comparison of antibiotic resistance

The ICE-1 knockout showed sensitivity to novobiocin (Figure 4-13) while the WT was resistant. Similar behaviour of an ABC exporter transporting novobiocin was reported in *Enterococcus faecalis* and *Streptococcus pneumoniae* (Davis et al., 2001, Robertson et al., 2005). Recently, Lam et al. (2017) described a link between emerging virulence, antibiotic resistant lineages and the Ybt system in *K. pneumoniae* strains.

4.4.6 ICE contribution to virulence

ICE-2 deletion caused attenuation that may be linked to the presence of several virulence associated components (section 3.3.2). The SecA translocase (*orf23*) was considered one of the major factors involved in virulence because it is responsible for translocation of various virulence associated effector proteins (Manting and Driessen, 2000). Another possible explanation for attenuation was the loss of methyl accepting chemotaxis protein (MCP) encoded by *orf47.* MCP was identified as the chemo-sensor interacting with T4 pili for surface-specific adhesion, twitching motility and expression of pathogenicity associated genes in *Ps. aeruginosa* (Persat et al., 2015). Several other virulence associated factors are present in ICE-2; these include the cold shock protein encoded by *orf13* and the toxin-antitoxin system *symE* (*orf24*). The findings here are also consistent with the associated genes described in PAPI-1 and PAPI-2 of *Ps. aeruginosa* PA14 (Miyata et al., 2003, He et al., 2004, Lee et al., 2006, Harrison et al., 2010).

An interesting and unexpected result was the lack of attenuation in the double mutant strain (Figure 4-14). Perhaps increased biofilm forming capacity may have counteracted the loss of virulence determinants in the Galleria model.

4.4.7 ICE-1 influenced *E. coli* phenotype

Three randomly selected transconjugants were studied for growth patterens, siderophore production and antibiotic susceptibilities. Consistant with the studies on the ΔICE-1 mutant, siderophore production and antibiotic resistance was significantly increased in transconjugants compared to the parent strain without obvious effects on growth. This provides further support for the role of the Ybt exporters discussed above.

4.5 Conclusions

1. Ybt produced by HPI enhaced growth of *K. pneumoniae* HS11286 in iron limited conditions.
2. Deletion of ICE-1 reduced the siderophore secretion and growth capabilities of bacteria in iron restricted enviroment.
3. Deletion of ICE-1 was associated with histidine dependence in the mutant strain but this was likely attributable to a lesion external to ICE-1.
4. Deletion of ICEs influenced biofilm formation by the host.
5. Presence of ICE-1 enhaced resistances against various antibiotics, especially to those associated with ABC and MFS exporters .
6. Deletion of ICE-2 increased attenuation but the effect was lost in the double mutant.
7. ICE-1 acquisition by *E. coli* had no effect on growth of transconjugants.
8. Transconjugants secreted significantly more siderophore compared to parent *E. coli*.
9. ICE-1 increased the antibiotic resistance of transconjugants against many ABC and MFS associated antibiotics.

Chapter 5 Mobilisation and integration of ICE-1

5.1 Introduction

Putative ICEs meet the definition of this class of genetic element if they can be shown to: (a) excise from the host chromosome, (b) generate extrachromosomal intermediates, (c) achieve horizontal transfer mediated by conjugation, and (d) integration into the recipient host chromosome (Johnson and Grossman, 2015).

ICEKP-1 elements are widely distributed in *Enterobacteriaceae* (chapter 3). However, whether or not they are functional in mobilisation has not been demonstrated for the majority. In recent studies, the functional elements of ICEKP-1 have been demonstrated in *E. coli* (ICEEc-1) (Schubert et al., 2004) and in *K. pneumoniae* NTUH-K2044 (ICEKp-1) (Lin et al., 2008). ICE excision from the genome and self-conjugation to other hosts has been shown to pass through episomal intermediates for the majority of elements (Schubert et al., 2004) and has been demonstrated for ICEKp-1 and ICEEc-1 (Schubert et al., 2004, Lin et al., 2008). However, in *E. coli* high excision of ICEEc-1 was achieved with induced integrase (Schubert et al., 2004). Generation of episomal intermediates is an essential step in the successful conjugative transfer of the majority of ICEs. Moreover, the ICE usually carries its own mobilisation system that mediates its transmission (Wozniak and Waldor, 2010). ICEEc-1 and ICEKp-1 have been shown to have functional modules that mediate mating pair formation and processing of DNA.

Stage (b) of the ICE mobilisation cycle is the assembly of several gene products into a mating channel that transfers DNA from donor to recipient (Johnson and Grossman, 2015); functional ICEs include *oriT* which includes *nic* sites for the generation of ssDNA. The *oriT* containing region of ICEKP-1 elements (ICEEc-1 and ICEKp1) normally lies upstream to *mobB* (Schubert et al., 2004, Lin et al., 2008), which was first described in the CloDF13 plasmid of *Enterobacter cloacae* (Hochhut and Waldor, 1999, Burrus et al., 2002). Unlike CloDF13, ICEEc-1 and ICEKp-1 have an inverted repeat region in *oriT* which means they have duplicated *nic* sequences (Figure 5-1). Similar duplicated *nic* sites have been described in the R6K plasmid (Avila et al., 1996, Schubert et al., 2004).

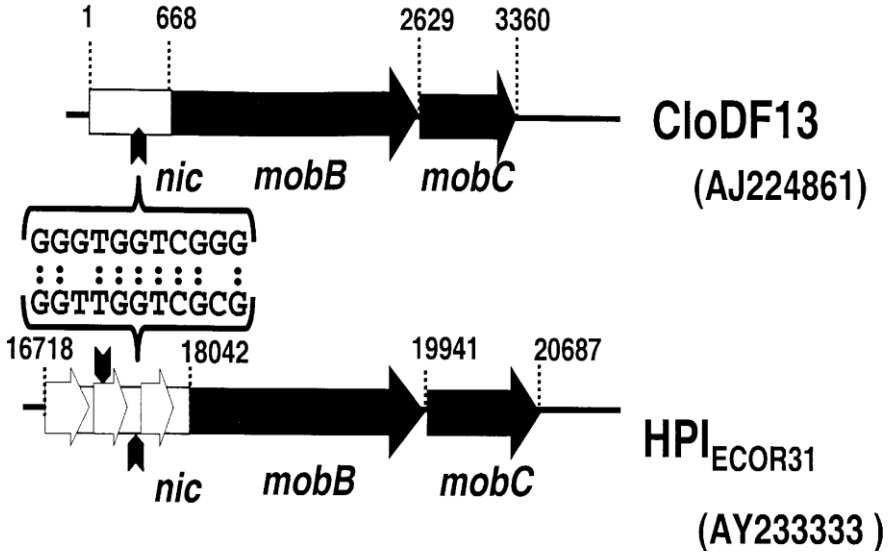

Figure 5-1 *nic* regions of CloDF13 and ICEEc-1 (HPI_{ECOR31}).
The brackets mark the map position of the *nic* site and its sequence similarities. The black arrow heads indicate the position of *nic* sites. (Schubert et al., 2004)

The T4SS of ICEKP-1 elements belong to the VirB/VirD4 system; this is a homologue of the T4SS found in *A. tumefaciens* (Juhas et al., 2008) (c.f. Chapter 1). The T4SS of ICEKp-1 was demonstrated to be functional for formation of mating pores and was capable of processing of DNA-protein complexes (Lin et al., 2008). To date little attention has been paid to the impact of effects of the ICEKP-1 cargo genes, such as HPI, on host phenotype.

5.1.1 Aim

To study the complete life cycle of ICE-1 and possible effects of its cargo genes on recipient phenotype.

5.1.2 Objectives

1. To determine the site-specific excision of ICE-1.
2. To investigate functionality of the mobilisation module of ICE-1 by;
    a. Conjugative-mobilisation of intact ICE-1 from host to recipient.
    b. Conjugative mobilisation of an ICE-1 marker plasmid (*E. coli* HB101).
3. To investigate the conservation of *oriT* and its repeated sequences among *Enterobacteriaceae* carrying putative ICEKP-1 elements.
4. To identify the minimal *oriT* sufficient for conjugative transfer of DNA in ICEKP-1 elements.

5.2 Methods

5.2.1 Excision assay

Episomal ICE intermediates were detected by PCR using genomic and plasmid DNA as template. To amplify either the chromosomal junction or the episomal form of ICE, minor modifications were made in the methods described by Lin et al. (2008), Schubert et al. (2004). DNA was extracted from a batch of culture at 4, 8 and 24 hr. The amount of DNA assayed was controlled at 10 and 100ng/reaction mix.

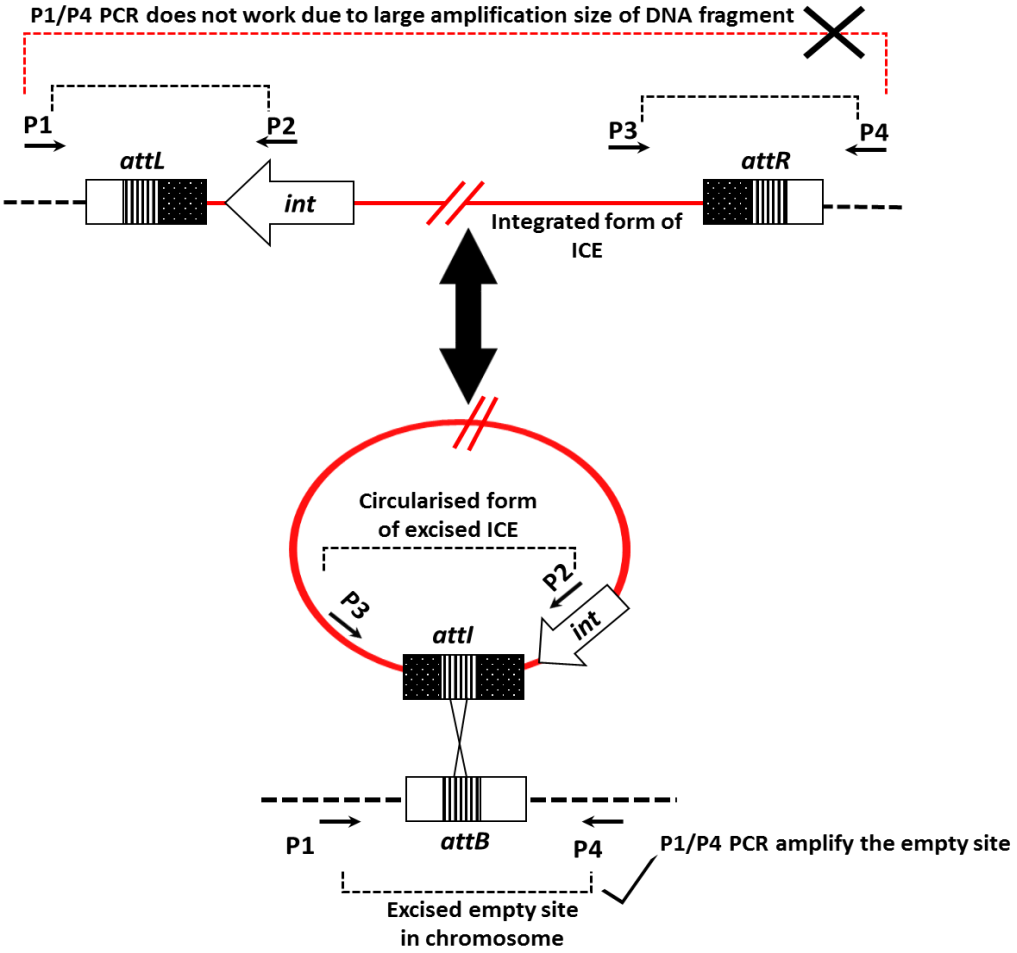

Figure 5-2 Schematics of ICE excision assay by PCR.
Primers P1, P2, P3 and P4 were used to confirm the integration/excision of ICE-1 .

The sensitivity of the experiment was controlled by the primers as shown in Figure 5-2. Primers pairs P1/P2 and P3/P4 were used to amplify the attL and attR sites. Whereas, P1/P4 and P2/P3 were used to detect empty sites in chromosome and the excised form, respectively. KOD Hot start DNA polymerase was used for all PCRs. To confirm the precise excision the PCR products were purified and sequenced.

5.2.2 Construction of ICE-1 marker plasmid

The purpose of the construction of ICE-1 marker conjugative plasmid was to analyse the DNA mobilization ability of ICE-1 and to confirm that it carries a functional T4SS. Plasmid pACYC184 was used to clone the *oriT* containing region of ICE-1. The pACYC184 was selected because it had previously been used for the construction of conjugative plasmid of other ICEKP-1 elements (Schubert et al., 2004, Lin et al., 2008).

Directed cloning by restriction and ligation was used to construct P-*oriT*1 (*oriT*1=1760bp region lies between *virB11* and *mobB* of ICE-1). The 1760bp region was amplified using *K. pneumoniae* HS11286 genomic DNA as template. HindIII and SalI restriction digestion sites were introduced in forward and reverse primers (Appendix III) used for the amplification of insert (Figure 5-5).

Both plasmid and *oriT* (PCR purified) fragment were double digested using HindIII and SalI endonucleases (NEB) (section 2.3.3). The fragments were gel purified and band sizes were again confirmed before the ligation. T4 ligase (Promega) was used for the ligation reaction (section 2.3.4), which was followed by its (4µl) electro transformation into electro competent *E. coli* DH5α (section 2.3.2). PCR assay was used to confirm the presence of the plasmid in the *E. coli* using pACYC184 specific primers (Appendix VIII). The precise construction was also confirmed via double digestion of plasmid extracted from culture transformants. *E.coli* DH5α transformed with the ICE-1 marker plasmid were archived at -20^{o}C and -80^{o}C for downstream experiments. Similar method were used to construct multiple versions of the ICE-1 marker plasmid for identification of the minimal *oriT*-1.

5.2.3 Conjugation assay

Mobilisation assays of ICE-1 marker plasmid and self-conjugation of ICE-1 was performed by filter mating assay (section 2.4.3).

5.3 Results

5.3.1 Site-specific excision of ICE-1

A PCR-based assay was developed to identify the generation of circular extrachromosomal intermediates of ICE-1; this is usually mediated by recombination between the direct repeats at the left and right junctions (*attL* and *attR*) of ICEs. Figure

5-3A outlines the assay used to detect the intact episomal state of ICE-1 and its empty chromosomal sites using specific primers (Appendix IX). Both genomic and plasmid DNA was used for the assay. Genomic DNA was used as a control for sensitivity and specificity of the assay. No PCR amplification was detected for the excised form of ICE-1 with 10ng of genomic DNA and a faint band could be seen with 100ng at 8 hr (Figure 5-3B). The empty chromosomal site was also not clearly detected. However, plasmid DNA analysis provided clear evidence of ICE-1 excision at 8 and 24 hr. Excision appeared to peak at early stationary phase then declined in established stationary phase (faint plasmid band at 24 hr). Sequencing of the PCR products confirmed the extrachromosomal and chromosomal junctions of ICE-1 (data not shown).

A.

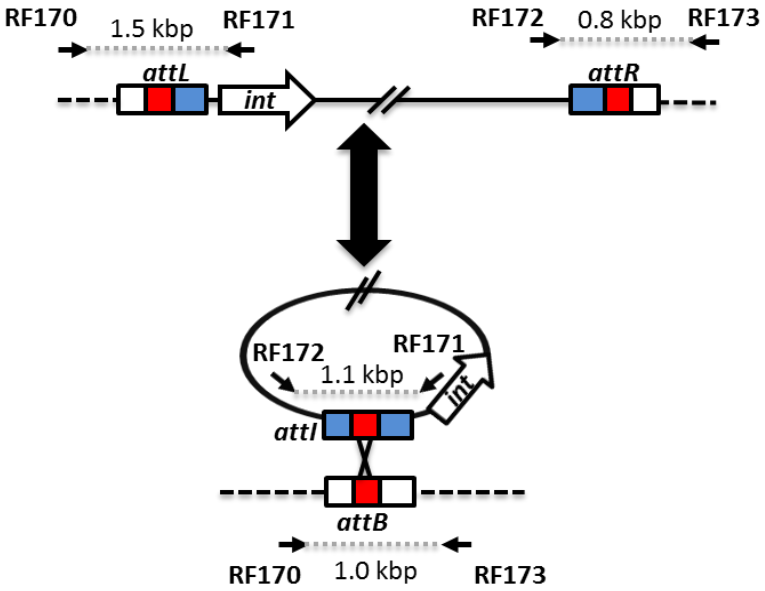

B.

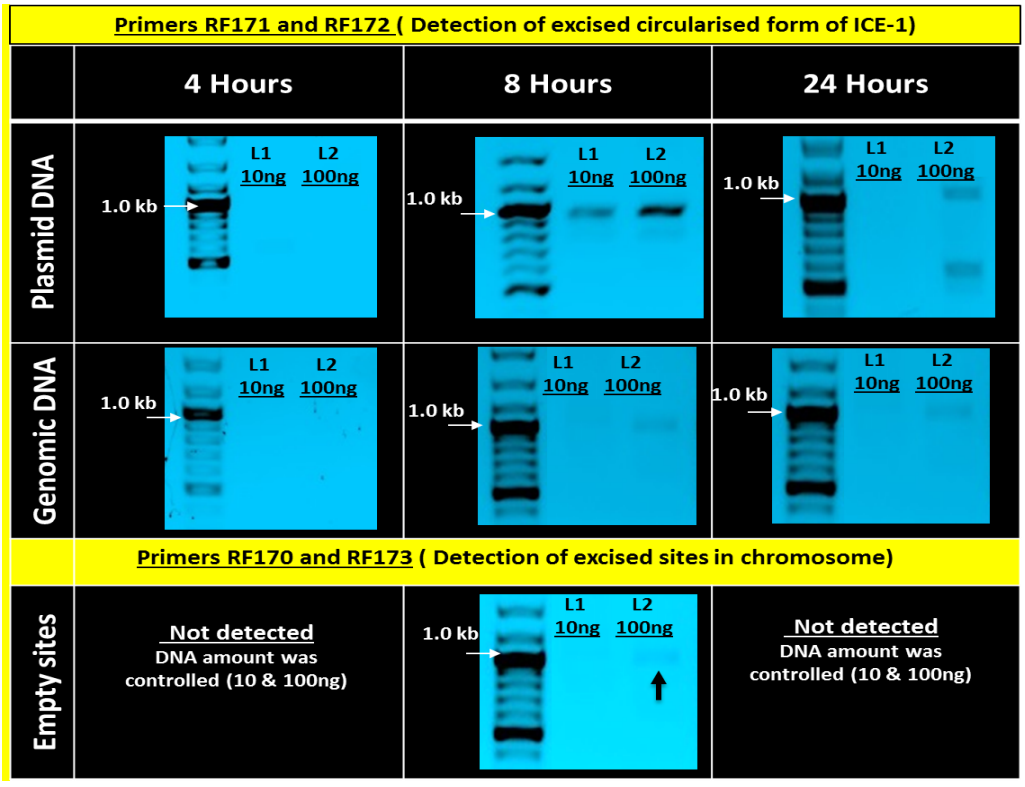

Figure 5-3 Site-specific excision and extrachromosomal circularisation of ICE-1.
A. Model of integration /excision of ICE-1. The small arrows above and below the map represents positions of primers used for different PCR assays. B. PCR results for the detection of empty sites in chromosome and excised form ICE-1 using both genomic and plasmid DNA.

5.3.2 Self-Conjugation of ICE-1

Mobilisation of ICE-1 to *E.coli* HB101 by conjugation was investigated. ICE-1 was marked with a hygromycin (hph) resistance cassette to enable selection of transconjugants. The *irp2* gene of ICE-1 was selected for (Figure 5-4) disruption as this was considered unlikely to interfere with ICE self-conjugation.

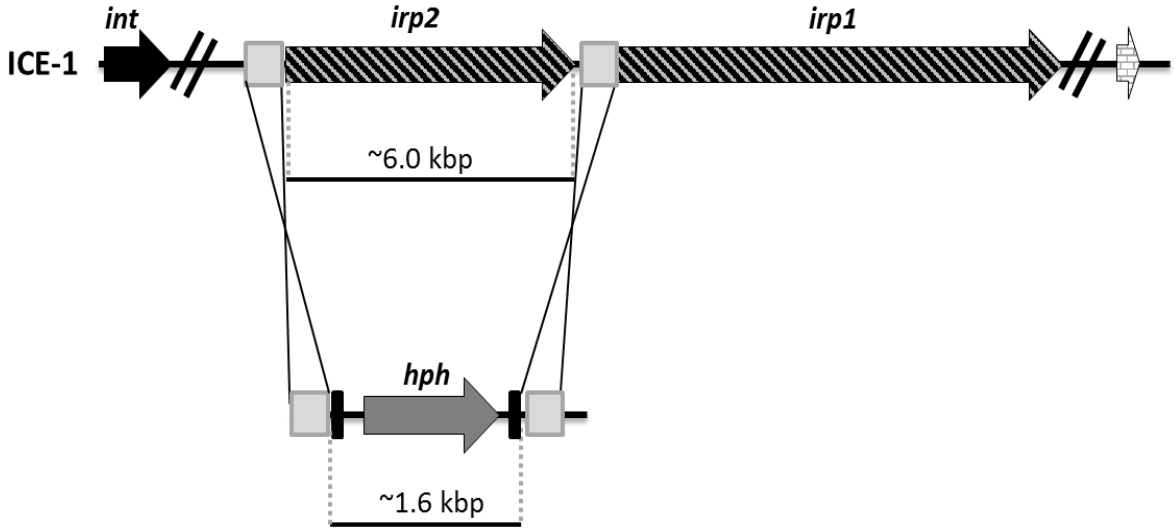

Figure 5-4 Schematics of ICE-1 tagging with hygromycin resistance cassette.
Irp2 of ICE-1 was replaced with *hph* cassette for self-conjugation assay of ICE-1. (This was done jointly with one of the collaborators Mr. Yingzhou Xie from Shanghai University China)

A conjugation assay was performed using the ICE-1^{hph} (donor). No transconjugants (limit of detection was <1×10^{-7}) were detected for the self-mobilised ICE-1^{hph}. Thus, either the ICE-1 was not able to mobilise itself or introduction of *hph* has affected the excision or transferability of the element. Potential effects of the *hph* cassette on the excision of ICE-1 were examined by performing an excision assay on the ICE-1^{hph} strain. No differences were apparent between excision of ICE-1 of the WT and the ICE-1^{hph} mutant strain (data not shown). These results are consistent either with ICE-1 being incapable of conjugative-mobilisation or with a defect in T4SS-1.

5.3.3 T4SS-1 of ICE-1 is functional and necessary for conjugative transfer of plasmid DNA

To verify that ICE-1 carries a functional T4SS (T4SS-1) an ICE-1 marker plasmid P-*oriT*-1 was constructed (Figure 5-5). The *oriT* region of ICE-1 was cloned into a low copy number plasmid, pACYC184 (section 5.2.2).

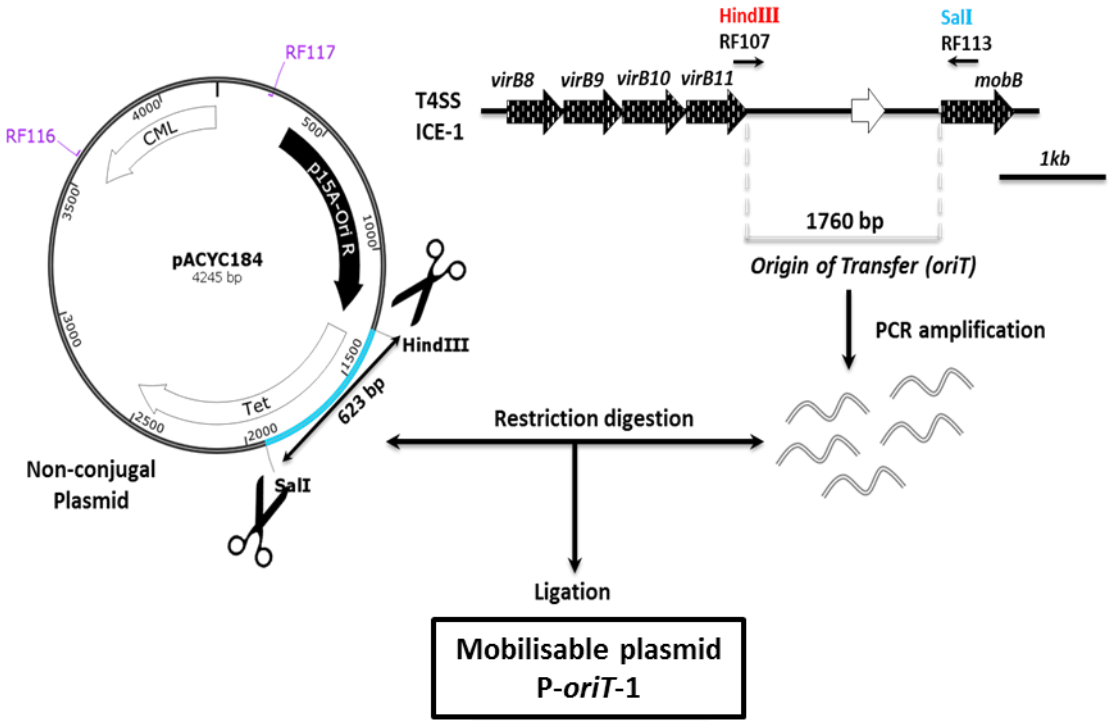

Figure 5-5 Schematics of construction of P-*oriT*-1 an ICE-1 marker plasmid for conjugation assay. For cloning, PCR amplified fragments of 1,760 bp from T4SS-1 and plasmid pACYC184 were double digested with HindIII and SalI followed by T4-ligation.

WT and ΔICE-1 strains were transformed with the P-*oriT*-1. *K. pneumoniae* NTUH-K2044 carrying P-*oriT*-1 and WT with pACYC184 were respectively used as positive and negative controls. To monitor the transfer of plasmid to the recipients (HB101; naturally resistant to streptomycin); transconjugants were selected on LB supplemented with streptomycin and chloramphenicol. The transfer frequencies of P-*oriT*-1 were calculated from data obtained from assays that were performed independently on four occasions with three biological replicates. As can be seen in Figure 5-6, the WT was able to mobilise the P-*oriT*-1 to recipient cells at a frequency of ~8.5×10^{-6}. The conjugation frequencies of WT were significantly higher compared to the control strain (Figure 5-6).

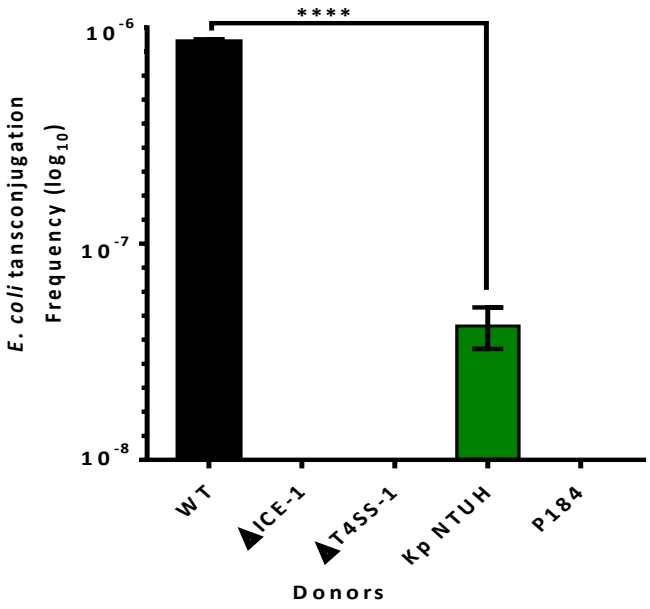

Figure 5-6 T4SS of ICE-1^{+poriT} is functional for mating pair formation.
K. pneumoniae NTUH-K2044 and WT+pACYC184 (P184) were used as positive and negative controls, respectively. (Error bars = Standard deviation, n=3, and **** = P<0.0001)

To confirm involvement of T4SS-1 in mobilisation, six genes (*virB1-virB6*) were mutated (Figure 5-7) to create the ΔT4SS-1 mutant strain. The mutated genes encode structural and functional proteins of the conjugative pilus. The ΔT4SS-1 strain was transformed with P-*oriT*-1 and conjugation assay showed no mobilisation of the ICE-1 marker plasmid (Figure 5-6). These results indicate that ICE-1 carries a functional conjugation module (T4SS-1).

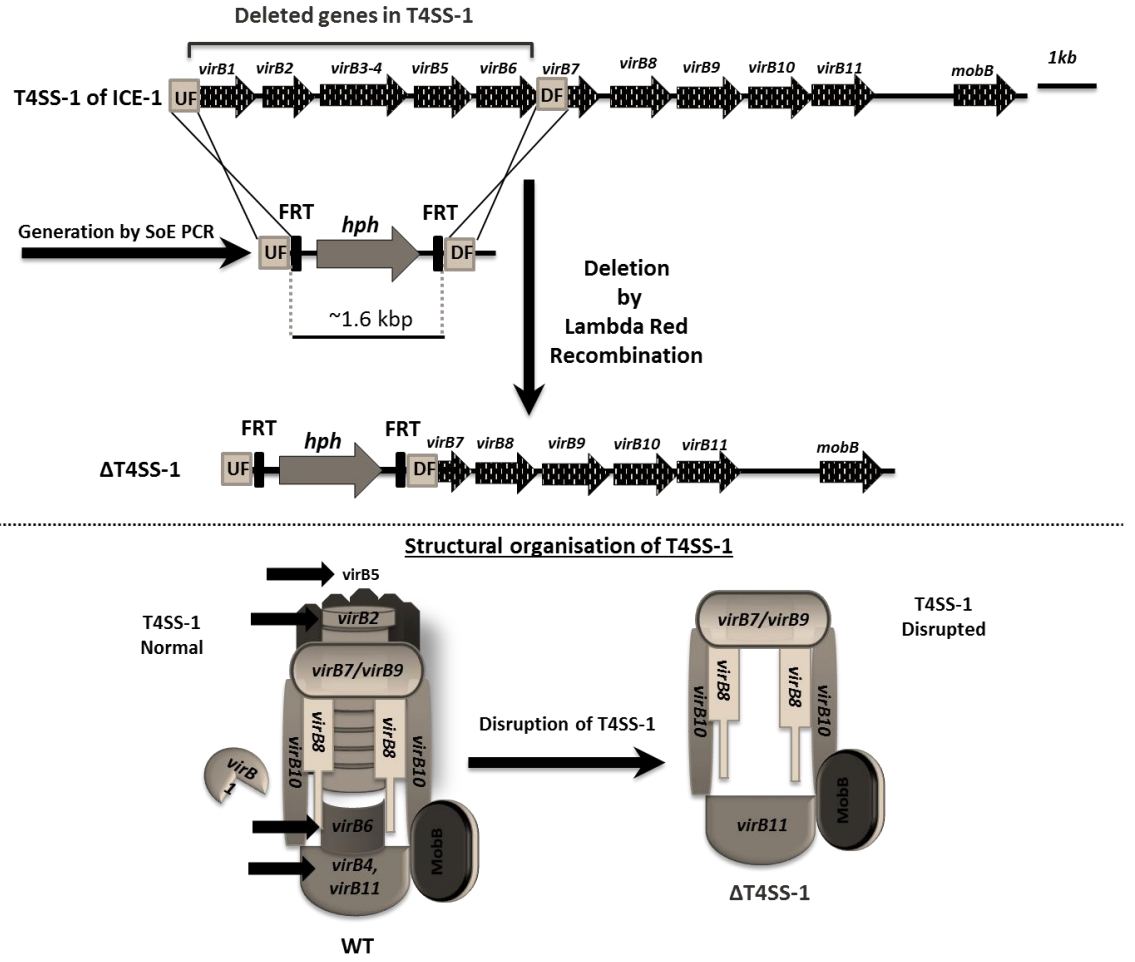

Figure 5-7 Schematic showing the disruption of T4SS-1 of ICE-1.
Six genes (virB1 to *virB*6) were deleted and this rendered the system non-functional for DNA transfer.

5.3.4 Plasmid mobilisation mediates self-conjugation of non-tagged ICE-1

While investigating transfer of the ICE-1 marker plasmid, transconjugants were PCR screened for the presence of marker genes (section 3.3.3.2 and Figure 3-8) of ICE-1. Surprisingly, all the transconjugants confirmed the presence of marker regions and also ICE-1 integration at the *asn-tRNA sites* (Figure 5-8). The transconjugants were identified to be *E. coli* by PCR (Appendix VIII). Moreover, to confirm that transconjugants were not contaminated by donor cells, the former were streaked for purity and genomic DNA extracted from overnight cultures. PCR screening was performed to confirm the presence of ICE-1 in *E. coli*.

Next, the conjugative-mobilisation of ICE-1^{hph} along with P-*oriT*-1 was investigated. The transconjugants were selected on three different sets of LB based selection media supplemented with: i) streptomycin and chloramphenicol, ii) streptomycin,

chloramphenicol and hygromycin and iii) streptomycin and hygromycin (Figure 5-9). Interestingly, no transconjugants were obtained on media containing hygromycin, however, plasmid mobilisation was observed on the streptomycin + chloramphenicol medium. These transconjugants were further investigated for the presence of ICE-1^{hph} but were found negative.

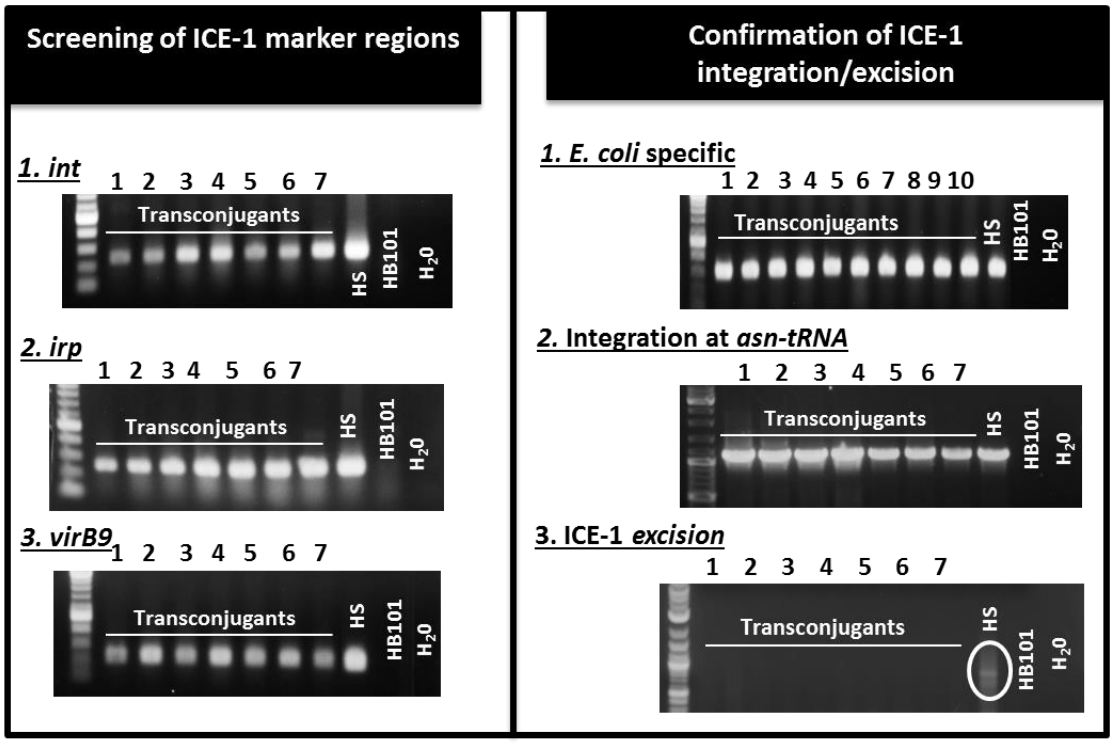

Figure 5-8 confirmation of presence and integration of ICE-1 in *E. coli* transconjugants.
Transfer of ICE-1 from *K. pneumoniae* to *E. coli* was confirmed by PCR. Presence of ICE-1 marker regions, integration site, and ICE-1 excision was confirmed in transconjugants. The transconjugants were also confirmed to be E.coli using its specific primers. *K. pneumoniae* Hs11286 and *E. coli* genomic DNA were used as positive and negative controls.

To exclude the possibility that the hygromycin resistance of the ICE-1^{hph} marked element was insufficient to detect mobilisation, selection of transconjugants was also attempted on lower concentrations of hygromycin (25 and 50 µg/ml) along with streptomycin (Figure 5-9). No transconjugants were obtained carrying ICE-1^{hph} but plasmid mobilisation was always observed. Finally, WT (with no P-oriT-1) was tested for mobilisation of ICE-1, *E.coli or* transconjugants were recovered on medium containing streptomycin only. Randomly 30 colonies of *E. coli* were PCR tested for the presence of ICE-1 but no amplification were obtained.

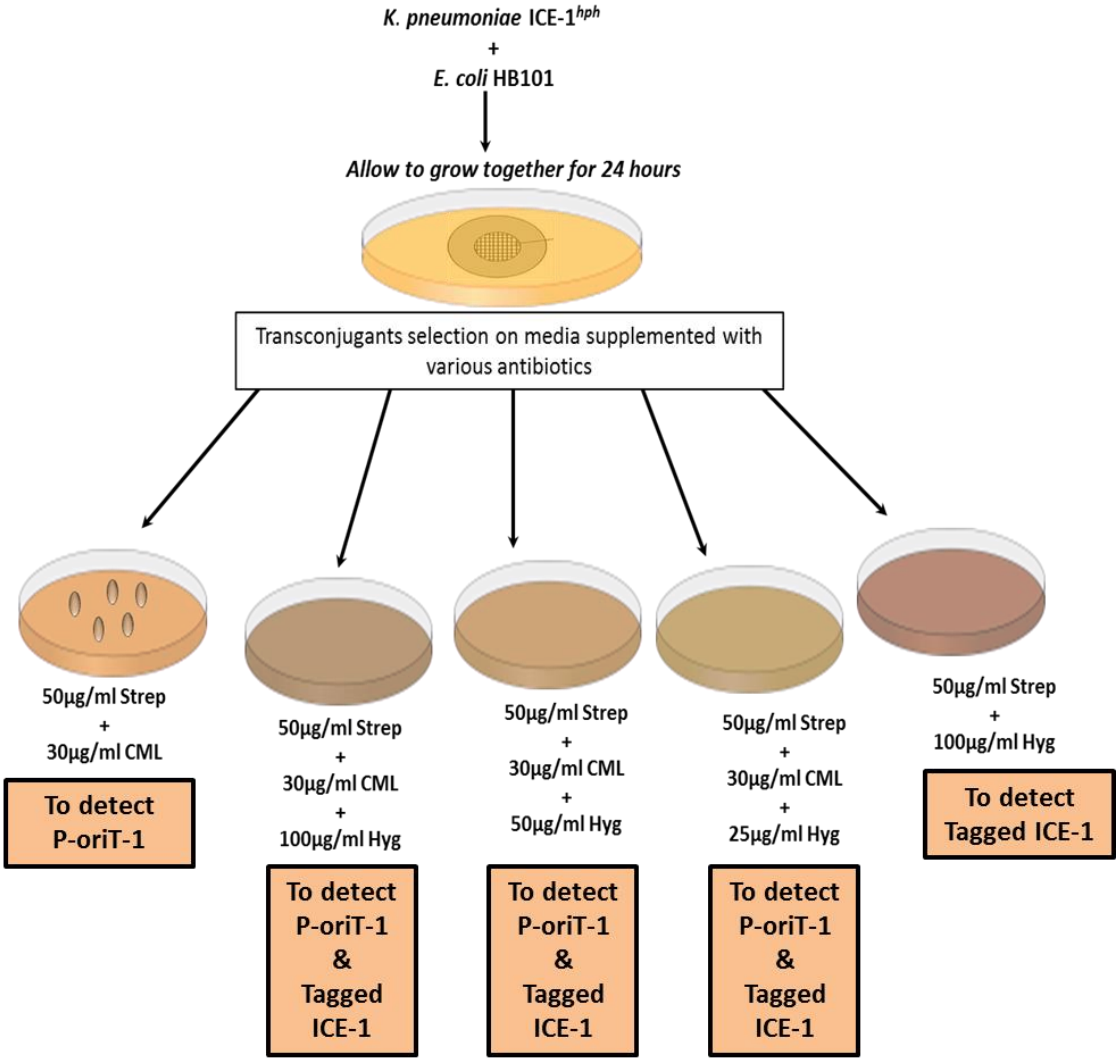

Figure 5-9 Strategies used for selection of transconjugants to detect the mobilisation of ICE^{hph}.

5.3.5 Identification of comprehensive sets of Inverted and Directly repeated sequences critical to *oriT*-1

Since direct (DR) and inverted repeats (IR) are major features of the *oriTs* of conjugal mobilising elements (Byrd and Matson, 1997, Llosa et al., 2002). *oriT*-1 was investigated using the web based tools Palindromic sequence finder (http://insilico.ehu.es/palindromes/) and REPuter (Kurtz et al., 2001). The conserved regions were also assessed in potential ICEKP-1 elements identified in other *Enterobacteriaceae*; these regions were found to be 92% identical (Figure 5-10). Interestingly, on reinvestigation of *oriT*-1, novel and previously unreported sequences of 10 bases in DR1 (CGCCCCAGCGA) and 13 bases in IR1 (CTTCATTATTTTT) were identified;

these repeated sequences were highly conserved in ICEKP-1 regions in other *Enterobacteriaceae* (Figure 5-10).

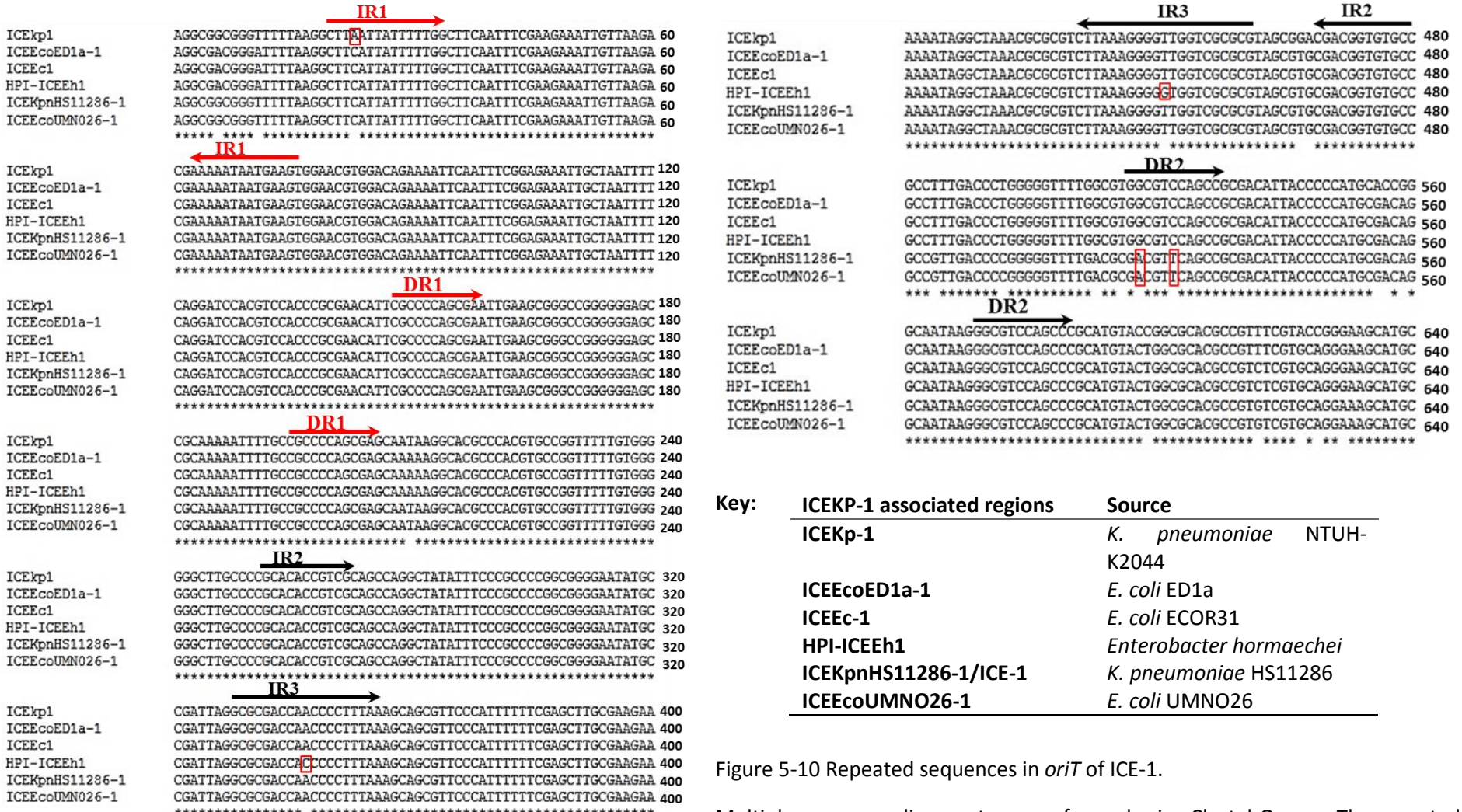

Key:

ICEKP-1 associated regions	Source
ICEKp-1	*K. pneumoniae* NTUH-K2044
ICEEcoED1a-1	*E. coli* ED1a
ICEEc-1	*E. coli* ECOR31
HPI-ICEEh1	*Enterobacter hormaechei*
ICEKpnHS11286-1/ICE-1	*K. pneumoniae* HS11286
ICEEcoUMNO26-1	*E. coli* UMNO26

Figure 5-10 Repeated sequences in *oriT* of ICE-1.

Multiple sequence alignment was performed using Clustal-Omega. The repeated sequence shown with black arrows were previously published by (Lin et al., 2008, Schubert et al., 2004); the red arrows show sequences identified in this study.

5.3.6 A 0.65 Kb region of ICE-1 contains the minimal *oriT* and its essential repeated sequences

In order to investigate the importance of the newly identified repeat sequences and to identify the minimal region of *oriT* (coordinates 3478265 to 3480025 in accession number CP003200) in ICE-1, multiple plasmids were constructed based on pACYC184 (Section 5.2.2 and Appendix III) as shown in Figure 5-11. In addition to P-*oriT*-1, five more plasmids (P-*oriT*956, P-*oriT*648, P-*oriT*568, P-*oriT*525 and P-*oriT*454) were constructed by reducing the length from both ends of the defined region. The truncation targeted repeat sequences and the 140 base region between the last DR2 and *mobB* (Figure 5-11). The WT was transformed with the five plasmids individually and conjugation assay performed. Conjugation frequency was significantly reduced when IR1 was absent (Figure 5-11). The highest transconjugant frequency was observed with P-*oriT*-648. No mobilisation was observed with deletion of the terminal 140 bp region.

Thus it appeared that the 140 bp region upstream of *mobB* was critical for the activity of *oriT-1*. To test the hypothesis P-*oriT*648 was modified to P-*oriT*-608 lacking the terminal 40 nucleotides of this region. Again no mobilisation was observed indicating the essential role of this 140 bp region, as a modest deletion reduced the highest transfer frequency to levels below the limit of detection (Figure 5-11). Taking these results together, it was concluded that 648bp of ICEKP-1 contains the minimal *oriT* and essential repeated sequences.

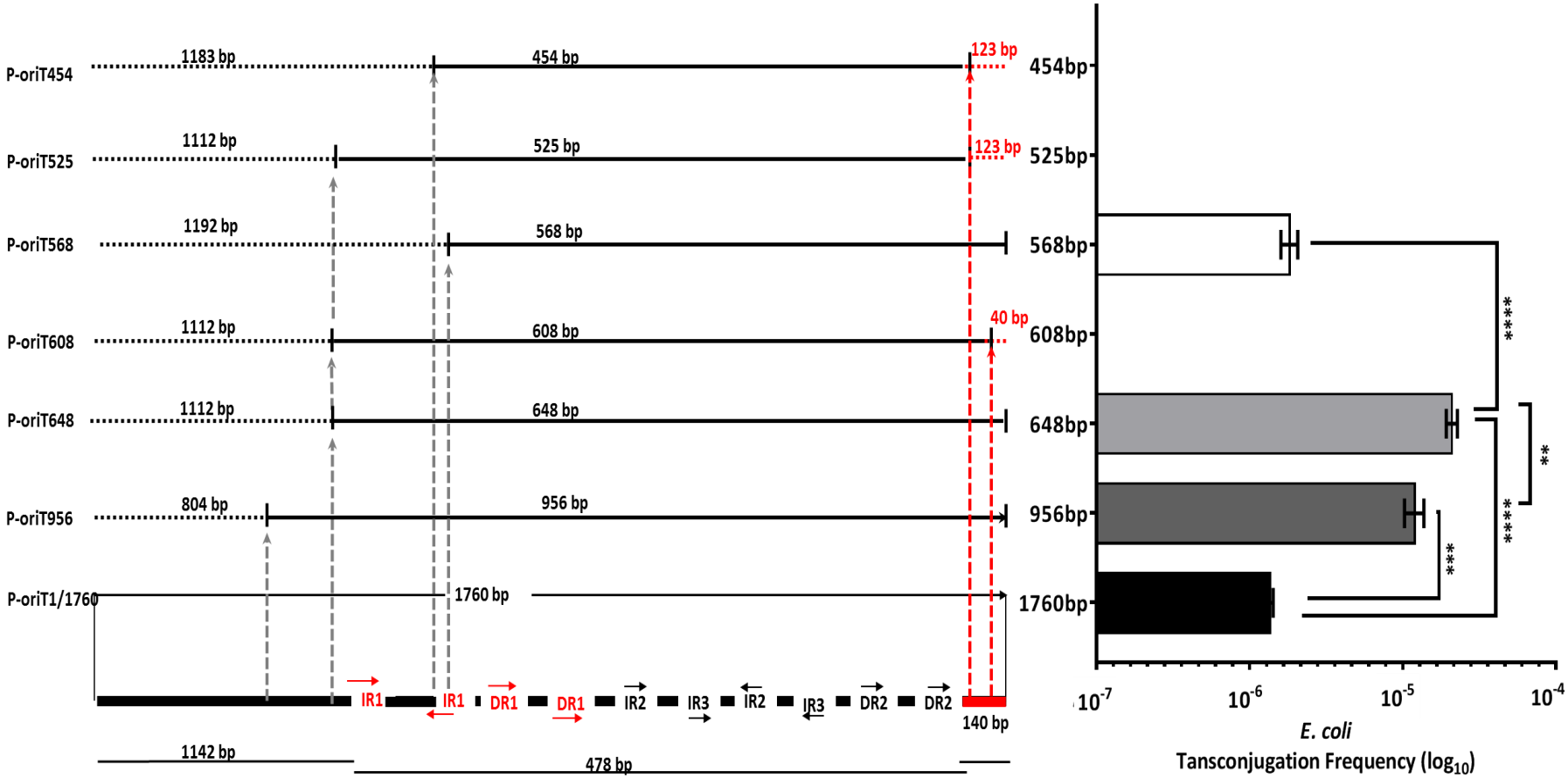

Figure 5-11. Identification of minimal *oriT*-1 region and importance of repeated sequences for the conjugative transfer of the plasmid.

Left side; Schematic representation of the 1760bp region (*oriT*) of ICE-1; black lines indicate the region cloned in pACYC184, grey dotted lines show the deleted region at 5´ end and red lines shows deletion of DNA sequence at 3´ end of the *oriT-1* containing region. Right side; Transconjugant frequencies from the *K. pneumoniae* HS11286 (WT) host. Un-paired t-tests (n=3) (** P= 0.003, *** P= 0.0004 and **** P = 0.0001). Schematic drawn is not the scale.

5.4 Discussion

5.4.1 Growth phase influenced the excision frequency of ICE-1

Before transfer to a new host, ICEs produce an intermediate extrachromosomal form. Excision results from integrase activity associated with homologous recombination between flanking direct repeat sequences (Wozniak and Waldor, 2010). The excision of ICE-1 shown here confirmed the presence of a functional integration and excision module. Sequencing of amplified fragments showed that excision / recombination occurred between the *attL* and *attR* sites of ICE-1. The precise excision and integration sites of ICEKP-1 elements have been previously demonstrated for ICE*Ec-1* and ICEKp-1. The circular form of ICE*Ec-1* was detected following induction of integrase, while ICEKp-1 appeared to be excised in this study without induction (Schubert et al., 2004, Lin et al., 2008).

The excision of ICEs could also be influenced by various environmental signals that provide selective pressure for this event (Wozniak and Waldor, 2010, Johnson and Grossman, 2015). These factors are generally ICE specific and include growth phase, responses to DNA damage (Beaber et al., 2004, Auchtung et al., 2005, Bellanger et al., 2007) and signal molecules produced by potential recipient partners (Ramsay et al., 2006, Ramsay et al., 2009).

The influence of growth phase on ICE-1 excision was assessed here. Based on previous growth studies (Figure 5-12) and the sample timings, the highest frequency of ICE-1 excision was observed in early stationary phase (8 hr). Similar patterns have been observed with ICE*clc*^{B13} of *Pseudomonas* B13 (Ravatn et al., 1998b), ICESt3 of *Streptococcus thermophiles* (Carraro et al., 2011) and ICE*MlSym*^{R74} of *Mesorhizobium loti* R7A (Ramsay et al., 2006).

Faint bands of the circularised ICE-1 at late stationary phase indicated its inefficient excision that also indicated the competition between intact and excised sites especially showing that latter dominated. The quantitative measurement of the frequencies of ICE-1 excision could be investigated in future using real time PCR or it could be more precise with digital PCR.

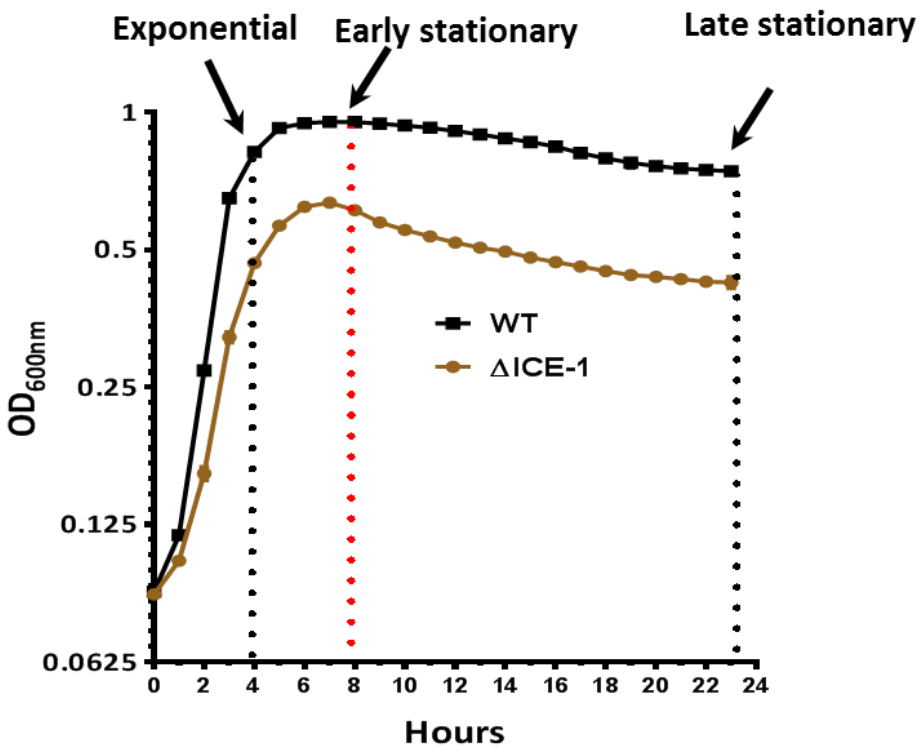

Figure 5-12 Growth pattern of WT and ΔICE-1 mutant at different time points.

5.4.2 ICE-1 was non-mobile

Self-conjugation of ICEKP-1 elements was previously examined for ICE*Ec-1* and ICEKp-1. Based on transmission of plasmids containing ICE*Ec-1* fragments of various sizes Schubert et al. (2004) showed that ICE*Ec-1* encoded a functional mating pair formation (Mpf) system. Similarly, ICEKp-1 has also been shown to be self-conjugated to both *K. pneumoniae* and *E. coli* strains lacking ICEKp-1. In this study, no evidence of ICE-1 self-conjugation was found. Previously, ICEKp-1 was tagged with a kanamycin resistance cassette while here hygromycin (*hph*) was selected. Thus it was possible that the *hph* tagging affected excision of ICE-1. However, excision experiments with both ICE-1^{hph} and native ICE-1 confirmed that tagging did not affect excision. One possible explanation could be that the Mpf system encoded by ICE-1 is non-functional.

5.4.3 ICE-1 encodes a functional Mpf-complex

Usually ICEs encode their own conjugative pili (c.f. chapter 1). ICE-1 encoding of a functional conjugative apparatus for Mpf and DNA mobilisation was investigated by construction of the ICE-1 marker plasmid (P-*oriT*-1) (Figure 5-5) using pACYC184 as a backbone. The selection of plasmid was based on its previous use for the construction

of a conjugative plasmid of ICEKP-1 elements (Schubert et al., 2004, Lin et al., 2008). The conjugative transfer of P-*oriT*-1 from WT to *E. coli* indicated the operational features of T4SS-1. These findings were supported when no transfer of P-*oriT*-1 was detected from a ΔICE-1 mutant strain. To investigate whether mobilisation of P-*oriT*-1 was mediated by the ICE-1 secretion system, a ΔT4SS-1 (*virB-1* to *virB6*) mutant was created (Figure 5-7) and mobilisation was thereby abolished. *VirB*1 encodes a periplasmic lytic transglycosylase providing space for the assembly of conjugative pili in the bacterial cell wall (Koraimann, 2003, Fronzes et al., 2009). VirB2 and VirB5 are the major structural proteins of the system forming the pilus structures extending extracellularly (Lawley et al., 2003, Aly and Baron, 2007, Kwok et al., 2007, Backert et al., 2008). VirB3 and 4 are transmembrane proteins that have been suggested to function together (Mossey et al., 2010), while VirB6 is a major candidate forming the pore within the pili (Cascales and Christie, 2004). It was assumed that deletion of these genes has disrupted both the pilus organisation and function. These findings were in accordance with the findings of Lin et al. (2008) who showed that a *virB*1 mutant of ICEKp-1 was unable to mobilise pACYC-*oriT*. Collectively, these findings confirmed that ICE-1 carried a functional conjugation module.

5.4.4 ICE-1 was mobilised by P-*oriT*-1 *in-trans*

Among MGEs some elements have been reported to encode their excision and integration systems but not to include all the factors required for their conjugative mobilisation. Such elements can be mobilised in-trans utilising the Mpf of any other co-resident ICE or conjugative plasmid (Burrus et al., 2002, Bellanger et al., 2013). The mechanism of *in-trans* mobilisation of integrative mobile elements (IMEs) has been linked to conjugative plasmids such as IncQ (Meyer, 2009). In addition, most of these IMEs carry their own *oriT* together with their relaxase and relaxosome related proteins (Li et al., 1995, Crellin and Rood, 1998, Vedantam et al., 2006); they were, nonetheless dependent on Mpfs of other related or unrelated ICEs or conjugative plasmids for transfer (Bellanger et al., 2013). In this study, the conjugative in-trans mobilisation of ICE-1 by P-*oriT*-1 occurred from *K. pneumoniae* HS11286 (donor) to *E. coli* HB101 (recipient). These results supported the idea of Tsvetkova et al. (2010), who showed in-trans mobilisation of a plasmid that carried *oriT*, *mobB* and *mobC* of ICE*Tn*1549 by RP4

(conjugative plasmid). Furthermore, high efficiency of in-trans mobilisation of plasmid CloDF13 was mediated by SXT (Hochhut et al., 2000). In addition, the findings of this study corroborated the results of previous researchers who showed that ICE SXT mobilised a chromosomal DNA fragment that was located 1.5 Mb far from SXT, in-trans (Hochhut et al., 2000, Daccord et al., 2010). Surprisingly, investigation of ICE^{hph} did not show any in-trans mobilisation of the element and this raised a question regarding the fitness cost to the recipient cell in the presence of hygromycin. To address this possibility, low concentrations of hygromycin were used for selection of transconjugants. However, ICE^{hph} transfer was not detected. Taking these results together it is suggested that the relaxosome formed during P-*oriT*-1 transfer triggered more assembly of the T4SS-1 and this mediated in-trans conjugative transfer of ICE-1 from donor to recipient. The reason why transfer of ICE-1^{hph} was not detected remains unclear.

5.4.5 Minimal *oriT*-1 contained 3 inverted and 2 directly repeated sequences

The *oriT*-1 (1760bp) was investigated for the presence of special features such DRs and IRs and also for AT rich areas. The region containing *oriT*-1 was sandwiched between *virB*11 and *mobB* of ICE-1, consistent with the findings of Lin et al. (2008), who demonstrated that the 1761bp region, *oriT*$^{Kp\text{-}1}$, lies between *virB*11 and *mobB* of ICEKp-1. The *oriT*$^{Ec\text{-}1}$ containing region of ICE*Ec-1*was 1838-bp region in the same location (Schubert et al., 2004). Previously, ICEKP-1 associated *oriT*s have been shown to include two IRs and one DR with the *nic* site in IR2 (Schubert et al., 2004, Lin et al., 2008). In contrast, this study has identified one novel set of IR and DR sequences localised upstream to the previously identified IR1 (Figure 5-10). It is interesting to note that these repeat sequences are highly conserved amongst multiple putative ICEKP-1 elements. Moreover, this study has determined that loss of these sequences increase the conjugative transfer of the marker plasmid (Figure 5-11). These results were contradictory to the findings of Guasch et al. (2003), who demonstrated that loss of only half of a repeated sequence resulted in a fivefold decrease in binding between relaxase and *oriT*. Thus it showed that newly identified repeated sequence had no significant impact on oriT-1 associated mobilisation.

In conjugative systems, *oriT* containing regions are usually positioned adjacent (upstream/downstream) to the DNA-processing genes *mobB* and *mobC* (Schubert et al., 2004). The $oriT^{Ec\text{-}1}$ and $oriT^{Kp\text{-}1}$ were respectively, 240bp and 140bp upstream to the *mobB*. Similarly, the *oriT*-1 containing region was 140bp upstream of *mob* and loss of 123bp from this region abolished conjugative transfer of the ICE-1 marker plasmid. These findings indicate a strong link between this region and DNA processing of ICE-1 during conjugation. To further confirm that the reduction in conjugative transfer was attributable to loss sequence from 140bp rather than interference with DR2, P-*oriT*608 was constructed leaving DR2 intact and this showed similar results to P-*oriT*568 (Figure 5-11). Thus it is suggested that the 140bp region might be important in enabling relaxase to form relaxase-DNA complexes.

As noted previously, relaxases control the conjugation process by site-specific binding to *nic* sites in the presence of a large excess non-target DNA both in the donor and the recipient (Carballeira et al., 2014). Relaxases recognise the hairpin loops formed by IR sequences in *oriT*s for binding and for nicking the DNA (Guasch et al., 2003). The results reported here raise two possibilities regarding the role of the 140bp region in *oriT*-1: 1) it acts as a helper sequence for relaxase to bind in donor cells or 2) it plays a role after the transfer of the ICE-1 marker plasmid to the recipient where the same or another molecule of relaxase binds the *nic* sites to join the fragments. In the second possibility two relaxase molecules would be attached to the DNA at same time. These suggestions are consistent with other studies concerned with relaxase activity during conjugative transfer (Lucas et al., 2010, Chandler et al., 2013, Carballeira et al., 2014). Moreover, loss ~1.0 kb region downstream to *virB*11 resulted in more than a 10-fold increase in conjugative transfer of the plasmid (P-*oriT*648), indicating that this region was not actually part of *oriT*-1. Overall, it was concluded that the 0.65 kb region upstream to *mobB* is the minimum for *oriT,* containing all its essential repeated sequences.

5.5 Conclusions;

1. ICE-1 excised site specifically and formed an intermediate episomal circularised form.
2. ICE-1 excised more frequently in early stationary growth phase.
3. ICE-1 conjugative-mobilisation was not detected.

4. ICE-1 has a functional conjugation module (T4SS-1) for nucleoprotein-complex processing via conjugation.
5. The ICE-1 marker plasmid meditated conjugative mobilisation of ICE-1 *in-trans*.
6. Newly identified repeat sequences had no significant impact on *oriT*-1 related function.
7. The 140bp upstream to *mobB* is critically required for the completion of *oriT*-1.

Chapter 6 Mobilisation cycle of ICE-2 and its interactions with ICE-1

6.1 Introduction

PAPI elements like other ICEs have modular structures that perform essential functions in different stages of their mobilisation cycle (Mohd et al., 2004, Wozniak and Waldor, 2010). PAPI elements can excise site specifically as shown for PAPI-1 and pKLC102 (Qiu et al., 2006, Klockgether et al., 2007). Moreover, ICEEc-2, which is a member of PAPI sub-family, was also documented for its successful excision (Roche et al., 2010). PAPI elements are self-mobile and can be disseminated among *Pseudomonas* spp. e.g. PAPI-1, PFGI-1, and pKLC102 (Qiu et al., 2006, Klockgether et al., 2007, Hong et al., 2017, Mavrodi et al., 2009). ICEEc-2 can also be transferred into *E. coli, Salmonella Typhimurium* and *Yersinia pseudotuberculosis* (Roche et al., 2010), indicating its broad host range.

In this study, two integrases (*int2a* and *int2b*) have been identified in ICE-2 (Figure 6-1), which were not reported by previous researchers. Therefore one aim was to investigate which integrase controls ICE-2 excision/integration. There has also been limited investigation of PAPI associated *oriT* regions. Previous work has been limited to studying mobilisation and prediction of the putative *oriT* containing region but no experimental evidence was provided (Mavrodi et al., 2009).

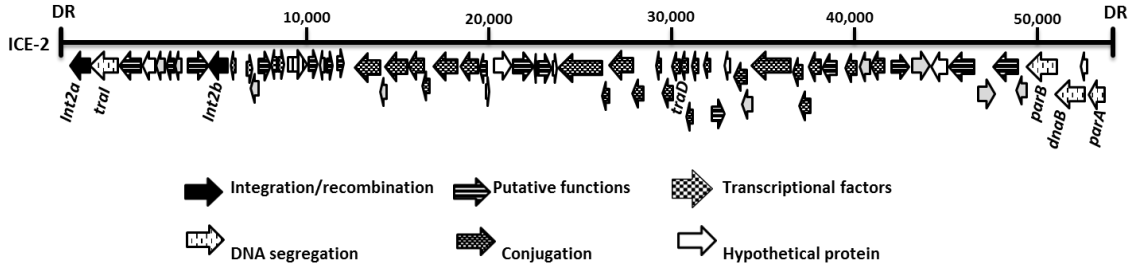

Figure 6-1 Schematics of ICE-2.

Cross-talk between two non-homologous MGEs in a single genome has been demonstrated in many cases. MGEs may interact in excision, transfer and metabolic function (Lopez-Garrido and Casadesus, 2012, Carpenter et al., 2015). As far as we are aware, the co-existence of ICEKP-1 and PAPI elements has not previously been reported. This study was focused on investigating the functional interactions between ICE-1 and ICE-2 during conjugative transfer of nucleoprotein complexes.

6.1.1 Aim

To study the mobilisation cycle of ICE-2 and its possible interactions with ICE-1 during DNA mobilisation.

6.1.2 Objectives

1. To investigate site-specific excision of ICE-2.
2. To identify the integrase that controls the excision of ICE-2.
3. To study the self-conjugation of ICE-2.
4. To construct a model mutant with higher frequencies of conjugative transfer of DNA.
5. To detect the region containing *oriT*-2.
6. To investigate the functional interactions between ICE-2 and ICE-1 during conjugation.
7. To identify components of ICE-2 that interact with ICE-1.

6.2 Methods

6.2.1 Construction of ICE-2 marker conjugative plasmid

ICE-2 marker plasmids were constructed for identification of *oriT*-2. The In-Fusion HD cloning kit (Takara) was used to construct the plasmids (section 4.2.4).

11 pairs of primers were designed (Appendix IV) to amplify A to K fragments of ICE-2 (Figure 6-2). Primers RF207 and 208 were used to amplify the pACYC184 backbone, and complementary sequences to these primers were used with 11 sets of ICE-2 associated primers to enable fusion of the plasmid backbone and the 11 amplified fragments (Figure 6-2).

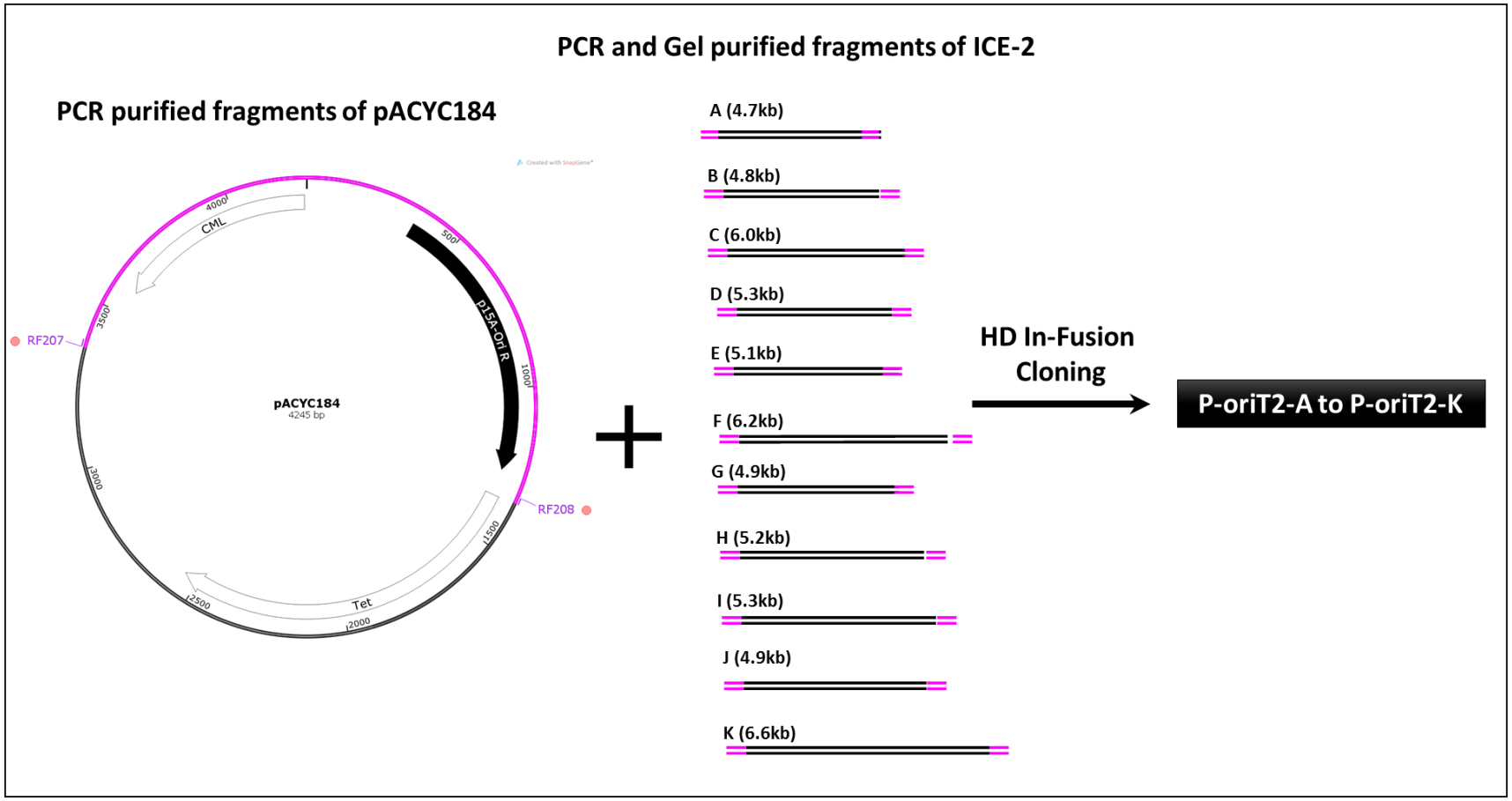

Figure 6-2 Construction of ICE-2 marker plasmids.

6.2.2 Construction of RFTool-1

A plasmid pWSK29-Apra, usually used for protein expression in *K. pneumoniae* (Table 2-3), and P-*oriT*-1 belongs to the same compatibility group, therefore to avoid incompatibility between the two plasmids in complementation experiments of *mob*-2 and *traI* RFTool-1 was constructed by restriction digestion and ligation. RFTool-1 contains the pBluescript region of pWSK29 and the broad host range (BHR) origin of replication of pFLP2-Apra. AflII restriction digestion sites were added at 5´ ends of the primers (Table 6-1) for the amplification of these two fragments. T4 ligase was used to ligate the fragments. Plasmid construction was confirmed using PCR and restriction digestion. The sequence of RFToo-1 is presented in Appendix XI.

Table 6-1 Primers used for the construction of RFTool-1.

Cat. No	5´- 3´ Sequence[a]	Features
RF172	ACCCTTAAGCGGCATCAGAGCAGATTGTA	Forward primer to amplify the BHR origin of replication using pFLP2-Apra as template
RF173	ACCCTTAAGATCGCCCTTCCCAACAGT	Reverse primer to amplify the BHR origin of replication using pFLP2-Apra as template
RF174	ACCCTTAAGGACGCTCAGTGGAACGAAAA	Forward primer to amplify the pBluescript DNA region containing multiple cloning sites (MCS) using pWSK29-Apra as template
RF175	ACCCTTAAGCACATGTTCTTTCCTGTTATCC	Reverse primer to amplify the pBluescript DNA region containing multiple cloning sites (MCS) using pWSK29-Apra as template

a= Sequence in red represents AflII restriction digestion site.

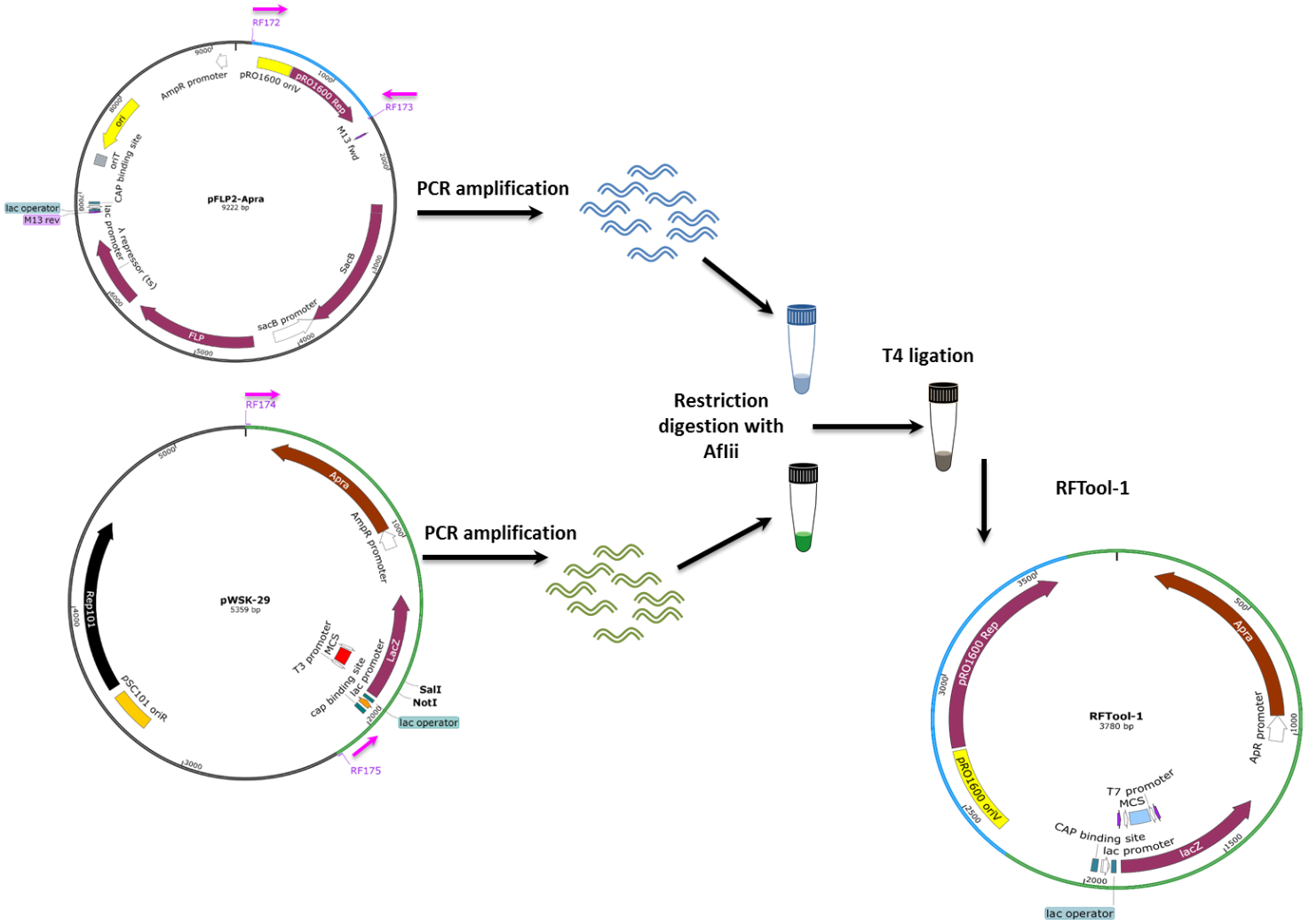

Figure 6-3 Construction of RFTool-1.

6.2.3 Point mutation

Multiple *mob*-2 sequences were constructed for cloning into the RFTool-1 plasmid for use in complementation experiments. Walker A&B motifs were identified; two base pair changes were introduced to lysine 199 (Walker A) and glutamic acid 507 (Walker B) residues in mob-2 into the non-polar amino acid Alanine. These alterations were introduced into primers overlapping the sequence upstream and downstream from the relevant codons and were paired with primers annealing at the beginning and end of the *mob*-2 gene. PCR resulted in two fragments each carrying a homologous complementary sequence that carried the desired point mutations and these were joined by SOE-PCR to create the mutant variant of the gene. The mutants were verified by sequencing.

Plasmid construction for complementation experiments

Conventional restriction site cloning was used for the plasmids constructed for complementation experiments.

6.3 Results

6.3.1 Mobilisation cycle of ICE-2

6.3.1.1 Identification of extrachromosomal ICE-2:

A PCR- based assay was developed to demonstrate the site-specific excision of ICE-2 (section 5.2.1). Different sets of primers were designed complementary to both ICE-2 and the chromosomal region outside ICE-2. Primer pairs RF160/RF161 and RF162/RF163 were used to detect the integrated form by amplification of attL and *attR* sites. Primer pair RF161/RF162 was used to detect the excised form by amplifying the *attI* sites of the element. Moreover, the *attB* (empty site) for *phe-tRNA* could be detected using RF160/RF163 (Figure 6-4A).

Both genomic and plasmid DNA (10ng/reaction mixture) was used as before (section 5.2.1), samples were taken at 4, 8 and 24 hr. The WT lanes in Figure 6-4B demonstrate site-specific excision of ICE-2 and formation of its circular intermediate. Unlike the ICE-1, excision did not appear to be growth phase dependant.

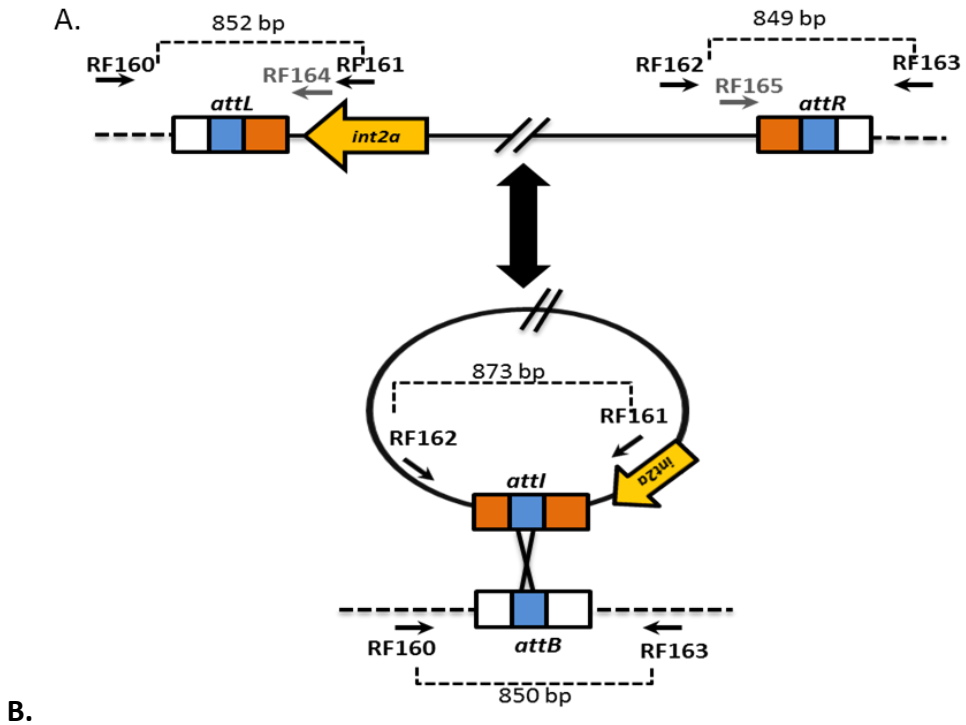

B.

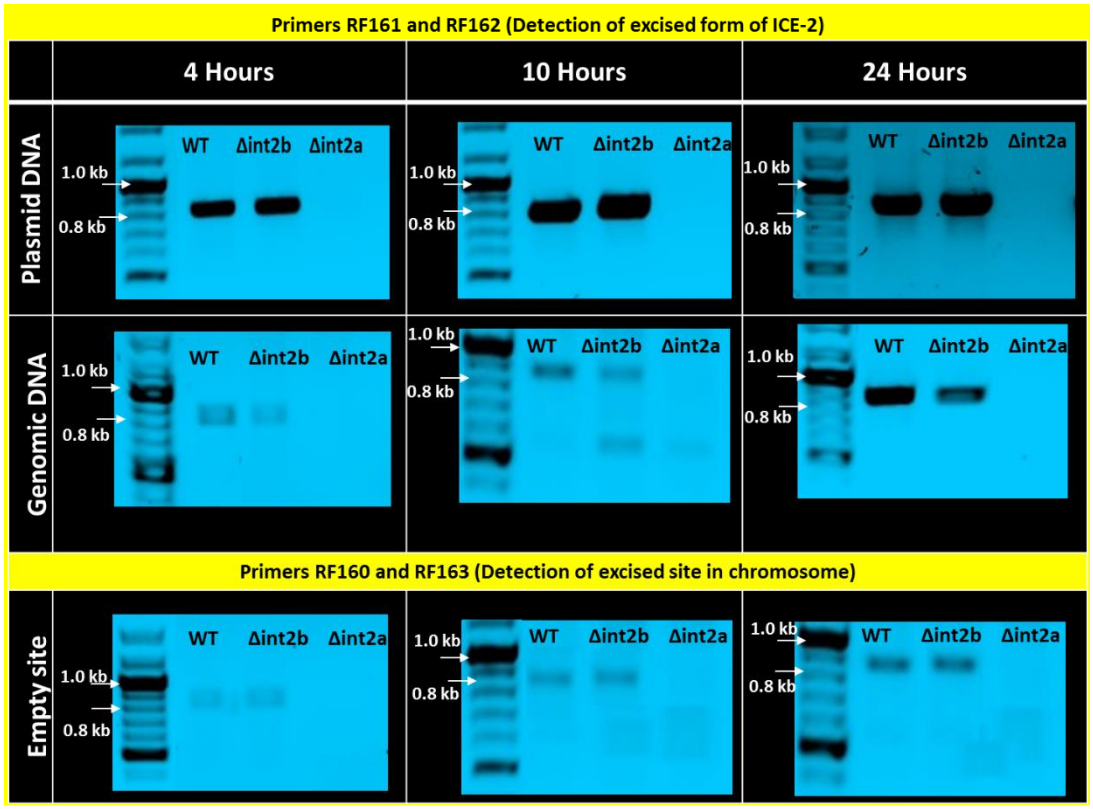

Figure 6-4 Site-specific excision and extrachromosomal circularisation of ICE-2.
A. ICE-2 model of integration/excision. The small arrows above and below the map represents positions of primers used for different PCRs. B. PCR results for the detection of excised form ICE-2 and empty sites in chromosome using both genomic and plasmid DNA. Note that different primers were used to interrogate the mutant strains (see below)

6.3.1.2 Identification of integrase responsible for ICE-2 excision

To identify which of the two integrase were required for excision of ICE-2, two mutant strains, Δint2a::hph and Δint2b::hph, were created. Similar primers to those described in section 6.3.1.1 but RF161' (annealing to the hph gene cassette) was substituted for RF161 for the Δint2a::hph mutant because int2a had been replaced with *hph*. The intermediate episomal state of ICE-2 was not detected in the *int2a* mutant strain whereas knockout of *int2b* did not affect the excision of ICE-2 (Figure 6-4B). These results indicate that *int2a* is responsible for excision of ICE-2.

6.3.1.3 Conjugative-mobilisation of ICE-2

ICE-2 was marked with *hph* on *orf8* (hypothetical gene) to enable the selection of transconjugants (Figure 6-5). The *orf8* was selected for disruption as it encodes hypothetical protein considered unlikely to interfere with conjugative-mobilisation.

A conjugation assay was performed, initially the transconjugants were selected on medium supplemented with hygromycin (100 µg/ml) and streptomycin (50 µg/ml). No transconjugants were detected for ICE-*2*^{hph}. Thus, either ICE-2 was not able to mobilise itself or *hph* has affected its ability to be excised and/or transfer. The possibility that the *hph* cassette reduced excision of ICE-2 was examined by performing an excision assay in ICE-*2*^{hph} strain. No differences were observed between excision of WT and ICE-*2*^{hph} (not shown).

Again the possible toxicity of hygromycin on ICE-*2*^{hph} transconjugants was explored by selection of transconjugants on lower concentrations (25 and 50 µg/ml) together with streptomycin (Figure 5-9). No ICE-*2*^{hph} transconjugants were obtained on any of the selection media suggesting inability of ICE-2 to self-mobilise.

To determine whether, like ICE-1, ICE-2 mobilisation could also be mediated by plasmid encoded elements the WT and Δorf8::hph strains were transformed with P-*oriT*-1 and a conjugation assay performed. No transconjugants were obtained carrying ICE-2 or ICE-*2*^{hph} but plasmid mobilisation was always observed. Based on these findings two hypotheses were proposed*;*

Conjugative-mobilisation of ICE-2 is too infrequent to detect *in vitro*. **Hypothesis 6-1**

ICE-2 lacks its origin of transfer (*oriT-2*). **Hypothesis 6-2**

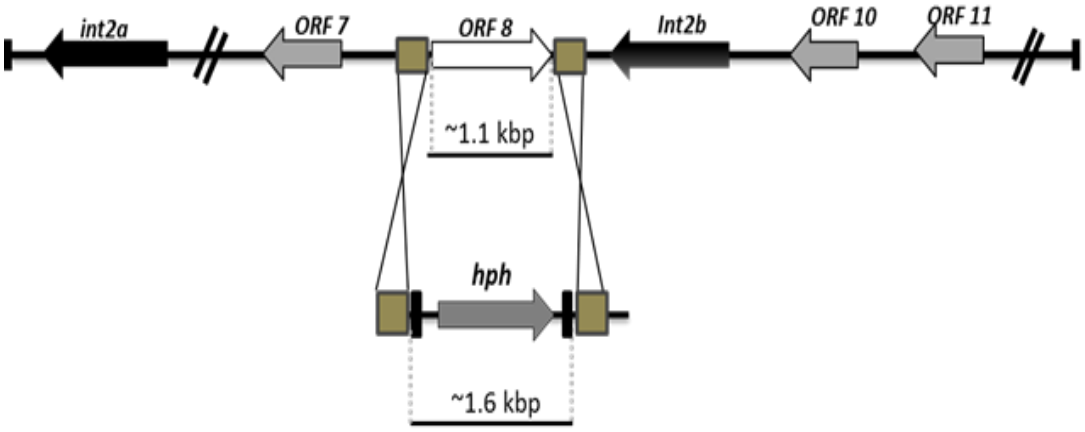

Figure 6-5 : Schematics showing ICE-2 tagging with *hph* cassette.
An orf8 was replaced with *hph* cassette for self-mobility assay of ICE-2. Lambda red recombination method was used for substitution of *orf8* with *hph*.

6.3.2 A double *K. pneumoniae* HS11286 mutant to increase transconjugation frequency

To investigate the hypothesis 6.1, there was a need to enhance the recovery of transconjugants. *K. pneumoniae* has many factors including type six secretion system (T6SS) that reduce *E. coli* viability (Rajakumar's unpublished data). In this study, two ΔT6SS-1 and ΔT6SS-3 mutant strains (kindly provided by David Ngmenterebo) were used to investigate the effect of deletion of T6SSs on conjugation frequencies of ICE-1 marker plasmid.

The capsulate parental strain of the *K. pneumoniae* HS11286 ΔMDRΔKPCΔCPS designated WT in this study was also used for comparison. Both transconjugation and *E. coli* recovery were highly increased in ΔT6SS-1 compared to the parental strain (Figure 6-6). The enhanced transconjugation frequencies of WT and ΔT6SS-1 compared to WT and ΔT6SS-3 was encouraging and, accordingly a double mutant was made in the ΔT6SS-1 strain by deleting the cps cluster (ΔT6SS-1Δcps::hph). Strikingly, the conjugation frequency of the double mutant was increased 2-log 100-fold compared to WT (Figure 6-6). This strain was designated ΔT6ΔC and used in further conjugation experiments.

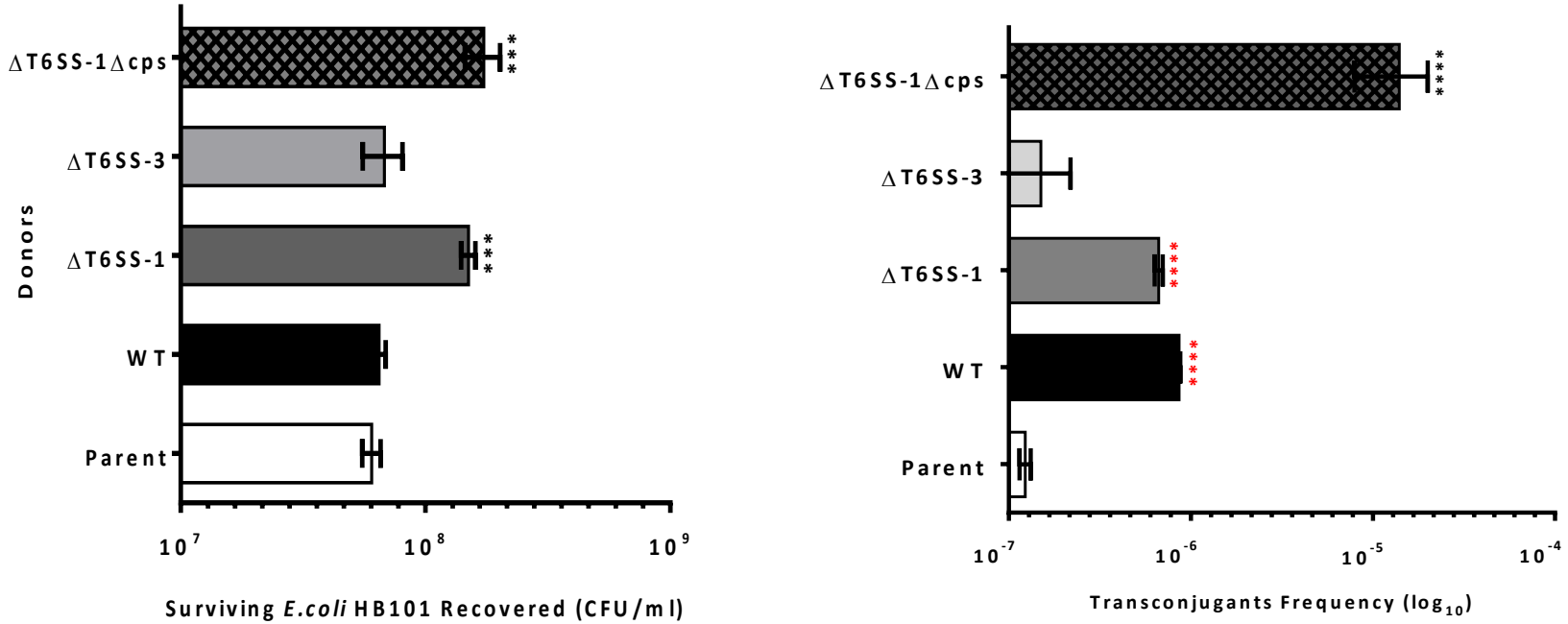

Figure 6-6 ΔT66-1Δcps has highest transconjugation frequency.

A. Recovered Cfu/ml of *E. coli* from the mixed culture, which was grown overnight for conjugation assay with each donor. Recovery of *E. coli* was measured by growing on medium containing streptomycin only. B. Transconjugants frequencies. Black asterisks '*' shows comparison between mutants and WT while red is for comparison between parent and other strains. (n=3, *** P= 0.0002 and **** P<0.0001).

6.3.3 Conjugative-mobilisation of ICE-2 using ΔT6ΔC as donor

Due to time limitation, ICE-2 was not marked in the ΔT6ΔC strain. Conjugation assays were performed using ΔT6ΔC-P-*oriT*-1 as donor and transconjugants were screened (PCR) for the presence of ICE-2 marker regions. No transconjugants carrying ICE-2 were detected but P-*oriT*-1 mobilisation was always detected. The possibility that lack of detected ICE-2 self-conjugation reflected a degenerated or lost *oriT* was therefore considered.

6.3.4 Screening for *oriT*-2 in ICE-2

To further investigate the possible location of *oriT*-2, the ~56 kb of ICE-2 was divided into 11 PCR fragments (A-K) using 11 pairs of primers (Appendix IV). In order to reduce the chance of truncation in *oriT*-2, each pair of primers had an overlap region with those adjacent (Figure 6-7). The HD In-Fusion cloning method was used to clone the 11 fragments into pACYC184. The plasmids were named as P-*oriT*2-A to P-*oriT*2-K (Figure 6-7).

Both WT and ΔT6ΔC mutant were transformed with each of these plasmids and conjugation experiments were performed. No mobilisation of any plasmid was observed.

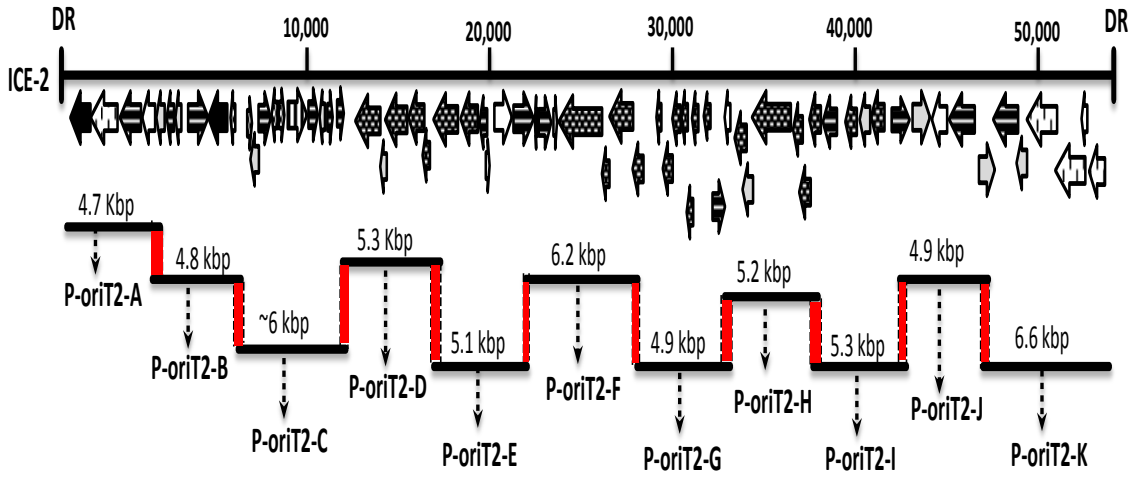

Overlapping regions	A-B	B-C	C-D	D-E	E-F	F-G	G-H	H-I	I-J	J-K
No. of overlapped nucleotides (bp)	300	381	300	280	333	266	293	375	505	500

Figure 6-7 Strategy used to identify the *oriT-2* in ICE-2.
Schematics of 11 fragments from A to K with small overlapping regions (shown in red rectangles).

6.3.5 Functional Interactions between ICE-2 and ICE-1

6.3.5.1 ICE-2 deletion reduced transconjugation of ICE-1 marker plasmid

In order to study the interactions between ICE-1 and ICE-2 during DNA mobilisation, ΔICE-2 mutant was transformed with P-*oriT*-1 and conjugation was performed. Remarkably, deletion of ICE-2 reduced the transconjugation frequency by ~6-fold compared to WT (Figure 6-8). The possibility that there were significant interactions between ICE-2 and the conjugation module of ICE-1 was therefore investigated and the following hypothesis proposed;

T4SS-2 facilitates the conjugation machinery of ICE-1 for mobilisation of its marker plasmid.

Hypothesis 6.3

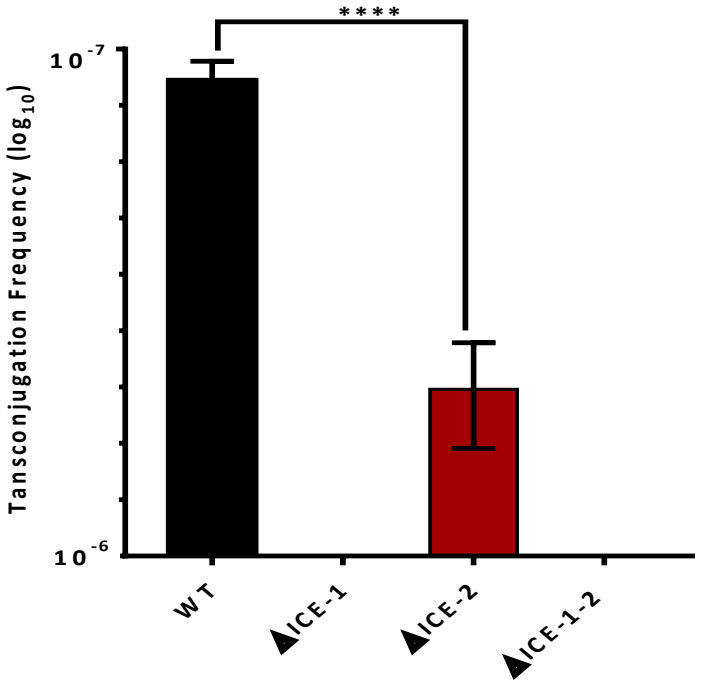

Figure 6-8 Transconjugation frequencies of ICE-1 marker plasmid (P-*oriT1*) by ΔICE-2. (Error bars = Standard deviation, n=3). **** P value <0.0001.

6.3.5.2 Identification of ICE-2 components involved in cross talk with ICE-1

A targeted strategy was used to investigate which component(s) of ICE-2 were contributing to P-*oriT*1 transfer. Candidate genes annotated as components of T4SS-2 were grouped according to their putative functions (Table 6-2). ORFs encoding proteins with specific function unidentified (SFU) and those annotated as pilus assembly and highly conserved PAPI elements were considered low priority. The remaining two genes *orf2* and *orf43*, annotated respectively as relaxase and T4CP were interrogated.

Table 6-2 Summary of ICE-2 genes associated to conjugative mobilisation of DNA.

ORF Position in ICE-2	Aa[a]	Homologue proteins	Possible Function[c]
ORF2	429	Relaxase	Nic at *oriT*
ORF17	509	TraG	Pilus assembly
ORF19	473	ICEs protein, PFL_4711	SFU
ORF20	313	ICEs protein, PFL_4710	SFU
ORF21	131	ICEs protein, PFL_4709 family	Transposition
ORF30	924	CT[b] ATPase, PFL_4706	Energy provider
ORF31	132	CT protein	Pilus assembly
ORF32	494	TrbI-like / PFL_4705	Transposition
ORF33	281	PFL_4704/TraK	SFU
ORF34	217	ICEs protein, PFL_4703	Transposition
ORF35	123	CT region protein, TIGR03750	Transposition
ORF36	117	ICEs membrane protein, PFL_4702	Assembly
ORF37	78	ICEs protein, PFL_4701	SFU
ORF38	105	ICEs protein	SFU
ORF41	252	Membrane protein PFL_4697	Transposition
ORF43	699	Coupling factor TraD	Transposition & Energy
ORF44	170	ICEs protein, PFL_4695	SFU
ORF46	205	ICEs protein, PFL_4693 family	SFU
ORF48	189	Type IV B pilus protein	Pilus assembly
ORF50	240	ICEs protein, PFL_4669 family	SFU

a=Amino acids, b = Conjugal transfer, c= colour codes based on similar functions

6.3.5.3 *orf43 encodes* homologue of MobB of ICE-1

Orf43 encodes a homologue of TraD a member of the VirD4 coupling protein of this family. MobB (619 amino acids) of ICE-1 is the VirD4 of T4SS-1.

The homology between $TraD^{ICE-2}$ and MobB was measured by a constraint based pair wise alignment using the COBALT multiple alignment tool (Figure 6-9). Based on this, MobB and $TraD^{ICE-2}$ were named Mob-1 and Mob-2, respectively. Table 6.3 shows the

domains identified in Mob1 and Mob2. It was speculated that Mob-2 might interact with the ICE-1 conjugation module.

Figure 6-9 Constrain based pair wise alignment of Mob-1 and Mob-2.
COBALT was used to identify the domain based homology between Mob-2 and Mob-1. Residues shown in red are conserved residues, blue indicates differences residues with no gaps and gray represents the residues where sequence gaps were <50%.

Table 6-3 Domains of Mob1 and Mob-2.

Domains	Accession No.	Mob-1 (619 aa*)	Mob-2 (699 aa)	Possible Functions
TraG-D_C	pfam12696	+	+	Coupling and DNA transfer
VirD4-component	COG3505	+	+	
SXT/TraD; SXT/TOL family	TIGR03743	+	-	Coupling protein
TraD:TOL family	TIGR03754	-	+	
T4SS-DNA-transfer	pfam02534	-	+	Coupling and relaxosome recruitment
TrwB	cd01127	-	+	
P-loop Ntapase family	cl21455	-	+	ATP utilisation
AAA_10	pfam12846	+	-	

6.3.5.4 *Mob-2* is required for enhanced mobilisation of P-*oriT*1

A Δ*mob-2* strain was created (see Appendix VII for primers) and was transformed with P-*oriT*-1 and conjugation assay (n=3) revealed a 6-fold reduction (P<0.0001) compared to WT.

Complementation was performed with an RFTool-1 based plasmid with *mob*-2 (Pmob-2) under the control of IPTG promoter (Figure 6-10) (see Appendix V for primers).

The plasmid was electro transformed into both Δmob2 and ΔICE-2 strains along with P-*oriT*-1. Pmob-2 restored transconjugation of the Δmob2 strain to WT levels and also produced a ~4 fold recovery in ΔICE2 (Figure 6-11). Thus, Mob2 appears to have a functional interaction with the ICE-1 mobilisation machinery acting on P-*oriT*-1

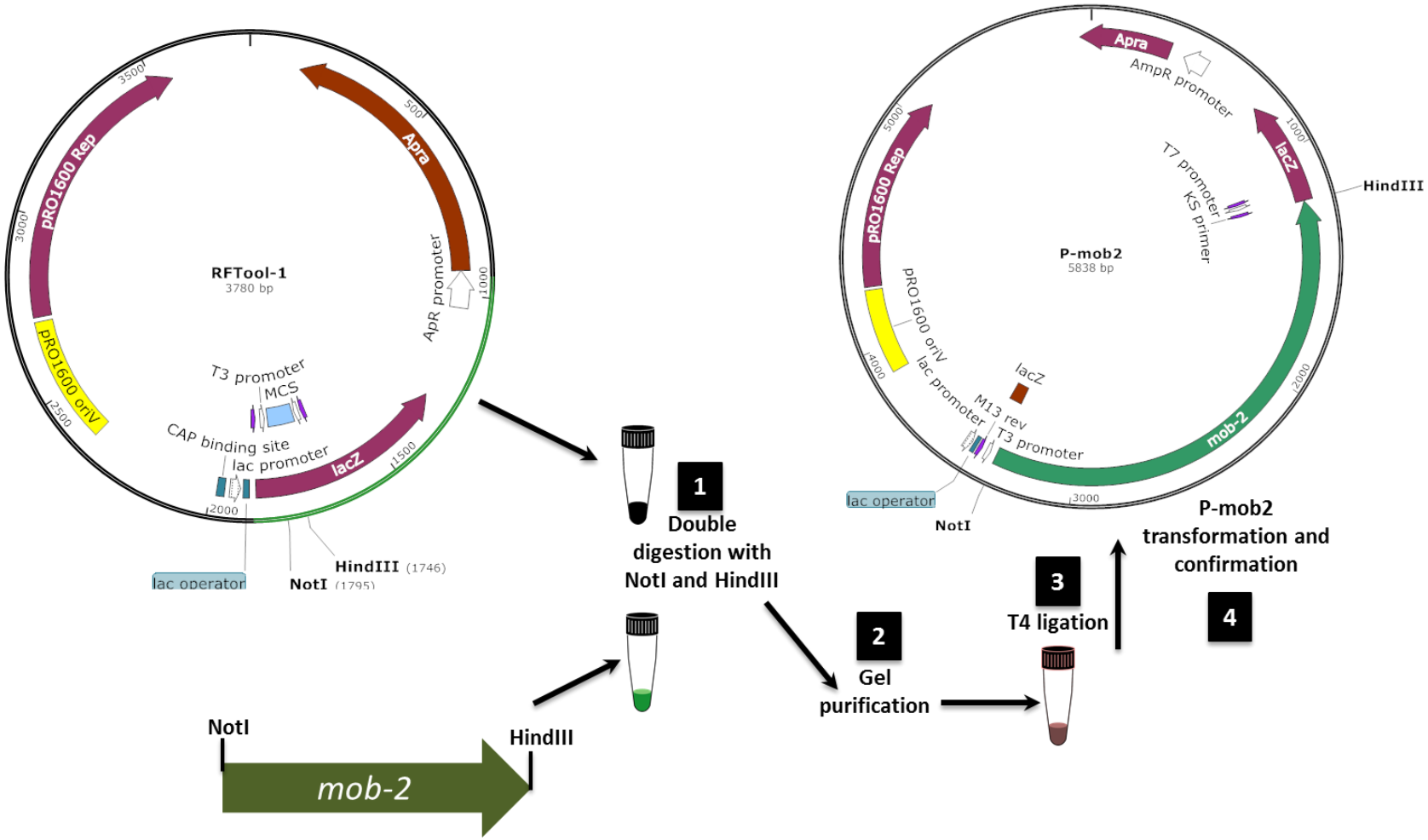

Figure 6-10 Schematics of construction of P-mob2 for complementation experiment.

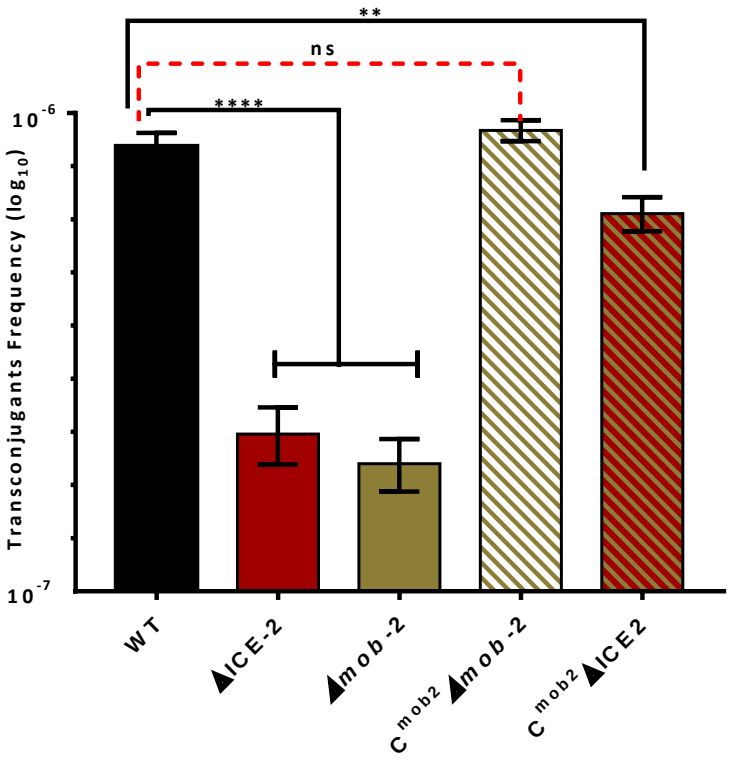

Donor strain	Conjugation frequency ±SD	P value (n=3)
WT	8.6×10^{-6} ± (2.0)	-
ΔICE-2	2.1×10^{-6} ± (4.7)	<0.0001
Δmob-2	1.8×10^{-6} ± (3.4)	<0.0001
C^{mob2} Δmob2	9.2×10^{-6} ± (4.0)	ns
C^{mob2}ΔICE-2	6.4×10^{-6} ± (2.0)	0.005

Figure 6-11 P-*oriT*-1 mobilisation was mediated by *mob-2* in ICE-2.
C^{mob2}Δmob-2 and C^{mob2}ΔICE-2 were mob-2 complemented strains. Unpaired t-test was used to measure the level of significance (n=3) P value was calculated compared to WT, ns = not significant.

6.3.5.5 *mob-2* did not substitute *mob-1*

To test whether *mob-2* could replace *mob-1* in T4SS-1, a *mob-1* deletion mutant was created and Δmob1 was transformed with P-*oriT*-1 and P-*oriT*-1+P-mob2. No transconjugants were obtained in either case except for the WT (8.7×10^{-6} ±7.0). Indicating that Mob-2 has functional rather than structural interactions with the ICE-1 conjugation system.

6.3.5.6 Mob2 may provide energy to the conjugation machinery of ICE-1

Mob1 and Mob2 are homologues of VirD4, which is involved in energy transduction to T4SS via its ATPase activity. Mob1 and Mob2 sequences were investigated for the presence of Walker A and B motifs as these are responsible for ATP binding and hydrolysis (Yuan et al., 2005, Stratford et al., 2007). Initial analysis showed that the Walker A motif was present in both proteins but Walker B was only detected in Mob-2 (Figure 6-12A). Thus it was speculated that Mob1 might be defective in ATP hydrolysis that is required for DNA transfer.

To determine examine possible significance of the absent Walker B motif in Mob-1, both Walker A and B motifs in Mob-2 were point mutated (section 6.2.3). Briefly, the lysine 199 residue (ATP binding site) in the Walker A motif and the glutamic acid 507 residue (ATP hydrolysis) in the Walker B motif were substituted with alanine (Figure 6-12B). The *mob*-2^{K199E507} (*mb* ^{K199E507}) was cloned into RFTool-1.

Mob-2^{K199E507} did not restore the mobilisation from the Δmob2 and ΔICE-2 strains (Figure 6-12C). These results strongly suggest that Mob2 made a significant contribution to energy transduction on the cytoplasmic aspect of T4SS-1.

A.

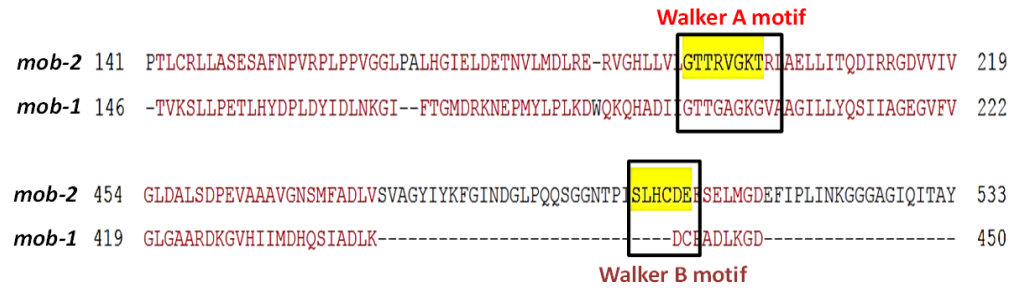

B.

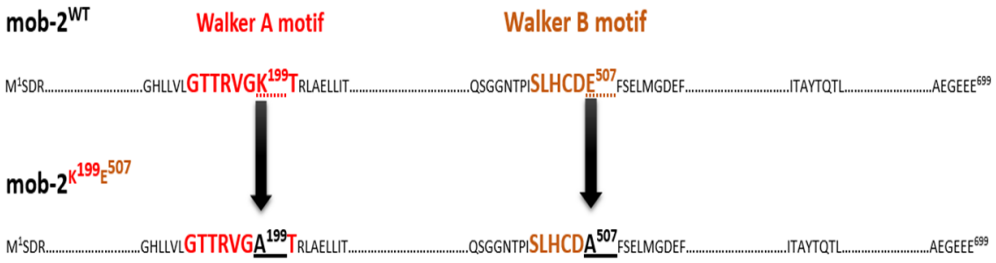

C.

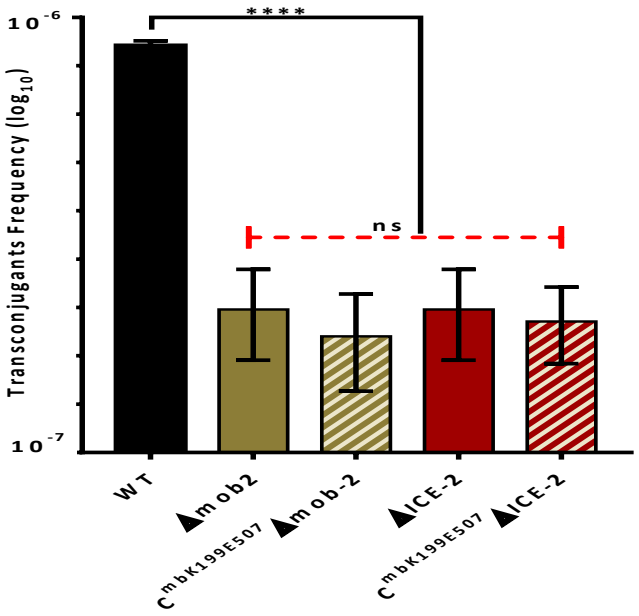

Figure 6-12 Point mutations in Walker motifs inactivated the Mob-2 activities.
A. position of walker motifs in mob genes; mob-1 is deficient for walker B motif. B. schematics of point mutations done in walker motifs of mob-2, which was cloned in RfTool-1 for complementation experiment. C. conjugation assay performed with mob2 and ICE2 mutant strains. $C^{mbK199E507}$ indicates the complementation of mutated mob-2.

6.3.5.7 Deletion of *traI* also reduced P-*oriT*-1 transport

TraI (*orf2*; relaxase) was also investigated for a potential contribution to ICE-1 / ICE-2 cross talk. An in-frame deletion of *traI* was made (see Appendix VII for primers) and transformed with P-*oriT*-1. Surprisingly, the *traI* deletion also reduced conjugative mobilisation of P-*oriT*-1 by ~5 fold compared to the WT (P = 0.0001) (Figure 6-13).

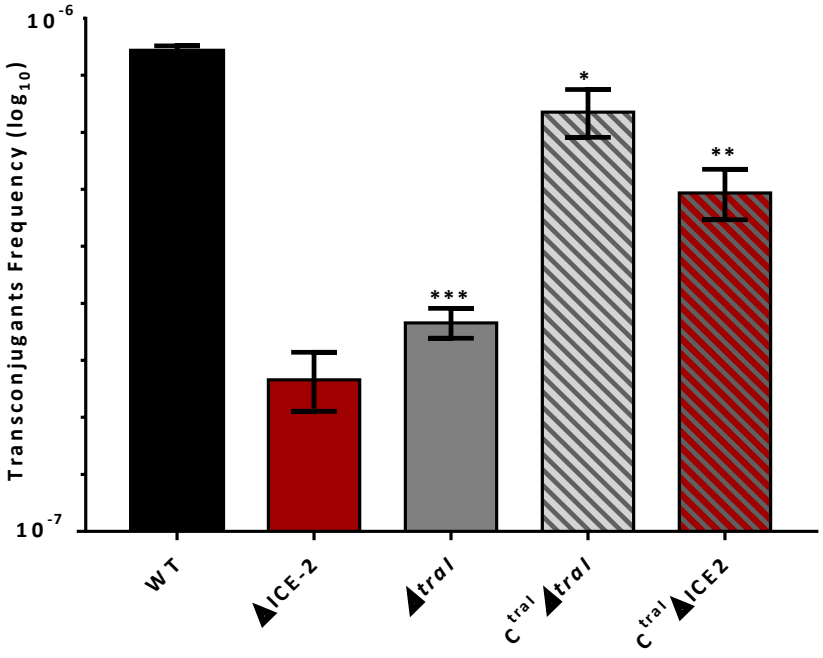

Donor strain	Conjugation frequency ±SD	P value (n=3)
WT	8.5×10^{-6} ± (2.0)	-
ΔICE-2	2.0×10^{-6} ± (4.7)	<0.0001
ΔtraI	3.5×10^{-6} ± (3.4)	0.0001
C^{traI} ΔtraI	6.9×10^{-6} ± (4.0)	0.01
C^{traI}ΔICE-2	5.3×10^{-6} ± (2.0)	0.008

Figure 6-13 *traI* deletion in ICE-2 reduced the conjugative transfer of P-*oriT*-1.
C^{traI} represents complementation of *traI* to the mutant strains. (n=3)

Complementation was achieved by was cloning *traI* into RFTool-1 between NotI and SalI restriction sites. P-*traI* construction was confirmed both by restriction digestion and PCR (Figure 6-14). Near complete complementation was seen with the Δ*traI* strain, while a lesser degree of complementation was achieved with the ΔICE-2 host.

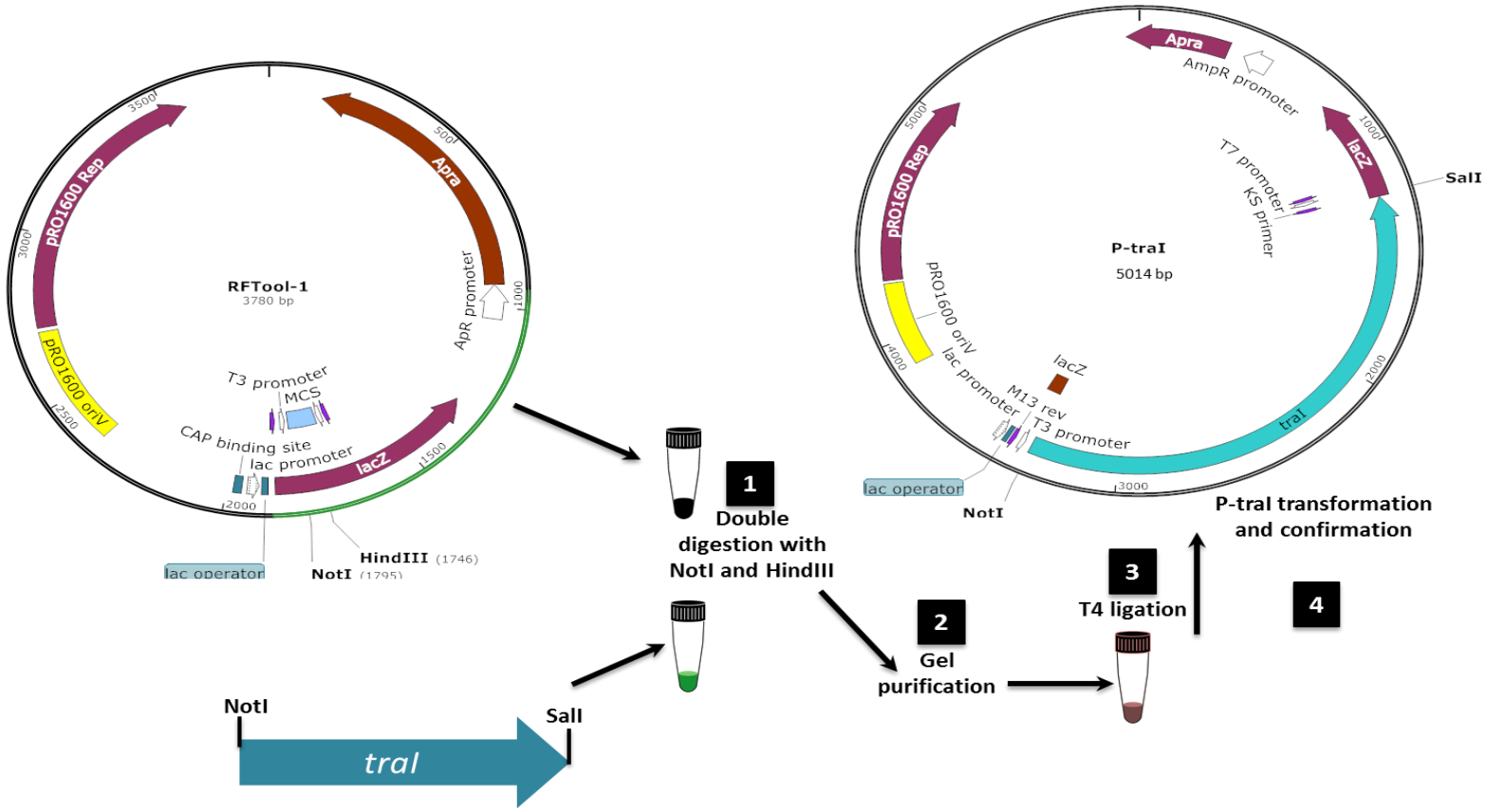

Figure 6-14 Schematics of construction of P-*traI*.

6.3.6 *Int2b* and *orf8* do not interact with the ICE-1 conjugation machinery

Conjugative mobilisation of P-*oriT*-1 was performed using Δ*int2b*::hph and Δ*orf8*::hph as donor strains. No differences in conjugation frequencies were observed between mutant strains and WT (Data not shown).

6.4 Discussion

6.4.1 Site specific excision of ICE-2 was not affected by growth phase

Successful excision of ICE-2 showed the presence of functional integration/excision module. These findings are consistent the work of Qiu et al. (2006), who demonstrated showed site-specific excision and integration of the PAPI-1 element in *Ps. aeruginosa*.

Generally, ICEs are dependent on various factors that provide selective pressure for their excision (Wozniak and Waldor, 2010, Johnson and Grossman, 2015), for example, environmental conditions such as growth phase or bacterial responses to DNA damage (Auchtung et al., 2005, Beaber et al., 2004, Bellanger et al., 2007). The influence of growth phase on ICE-2 excision was studied here for the first time. ICE-2 was found to be excised at sampling point but the level increased in early stationary where the circularised form of the element was detected equally in the genomic DNA fraction (Figure 6-4). Similar patterns have been observed with ICEclcB13 (Ravatn et al., 1998), ICESt3 (Carraro et al., 2011) and ICEMlSymR74 (Ramsay et al., 2006). The quantitative measurement of the frequencies of ICE-1 excision could be investigated in future using real time PCR.

6.4.2 Deletion of *int2a* abolished excision of ICE-2

ICE-2 contained two integrases (*int2a* and *int2b*) (section 3.3.2 & Table 3-3) and both belong to the same family of tyrosine recombinases that catalyse site-specific recombination between double stranded DNA via short segments with identical sequences (Grindley et al., 2006, Rajeev et al., 2009). Deletion of int2a abolished the excision of ICE-2. Moreover, no cross talk was detected between *int2a* and *int2b*, indicating that only *int2a* was required under the conditions applied here.

6.4.3 No evidence for ICE-2 mobilisation

Self-conjugation of PAPI elements was previously examined for pKLC102 and ICEEc-2. However, no evidence of ICE-2 self-conjugation was observed (limit of detection was $<1\times10^{-7}$). As previously with ICE-1, ICE-2 was tagged with hph and excision experiments with both native and tagged ICE-2 showed no difference, confirming that tagging did not affect the excision.

In-trans mobilisation of ICE-2 by P-*oriT*-1 was also tested. However, conjugative transfer of ICE-2 was not detected. This may have reflected very low conjugation frequencies of with ICE-2. One contribution to this could have been lethality of the *K. pneumoniae* donors to the recipient *E. coli* mediated by their T6SSs. These secretion systems have been identified in more than 25 % of Gram-negative bacteria (Bingle et al., 2008) and have the capacity to kill other co-localised cells. For example, *V. chloerae* uses its T6SS to kill *E. coli*, *Dictyostelium discoideum*, and even macrophage cell lines (Pukatzki et al., 2006, Ma et al., 2009).

Among the three T6SSs (T6SS-1, T6SS-2 and T6SS-3) of *K. pneumoniae* HS11286, deletion of T6SS-1 significantly attenuated its predatory effects on *E. coli* (Figure 6-6), accordingly a double mutant (ΔT6Δc) was created and this significantly increased the transconjugant frequency. However, investigation of ICE-2 transfer from this strain did not detect any self or in-trans mobilisation of the element (limit of detection $<1\times10^{-6}$). Although it is possible that the sensitivity of the assay was insufficient to detect transconjugants, this result raised the possibility that the conjugative machinery of ICE-2 might be inactive. This suggestion accords with the findings of Croucher et al. (2009), who showed that variations in insertion sites and loss of any gene in the conjugative-machinery resulted in degeneration of the element's autonomous mobility.

6.4.4 *oriT* was not detected in ICE-2

The presence of relaxase and *oriT* are necessary for mobility of ICEs (Lee and Grossman, 2007, Smillie et al., 2010). Relaxases recognise the nick sites in *oriT* to produce a single strand DNA break (Byrd and Matson, 1997). The relaxase of ICE-2 was identified as *orf2* in Chapter 3, thus the location of *oriT* was investigated here.

There is little experimental evidence regarding the location of *oriT* in PAPI elements. Investigators have documented the presence of relaxases in ICEEc-2, PAPI-1 and pKLC102 but did not identify their *oriT* sequences (Klockgether et al., 2007, Qiu et al., 2006, Roche et al., 2010). Nevertheless, conjugative transfer of these elements confirm the presence of *oriTs*.

11 fragments from ICE-2 were cloned into pACYC184 but no plasmid mobilisation was detected. Although, the strategy used could be modified further but it seems that none

of these fragments were found to contain the oriT-2. These results might reflect degeneration or loss of *oriT* in ICE-2. However, the presence of many repeated sequences and AT rich regions in ICE-2 indicate the possible presence of a functional *oriT.* It seems most likely that lack of a functional Mpf system in ICE-2 was responsible. Loss of components from a conjugation system are well-recognised to result in loss of conjugative mobilisation (Croucher et al., 2009).

6.4.5 ICE-2 cross talk with ICE-1 during conjugative DNA transfer

Functional interactions between the two non-homologous T4SSs (T4SS-1 and T4SS-2) were investigated. Interactions between two non-homologous MGEs are common and have been described in several bacterial systems. In *V. cholerae*, the recombination directionality factor VPI-1 interacts with VPI-2 for its excision (Carpenter et al., 2015). Integrase cross-talk between two PAIs of *E. coli* 536 has also been documented by Middendorf et al. (2004).

Deletion of ICE-2 showed a 6-fold reduction in conjugative mobilisation of the ICE-1 marker plasmid P-oriT1. This result fits with the findings of de Paz et al. (2005), who demonstrated the functional interactions between two non-homologous T4SSs in *Agrobacterium*. In their study, VirB10 from one T4SS was partially substituted by TrwE of the other system during conjugation (de Paz et al., 2005).

6.4.6 MobB is a TraD homologue

To identify components involved in this cross talk, T4SS-2 components were reviewed on the basis of their putative functions and prioritised for further analysis. Because they are highly specific for their own systems (Zechner et al., 2012) genes involved in pilus assembly were given low priority as were those highly conserved in PAPI elements.

TraI (relaxase) and *traD* (T4CP), were investigated (Table 6-2) because they share common features even though they are from different systems (Juhas et al., 2008). Relaxase binds DNA in a sequence-specific manner (Nash et al., 2010) but the sequences could be variable even for the same relaxase, thus the relaxase of T4SS-2 might have been involved. In addition, T4CP mediates DNA transport to the secretion channel by interacting with both the relaxosome and the secretory channel (Schroder and Lanka, 2005, Wallden et al., 2010).

The amino acid sequence analysis of coupling proteins of ICE-1 (MobB) and ICE-2 (TraD) showed that both shared similar domains. TraG-D_C was one of the common domains that has a role in DNA transposition during conjugation. The other common domain was VirD4-components that translocate DNA to the secretion channel (Cascales et al., 2013, Cascales and Christie, 2004, Jakubowski et al., 2004). In addition, COBALT analysis confirmed that these domains showed 80% similarity and, based on these findings, the genes were named as *mob-1* (*mobB*) and *mob-2* (*traD*).

6.4.7 Mob-2 was an energy amplifier that enhanced conjugative transfer of ICE-1 marker DNA

The Δmob-2 stain showed a 6-fold reduction in P-oriT1 transconjugants, indicating that this gene contributed to the cross talk and this was further confirmed by complementation with P-mob2. These findings were extended by demonstrating enhancement of conjugative transfer of P-oriT1 by P-mob2 in the ΔICE-2 strain.

A Δmob-1 strain was also created to investigate whether *mob-2* could substitute for *mob-1*. DNA transfer was completely abolished and P-mob2 did not provide complementation. Thus Mob-2 appears to have an enhancing rather than an essential role in ICE-1 mobilisation.

In conjugative transfer, VirD4 (T4CP) delivers the DNA substrate to VirB11 and this is translocated to the recipient via the VirB2 channel (Cascales and Christie, 2004). Cascales et al. (2013) showed that engagement of DNA substrates with T4CP was necessary for VirB10 activation. For DNA translocation, an energy hub is provided by three ATPases (VirB4, VirB11, VirD4) and this is referred to the cytoplasmic power house of conjugation (Banta et al., 2011, Atmakuri et al., 2004). VirD4 is involved in sensing intracellular signals from the relaxosome (Figure 6-15) and processes the nucleoprotein complexes to the secretion channel (Lang et al., 2011). In addition, T4CP (TrwB) possesses ATPase activity with specificity for the DNA to be translocated (Gomis-Ruth et al., 2001, Moncalian et al., 1999, Hormaeche et al., 2006). It was therefore suggested that Mob-2 might act as an amplifier enhancing T4SS-1 mediated transfer by contributing more energy.

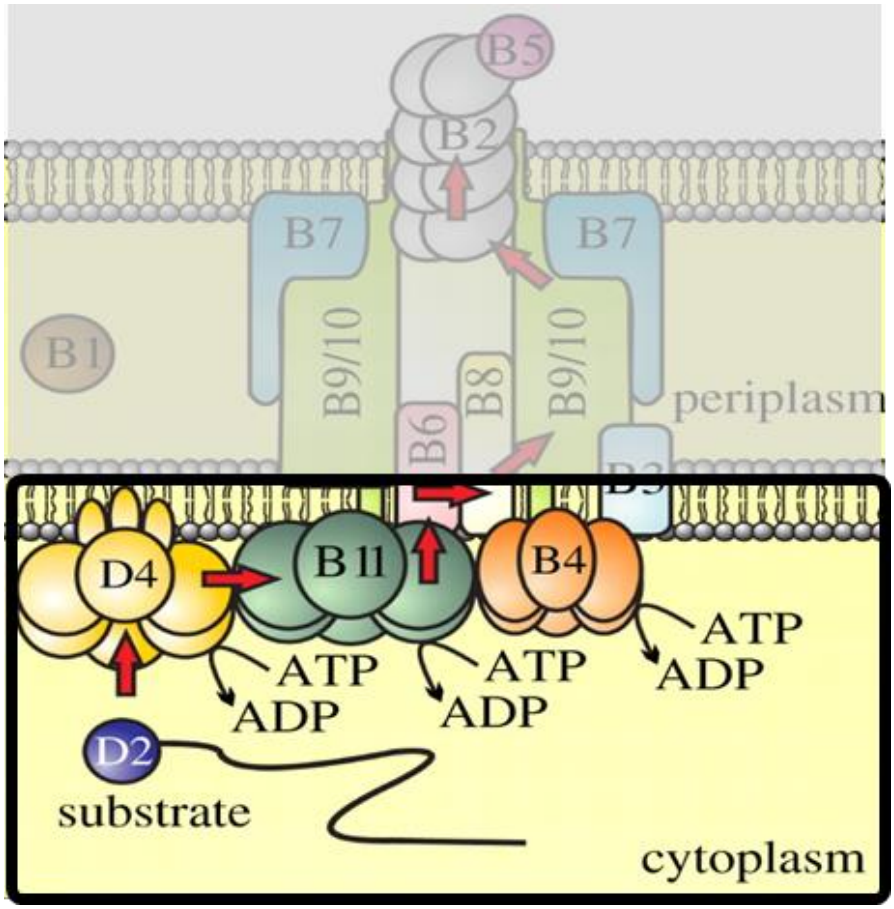

Figure 6-15 General DNA translocation pathway and core structure of a T4SS-1. Adapted from (Zechner et al., 2012)

The recognition that Mob-1 apparently lacked a Walker B motif whereas Mob-2 was intact added further weight to this possibility. Analysis of the the point mutations in the Walker motifs of *mob-2* provided further evidence for a role of this protein in energy provision enhancing ICE-1 mediated conjugative transfer. Based on these findings a model of interactions/crosstalk between T4SS-1 and T4SS-2 is presented in Figure (6-16).

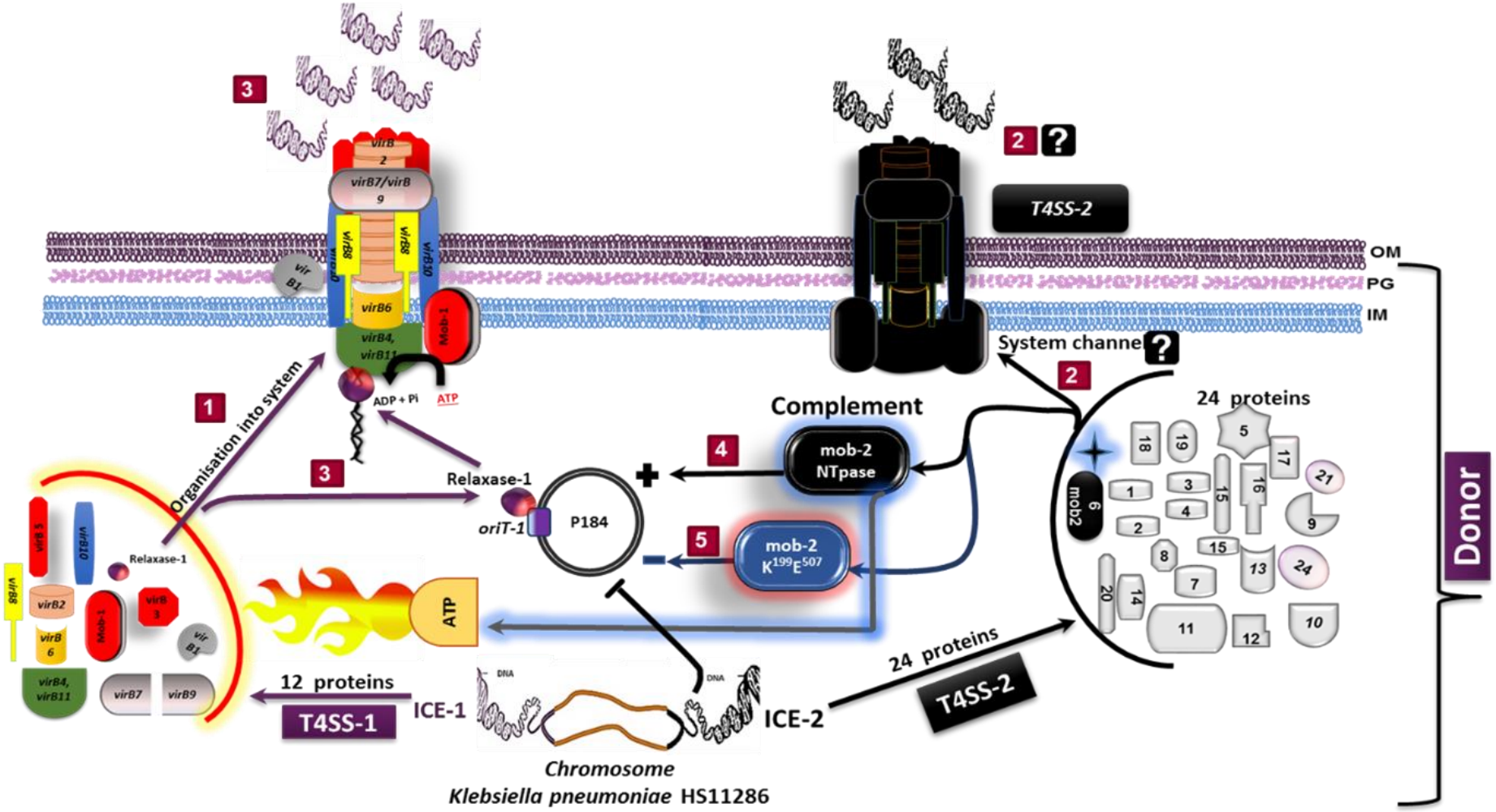
3
virB 2
virB7/virB 9
virB8
virB8
virB10
vir B1
virB6
virB4, virB11
Mob-1
ADP + Pi
ATP
1
Organisation into system
3
Relaxase-1
oriT-1
P184
4
mob-2 NTpase
5
mob-2 K199E507
ATP
12 proteins
T4SS-1
ICE-1
DNA
ICE-2
24 proteins
T4SS-2
2 ?
T4SS-2
OM
PG
IM
System channel ?
2
Complement
24 proteins
mob2
Donor
Chromosome
Klebsiella pneumoniae HS11286

Figure 6-16 Model of interactions/crosstalk between T4SS-1 and T4SS-2.
1. ICE-1 encodes 12 proteins that form a functional Mpf system of T4SS-1. 2. ICE-2 has 24 genes encoding proteins for T4SS-2 but whether or not these organised into a functional Mpf system is unknown. 3. T4SS-1 was able to mobilise ICE-1 marker plasmid and deletion of ICE-2 reduced the transconjugation frequency by T4SS-1 4. The *mob-2* complemented the defects in mobilisation of ICE-1 marker plasmid. 5. Point mutations in Walker (A & B) motifs of *mob-2* indicated that it provides energy to the conjugation machinery of ICE-1.

6.4.8 TraI also exerted effects on ICE-1 marker DNA transfer

Partial complementation of P-mob2 in ΔICE-2 strain indicated that other components of ICE-2 might contribute. The other prioritized target was *traI* and the ΔtraI mutant was shown to produce a 4-fold declined in conjugative transfer of P-*oriT*-1. The defects was more effectively complemented in ΔtraI than in ΔICE-2. Thus both *mob-2* and *traI* contributed to the enhanced DNA transfer.

Tato et al. (2007) showed that the ATPase activity of T4CP contributing to substrate transfer was regulated by components of the relaxosome. Functional interactions between TraI and T4CP were also documented by Szpirer et al. (2000), who demonstrated that these proteins could interact with other systems even in the absence of their cognate *oriT*. Thus the roles of traI and mob-2 in the present context are further supported; combined complementation of traI and mob-2 would provide definitive evidence. Furthermore the interaction of TraI and *oriT*-1 could be investigated in future by DNA binding assays and transfer DNA immunoprecipitation (TrLp) assay.

The Δorf8 and Δint2b mutant strains effectively provided negative controls as components with no predicted contribution to cross talk. Thus not every gene mutation in ICE-2 reduced DNA transfer of ICE-1 thereby further reinforcing the conclusion that mob-2 and traI were critical to the interactions with T4SS-1.

6.5 Conclusions:

1. Excision/integration module of ICE-2 is functional.
2. Growth phase had no effects on excision of ICE-2.
3. *Int2a* controlled the excision of ICE-2.
4. ICE-2 conjugative mobilisation was not detected suggesting an incomplete mobilisation cycle of this element.
5. An origin of transfer was not detected in ICE-2.

6. Functional interactions were detected between ICE-1 and ICE-2 for conjugative transfer of the ICE-1 marker plasmid.
7. Mob-2 and TraI mediated cross talk between the ICEs.
8. Mob-2 enhanced conjugative transfer of ICE-1 marker DNA, probably by providing energy to the hub.

Chapter 7 General discussion and final conclusion

7.1 General discussion

This study was developed to characterize two ICEs of an extensively studied *K. pneumoniae* strain (HS11286) with a view to further understanding their contributions to HGT, cell physiology, virulence and antibiotic resistance.

ICEs are self-conjugative MGEs that encode their own machineries for transmission regulation and maintenance. Findings of this study demonstrated that organisation of various modules in ICEKP-1 associated elements are stable. The 5´ region carries the HPI of *Y. pestis* and *Y. pseudotuberculosis*, while the 3´ region contains the conjugation module. These two regions are highly conserved in elements found in *Enterobacteriaceae*. In addition, two regions were found to show variation. First, at the 3'-end of the HPI the *IS100* found in *Yersinia* spp., was replaced and marked by a 17bp DR, a common feature in both HPI and ICEKP-1 elements. ICEKP-1 was first identified in *E. coli* and it was believed to have originated by insertion of plasmid R6K at the *IS100* of HPI (Schubert et al., 2004). The second region of variation generally lies between the conjugative module and the DR at the 3´-end. *In-silico* characterisation and PCR screening of ICE-1 (Figure 3-9) in clinical isolates also demonstrated variations between elements exist in these two regions. Thus it is suggested that gene content variation in ICE families can arise from transposases and other insertions or deletions in the middle and at the 3´ end of ICEKP-1 elements.

Characterisation and classification of ICE-2 highlighted the need to develop the classification system further (Burrus et al., 2002, Bi et al., 2012). As ICEs come into existence after one or many HGT events, variations are expected leading to members of the same family with regions that vary from their ancestors. For example, the existing classification system is based on the similarities of integration sites and the nature of the conjugative module. Integrases are generally site-specific for ICE integrations but any flexibilities in their recognition and binding sites could alter the insertion, thereby producing a challenge for classification. To facilitate classification, both the integration site and the integrase family should be considered equally. Thus, a major modification suggested here is to categorise the existing 28 families of ICEs into subfamilies; this will enable the classification of the majority of unclassified elements. However, many ICEs

may not be recognisable by bioinformatic approaches, and devising experimental methods to identify new ICEs is an important challenge for future studies.

Siderophore systems are common in *K. pneumoniae* and other Gram negative bacteria (Koczura and Kaznowski, 2003) and have long been known to contribute to virulence and growth fitness (Holden and Bachman, 2015). Enterobactin (catecholate) is among first characterised siderophores and is produced by more than 90% of examined enetrobacterial isolates whereas, yersiniabactin was found in few isolates (Lawlor et al., 2007). Nearly all *K. pneumoniae* produce enterobactin, however yersiniabactin (Ybt) is the next most commonly produced siderophore; the latter is frequently found on an ICE (ICEKP-1). Recently the Ybt locus was detected in 39.5 % of 2499 *K. pneumoniae* genomes and the majority of these were clinical isolates, demonstrating a strong association between Ybt and human infections (Lam et al., 2017). In *Yersinia* the major differences between high and low virulence strains has been related to their ability to capture iron molecules (Brem et al., 2001).

K. pneumoniae HS11286 carries loci for enterobactin and Ybt, evidence from this study indicated that ICE-1 mutant produced siderophore (Figure 4-7) in the absence of Ybt locus, thus showed that enterobactin production was active. Halo-zones produced by ΔICE-1 (Figure 4-7B) suggesting that enterobactin might be the major siderophore produced by *K. pneumoniae* HS11286. However, ICE-1 mutant did not show improved growth in the presence of WT supernatant (section 4.3.2) that supported the hypothesis 4-1 and the importance of Ybt in *K. pneumoniae* HS11286. Although measurements of siderophore release were only comparative and did not differentiate the specific contributions of Ybt. Direct quantification of Ybt would provide a better and direct comparison. In general, siderophore uptake by Gram-negative bacteria requires genes encoding a TonB-dependent receptor, a periplasmic binding protein and an ABC transporter that enables transfer of siderophore-bound iron from periplasm to cytoplasm (Brem et al., 2001). In the Ybt system, FyuA is the TonB-dependent receptor, YbtP and Q are the ABC transporters but identification of a periplasmic binding protein has not been reported. It was suggested that such genes might be located outside the HPI or are not required by the system. The synthesised Ybt is exported by an unknown method that might be facilitated by YbtX (Figure 3-1).

YbtP and Q were assumed to be important for internalisation of bound iron and complementation of the ICE-1 mutant with Pybt supported this view. Direct measurement of internalisation of radiolabelled iron would provide clearer in this regard. The question of how the growth defect was complemented in the absence of FyuA remains answered. It was speculated that alternative TonB-dependent siderophore receptors might have been used to achieve growth recovery. These findings have gone some way towards enhancing our understanding of how an HGT derived additional siderophore system could enhance survival in harsh conditions.

Another interesting finding was the apparent contributions of Ybt exporters to antibiotic resistance. As far as we are aware, this is the first study to highlight this role. As explained earlier, YbtP and Q belong to the ABC transporter family while YbtX belongs to the MFS major drug efflux system. Both the deletion and reserpine studies related antibiotics supported the proposal that Ybt exporters contributed to resistance in both *K. pneumoniae* and *E. coli*. Some cautions should be attached to this conclusion. The deletion of ICE-1 affected growth rate and this could, in turn affect zone sizes. In addition, complementation with Pybt did not allow attribution of the effects to specific genes. These findings reported here are very promising; however, single gene mutations/complementation would provide definitive results.

K. pneumoniae HS11286 carried six natural plasmids (section 1.16). Plasmid Miniprep was performed to address the possibility of loss of any natural plasmid. However, no loss was observed (Figure S2 Appendix XIII) that confirmed that phenotypes of ICE mutants were not due to the loss of natural plasmids from the strain. Overall, the in-vitro experiments clearly identified important roles for the ICEs in growth, biofilm formation and antibiotic resistance. The virulence studies do not allow firm conclusions at this stage. In general the results represent good examples of how cargo genes carried by elements benefited the host in various conditions.

ICEs primarily reside in a host but retain the ability to excise and to transfer by conjugation (Johnson and Grossman, 2015). ICEs typically have a modular structures, with gene clustered according to the process to which they contribute. ICEs all share the core functions of the mobilisation cycle but these are not carried out in the same way by all; instead they regulate and maintain their existence using diverse range of genes

and mechanisms (Wozniak and Waldor, 2010). The integration/ excision module plays important role in the maintenance of ICEs, and functional Mpf systems are required for successful conjugative transfer. Disruption and lack of any of the genes encoding the Mpf system abolishes the transfer of element. Moreover, ICE excision and transmission may also be affected by environmental factors including growth phase and metabolic burden. For example, excision of ICE-1 increases as the host cell enters stationary phase, whereas, no obvious effects was observed in excision of ICE-2. These results illustrate that different mechanisms and environmental conditions affect mobilisation of different ICEs.

T4SSs are multisubunit cell envelope spanning structures enabling conjugative transfer of nucleoprotein complexes across the cell envelope. T4SSs are encoded by multiple genes usually organised into a single functional unit. Mobilisation of non-conjugative elements by ICEs and conjugative plasmids were reported previously (Naglich and Andrews, 1988, Valentine et al., 1988, Hochhut et al., 2000, Lee et al., 2012). In the present study a novel phenomenon of conjugative mobilisation of ICE-1 by its own marker plasmid P-oriT-1 was observed. It was speculated that relaxosome and Mpf formed during plasmid mobilisation triggered in-trans the transfer ICE-1 such that the transconjugant frequency reached the level of assay detection. Quantification of expression of from the ICE-1 conjugation module with and without P-oriT-1 could deliver a better level of understanding regarding the apparent *in-trans* mobilisation.

The conjugation process begins with recognition of *oriT* by its cognate relaxase. Generally, *oriT* regions are recognised as A+T rich regions with several conserved DR and IR sequences. A novel set of IR and DR regions was defined here and were demonstrated to be critical for *oriT* function and conserved in related ICEs. Demonstration that the 140bp region between *mobB* and DR2 was essential for mobilisation was also an original finding. Although these sequences are highly conserved in ICEKP-1 associated elements their importance was not previously recognised. The results reported are comprehensive and can be regarded as definitive.

On screening the PAPI associated elements were found to have two integrases belonging to different families. This the first study in which the role of each integrase in excision was studied. *Int2a* which belongs to (XerC/D) family was found responsible for

excision. These findings also support the classification of ICE-2 based on *int2a*. This strategy helped to understand how bioinformatic analysis together with experimental data could sort out the challenges in classification of novel ICEs.

No self-conjugation and oriT-2 was detected in ICE-2, although significant conserved IR and DR sequences (data not shown) were detected in the element. One possibility could be a non-functional Mpf system in ICE-2. Generally the gene clusters encoding Mpf in the of PAPI family are intact and organised into a single operon (Mavrodi et al., 2009). However, in case of ICE-2, the components of T4SS-2 are localised in various regions (Figure 3-5) and this could have affected the expression of essential components. A not functional Mpf could explain the lack of observed conjugative-mobilisation of ICE-2 and the failure to define *oriT* in ICE-2. It would be informative to investigate the organisation and structural assembly of the ICE-2 Mpf system to gain understanding of the results obtained here.

Interactions between non-homologous MGEs have been described in several bacterial systems (Carpenter et al., 2015, Middendorf et al., 2004). Here, TraI and Mob-2 of ICE-2 were shown to be involved in crosstalk with T4SS of ICE-1 leading to enhanced mobilisation of P-oriT-1. It was also shown that Mob-1 lacked a Walker B motif and that Mob-2 could enhance the mobilisation of the ICE-1 marker plasmid, presumably by increasing the energy available to support transfer. Further studies taking into account the currently unexplained role of TraI, will need to fully explain the cross talk in conjugation between the two ICEs observed here.

Finally, a number of potential limitations need to be considered. Firstly, the contribution of ICE-1 to the histidine dependant phenotype should have been investigated in multiple derived mutant strains. Unfortunately, due to switching between labs, five additional ICE-1 mutants were lost. It seems likely that histidine dependence would not have been present in strains other than the one investigated. Second, the virulence assay should be repeated to confirm or resolve the anomaly between the single and double mutants. Thirdly, while identification of oriT-2 in ICE-2, was limited by construction of only a few ICE-2 marker plasmids, several other combinations could also be investigated. Other approaches such as assay of TraI binding to ICE-2 sequences could provide clear evidence of an *oriT* in the element.

7.2 Final Conclusions

The specific objectives of this study are stated with final conclusions:

1. To characterise and annotate uncharacterised contents of ICE-1 and ICE-2 of *K. pneumoniae* HS11286 and to study their prevalence in 42 local clinical isolates.

Conclusion 1 "ICE-1 belongs to ICEKP-1 family, whereas ICE-2 was classified as PAPI element and compared to ICE-2, ICE-1 was more prevalent in local isolates of *K. pneumoniae.*

2. To investigate the contribution of ICE-1 and ICE-2 on the phenotypes of *K. pneumoniae* HS11286 including: Growth characteristics; Biofilm formation; Antibiotic resistance; and contribution to virulence.

Conclusion 2 "ICEs have shown contribution to the growth dynamics, biofilm formation, antibiotic resistance and virulence of the host"

3. To study the mobilisation cycle of ICE-1 and ICE-2 and its effects on recipient phenotypic biology.

Conclusion 3 "Both ICE1 and ICE-2 were non-mobile, however ICE-1 was mobilised *in-trans* by P-*oriT*-1 and siderophore production and antibiotic resistance was significantly increased in transconjugants"

4. To investigate whether or not ICE-1 and ICE-2 has functional interactions during conjugative transfer of DNA.

Conclusion 4 "Mob-2 and TraI of ICE-2 has functional interactions with ICE-1 during conjugative transfer of ICE-1 marker DNA."

7.3 Future recommendations

1. Whole genome sequencing of the ΔICE-1 mutant that will help to identify the lesion(s) that affected histidine biosynthesis.
2. Deletion of *ybtX* will prove the role of Ybt exporters in antibiotic resistance.
3. Deletion of the *fhuA* and *fepA* homologues in HS11286 strain is desirable to understand whether Ybt could internalise Ybt-bound iron through an alternative TonB-siderophore receptor.
4. The quantitative measurement of ICE-1 and ICE-2 excision will provide clear evidences of the effects of growth phase on their excision.
5. Combined complementation of *traI* and *mob*-2 will prove that cross talk between T4SS-1 and T4SS-2 was mediated by both.
6. Interactions between Mob-2 and TraI will help to understand their real role in cross talk.
7. The examination of organisation and structural assembly of ICE-2 Mpf system will confirm that the system is functional.

Bibliography

AARTSEN, J. J. V. 2008. <The Klebsiella pheV tRNA locus: a hotspot for integration of alien genomic islands>. *Bioscience Horizons,* 1**,** 51-60.

AL-MADADHA, M. E. 2017. Functional Analysis of Fic Domain Bearing Proteins in *Klebsiella pneumoniae*. *University of Leicester; Thesis***,** 1-168.

ALTSCHUL, S. F., THOMAS L. MADDEN, ALEJANDRO A. SCHÄFFER, JINGHUI ZHANG, ZHENG ZHANG, MILLER, W. & LIPMAN, D. J. 1997. Gapped BLAST and PSI-BLAST: a new generation of protein database search programs. *Nucleic Acids Research,* 25**,** 3389-3402.

ALY, K. A. & BARON, C. 2007. The VirB5 protein localizes to the T-pilus tips in Agrobacterium tumefaciens. *Microbiology,* 153**,** 3766-75.

ANDAM, C. P. & GOGARTEN, J. P. 2011. Biased gene transfer in microbial evolution. *Nature Reviews Microbiology,* 9**,** 543-555.

ANDREWS, S. C., ROBINSON, A. K. & RODRÍGUEZ-QUIÑONES, F. 2003. Bacterial iron homeostasis. *FEMS Microbiology Reviews,* 27**,** 215-237.

ANDRZEJEWSKA, J., LEE, S. K., OLBERMANN, P., LOTZING, N., KATZOWITSCH, E., LINZ, B., ACHTMAN, M., KADO, C. I., SUERBAUM, S. & JOSENHANS, C. 2006. Characterization of the pilin ortholog of the Helicobacter pylori type IV cag pathogenicity apparatus, a surface-associated protein expressed during infection. *Journal of bacteriology,* 188**,** 5865-5877.

ARBER., W. 2000. Genetic variation: molecular mechanisms and impact on microbial evolution. *FEMS Microbiology Reviews,* 24**,** 1-7.

ARNOLD, R. S., THOM, K. A., SHARMA, S., PHILLIPS, M., JOHNSON, J. K. & MORGAN, D. J. 2011. Emergence of *Klebsiella pneumoniae* carbapenemase (KPC)-producing bacteria. *Southern medical journal,* 104**,** 40.

ATMAKURI, K., CASCALES, E. & CHRISTIE, P. J. 2004. Energetic components VirD4, VirB11 and VirB4 mediate early DNA transfer reactions required for bacterial type IV secretion. *Mol Microbiol,* 54**,** 1199-211.

AUCHTUNG, J. M., LEE, C. A., MONSON, R. E., LEHMAN, A. P. & GROSSMAN, A. D. 2005. Regulation of a Bacillus subtilis mobile genetic element by intercellular signaling and the global DNA damage response. *Proceedings of the National Academy of Sciences of the United States of America,* 102**,** 12554-12559.

AVILA, P., NÚÑEZ, B. & DE LA CRUZ, F. 1996. Plasmid R6K Contains Two FunctionaloriTswhich can Assemble Simultaneously in Relaxosomesin vivo. *Journal of molecular biology,* 261**,** 135-143.

AZIZ, R. K., BARTELS, D., BEST, A. A., DEJONGH, M., DISZ, T., EDWARDS, R. A., FORMSMA, K., GERDES, S., GLASS, E. M., KUBAL, M., MEYER, F., OLSEN, G. J., OLSON, R., OSTERMAN, A. L., OVERBEEK, R. A., MCNEIL, L. K., PAARMANN, D., PACZIAN, T., PARRELLO, B., PUSCH, G. D., REICH, C., STEVENS, R., VASSIEVA, O., VONSTEIN, V.,

WILKE, A. & ZAGNITKO, O. 2008. The RAST Server: rapid annotations using subsystems technology. *BMC Genomics,* 9**,** 75.

BAAR, C., EPPINGER, M., RADDATZ, G., SIMON, J., LANZ, C., KLIMMEK, O., NANDAKUMAR, R., GROSS, R., ROSINUS, A., KELLER, H., JAGTAP, P., LINKE, B., MEYER, F., LEDERER, H. & SCHUSTER, S. C. 2003. Complete genome sequence and analysis of Wolinella succinogenes. *Proc Natl Acad Sci U S A,* 100**,** 11690-5.

BACH, S., DE ALMEIDA, A. & CARNIEL, E. 2000. The Yersinia high-pathogenicity island is present in different members of the family Enterobacteriaceae. *FEMS microbiology letters,* 183**,** 289-294.

BACHMAN, M. A., OYLER, J. E., BURNS, S. H., CAZA, M., LEPINE, F., DOZOIS, C. M. & WEISER, J. N. 2011. *Klebsiella pneumoniae* yersiniabactin promotes respiratory tract infection through evasion of lipocalin 2. *Infect Immun,* 79**,** 3309-16.

BACKERT, S., FRONZES, R. & WAKSMAN, G. 2008. VirB2 and VirB5 proteins: specialized adhesins in bacterial type-IV secretion systems? *Trends Microbiol,* 16**,** 409-13.

BACKERT, S. & MEYER, T. F. 2006. Type IV secretion systems and their effectors in bacterial pathogenesis. *Current opinion in microbiology,* 9**,** 207-217.

BAMBEKE, F. V., BALZI, E. & TULKENS, P. M. 2000. Antibiotic efflux pumps. *Biochemical Pharmacology,* 60**,** 457-470.

BANTA, L. M., KERR, J. E., CASCALES, E., GIULIANO, M. E., BAILEY, M. E., MCKAY, C., CHANDRAN, V., WAKSMAN, G. & CHRISTIE, P. J. 2011. An Agrobacterium VirB10 mutation conferring a type IV secretion system gating defect. *Journal of bacteriology,* 193**,** 2566-2574.

BATTLE, S. E., MEYER, F., RELLO, J., KUNG, V. L. & HAUSER, A. R. 2008. Hybrid pathogenicity island PAGI-5 contributes to the highly virulent phenotype of a Pseudomonas aeruginosa isolate in mammals. *J Bacteriol,* 190**,** 7130-40.

BEABER, J. W., HOCHHUT, B. & WALDOR, M. K. 2002. Genomic and functional analyses of SXT, an integrating antibiotic resistance gene transfer element derived from Vibrio cholerae. *Journal of bacteriology,* 184**,** 4259-4269.

BEABER, J. W., HOCHHUT, B. & WALDOR, M. K. 2004. SOS response promotes horizontal dissemination of antibiotic resistance genes. *Nature,* 427**,** 72-74.

BELLANGER, X., MOREL, C., DECARIS, B. & GUÉDON, G. 2007. Derepression of excision of integrative and potentially conjugative elements from Streptococcus thermophilus by DNA damage response: implication of a cI-related repressor. *Journal of bacteriology,* 189**,** 1478-1481.

BELLANGER, X., MOREL, C., GONOT, F., PUYMEGE, A., DECARIS, B. & GUEDON, G. 2011. Site-specific accretion of an integrative conjugative element together with a related genomic island leads to cis mobilization and gene capture. *Mol Microbiol,* 81**,** 912-25.

BELLANGER, X., PAYOT, S., LEBLOND-BOURGET, N. & GUEDON, G. 2013. Conjugative and mobilizable genomic islands in bacteria: evolution and diversity. *FEMS Microbiol Rev*.

BI, D., JIANG, X., SHENG, Z.-K., NGMENTEREBO, D., TAI, C., WANG, M., DENG, Z., RAJAKUMAR, K. & OU, H.-Y. 2015. Mapping the resistance-associated mobilome of a carbapenem-resistant *Klebsiella pneumoniae* strain reveals insights into factors shaping these regions and facilitates generation of a 'resistance-disarmed'model organism. *Journal of Antimicrobial Chemotherapy,* 70**,** 2770-2774.

BI, D., LIU, L., TAI, C., DENG, Z., RAJAKUMAR, K. & OU, H. Y. 2013. SecReT4: a web-based bacterial type IV secretion system resource. *Nucleic Acids Res,* 41**,** D660-5.

BI, D., XU, Z., HARRISON, E. M., TAI, C., WEI, Y., HE, X., JIA, S., DENG, Z., RAJAKUMAR, K. & OU, H. Y. 2012. ICEberg: a web-based resource for integrative and conjugative elements found in Bacteria. *Nucleic Acids Res,* 40**,** D621-6.

BIALEK-DAVENET, S., CRISCUOLO, A., AILLOUD, F., PASSET, V., JONES, L., DELANNOY-VIEILLARD, A.-S., GARIN, B., LE HELLO, S., ARLET, G. & NICOLAS-CHANOINE, M.-H. 2014. Genomic definition of hypervirulent and multidrug-resistant *Klebsiella pneumoniae* clonal groups. *Emerging infectious diseases,* 20**,** 1812-20.

BIKANDI, J., SAN MILLAN, R., REMENTERIA, A. & GARAIZAR, J. 2004. In silico analysis of complete bacterial genomes: PCR, AFLP-PCR and endonuclease restriction. *Bioinformatics,* 20**,** 798-9.

BINGLE, L. E., BAILEY, C. M. & PALLEN, M. J. 2008. Type VI secretion: a beginner's guide. *Current opinion in microbiology,* 11**,** 3-8.

BISTUÉ, A. J. S., BIRSHAN, D., TOMARAS, A. P., DANDEKAR, M., TRAN, T., NEWMARK, J., BUI, D., GUPTA, N., HERNANDEZ, K. & SARNO, R. 2008. *Klebsiella pneumoniae* multiresistance plasmid pMET1: similarity with the Yersinia pestis plasmid pCRY and integrative conjugative elements. *PloS one,* 3**,** e1800.

BOLTNER, D., MACMAHON, C., PEMBROKE, J. T., STRIKE, P. & OSBORN, A. M. 2002. R391: a Conjugative Integrating Mosaic Comprised of Phage, Plasmid, and Transposon Elements. *Journal of Bacteriology,* 184**,** 5158-5169.

BREM, D., C. PELLUDAT, A. RAKIN, AND, C. A. J. & HEESEMANN., J. 2001. Functional analysis of yersiniabactin transport genes of Yersinia enterocolitica. *Microbiology Today,* 147**,** 1115–1127.

BRISSE, S., FEVRE, C., PASSET, V., ISSENHUTH-JEANJEAN, S., TOURNEBIZE, R., DIANCOURT, L. & GRIMONT, P. 2009. Virulent clones of *Klebsiella pneumoniae*: identification and evolutionary scenario based on genomic and phenotypic characterization. *PloS one,* 4**,** e4982.

BRISSE, S., GRIMONT, F. & GRIMONT, P. 2006. The genus Klebsiella, p 159–196. *The prokaryotes,* 6.

BROCHET, M., DA CUNHA, V., COUVÉ, E., RUSNIOK, C., TRIEU-CUOT, P. & GLASER, P. 2009. Atypical association of DDE transposition with conjugation specifies a new family of mobile elements. *Molecular microbiology,* 71**,** 948-959.

BROMKE, M. A. 2013. Amino acid biosynthesis pathways in diatoms. *Metabolites,* 3**,** 294-311.

BUHRDORF, R., FÖRSTER, C., HAAS, R. & FISCHER, W. 2003. Topological analysis of a putative virB8 homologue essential for the cag type IV secretion system in Helicobacter pylori. *International journal of medical microbiology,* 293**,** 213-217.

BURRUS, V., PAVLOVIC G, DECARIS B & G, G. 2002. Conjugative transposons: the tip of the iceberg. *Molecular Microbiology,* 46**,** 601–610.

BURRUS, V. & WALDOR, M. K. 2003. Control of SXT integration and excision. *Journal of bacteriology,* 185**,** 5045-5054.

BURRUS, V. & WALDOR, M. K. 2004. Shaping bacterial genomes with integrative and conjugative elements. *Res Microbiol,* 155**,** 376-86.

BYRD, D. R. A. & MATSON, S. W. 1997. Nicking by transesterification: the reaction catalysed by a relaxase. *Molecular Microbiology.,* 25**,** 1011–1022.

CAMPBELL, A. 2007. Phage integration and chromosome structure. A personal history. *Annu. Rev. Genet.,* 41**,** 1-11.

CAPITANI, G., EIDAM, O., GLOCKSHUBER, R. & GRÜTTER, M. G. 2006. Structural and functional insights into the assembly of type 1 pili from Escherichia coli. *Microbes and infection,* 8**,** 2284-2290.

CARBALLEIRA, J. D., GONZALEZ-PEREZ, B., MONCALIAN, G. & DE LA CRUZ, F. 2014. A high security double lock and key mechanism in HUH relaxases controls oriT-processing for plasmid conjugation. *Nucleic Acids Res,* 42**,** 10632-43.

CARMEN, B., CHRISTOPHE, R., LIONEL, F., ELISABETH, C., ALAIN, B., FRANK, K., ELISABETH, C. & PHILIPPE, G. 1999. The 102-kilobase pgm locus of Yersinia pestis: Sequence analysis and comparison of selected regions among different Yersinia pestis and Yersinia pseudotuberculosis strains. *Infection and Immunity,* 67**,** 4851–4861.

CARNIEL, E. 2001. The Yersinia high-pathogenicity island: an iron-uptake island. *Microbes and Infection,* 3**,** 561−569.

CARPENTER, J. L. 1990. Klebsiella pulmonary infections: occurrence at one medical center and review. *Review of Infectious Diseases,* 12**,** 672-682.

CARPENTER, M. R., ROZOVSKY, S. & BOYD, E. F. 2015. Pathogenicity Island Cross Talk Mediated by Recombination Directionality Factors Facilitates Excision from the Chromosome. *J Bacteriol,* 198**,** 766-76.

CARRARO, N. & BURRUS, V. 2015. The dualistic nature of integrative and conjugative elements. *Mob Genet Elements,* 5**,** 98-102.

CARRARO, N., LIBANTE, V., MOREL, C., DECARIS, B., CHARRON-BOURGOIN, F., LEBLOND, P. & GUEDON, G. 2011. Differential regulation of two closely related integrative and conjugative elements from Streptococcus thermophilus. *BMC Microbiol,* 11**,** 238.

CASCALES, E., ATMAKURI, K., SARKAR, M. K. & CHRISTIE, P. J. 2013. DNA substrate-induced activation of the Agrobacterium VirB/VirD4 Type IV secretion system. *Journal of Bacteriology,* 195**,** 2691–2704.

CASCALES, E. & CHRISTIE, P. J. 2003. The versatile bacterial type IV secretion systems. *Nature Reviews Microbiology,* 1**,** 137-149.

CASCALES, E. & CHRISTIE, P. J. 2004. Definition of a Bacterial Type IV Secretion Pathway for a DNA Substrate. *SCIENCE,* 304**,** 1170-1173.

CASSAT, J. E. & SKAAR, E. P. 2013. Iron in infection and immunity. *Cell Host Microbe,* 13**,** 509-19.

CECCARELLI, D., DACCORD, A., RENÉ, M. & BURRUS, V. 2008. Identification of the origin of transfer (oriT) and a new gene required for mobilization of the SXT/R391 family of integrating conjugative elements. *Journal of bacteriology,* 190**,** 5328-5338.

CHANDLER, M., DE LA CRUZ, F., DYDA, F., HICKMAN, A. B., MONCALIAN, G. & TON-HOANG, B. 2013. Breaking and joining single-stranded DNA: the HUH endonuclease superfamily. *Nature Reviews Microbiology,* 11**,** 525-538.

CHEN, I., CHRISTIE, P. J. & DUBNAU, D. 2005. The ins and outs of DNA transfer in bacteria. *Science,* 310**,** 1456-1460.

CHEN, N., OU, H. Y., VAN AARTSEN, J. J., JIANG, X., LI, M., YANG, Z., WEI, Q., CHEN, X., HE, X., DENG, Z., RAJAKUMAR, K. & LU, Y. 2010. The pheV phenylalanine tRNA gene *Klebsiella pneumoniae* clinical isolates is an integration hotspot for possible niche-adaptation genomic islands. *Curr Microbiol,* 60**,** 210-6.

CHEN, Y.-T., LIAO, T.-L., WU, K.-M., LAUDERDALE, T.-L., YAN, J.-J., HUANG, I.-W., LU, M.-C., LAI, Y.-C., LIU, Y.-M. & SHU, H.-Y. 2009. Genomic diversity of citrate fermentation in *Klebsiella pneumoniae*. *BMC microbiology,* 9**,** 168.

CHEN, Y. T., CHANG, H. Y., LAI, Y. C., PAN, C. C., TSAI, S. F. & PENG, H. L. 2004. Sequencing and analysis of the large virulence plasmid pLVPK of *Klebsiella pneumoniae* CG43. *Gene,* 337**,** 189-98.

CHENG, H., CHEN, Y., WU, C., CHANG, H., LAI, Y. & PENG, H. 2010. RmpA regulation of capsular polysaccharide biosynthesis in *Klebsiella pneumoniae* CG43. *Journal of bacteriology,* 192**,** 3144-3158.

CHENG, Q., PASZKIET, B. J., SHOEMAKER, N. B., GARDNER, J. F. & SALYERS, A. A. 2000. Integration and Excision of aBacteroides Conjugative Transposon, CTnDOT. *Journal of bacteriology,* 182**,** 4035-4043.

CHIMILESKI, S., DOLAS, K., NAOR, A., GOPHNA, U. & PAPKE, R. T. 2014. Extracellular DNA metabolism in Haloferax volcanii.

CHOU, H.-C., LEE, C.-Z., MA, L.-C., FANG, C.-T., CHANG, S.-C. & WANG, J.-T. 2004. Isolation of a chromosomal region of *Klebsiella pneumoniae* associated with allantoin metabolism and liver infection. *Infection and immunity,* 72**,** 3783-3792.

CHRISTIE, P. J. 2004. Type IV secretion: the Agrobacterium VirB/D4 and related conjugation systems. *Biochimica et Biophysica Acta (BBA)-Molecular Cell Research,* 1694**,** 219-234.

CHRISTIE, P. J., ATMAKURI, K., KRISHNAMOORTHY, V., JAKUBOWSKI, S. & CASCALES, E. 2005. Biogenesis, architecture, and function of bacterial type IV secretion systems. *Annu. Rev. Microbiol.,* 59**,** 451-485.

CHRISTIE, P. J. & CASCALES, E. 2005. Structural and dynamic properties of bacterial type IV secretion systems (review). *Molecular membrane biology,* 22**,** 51-61.

COLLYN, F., BILLAULT, A., MULLET, C., SIMONET, M. & MARCEAU, M. 2004. YAPI, a new Yersinia pseudotuberculosis pathogenicity island. *Infect Immun,* 72**,** 4784-90.

COLSTON, S. M., FULLMER, M. S., BEKA, L., LAMY, B., GOGARTEN, J. P. & GRAF, J. 2014. Bioinformatic genome comparisons for taxonomic and phylogenetic assignments using Aeromonas as a test case. *MBio,* 5**,** e02136-14.

CONNOLLY, K. M., IWAHARA, M. & CLUBB, R. T. 2002. Xis protein binding to the left arm stimulates excision of conjugative transposon Tn916. *Journal of bacteriology,* 184**,** 2088-2099.

CORDERO, L., RAU, R., TAYLOR, D. & AYERS, L. W. 2004. Enteric gram-negative bacilli bloodstream infections: 17 years' experience in a neonatal intensive care unit. *American journal of infection control,* 32**,** 189-195.

CORREIA, M., BOAVIDA, F., GROSSO, F., SALGADO, M., LITO, L., CRISTINO, J. M., MENDO, S. & DUARTE, A. 2003. Molecular characterization of a new class 3 integron in *Klebsiella pneumoniae*. *Antimicrobial agents and chemotherapy,* 47**,** 2838-2843.

COSTA, T. R., FELISBERTO-RODRIGUES, C., MEIR, A., PREVOST, M. S., REDZEJ, A., TROKTER, M. & WAKSMAN, G. 2015. Secretion systems in Gram-negative bacteria: structural and mechanistic insights. *Nature Reviews Microbiology,* 13**,** 343-359.

CRELLIN, P. K. & ROOD, J. I. 1998. Tn4451 from Clostridium perfringens is a mobilizable transposon that encodes the functional Mob protein, TnpZ. *Molecular microbiology,* 27**,** 631-642.

CROUCHER, N. J., WALKER, D., ROMERO, P., LENNARD, N., PATERSON, G. K., BASON, N. C., MITCHELL, A. M., QUAIL, M. A., ANDREW, P. W., PARKHILL, J., BENTLEY, S. D. & MITCHELL, T. J. 2009. Role of conjugative elements in the evolution of the multidrug-resistant pandemic clone Streptococcus pneumoniaeSpain23F ST81. *J Bacteriol,* 191**,** 1480-9.

CRUZ, B. N. A. F. D. L. 2001. Two atypical mobilization proteins are involved in plasmid CloDF13 relaxation. *Molecular Microbiology,* 39**,** 1088-1099.

CURCIO, M. J. & DERBYSHIRE, K. M. 2003. The outs and ins of transposition: from mu to kangaroo. *Nature Reviews Molecular Cell Biology,* 4**,** 865-877.

DACCORD, A., CECCARELLI, D. & BURRUS, V. 2010. Integrating conjugative elements of the SXT/R391 family trigger the excision and drive the mobilization of a new class of Vibrio genomic islands. *Mol Microbiol,* 78**,** 576-88.

DACCORD, A., MURSELL, M., POULIN-LAPRADE, D. & BURRUS, V. 2012. Dynamics of the SetCD-regulated integration and excision of genomic islands mobilized by integrating conjugative elements of the SXT/R391 family. *J Bacteriol,* 194**,** 5794-802.

DAMJANOVA, I., TÓTH, Á., PÁSZTI, J., JAKAB, M., MILCH, H., BAUERNFEIND, A. & FÜZI, M. 2007. Epidemiology of SHV-type β-lactamase-producing Klebsiella spp. from outbreaks in five geographically distant Hungarian neonatal intensive care units: widespread dissemination of epidemic R-plasmids. *International journal of antimicrobial agents,* 29**,** 665-671.

DAS, A. & DAS, A. 2014. Delineation of polar localization domains of Agrobacterium tumefaciens type IV secretion apparatus proteins VirB4 and VirB11. *Microbiologyopen,* 3**,** 793-802.

DAVIES, M. R., SHERA, J., VAN DOMSELAAR, G. H., SRIPRAKASH, K. S. & MCMILLAN, D. J. 2009. A novel integrative conjugative element mediates genetic transfer from group G Streptococcus to other {beta}-hemolytic Streptococci. *J Bacteriol,* 191**,** 2257-65.

DAVIS, D., JAMES B. MCALPINE, CHRISTOPHER, PAZOLES, J., TALBOT, M. K., ALDER, E. A., WHITE, A. C., JONAS, B. M., MURRAY, B. E., WEINSTOCK, G. M. & ROGERS, B. L. 2001. Enterococcus faecalis multi-drug resistance transporters: application for antibiotic discovery. *J. Mol. Microbiol. Biotechnol,* 3**,** 179-184.

DAVIS, T. J. & MATSEN, J. M. 1974. Prevalence and characteristics of Klebsiella species: relation to association with a hospital environment. *Journal of Infectious Diseases,* 130**,** 402-405.

DE PAZ, H. D., SANGARI, F. J., BOLLAND, S., GARCIA-LOBO, J. M., DEHIO, C., DE LA CRUZ, F. & LLOSA, M. 2005. Functional interactions between type IV secretion systems involved in DNA transfer and virulence. *Microbiology,* 151**,** 3505-16.

DELAMUTA, J. R. M., RIBEIRO, R. A., MENNA, P., BANGEL, E. V. & HUNGRIA, M. 2012. Multilocus sequence analysis (MLSA) of Bradyrhizobium strains: revealing high diversity of tropical diazotrophic symbiotic bacteria. *Brazilian Journal of Microbiology,* 43**,** 698-710.

DIMOPOULOU, I. D., RUSSELL, J. E., MOHD-ZAIN, Z., HERBERT, R. & CROOK, D. W. 2002. Site-Specific Recombination with the Chromosomal tRNALeu Gene by the Large Conjugative Haemophilus Resistance Plasmid. *Antimicrobial Agents and Chemotherapy,* 46**,** 1602-1603.

DOBRINDT, U. & HACKER, J. 2001. Whole genome plasticity in pathogenic bacteria. *Curr Opin Microbiol.,* 4**,** 550-7.

DOBRINDT, U., HOCHHUT, B., HENTSCHEL, U. & HACKER, J. 2004. Genomic islands in pathogenic and environmental microorganisms. *Nat Rev Microbiol,* 2**,** 414-24.

DORDET FRISONI, E., MARENDA, M. S., SAGNÉ, E., NOUVEL, L. X., GUÉRILLOT, R., GLASER, P., BLANCHARD, A., TARDY, F., SIRAND-PUGNET, P. & BARANOWSKI, E. 2013. ICEA of Mycoplasma agalactiae: a new family of self-transmissible integrative elements that confers conjugative properties to the recipient strain. *Molecular microbiology,* 89**,** 1226-1239.

DOWER, W. J., MILLER, J. F. & RAGSDALE, C. W. 1988. High efficiency transformation of E. coli by high voltage electroporation. *Nucleic acids research,* 16**,** 6127-6145.

DRAPER, O., CÉSAR, C. E., MACHÓN, C., DE LA CRUZ, F. & LLOSA, M. 2005. Site-specific recombinase and integrase activities of a conjugative relaxase in recipient cells. *Proceedings of the National Academy of Sciences of the United States of America,* 102**,** 16385-16390.

DROPA, M., BALSALOBRE, L. C., LINCOPAN, N., MAMIZUKA, E. M., CASSETTARI, V. C., MATTÉ, G. R. & MATTÉ, M. H. 2010. Emergence of *Klebsiella pneumoniae* carrying the novel extended-spectrum β-lactamase gene variants blaSHV-40, blaTEM-116 and the class 1 integron-associated blaGES-7 in Brazil. *Clinical Microbiology and Infection,* 16**,** 630-632.

EDWARDS, A. W. F. 2004. *Cogwheels of the mind: the story of Venn diagrams*, JHU Press.

ELIANA, D. & FREDERICK, M. A. 2002. Pseudomonas biofilm formation and antibiotic resistance are linked to phenotypic variation. *letters to nature,* 416**,** 740-743.

EPPINGER, M., ROSOVITZ, M. J., FRICKE, W. F., RASKO, D., KOKORINA, G., FAYOLLE, C., LINDLER, L. E., CARNIEL, E. & RAVEL, J. 2007. Genome Sequence of Y. pseudotuberculosis IP31758, the Causative Agent of Far East Scarlet Like Fever: Linking Genomic Plasticity to Pathogenicity. *PLoS Genetics,* preprint**,** e142.

ERIC, C., KRISHNAMOHAN ATMAKURI, MAYUKH K. SARKAR & CHRISTIE., P. J. 2013. DNA Substrate-Induced Activation of the Agrobacterium VirB/VirD4 Type IV Secretion System. *Journal of Bacteriology,* 195**,** 2691–2704.

ESPINOSA, M., R., SOBERON-CHAVEZ, G., DELGADO-SAPIEN, G., SANDNER-MIRANDA, L., MENDEZ, J. L., GONZALEZ-VALENCIA, G. & CRAVIOTO, A. 2012. Genetic and phenotypic characterization of a Pseudomonas aeruginosa population with high frequency of genomic islands. *PLoS One,* 7**,** e37459.

FANI, R., MORI, E., TAMBURINI, E. & LAZCANO, A. 1998. Evolution of the structure and chromosomal distribution of histidine biosynthetic genes. *Origins of Life and Evolution of the Biosphere,* 28**,** 555-570.

FETHERSTON, J. D., KIRILLINA, O., BOBROV, A. G., PAULLEY, J. T. & PERRY, R. D. 2010. The yersiniabactin transport system is critical for the pathogenesis of bubonic and pneumonic plague. *Infect Immun,* 78**,** 2045-52.

FINN, R. D., BATEMAN, A., CLEMENTS, J., COGGILL, P., EBERHARDT, R. Y., EDDY, S. R., HEGER, A., HETHERINGTON, K., HOLM, L. & MISTRY, J. 2014. Pfam: the protein families database. *Nucleic acids research,* 42**,** D222-D230.

FLANNERY, E. L., ANTCZAK, S. M. & MOBLEY, H. L. 2011. Self-transmissibility of the integrative and conjugative element ICEPm1 between clinical isolates requires a functional integrase, relaxase, and type IV secretion system. *J Bacteriol,* 193**,** 4104-12.

FLANNERY, E. L., MODY, L. & MOBLEY, H. L. 2009. Identification of a modular pathogenicity island that is widespread among urease-producing uropathogens and shares features with a diverse group of mobile elements. *Infect Immun,* 77**,** 4887-94.

FOUTS, D. E., TYLER, H. L., DEBOY, R. T., DAUGHERTY, S., REN, Q., DURKIN, A. S., HUOT, H., SHRIVASTAVA, S., KOTHARI, S. & DODSON, R. J. 2008. Complete genome sequence of the N 2-fixing broad host range endophyte *Klebsiella pneumoniae* 342 and virulence predictions verified in mice. *PLoS Genet,* 4**,** e1000141.

FOX, J. & ROHOVSKY, M. 1975. Meningitis caused by Klebsiella spp in two rhesus monkeys. *Journal of the American Veterinary Medical Association,* 167**,** 634-636.

FRONZES, R., CHRISTIE, P. J. & WAKSMAN, G. 2009. The structural biology of type IV secretion systems. *Nat Rev Microbiol,* 7**,** 703-14.

FROST, L. S., LEPLAE, R., SUMMERS, A. O. & TOUSSAINT, A. 2005. Mobile genetic elements: the agents of open source evolution. *Nat Rev Microbiol,* 3**,** 722-32.

GAL-MOR, O. & FINLAY, B. B. 2006. Pathogenicity islands: a molecular toolbox for bacterial virulence. *Cell Microbiol,* 8**,** 1707-19.

GARCILLÁN-BARCIA, M. P., JURADO, P., GONZÁLEZ-PÉREZ, B., MONCALIÁN, G., FERNÁNDEZ, L. A. & DE LA CRUZ, F. 2007. Conjugative transfer can be inhibited by blocking relaxase activity within recipient cells with intrabodies. *Molecular microbiology,* 63**,** 404-416.

GARVEY, M. I. & PIDDOCK, L. J. 2008. The efflux pump inhibitor reserpine selects multidrug-resistant Streptococcus pneumoniae strains that overexpress the ABC transporters PatA and PatB. *Antimicrob Agents Chemother,* 52**,** 1677-85.

GHIGO, J.-M. 2001. Natural conjugative plasmids induce bacterial biofilm development. *Nature,* 412**,** 442-445.

GIOBBIA, M., SCOTTON, P. G., CARNIATO, A., CRUCIANI, M., FARNIA, A., DANIOTTI, E., SCARPA, G. & VAGLIA, A. 2003. Community-acquired *Klebsiella pneumoniae* bacteremia with meningitis and endophthalmitis in Italy. *International Journal of Infectious Diseases,* 7**,** 234-235.

GLICKMAN, L. 1981. Veterinary nosocomial (hospital-acquired) Klebsiella infections. *Journal of the American Veterinary Medical Association,* 179**,** 1389-1392.

GOGARTEN, J. P. & TOWNSEND, J. P. 2005a. Horizontal gene transfer, genome innovation and evolution. *Nature Reviews Microbiology,* 3**,** 679-687.

GOGARTEN, J. P. & TOWNSEND, J. P. 2005b. Horizontal gene transfer, genome innovation and evolution. *Nat Rev Microbiol,* 3**,** 679-87.

GOMIS-RUTH, F. X., M. SOLA, F. DE LA CRUZ & COLL., M. 2004. Coupling factors in macromolecular type IV secretion machineries. *Curr. Pharm. Des,* 10**,** 1551-1565.

GOMIS-RUTH, F. X., MONCALIAN, G., PEREZ-LUQUE, R., GONZALEZ, A., CABEZON, E., DE LA CRUZ, F. & COLL, M. 2001. The bacterial conjugation protein TrwB resembles ring helicases and F1-ATPase. *Nature,* 409**,** 637-641.

GRINDLEY, N. D. F., WHITESON, K. L. & RICE, P. A. 2006. Mechanisms of site-specific recombination. *Annu. Rev. Biochem.,* 75**,** 567–605.

GUASCH, A., LUCAS, M., MONCALIAN, G., CABEZAS, M., PEREZ-LUQUE, R., GOMIS-RUTH, F. X., DE LA CRUZ, F. & COLL, M. 2003. Recognition and processing of the origin of transfer DNA by conjugative relaxase TrwC. *Nat Struct Biol,* 10**,** 1002-10.

GUÉRILLOT, R., SIGUIER, P., GOURBEYRE, E., CHANDLER, M. & GLASER, P. 2014. The diversity of prokaryotic DDE transposases of the mutator superfamily, insertion specificity, and association with conjugation machineries. *Genome biology and evolution,* 6**,** 260-272.

HACKER, J., BENDER, L., OTT, M., WINGENDER, J., LUND, B., MARRE, R. & GOEBEL, W. 1990. Deletions of chromosomal regions coding for fimbriae and hemolysins occur in vitro and in vivo in various extraintestinal Escherichia coli isolates. *Microb Pathog,* 8**,** 213-25.

HACKER, J. & KAPER, J., B. 2000. Pathogenicity islands and the evolution of microbes. *Annu. Rev. Microbiol,* 54**,** 641-79.

HACKER., J. 2000. Pathogenicity islands and the evolution of microbes. *Annu. Rev. Microbiol.,* 54**,** 641–79.

HAMBURGER, P. 2005. Cogwheels of the mind. The story of venn diagrams. *The Mathematical Intelligencer,* 27**,** 36-38.

HAMILTON, C. M., LEE, H., LI, P.-L., COOK, D. M., PIPER, K. R., VON BODMAN, S. B., LANKA, E., REAM, W. & FARRAND, S. K. 2000. TraG from RP4 and TraG and VirD4 from Ti plasmids confer relaxosome specificity to the conjugal transfer system of pTiC58. *Journal of bacteriology,* 182**,** 1541-1548.

HAN WANG, D. C. 2014. An Accurate Genomic Island Prediction Method for Sequenced Bacterial and Archaeal Genomes. *Journal of Proteomics & Bioinformatics,* 07.

HANCOCK, V., FERRIERES, L. & KLEMM, P. 2008. The ferric yersiniabactin uptake receptor FyuA is required for efficient biofilm formation by urinary tract infectious Escherichia coli in human urine. *Microbiology,* 154**,** 167-75.

HANCOCK, V. & KLEMM, P. 2007. Global gene expression profiling of asymptomatic bacteriuria Escherichia coli during biofilm growth in human urine. *Infect Immun,* 75**,** 966-76.

HANEDA, T., ISHII, Y., DANBARA, H. & OKADA, N. 2009. Genome-wide identification of novel genomic islands that contribute to Salmonella virulence in mouse systemic infection. *FEMS Microbiol Lett,* 297**,** 241-9.

HARDING, C. R., SCHROEDER, G. N., COLLINS, J. W. & FRANKEL, G. 2013. Use of Galleria mellonella as a model organism to study Legionella pneumophila infection. *JoVE (Journal of Visualized Experiments)***,** e50964-e50964.

HARRISON, E. M., CARTER, M. E., LUCK, S., OU, H. Y., HE, X., DENG, Z., O'CALLAGHAN, C., KADIOGLU, A. & RAJAKUMAR, K. 2010. Pathogenicity islands PAPI-1 and PAPI-2 contribute individually and synergistically to the virulence of Pseudomonas aeruginosa strain PA14. *Infect Immun,* 78**,** 1437-46.

HE, J., BALDINI, R. L., DEZIEL, E., SAUCIER, M., ZHANG, Q., LIBERATI, N. T., LEE, D., URBACH, J., GOODMAN, H. M. & RAHME, L. G. 2004. The broad host range pathogen Pseudomonas aeruginosa strain PA14 carries two pathogenicity islands harboring plant and animal virulence genes. *Proceedings of the National Academy of Sciences,* 101**,** 2530-2535.

HENDERSON, I. R., NAVARRO-GARCIA, F., DESVAUX, M., FERNANDEZ, R. C. & ALA'ALDEEN, D. 2004. Type V protein secretion pathway: the autotransporter story. *Microbiology and molecular biology reviews,* 68**,** 692-744.

HICKMAN, J. W., TIFREA, D. F. & HARWOOD, C. S. 2005. A chemosensory system that regulates biofilm formation through modulation of cyclic diguanylate levels. *Proceedings of the National Academy of Sciences of the United States of America,* 102**,** 14422-14427.

HINERFELD, D. & CHURCHWARD, G. 2001. Xis protein of the conjugative transposon Tn916 plays dual opposing roles in transposon excision. *Molecular microbiology,* 41**,** 1459-1467.

HIRANO, N., MUROI, T., TAKAHASHI, H. & HARUKI, M. 2011. Site-specific recombinases as tools for heterologous gene integration. *Applied microbiology and biotechnology,* 92**,** 227.

HOCHHUT, B., JOELI, M. & MATTHEW, K. W. 2000. Mobilization of Plasmids and Chromosomal DNA Mediated by the SXT Element, a Constin Found in Vibrio cholerae O139. *Journal Of Bacteriology,* 182**,** 2043-2047.

HOCHHUT, B., LOTFI, Y., MAZEL, D., FARUQUE, S. M., WOODGATE, R. & WALDOR, M. K. 2001. Molecular analysis of antibiotic resistance gene clusters in vibrio cholerae O139 and O1 SXT constins. *Antimicrob Agents Chemother,* 45**,** 2991-3000.

HOCHHUT, B. & WALDOR, M. K. 1999. Site-specific integration of the conjugal Vibrio cholerae SXT element into prfC. *Molecular microbiology,* 32**,** 99-110.

HOLDEN, V. I. & BACHMAN, M. A. 2015. Diverging roles of bacterial siderophores during infection. *Metallomics,* 7**,** 986-995.

HOLDEN, V. I., BREEN, P., HOULE, S., DOZOIS, C. M. & BACHMAN, M. A. 2016. *Klebsiella pneumoniae* Siderophores Induce Inflammation, Bacterial Dissemination, and HIF-1alpha Stabilization during Pneumonia. *MBio,* 7**,** 1-10.

HOLT, K. E., WERTHEIM, H., ZADOKS, R. N., BAKER, S., WHITEHOUSE, C. A., DANCE, D., JENNEY, A., CONNOR, T. R., HSU, L. Y. & SEVERIN, J. 2015. Genomic analysis of diversity, population structure, virulence, and antimicrobial resistance in

Klebsiella pneumoniae, an urgent threat to public health. *Proceedings of the National Academy of Sciences,* 112**,** E3574-E3581.

HONG, T. P., CARTER, M. Q., STRUFFI, P., CASONATO, S., HAO, Y., LAM, J. S., LORY, S. & JOUSSON, O. 2017. Conjugative type IVb pilus recognizes lipopolysaccharide of recipient cells to initiate PAPI-1 pathogenicity island transfer in Pseudomonas aeruginosa. *BMC Microbiol,* 17**,** 31.

HORMAECHE, I., SEGURA, R. L., VECINO, A. J., GONI, F. M., DE LA CRUZ, F. & ALKORTA, I. 2006. The transmembrane domain provides nucleotide binding specificity to the bacterial conjugation protein TrwB. *FEBS Lett,* 580**,** 3075-82.

HOWARD, O., JEFFREY, G. L. & EDUARDO, A. G. 2000. Lateral gene transfer and the nature of bacterial innovation. *Nature,* 405**,** 299-304.

HSIEH, P. F., LIN, T. L., LEE, C. Z., TSAI, S. F. & WANG, J. T. 2008. Serum-induced iron-acquisition systems and TonB contribute to virulence in *Klebsiella pneumoniae* causing primary pyogenic liver abscess. *J Infect Dis,* 197**,** 1717-27.

JAKUBOWSKI, S. J., KRISHNAMOORTHY, V., CASCALES, E. & CHRISTIE, P. J. 2004. Agrobacterium tumefaciens VirB6 domains direct the ordered export of a DNA substrate through a type IV secretion system. *Journal of molecular biology,* 341**,** 961-977.

JOHNSON, C. M. & GROSSMAN, A. D. 2015. Integrative and Conjugative Elements (ICEs): What They Do and How They Work. *Annu Rev Genet,* 49**,** 577-601.

JOHNSTON, C., MARTIN, B., FICHANT, G., POLARD, P. & CLAVERYS, J.-P. 2014. Bacterial transformation: distribution, shared mechanisms and divergent control. *Nature Reviews Microbiology,* 12**,** 181-196.

JUHAS, M., CROOK, D. W., DIMOPOULOU, I. D., LUNTER, G., HARDING, R. M., FERGUSON, D. J. & HOOD, D. W. 2007a. Novel type IV secretion system involved in propagation of genomic islands. *J Bacteriol,* 189**,** 761-71.

JUHAS, M., CROOK, D. W. & HOOD, D. W. 2008. Type IV secretion systems: tools of bacterial horizontal gene transfer and virulence. *Cell Microbiol,* 10**,** 2377-86.

JUHAS, M., POWER, P. M., HARDING, R. M., FERGUSON, D. J., DIMOPOULOU, I. D., ELAMIN, A. R., MOHD-ZAIN, Z., HOOD, D. W., ADEGBOLA, R., ERWIN, A., SMITH, A., MUNSON, R. S., HARRISON, A., MANSFIELD, L., BENTLEY, S. & CROOK, D. W. 2007b. Sequence and functional analyses of Haemophilus spp. genomic islands. *Genome Biol,* 8**,** R237.

JUHAS, M., VAN DER MEER, J. R., GAILLARD, M., HARDING, R. M., HOOD, D. W. & CROOK, D. W. 2009a. Genomic islands: tools of bacterial horizontal gene transfer and evolution. *FEMS Microbiol Rev,* 33**,** 376-93.

JUHAS, M., VAN DER MEER, J. R., GAILLARD, M., HARDING, R. M., HOOD, D. W. & CROOK, D. W. 2009b. Genomic islands: tools of bacterial horizontal gene transfer and evolution. *Microbiol Rev,* 33**,** 376-93.

JULIAO, P. C., MARRS, C. F., XIE, J. & GILSDORF, J. R. 2007. Histidine auxotrophy in commensal and disease-causing nontypeable Haemophilus influenzae. *Journal of bacteriology,* 189**,** 4994-5001.

KAMENŠEK, S., PODLESEK, Z., GILLOR, O. & ŽGUR-BERTOK, D. 2010. Genes regulated by the Escherichia coli SOS repressor LexA exhibit heterogenous expression. *BMC microbiology,* 10**,** 283.

KARAMA, E. M., WILLERMAIN, F., JANSSENS, X., CLAUS, M., VAN DEN WIJNGAERT, S., WANG, J.-T., VEROUGSTRAETE, C. & CASPERS, L. 2008. Endogenous endophthalmitis complicating *Klebsiella pneumoniae* liver abscess in Europe: case report. *International ophthalmology,* 28**,** 111-113.

KELLY, P. W. 2002. Survey and summary Integration sites for genetic elements in prokaryotic tRNA and tmRNA genes: sublocation preference of integrase subfamilies. *Nucleic Acids Research.,* 30**,** 866–875.

KIBBE, W. A. 2007. OligoCalc: an online oligonucleotide properties calculator. *Nucleic Acids Res,* 35**,** W43-6.

KINKLER JR, R., WAGNER, J., DOYLE, R. & OWENS, D. 1976. Bacterial mastitis in guinea pigs. *Laboratory animal science,* 26**,** 214-217.

KLOCKGETHER, J., REVA, O., LARBIG, K. & TUMMLER, B. 2004. Sequence Analysis of the Mobile Genome Island pKLC102 of Pseudomonas aeruginosa C. *Journal of Bacteriology,* 186**,** 518-534.

KLOCKGETHER, J., WURDEMANN, D., REVA, O., WIEHLMANN, L. & TUMMLER, B. 2007. Diversity of the abundant pKLC102/PAGI-2 family of genomic islands in Pseudomonas aeruginosa. *J Bacteriol,* 189**,** 2443-59.

KO, W.-C., PATERSON, D. L., SAGNIMENI, A. J., HANSEN, D. S., VON GOTTBERG, A., MOHAPATRA, S., CASELLAS, J. M., GOOSSENS, H., MULAZIMOGLU, L. & TRENHOLME, G. 2002. Community-acquired *Klebsiella pneumoniae* bacteremia: global differences in clinical patterns. *Emerging infectious diseases,* 8**,** 160-166.

KOCZURA, R. & KAZNOWSKI, A. 2003. Occurrence of the Yersinia high-pathogenicity island and iron uptake systems in clinical isolates of *Klebsiella pneumoniae*. *Microbial Pathogenesis,* 35**,** 197-202.

KORAIMANN, G. 2003. Lytic transglycosylases in macromolecular transport systems of Gram-negative bacteria. *Cellular and molecular life sciences,* 60**,** 2371-2388.

KREWULAK, K. D. & VOGEL, H. J. 2008. Structural biology of bacterial iron uptake. *Biochim Biophys Acta,* 1778**,** 1781-804.

KULIS, H., R. K., PERSICKE, M. & KALINOWSKI, J. 2014. Histidine biosynthesis, its regulation and biotechnological application in Corynebacterium glutamicum. *Microb Biotechnol,* 7**,** 5-25.

KURTZ, S., CHOUDHURI, J. V., OHLEBUSCH, E., SCHLEIERMACHER, C., STOYE, J. & GIEGERICH, R. 2001. REPuter: the manifold applications of repeat analysis on a genomic scale. *Nucleic acids research,* 29**,** 4633-4642.

KWOK, T., ZABLER, D., URMAN, S., ROHDE, M., HARTIG, R., WESSLER, S., MISSELWITZ, R., BERGER, J., SEWALD, N., KONIG, W. & BACKERT, S. 2007. Helicobacter exploits integrin for type IV secretion and kinase activation. *Nature,* 449**,** 862-6.

KYNDT, T., QUISPE, D., ZHAI, H., JARRET, R., GHISLAIN, M., LIU, Q., GHEYSEN, G. & KREUZE, J. F. 2015. The genome of cultivated sweet potato contains Agrobacterium T-DNAs with expressed genes: an example of a naturally transgenic food crop. *Proceedings of the National Academy of Sciences,* 112**,** 5844-5849.

LAM, M. M., WICK, R. R., WYRES, K. L., GORRIE, C., JUDD, L. M., BRISSE, S., JENNEY, A. & HOLT, K. E. 2017. Frequent emergence of pathogenic lineages of *Klebsiella pneumoniae* via mobilisation of yersiniabactin and colibactin. *bioRxiv***,** 1-29.

LANG, S., KIRCHBERGER, P. C., GRUBER, C. J., REDZEJ, A., RAFFL, S., ZELLNIG, G., ZANGGER, K. & ZECHNER, E. L. 2011. An activation domain of plasmid R1 TraI protein delineates stages of gene transfer initiation. *Mol Microbiol,* 82**,** 1071-85.

LANGILLE, M. G., HSIAO, W. W. & BRINKMAN, F. S. 2010. Detecting genomic islands using bioinformatics approaches. *Nature Reviews Microbiology,* 8**,** 373-382.

LANK, E. 1995. DNA processing reactions in bacterial conjugation. *Annu. Rev. Biochem.,* 64**,** 141-69.

LAPIERRE, P. & GOGARTEN, J. P. 2009. Estimating the size of the bacterial pan-genome. *Trends in genetics,* 25**,** 107-110.

LARBIG, K. D., CHRISTMANN, A., JOHANN, A., KLOCKGETHER, J., HARTSCH, T., MERKL, R., WIEHLMANN, L., FRITZ, H. J. & TUMMLER, B. 2002. Gene Islands Integrated into tRNAGly Genes Confer Genome Diversity on a Pseudomonas aeruginosa Clone. *Journal of Bacteriology,* 184**,** 6665-6680.

LARKIN, M. A., BLACKSHIELDS, G., BROWN, N. P., CHENNA, R., MCGETTIGAN, P. A., MCWILLIAM, H., VALENTIN, F., WALLACE, I. M., WILM, A., LOPEZ, R., THOMPSON, J. D., GIBSON, T. J. & HIGGINS, D. G. 2007. Clustal W and Clustal X version 2.0. *Bioinformatics,* 23**,** 2947-8.

LAWLEY, T. D., GORDON, G. S., WRIGHT, A. & TAYLOR, D. E. 2002. Bacterial conjugative transfer: visualization of successful mating pairs and plasmid establishment in live Escherichia coli. *Molecular microbiology,* 44**,** 947-956.

LAWLEY, T. D., KLIMKE, W. A., GUBBINS, M. J. & FROST, L. S. 2003. F factor conjugation is a true type IV secretion system. *FEMS Microbiology Letters,* 224**,** 1-15.

LAWLOR, M. S., O'CONNOR, C. & MILLER, V. L. 2007. Yersiniabactin is a virulence factor for *Klebsiella pneumoniae* during pulmonary infection. *Infect Immun,* 75**,** 1463-72.

LEE, C. A., BABIC, A. & GROSSMAN, A. D. 2010. Autonomous plasmid-like replication of a conjugative transposon. *Molecular microbiology,* 75**,** 268-279.

LEE, C. A. & GROSSMAN, A. D. 2007. Identification of the origin of transfer (oriT) and DNA relaxase required for conjugation of the integrative and conjugative element ICEBs1 of Bacillus subtilis. *J Bacteriol,* 189**,** 7254-61.

LEE, C. A., THOMAS, J. & GROSSMAN, A. D. 2012. The Bacillus subtilis conjugative transposon ICEBs1 mobilizes plasmids lacking dedicated mobilization functions. *Journal of bacteriology,* 194**,** 3165-3172.

LEE, D. G., URBACH, J. M., WU, G., LIBERATI, N. T., FEINBAUM, R. L., MIYATA, S., DIGGINS, L. T., HE, J., SAUCIER, M., DEZIEL, E., FRIEDMAN, L., LI, L., GRILLS, G., MONTGOMERY, K., KUCHERLAPATI, R., RAHME, L. G. & AUSUBEL, F. M. 2006. Genomic analysis reveals that Pseudomonas aeruginosa virulence is combinatorial. *Genome Biol,* 7**,** R90.

LEWIS, J. A. & HATFULL, G. F. 2001. Control of directionality in integrase-mediated recombination: examination of recombination directionality factors (RDFs) including Xis and Cox proteins. *Nucleic acids research,* 29**,** 2205-2216.

LI, C., MA., CHI, T., FANG., CHA-ZE, L., CHIA-TUNG, S. & JIN-TOWN, W. 2005. Genomic heterogeneity in *Klebsiella pneumoniae* strains is associated with primary pyogenic liver abscess and metastatic infection. *The Journal of Infectious Diseases,* 192**,** 117–128.

LI, L.-Y., SHOEMAKER, N. B., WANG, G.-R., COLE, S. P., HASHIMOTO, M. K., WANG, J. & SALYERS, A. A. 1995. The mobilization regions of two integrated Bacteroides elements, NBU1 and NBU2, have only a single mobilization protein and may be on a cassette. *Journal of bacteriology,* 177**,** 3940-3945.

LIN, A. C., LIAO, T. L., LIN, Y. C., LAI, Y. C., LU, M. C. & CHEN, Y. T. 2012. Complete genome sequence of *Klebsiella pneumoniae* 1084, a hypermucoviscosity-negative K1 clinical strain. *J Bacteriol,* 194**,** 6316.

LIN, T. L., LEE, C. Z., HSIEH, P. F., TSAI, S. F. & WANG, J. T. 2008. Characterization of integrative and conjugative element ICEKp1-associated genomic heterogeneity in a *Klebsiella pneumoniae* strain isolated from a primary liver abscess. *J Bacteriol,* 190**,** 515-26.

LIU, P., LI, P., JIANG, X., BI, D., XIE, Y., TAI, C., DENG, Z., RAJAKUMAR, K. & OU, H. Y. 2012. Complete genome sequence of *Klebsiella pneumoniae* subsp. pneumoniae HS11286, a multidrug-resistant strain isolated from human sputum. *J Bacteriol,* 194**,** 1841-2.

LLOSA, M., GOMIS-RÜTH, F. X., COLL, M. & CRUZ, F. D. L. 2002. Bacterial conjugation: a two-step mechanism for DNA transport. *Molecular microbiology,* 45**,** 1-8.

LOBKOVSKY, A. E., WOLF, Y. I. & KOONIN, E. V. 2014. Estimation of prokaryotic supergenome size and composition from gene frequency distributions. *BMC genomics,* 15**,** S14.

LÖHR, I. H., HÜLTER, N., BERNHOFF, E., JOHNSEN, P. J., SUNDSFJORD, A. & NASEER, U. 2015. Persistence of a pKPN3-Like CTX-M-15-Encoding IncFII K Plasmid in a

Klebsiella pneumonia ST17 Host during Two Years of Intestinal Colonization. *PloS one,* 10**,** e0116516.

LOPEZ-GARRIDO, J. & CASADESUS, J. 2012. Crosstalk between virulence loci: regulation of Salmonella enterica pathogenicity island 1 (SPI-1) by products of the std fimbrial operon. *PLoS One,* 7**,** e30499.

LOUDEN, B., C. , DANIEL HAARMANN & LYNNE, A. M. 2011. Use of blue agar cas assay for siderophore detection. *Microbiology & Biology Education,* 12**,** 51-53.

LU, B. & LEONG, H. W. 2016. Computational methods for predicting genomic islands in microbial genomes. *Comput Struct Biotechnol J,* 14**,** 200-6.

LUBELSKI, J., KONINGS, W. N. & DRIESSEN, A. J. 2007. Distribution and physiology of ABC-type transporters contributing to multidrug resistance in bacteria. *Microbiol Mol Biol Rev,* 71**,** 463-76.

LUCAS, M., GONZALEZ-PEREZ, B., CABEZAS, M., MONCALIAN, G., RIVAS, G. & DE LA CRUZ, F. 2010. Relaxase DNA binding and cleavage are two distinguishable steps in conjugative DNA processing that involve different sequence elements of the nic site. *J Biol Chem,* 285**,** 8918-26.

LUKJANCENKO, O., WASSENAAR, T. M. & USSERY, D. W. 2010. Comparison of 61 sequenced Escherichia coli genomes. *Microbial ecology,* 60**,** 708-720.

MA, A. T., MCAULEY, S., PUKATZKI, S. & MEKALANOS, J. J. 2009. Translocation of a Vibrio cholerae type VI secretion effector requires bacterial endocytosis by host cells. *Cell host & microbe,* 5**,** 234-243.

MA, L.-C., FANG, C.-T., LEE, C.-Z., SHUN, C.-T. & WANG, J.-T. 2005. Genomic heterogeneity in *Klebsiella pneumoniae* strains is associated with primary pyogenic liver abscess and metastatic infection. *Journal of Infectious Diseases,* 192**,** 117-128.

MACHUCA, A. & MILAGRES, A. 2003. Use of CAS-agar plate modified to study the effect of different variables on the siderophore production by Aspergillus. *Letters in applied microbiology,* 36**,** 177-181.

MANTING, E., H. & DRIESSEN, A. J. M. 2000. Escherichia coli translocase: the unravelling of a molecular machine. *Molecular Microbiology,* 37**,** 226±238.

MANTRI, Y. & WILLIAMS, K. P. 2004. Islander: a database of integrative islands in prokaryotic genomes, the associated integrases and their DNA site specificities. *Nucleic acids research,* 32**,** D55-D58.

MARCHAIM, D., ZAIDENSTEIN, R., LAZAROVITCH, T., KARPUCH, Y., ZIV, T. & WEINBERGER, M. 2008. Epidemiology of bacteremia episodes in a single center: increase in Gram-negative isolates, antibiotics resistance, and patient age. *European journal of clinical microbiology & infectious diseases,* 27**,** 1045-1051.

MARCOLETA, A. E., BERRIOS-PASTEN, C., NUNEZ, G., MONASTERIO, O. & LAGOS, R. 2016. *Klebsiella pneumoniae* Asparagine tDNAs Are Integration Hotspots for Different Genomic Islands Encoding Microcin E492 Production Determinants and Other

Putative Virulence Factors Present in Hypervirulent Strains. *Front Microbiol,* 7**,** 849.

MARGER, M. D. & SAIER, M. H. 1993. A major superfamily of transmembrane facilitators that catalyse uniport, symport and antiport. *Trends in biochemical sciences,* 18**,** 13-20.

MATA, C., NAVARRO, F., MIRO, E., WALSH, T. R., MIRELIS, B. & TOLEMAN, M. 2011. Prevalence of SXT/R391-like integrative and conjugative elements carrying blaCMY-2 in Proteus mirabilis. *J Antimicrob Chemother,* 66**,** 2266-70.

MATHEE, K., NARASIMHAN, G., VALDES, C., QIU, X., MATEWISH, J. M., KOEHRSEN, M., ROKAS, A., YANDAVA, C. N., ENGELS, R. & ZENG, E. 2008. Dynamics of Pseudomonas aeruginosa genome evolution. *Proceedings of the National Academy of Sciences,* 105**,** 3100-3105.

MAURIZI, M. R. & LI, C.-C. H. 2001. AAA proteins: in search of a common molecular basis. *EMBOreports,* 2**,** 980–985.

MAVRODI, D. V., LOPER, J. E., PAULSEN, I. T. & THOMASHOW, L. S. 2009. Mobile genetic elements in the genome of the beneficial rhizobacterium Pseudomonas fluorescens Pf-5. *BMC Microbiol,* 9**,** 8.

MCMORRAN, B., TOWN, L., COSTELLOE, E., PALMER, J., ENGEL, J., HUME, D. & WAINWRIGHT, B. 2003. Effector ExoU from the Type III Secretion System Is an Important Modulator of Gene Expression in Lung Epithelial Cells in Response to Pseudomonas aeruginosa Infection. *Infection and Immunity,* 71**,** 6035-6044.

MEATHERALL, B. L., GREGSON, D., ROSS, T., PITOUT, J. D. & LAUPLAND, K. B. 2009. Incidence, risk factors, and outcomes of *Klebsiella pneumoniae* bacteremia. *The American journal of medicine,* 122**,** 866-873.

MEDINI, D., DONATI, C., TETTELIN, H., MASIGNANI, V. & RAPPUOLI, R. 2005. The microbial pan-genome. *Current opinion in genetics & development,* 15**,** 589-594.

MENARD, K. L. & GROSSMAN, A. D. 2013. Selective pressures to maintain attachment site specificity of integrative and conjugative elements. *PLoS Genet,* 9**,** e1003623.

METCALF, J. A., FUNKHOUSER-JONES, L. J., BRILEYA, K., REYSENBACH, A. L. & BORDENSTEIN, S. R. 2014. Antibacterial gene transfer across the tree of life. *Elife,* 3.

MEYER, R. 2009. Replication and conjugative mobilization of broad host-range IncQ plasmids. *Plasmid,* 62**,** 57-70.

MICHEL, B., YVON. & BAYSSE, C. 2002. The pyocins of Pseudomonas aeruginosa. *Biochimie,* 84**,** 499-510.

MIDDENDORF, B., HOCHHUT, B., LEIPOLD, K., DOBRINDT, U., BLUM-OEHLER, G. & HACKER, J. 2004. Instability of Pathogenicity Islands in Uropathogenic Escherichia coli 536. *Journal of Bacteriology,* 186**,** 3086-3096.

MILLER, M. C., FETHERSTON, J. D., PICKETT, C. L., BOBROV, A. G., WEAVER, R. H., DEMOLL, E. & PERRY, R. D. 2010. Reduced synthesis of the Ybt siderophore or production of aberrant Ybt-like molecules activates transcription of yersiniabactin genes in Yersinia pestis. *Microbiology,* 156**,** 2226-38.

MINOIA, M., GAILLARD, M., REINHARD, F., STOJANOV, M., SENTCHILO, V. & VAN DER MEER, J. R. 2008. Stochasticity and bistability in horizontal transfer control of a genomic island in Pseudomonas. *Proceedings of the National Academy of Sciences,* 105**,** 20792-20797.

MIRA, A., MARTÍN-CUADRADO, A. B., D'AURIA, G. & RODRÍGUEZ-VALERA, F. 2010. The bacterial pan-genome: a new paradigm in microbiology. *International Microbiology,* 13**,** 45-57.

MIYATA, S., CASEY, M., FRANK, D. W., AUSUBEL, F. M. & DRENKARD, E. 2003. Use of the Galleria mellonella caterpillar as a model host to study the role of the type III secretion system in Pseudomonas aeruginosa pathogenesis. *Infection and immunity,* 71**,** 2404-2413.

MIYAZAKI, R., MINOIA, M., PRADERVAND, N., SULSER, S., REINHARD, F. & VAN DER MEER, J. R. 2012. Cellular variability of RpoS expression underlies subpopulation activation of an integrative and conjugative element. *PLoS Genet,* 8**,** e1002818.

MOHD, Z., Z., TURNER, S. L., CERDENO-TARRAGA, A. M., LILLEY, A. K., INZANA, T. J., DUNCAN, A. J., HARDING, R. M., HOOD, D. W., PETO, T. E. & CROOK, D. W. 2004. Transferable antibiotic resistance elements in Haemophilus influenzae share a common evolutionary origin with a diverse family of syntenic genomic islands. *J Bacteriol,* 186**,** 8114-22.

MOKRACKA, J., KOCZURA, R. & KAZNOWSKI, A. 2004. Yersiniabactin and other siderophores produced by clinical isolates of Enterobacter spp. and Citrobacter spp. *FEMS Immunology & Medical Microbiology,* 40**,** 51-55.

MONCALIAN, G., CABEZON, E., ALKORTA, I., VALLE, M., MORO, F., VALPUESTA, J. M., GONI, F. M. & DE LA CRUZ, F. 1999. Characterization of ATP and DNA binding activities of TrwB, the coupling protein essential in plasmid R388 conjugation. *The Journal of Biological Chemistry,* 274**,** 36117–36124.

MORENO, S., A. I., DEN BAKKER, H. C., CUMMINGS, C. A., RODRIGUEZ-RIVERA, L. D., GOVONI, G., RANEIRI, M. L., DEGORICIJA, L., BROWN, S., HOELZER, K., PETERS, J. E., BOLCHACOVA, E., FURTADO, M. R. & WIEDMANN, M. 2012. Identification and characterization of novel Salmonella mobile elements involved in the dissemination of genes linked to virulence and transmission. *PLoS One,* 7**,** e41247.

MORGAN, R., KOHN, S., HWANG, S.-H., HASSETT, D. J. & SAUER, K. 2006. BdlA, a chemotaxis regulator essential for biofilm dispersion in Pseudomonas aeruginosa. *Journal of bacteriology,* 188**,** 7335-7343.

MORRIS, J. J., LENSKI, R. E. & ZINSER, E. R. 2012. The Black Queen Hypothesis: evolution of dependencies through adaptive gene loss. *MBio,* 3**,** e00036-12.

MOSSEY, P., HUDACEK, A. & DAS, A. 2010. Agrobacterium tumefaciens type IV secretion protein VirB3 is an inner membrane protein and requires VirB4, VirB7, and VirB8 for stabilization. *J Bacteriol,* 192**,** 2830-8.

MOUGOUS, J. D., CUFF, M. E., RAUNSER, S., SHEN, A., ZHOU, M., GIFFORD, C. A., GOODMAN, A. L., JOACHIMIAK, G., ORDOÑEZ, C. L. & LORY, S. 2006. A virulence locus of Pseudomonas aeruginosa encodes a protein secretion apparatus. *Science,* 312**,** 1526-1530.

MULLANY, P., WILLIAMS, R., LANGRIDGE, G. C., TURNER, D. J., WHALAN, R., CLAYTON, C., LAWLEY, T., HUSSAIN, H., MCCURRIE, K., MORDEN, N., ALLAN, E. & ROBERTS, A. P. 2012. Behavior and target site selection of conjugative transposon Tn916 in two different strains of toxigenic Clostridium difficile. *Appl Environ Microbiol,* 78**,** 2147-53.

MURPHY, K. C. & CAMPELLONE, K. G. 2003. Lambda Red-mediated recombinogenic engineering of enterohemorrhagic and enteropathogenic E. coli. *BMC molecular biology,* 4**,** 11.

NADASY, K. A., DOMIATI-SAAD, R. & TRIBBLE, M. A. 2007. Invasive *Klebsiella pneumoniae* syndrome in North America. *Clinical Infectious Diseases,* 45**,** e25-e28.

NAGLICH, J. G. & ANDREWS, R. E. 1988. Tn916-dependent conjugal transfer of pC194 and pUB110 from Bacillus subtilis into Bacillus thuringiensis subsp. israelensis. *Plasmid,* 20**,** 113-126.

NANCHARAIAH, Y. V., WATTIAU, P., WUERTZ, S., BATHE, S., MOHAN, S. V., WILDERER, P. A. & HAUSNER, M. 2003. Dual Labeling of Pseudomonas putida with Fluorescent Proteins for In Situ Monitoring of Conjugal Transfer of the TOL Plasmid. *Applied and Environmental Microbiology.,* 69**,** 4846-4852.

NASH, R. P., HABIBI, S., CHENG, Y., LUJAN, S. A. & REDINBO, M. R. 2010. The mechanism and control of DNA transfer by the conjugative relaxase of resistance plasmid pCU1. *Nucleic Acids Res,* 38**,** 5929-43.

NIYAZ, A., ULRICH, D., JORG, H. & HASNAIN., S. E. 2008. Genomic fluidity and pathogenic bacteria: applications in diagnostics, epidemiology and intervention. *Nature Reviews Microbiology,* 6**,** 389-394.

NORMAN, A., HANSEN, L. H. & SØRENSEN, S. J. 2009. Conjugative plasmids: vessels of the communal gene pool. *Philosophical Transactions of the Royal Society of London B: Biological Sciences,* 364**,** 2275-2289.

OLSEN, R. J., WATKINS, M. E., CANTU, C. C., BERES, S. B. & MUSSER, J. M. 2011. Virulence of serotype M3 Group A Streptococcus strains in wax worms (Galleria mellonella larvae). *Virulence,* 2**,** 111-119.

OSBORN, A. M. & BÖLTNER, D. 2002. When phage, plasmids, and transposons collide: genomic islands, and conjugative-and mobilizable-transposons as a mosaic continuum. *Plasmid,* 48**,** 202-212.

OU, H.-Y., HE, X., HARRISON, E. M., KULASEKARA, B. R., THANI, A. B., KADIOGLU, A., LORY, S., HINTON, J. C., BARER, M. R. & DENG, Z. 2007. MobilomeFINDER: web-based tools for in silico and experimental discovery of bacterial genomic islands. *Nucleic acids research,* 35**,** W97-W104.

OU, H. Y., CHEN, L. L., LONNEN, J., CHAUDHURI, R. R., THANI, A. B., SMITH, R., GARTON, N. J., HINTON, J., PALLEN, M., BARER, M. R. & RAJAKUMAR, K. 2006. A novel strategy for the identification of genomic islands by comparative analysis of the contents and contexts of tRNA sites in closely related bacteria. *Nucleic Acids Res,* 34**,** e3.

PAAUW, A., LEVERSTEIN-VAN HALL, M. A., VAN KESSEL, K. P., VERHOEF, J. & FLUIT, A. C. 2009. Yersiniabactin reduces the respiratory oxidative stress response of innate immune cells. *PLoS One,* 4**,** e8240.

PAAUW, A., LEVERSTEIN-VAN HALL, M. A., VERHOEF, J. & FLUIT, A. C. 2010. Evolution in quantum leaps: multiple combinatorial transfers of HPI and other genetic modules in Enterobacteriaceae. *PLoS One,* 5**,** e8662.

PACZOSA, M. K. & MECSAS, J. 2016. *Klebsiella pneumoniae*: going on the offense with a strong defense. *Microbiology and Molecular Biology Reviews,* 80**,** 629-661.

PAPADOPOULOS, J. S. & AGARWALA, R. 2007. COBALT: constraint-based alignment tool for multiple protein sequences. *Bioinformatics,* 23**,** 1073-1079.

PAPKE, R. T. & GOGARTEN, J. P. 2012. How bacterial lineages emerge. *Science,* 336**,** 45-46.

PARK, C. & ZHANG, J. 2012. High expression hampers horizontal gene transfer. *Genome biology and evolution,* 4**,** 523-532.

PARTRIDGE, S. R. 2011. Analysis of antibiotic resistance regions in Gram-negative bacteria. *FEMS microbiology reviews,* 35**,** 820-855.

PATERSON, D. L., HUJER, K. M., HUJER, A. M., YEISER, B., BONOMO, M. D., RICE, L. B. & BONOMO, R. A. 2003. Extended-spectrum β-lactamases in *Klebsiella pneumoniae* bloodstream isolates from seven countries: dominance and widespread prevalence of SHV-and CTX-M-type β-lactamases. *Antimicrobial agents and chemotherapy,* 47**,** 3554-3560.

PAULSEN, I. T. & LEWIS, K. 2001. Microbial multidrug efflux: introduction. HORIZON SCIENTIFIC PRESS PO BOX 1, NORFOLK, WYMONDHAM NR18 0JA, ENGLAND.

PAVLOVIC, G., BURRUS, V., GINTZ, B., DECARIS, B. & GUEDON, G. 2004. Evolution of genomic islands by deletion and tandem accretion by site-specific recombination: ICESt1-related elements from Streptococcus thermophilus. *Microbiology,* 150**,** 759-774.

PENNINGTON, J. M. & ROSENBERG, S. M. 2007. Spontaneous DNA breakage in single living Escherichia coli cells. *Nature genetics,* 39**,** 797-802.

PÉREZ-MIRANDA, S., CABIROL, N., GEORGE-TÉLLEZ, R., ZAMUDIO-RIVERA, L. & FERNÁNDEZ, F. 2007. O-CAS, a fast and universal method for siderophore detection. *Journal of microbiological methods,* 70**,** 127-131.

PERRY, R. D., BALBO, P. B., JONES, H. A., FETHERSTON, J. D. & DEMOLL, E. 1999. Yersiniabactin from Yersinia pestis: biochemical characterization of the siderophore and its role in iron transport and regulation. *Microbiology,* 145**,** 1181-1190.

PERSAT, A., INCLAN, Y. F., ENGEL, J. N., STONE, H. A. & GITAI, Z. 2015. Type IV pili mechanochemically regulate virulence factors in Pseudomonas aeruginosa. *Proc Natl Acad Sci U S A,* 112**,** 7563-8.

PETERS, J. E. & CRAIG, N. L. 2001. Tn7: smarter than we thought. *Nature Reviews Molecular Cell Biology,* 2**,** 806-814.

PIDDOCK, L., J. V. 2006a. Multidrug-resistance efflux pumps-not just for resistance. *Nature Reviews | Microbiology,* 4**,** 629-636.

PIDDOCK, L. J. 2006b. Clinically relevant chromosomally encoded multidrug resistance efflux pumps in bacteria. *Clinical microbiology reviews,* 19**,** 382-402.

PODSCHUN, R., PIETSCH, S., HÖLLER, C. & ULLMANN, U. 2001. Incidence of Klebsiella species in surface waters and their expression of virulence factors. *Applied and environmental microbiology,* 67**,** 3325-3327.

PODSCHUN, R. & ULLMANN, U. 1998. Klebsiella spp. as Nosocomial Pathogens: Epidemiology, Taxonomy, Typing Methods, and Pathogenicity Factors. *CLINICAL MICROBIOLOGY REVIEWS,* 11**,** 589–603.

POLZ, M. F., ALM, E. J. & HANAGE, W. P. 2013. Horizontal gene transfer and the evolution of bacterial and archaeal population structure. *Trends Genet,* 29**,** 170-5.

POOLE, K. 2005. Efflux-mediated antimicrobial resistance. *J Antimicrob Chemother,* 56**,** 20-51.

POPA, O., HAZKANI-COVO, E., LANDAN, G., MARTIN, W. & DAGAN, T. 2011. Directed networks reveal genomic barriers and DNA repair bypasses to lateral gene transfer among prokaryotes. *Genome research,* 21**,** 599-609.

PUIGBÒ, P., LOBKOVSKY, A. E., KRISTENSEN, D. M., WOLF, Y. I. & KOONIN, E. V. 2014. Genomes in turmoil: quantification of genome dynamics in prokaryote supergenomes. *BMC biology,* 12**,** 66.

PUKATZKI, S., MA, A. T., STURTEVANT, D., KRASTINS, B., SARRACINO, D., NELSON, W. C., HEIDELBERG, J. F. & MEKALANOS, J. J. 2006. Identification of a conserved bacterial protein secretion system in Vibrio cholerae using the Dictyostelium host model system. *Proc Natl Acad Sci U S A,* 103**,** 1528-33.

PUTZE, J., HENNEQUIN, C., NOUGAYREDE, J. P., ZHANG, W., HOMBURG, S., KARCH, H., BRINGER, M. A., FAYOLLE, C., CARNIEL, E., RABSCH, W., OELSCHLAEGER, T. A., OSWALD, E., FORESTIER, C., HACKER, J. & DOBRINDT, U. 2009. Genetic structure

and distribution of the colibactin genomic island among members of the family Enterobacteriaceae. *Infect Immun,* 77**,** 4696-703.

QIU, X., GURKAR, A. U. & LORY, S. 2006. Interstrain transfer of the large pathogenicity island (PAPI-1) of Pseudomonas aeruginosa. *Proc Natl Acad Sci U S A,* 103**,** 19830-5.

QURESHI, S. 2016. Klbesiella Infections. *Medscape***,** http://emedicine.medscape.com/article/219907-overview#showall.

RAHIMIAN, J., WILSON, T., ORAM, V. & HOLZMAN, R. S. 2004. Pyogenic liver abscess: recent trends in etiology and mortality. *Clinical infectious diseases,* 39**,** 1654-1659.

RAJEEV, L., MALANOWSKA, K. & GARDNER, J. F. 2009. Challenging a paradigm: the role of DNA homology in tyrosine recombinase reactions. *Microbiol Mol Biol Rev,* 73**,** 300-9.

RAMIREZ, M. S., TRAGLIA, G. M., LIN, D. L., TRAN, T. & TOLMASKY, M. E. 2014. Plasmid-mediated antibiotic resistance and virulence in gram-negatives: the *Klebsiella pneumoniae* paradigm. *Microbiology spectrum,* 2**,** 1.

RAMSAY, J. P., SULLIVAN, J. T., JAMBARI, N., ORTORI, C. A., HEEB, S., WILLIAMS, P., BARRETT, D. A., LAMONT, I. L. & RONSON, C. W. 2009. A LuxRI-family regulatory system controls excision and transfer of the Mesorhizobium loti strain R7A symbiosis island by activating expression of two conserved hypothetical genes. *Molecular microbiology,* 73**,** 1141-1155.

RAMSAY, J. P., SULLIVAN, J. T., STUART, G. S., LAMONT, I. L. & RONSON, C. W. 2006. Excision and transfer of the Mesorhizobium loti R7A symbiosis island requires an integrase IntS, a novel recombination directionality factor RdfS, and a putative relaxase RlxS. *Molecular microbiology,* 62**,** 723-734.

RANDRIANIRINA, F., VEDY, S., RAKOTOVAO, D., RAMAROKOTO, C.-E., RATSITOHAINA, H., CAROD, J., RATSIMA, E., MORILLON, M. & TALARMIN, A. 2009. Role of contaminated aspiration tubes in nosocomial outbreak of *Klebsiella pneumoniae* producing SHV-2 and CTX-M-15 extended-spectrum β-lactamases. *Journal of Hospital Infection,* 72**,** 23-29.

RANKIN, D. J., ROCHA, E. P. & BROWN, S. P. 2011. What traits are carried on mobile genetic elements, and why? *Heredity,* 106**,** 1-10.

RATLEDGE, C. & DOVER, L., G. 2000. Iron metabolism in pathogenic bacteria. *Annu. Rev. Microbiology,* 54**,** 881-941.

RAVATN, R., ALEXANDER J. B. ZEHNDER & MEER, J. R. V. D. 1998a. Low-Frequency Horizontal Transfer of an Element Containing the Chlorocatechol Degradation Genes from Pseudomonas sp. Strain B13 to Pseudomonas putida F1 and to Indigenous Bacteria in Laboratory-Scale Activated-Sludge Microcosms. *Applied and Environmental Microbiology,* 64.

RAVATN, R., SONJA STUDER, ALEXANDER J. B. ZEHNDER & MEER, J. R. V. D. 1998b. Int-B13, an Unusual Site-Specific Recombinase of the Bacteriophage P4 Integrase

Family, Is Responsible for Chromosomal Insertion of the 105-Kilobase clc Element of Pseudomonas sp. Strain B13. *JOURNAL OF BACTERIOLOGY,* 180**,** 5505-5514.

RAYMOND, K. N., DERTZ, E. A. & KIM, S. S. 2003. Enterobactin: an archetype for microbial iron transport. *Proc Natl Acad Sci U S A,* 100**,** 3584-8.

REINEKE, W., STEPHEN W. WESSELS, MIGUEL A. RUBIO, JAVIER, L., UWE, S., EBERHARDT, S., SCHL6MANN, M. & HANS, J. K. 1982. Degradation of monochlorinated aromatics following transfer of genes encoding chlorocatechol catabolism. *FEMS Microbiology Letters,* 14**,** 291-294.

REISNER, A., HAAGENSEN, J. A., SCHEMBRI, M. A., ZECHNER, E. L. & MOLIN, S. 2003. Development and maturation of Escherichia coli K-12 biofilms. *Molecular microbiology,* 48**,** 933-946.

ROBERTS, A. P. & MULLANY, P. 2009. A modular master on the move: the Tn916 family of mobile genetic elements. *Trends Microbiol,* 17**,** 251-8.

ROBERTSON, G. T., DOYLE, T. B. & LYNCH, A. S. 2005. Use of an efflux-deficient Streptococcus pneumoniae strain panel to identify ABC-class multidrug transporters involved in intrinsic resistance to antimicrobial agents. *Antimicrobial agents and chemotherapy,* 49**,** 4781-4783.

ROCHE, D., FLECHARD, M., LALLIER, N., REPERANT, M., BREE, A., PASCAL, G., SCHOULER, C. & GERMON, P. 2010. ICEEc2, a new integrative and conjugative element belonging to the pKLC102/PAGI-2 family, identified in Escherichia coli strain BEN374. *J Bacteriol,* 192**,** 5026-36.

ROSENBLUETH, M., MARTÍNEZ, L., SILVA, J. & MARTÍNEZ-ROMERO, E. 2004. Klebsiella variicola, a novel species with clinical and plant-associated isolates. *Systematic and applied microbiology,* 27**,** 27-35.

ROSSELLÓ-MORA, R. & AMANN, R. 2001. The species concept for prokaryotes. *FEMS microbiology reviews,* 25**,** 39-67.

ROY, C. R. & CHERFILS, J. 2015. Structure and function of Fic proteins. *Nat Rev Microbiol,* 13**,** 631-40.

ROY, P. H. 1999. Horizontal transfer of genes in bacteria. *Microbiology Today,* 26**,** 168-170.

RUMER, L., JORES, J., KIRSCH, P., CAVIGNAC, Y., ZEHMKE, K. & WIELER, L. H. 2003. Dissemination of pheU- and pheV-located genomic islands among enteropathogenic (EPEC) and enterohemorrhagic (EHEC) E. coli and their possible role in the horizontal transfer of the locus of enterocyte effacement (LEE). *Int J Med Microbiol,* 292**,** 463-75.

RUSSO, T. A., OLSON, R., MACDONALD, U., BEANAN, J. & DAVIDSON, B. A. 2015. Aerobactin, but not yersiniabactin, salmochelin, or enterobactin, enables the growth/survival of hypervirulent (hypermucoviscous) *Klebsiella pneumoniae* ex vivo and in vivo. *Infect Immun,* 83**,** 3325-33.

SALYERS, A. A., SHOEMAKER, N. B., STEVENS, A. M. & LI, L.-Y. 1995. Conjugative transposons: an unusual and diverse set of integrated gene transfer elements. *Microbiological reviews,* 59**,** 579-590.

SCHMID, M. C., SCHULEIN, R., DEHIO, M., DENECKER, G., CARENA, I. & DEHIO, C. 2004. The VirB type IV secretion system of Bartonella henselae mediates invasion, proinflammatory activation and antiapoptotic protection of endothelial cells. *Molecular microbiology,* 52**,** 81-92.

SCHMIDT, H. & HENSEL, M. 2004. Pathogenicity islands in bacterial pathogenesis. *Clinical microbiology reviews,* 17**,** 14-56.

SCHRODER, G. & LANKA, E. 2005. The mating pair formation system of conjugative plasmids-A versatile secretion machinery for transfer of proteins and DNA. *Plasmid,* 54**,** 1-25.

SCHUBERT, SÖREN, DUFKE, SEVERIN, SORSA, JOHANNA, HEESEMANN & JÜRGEN 2004. A novel integrative and conjugative element (ICE) of Escherichia coli: the putative progenitor of the Yersinia high-pathogenicity island. *Molecular Microbiology,* 51**,** 837-848.

SCHUBERT, SÖREN, SONJA CUENCA, DANIELA FISCHER & HEESEMANN., J. 2000. High-Pathogenicity Island of Yersinia pestis in Enterobacteriaceae Isolated from Blood Cultures and Urine Samples: Prevalence and Functional Expression. *The Journal of Infectious Diseases,* 182**,** 1268–1271.

SCHULERT, G. S., HEATHER FELTMAN, SHIRA D. P. RABIN, CIARA G. MARTIN, SCOTT E. BATTLE, JORDI RELLO & HAUSER, A. R. 2003. Secretion of the toxin exou is a marker for highly virulent Pseudomonas aeruginosa isolates obtained from patients with hospital-acquired pneumonia. *Journal of Infectious Diseases,* 188**,** 1695–1706.

SCOTT, W. B., JACQUELINE D. FETHERSTON & PERRY, R. D. 1997. Genetic organization of the yersiniabactin biosynthetic region and construction of avirulent mutants in Yersinia pestis. *Infection and Immunity,* 65**,** 1659–1668.

SENTCHILO, V., ZEHNDER, A. J. B. & VAN DER MEER, J. R. 2003. Characterization of two alternative promoters for integrase expression in the clc genomic island of Pseudomonas sp. strain B13. *Molecular Microbiology,* 49**,** 93-104.

SETH, S., H. M., FOOKES, M. C., OKORO, C. K., BAKER, S., HARRIS, S. R., SCOTT, P., PICKARD, D., QUAIL, M. A., CHURCHER, C., SANDERS, M., HARMSE, J., DOUGAN, G., PARKHILL, J. & THOMSON, N. R. 2012. Structure, diversity, and mobility of the Salmonella pathogenicity island 7 family of integrative and conjugative elements within Enterobacteriaceae. *J Bacteriol,* 194**,** 1494-504.

SETH, S., HELENA, & CROUCHER, N. J. 2009. ice breakdown. *NATURE REVIEWS | MICROBIOLOGY,* VOLUME 7**,** 328-329.

SHAO, Y., HE, X., HARRISON, E. M., TAI, C., OU, H.-Y., RAJAKUMAR, K. & DENG, Z. 2010. mGenomeSubtractor: a web-based tool for parallel in silico subtractive

hybridization analysis of multiple bacterial genomes. *Nucleic acids research,* 38**,** W194-W200.

SHAPIRO, B. J., FRIEDMAN, J., CORDERO, O. X., PREHEIM, S. P., TIMBERLAKE, S. C., SZABÓ, G., POLZ, M. F. & ALM, E. J. 2012. Population genomics of early events in the ecological differentiation of bacteria. *science,* 336**,** 48-51.

SIGUIER, P., GOURBEYRE, E. & CHANDLER, M. 2014. Bacterial insertion sequences: their genomic impact and diversity. *FEMS microbiology reviews,* 38**,** 865-891.

SITKIEWICZ, I., GREEN, N. M., GUO, N., MEREGHETTI, L. & MUSSER, J. M. 2011. Lateral gene transfer of streptococcal ICE element RD2 (region of difference 2) encoding secreted proteins. *BMC microbiology,* 11**,** 65.

SKIPPINGTON, E. & RAGAN, M. A. 2012. Phylogeny rather than ecology or lifestyle biases the construction of Escherichia coli–Shigella genetic exchange communities. *Open biology,* 2**,** 120112.

SMATI, M., MAGISTRO, G., ADIBA, S., WIESER, A., PICARD, B., SCHUBERT, S. & DENAMUR, E. 2017. Strain-specific impact of the high-pathogenicity island on virulence in extra-intestinal pathogenic Escherichia coli. *Int J Med Microbiol,* 307**,** 44-56.

SMILLIE, C., GARCILLAN-BARCIA, M. P., FRANCIA, M. V., ROCHA, E. P. & DE LA CRUZ, F. 2010. Mobility of plasmids. *Microbiol Mol Biol Rev,* 74**,** 434-52.

SMILLIE, C. S., SMITH, M. B., FRIEDMAN, J., CORDERO, O. X., DAVID, L. A. & ALM, E. J. 2011. Ecology drives a global network of gene exchange connecting the human microbiome. *Nature,* 480**,** 241-244.

SNIDER, J., THIBAULT, G. & HOURY, W. A. 2008. The AAA+ superfamily of functionally diverse proteins. *Genome Biol,* 9**,** 216.

SOBIRK, S. K., STRUVE, C. & JACOBSSON, S. G. 2010. Primary *Klebsiella pneumoniae* liver abscess with metastatic spread to lung and eye, a North-European case report of an emerging syndrome. *The open microbiology journal,* 4.

SOLER, B., A. J., BIRSHAN, D., TOMARAS, A. P., DANDEKAR, M., TRAN, T., NEWMARK, J., BUI, D., GUPTA, N., HERNANDEZ, K., SARNO, R., ZORREGUIETA, A., ACTIS, L. A. & TOLMASKY, M. E. 2008. *Klebsiella pneumoniae* multiresistance plasmid pMET1: similarity with the Yersinia pestis plasmid pCRY and integrative conjugative elements. *PLoS One,* 3**,** e1800.

SOTO, S. M. 2013. Role of efflux pumps in the antibiotic resistance of bacteria embedded in a biofilm. *Virulence,* 4**,** 223-9.

SOUCY, S. M., HUANG, J. & GOGARTEN, J. P. 2015. Horizontal gene transfer: building the web of life. *Nat Rev Genet,* 16**,** 472-82.

SRINIVASAN, V. B., SINGH, B. B., PRIYADARSHI, N., CHAUHAN, N. K. & RAJAMOHAN, G. 2014. Role of novel multidrug efflux pump involved in drug resistance in *Klebsiella pneumoniae*. *PLoS One,* 9**,** e96288.

STEVE ROZEN & SKALETSKY, H. 2000. Primer3 on the WWW for General Users and for Biologist Programmers. *Methods Mol. Biol.,* 132**,** 365-86.

STRATFORD, F. L., RAMJEESINGH, M., CHEUNG, J. C., HUAN, L.-J. & BEAR, C. E. 2007. The Walker B motif of the second nucleotide-binding domain (NBD2) of CFTR plays a key role in ATPase activity by the NBD1–NBD2 heterodimer. *Biochemical Journal,* 401**,** 581-586.

SZPIRER, C. Y., FAELEN, M. & COUTURIER, M. 2000. Interaction between the RP4 coupling protein TraG and the pBHR1 mobilization protein Mob. *Molecular Microbiology,* 37**,** 1283-1292.

TATO, I., MATILLA, I., ARECHAGA, I., ZUNZUNEGUI, S., DE LA CRUZ, F. & CABEZON, E. 2007. The ATPase activity of the DNA transporter TrwB is modulated by protein TrwA: implications for a common assembly mechanism of DNA translocating motors. *J Biol Chem,* 282**,** 25569-76.

TATUM, E. & LEDERBERG, J. 1947. Gene recombination in the bacterium Escherichia coli. *Journal of bacteriology,* 53**,** 673.

TETTELIN, H., RILEY, D., CATTUTO, C. & MEDINI, D. 2008. Comparative genomics: the bacterial pan-genome. *Current opinion in microbiology,* 11**,** 472-477.

THANASSI, D. G. & HULTGREN, S. J. 2000. Multiple pathways allow protein secretion across the bacterial outer membrane. *Current opinion in cell biology,* 12**,** 420-430.

THOMAS, J., LEE, C. A. & GROSSMAN, A. D. 2013. A conserved helicase processivity factor is needed for conjugation and replication of an integrative and conjugative element. *PLoS Genet,* 9**,** e1003198.

THOMSEN, R. W., JEPSEN, P. & SØRENSEN, H. T. 2007. Diabetes mellitus and pyogenic liver abscess: risk and prognosis. *Clinical infectious diseases,* 44**,** 1194-1201.

TOLMASKY, M. E., CHAMORRO, R., CROSA, J. & MARINI, P. 1988. Transposon-mediated amikacin resistance in *Klebsiella pneumoniae*. *Antimicrobial agents and chemotherapy,* 32**,** 1416-1420.

TOUSSAINT, A. & MERLIN, C. 2002. Mobile elements as a combination of functional modules. *Plasmid,* 47**,** 26-35.

TROKTER, M., FELISBERTO-RODRIGUES, C., CHRISTIE, P. J. & WAKSMAN, G. 2014. Recent advances in the structural and molecular biology of type IV secretion systems. *Curr Opin Struct Biol,* 27**,** 16-23.

TSVETKOVA, K., MARVAUD, J. C. & LAMBERT, T. 2010. Analysis of the mobilization functions of the vancomycin resistance transposon Tn1549, a member of a new family of conjugative elements. *J Bacteriol,* 192**,** 702-13.

TUANYOK, A., LEADEM, B. R., AUERBACH, R. K., BECKSTROM-STERNBERG, S. M., BECKSTROM-STERNBERG, J. S., MAYO, M., WUTHIEKANUN, V., BRETTIN, T. S., NIERMAN, W. C., PEACOCK, S. J., CURRIE, B. J., WAGNER, D. M. & KEIM, P. 2008.

Genomic islands from five strains of Burkholderia pseudomallei. *BMC Genomics,* 9**,** 566.

VALENTINE, P. J., SHOEMAKER, N. B. & SALYERS, A. A. 1988. Mobilization of Bacteroides plasmids by Bacteroides conjugal elements. *Journal of bacteriology,* 170**,** 1319-1324.

VAN DER MEER, J. R. & SENTCHILO, V. 2003. Genomic islands and the evolution of catabolic pathways in bacteria. *Current Opinion in Biotechnology,* 14**,** 248-254.

VEDANTAM, G., KNOPF, S. & HECHT, D. W. 2006. Bacteroides fragilis mobilizable transposon Tn5520 requires a 71 base pair origin of transfer sequence and a single mobilization protein for relaxosome formation during conjugation. *Mol Microbiol,* 59**,** 288-300.

VERMA, A. & BURNS, D. L. 2007. Requirements for assembly of PtlH with the pertussis toxin transporter apparatus of Bordetella pertussis. *Infection and immunity,* 75**,** 2297-2306.

VERNIKOS, G. 2008. *In silico prediction of genomic islands in microbial genomes.* University of Cambridge.

VERNIKOS, G. S. & PARKHILL, J. 2008a. Resolving the structural features of genomic islands: a machine learning approach. *Genome Res,* 18**,** 331-42.

VERNIKOS, G. S. & PARKHILL, J. 2008b. Resolving the structural features of genomic islands: a machine learning approach. *Genome research,* 18**,** 331-342.

VINCZE, T. 2003. NEBcutter: a program to cleave DNA with restriction enzymes. *Nucleic Acids Research,* 31**,** 3688-3691.

WALDOR, M. K., TSCHAPE, H. & MEKALANOS, J. J. 1996. A New Type of Conjugative Transposon Encodes Resistance to Sulfamethoxazole, Trimethoprim, and Streptomycin in Vibrio cholerae O139. *JOURNAL OF BACTERIOLOGY,* 178**,** 4157–4165.

WALLDEN, K., RIVERA-CALZADA, A. & WAKSMAN, G. 2010. Type IV secretion systems: versatility and diversity in function. *Cell Microbiol,* 12**,** 1203-12.

WANDERSMAN, C. & DELEPELAIRE, P. 2004. Bacterial iron sources: from siderophores to hemophores. *Annu Rev Microbiol,* 58**,** 611-47.

WENT, F. 1971. Parallel evolution. *Taxon***,** 197-226.

WEST, S. C. 1997. Processing of recombination intermediates by the RuvABC proteins. *Annual review of genetics,* 31**,** 213-244.

WHITTLE, G., SHOEMAKER, N. B. & SALYERS., A. A. 2002. The role of Bacteroides conjugative transposons in the dissemination of antibiotic resistance genes. *Cellular and Molecular Life Sciences,* 59**,** 2044–2054.

WILLIAMS, D., FOURNIER, G. P., LAPIERRE, P., SWITHERS, K. S., GREEN, A. G., ANDAM, C. P. & GOGARTEN, J. P. 2011. A rooted net of life. *Biology direct,* 6**,** 45.

WILLIAMS, D., GOGARTEN, J. P. & PAPKE, R. T. 2012. Quantifying homologous replacement of loci between haloarchaeal species. *Genome biology and evolution,* 4**,** 1223-1244.

WILSON, R. B. 1994. Hepatic hemosiderosis and Klebsiella bacteremia in a green aracari (Pteroglossus viridis). *Avian diseases***,** 679-681.

WOZNIAK, R. A., FOUTS, D. E., SPAGNOLETTI, M., COLOMBO, M. M., CECCARELLI, D., GARRISS, G., DERY, C., BURRUS, V. & WALDOR, M. K. 2009. Comparative ICE genomics: insights into the evolution of the SXT/R391 family of ICEs. *PLoS Genet,* 5**,** e1000786.

WOZNIAK, R. A. & WALDOR, M. K. 2010. Integrative and conjugative elements: mosaic mobile genetic elements enabling dynamic lateral gene flow. *Nat Rev Microbiol,* 8**,** 552-63.

WU, K. M., LI, L. H., YAN, J. J., TSAO, N., LIAO, T. L., TSAI, H. C., FUNG, C. P., CHEN, H. J., LIU, Y. M., WANG, J. T., FANG, C. T., CHANG, S. C., SHU, H. Y., LIU, T. T., CHEN, Y. T., SHIAU, Y. R., LAUDERDALE, T. L., SU, I. J., KIRBY, R. & TSAI, S. F. 2009. Genome sequencing and comparative analysis of *Klebsiella pneumoniae* NTUH-K2044, a strain causing liver abscess and meningitis. *J Bacteriol,* 191**,** 4492-501.

WURDEMANN, D. & TUMMLER, B. 2007. In silico comparison of pKLC102-like genomic islands of Pseudomonas aeruginosa. *FEMS Microbiol Lett,* 275**,** 244-9.

WYRES, K. L. & HOLT, K. E. 2016. *Klebsiella pneumoniae* Population Genomics and Antimicrobial-Resistant Clones. *Trends Microbiol,* 24**,** 944-956.

YOON, S. H., PARK, Y.-K., LEE, S., CHOI, D., OH, T. K., HUR, C.-G. & KIM, J. F. 2007. Towards pathogenomics: a web-based resource for pathogenicity islands. *Nucleic acids research,* 35**,** D395-D400.

YUAN, Q., CARLE, A., GAO, C., SIVANESAN, D., ALY, K. A., HÖPPNER, C., KRALL, L., DOMKE, N. & BARON, C. 2005. Identification of the VirB4-VirB8-VirB5-VirB2 pilus assembly sequence of type IV secretion systems. *Journal of Biological Chemistry,* 280**,** 26349-26359.

ZADOKS, R., GRIFFITHS, H., MUNOZ, M., AHLSTROM, C., BENNETT, G., THOMAS, E. & SCHUKKEN, Y. 2011. Sources of Klebsiella and Raoultella species on dairy farms: be careful where you walk. *Journal of dairy science,* 94**,** 1045-1051.

ZECHNER, E., DE LA CRUZ, F., EISENBRANDT, R., GRAHN, A., KORAIMANN, G., LANKA, E., MUTH, G., PANSEGRAU, W., THOMAS, C. & WILKINS, B. 2000. Conjugative-DNA transfer processes. *The horizontal gene pool: bacterial plasmids and gene spread***,** 87-174.

ZECHNER, E. L., LANG, S. & SCHILDBACH, J. F. 2012. Assembly and mechanisms of bacterial type IV secretion machines. *Philos Trans R Soc Lond B Biol Sci,* 367**,** 1073-87.

ZHANG, J., VAN AARTSEN, J. J., JIANG, X., SHAO, Y., TAI, C., HE, X., TAN, Z., DENG, Z., JIA, S., RAJAKUMAR, K. & OU, H. Y. 2011. Expansion of the known *Klebsiella*

pneumoniae species gene pool by characterization of novel alien DNA islands integrated into tmRNA gene sites. *J Microbiol Methods,* 84**,** 283-9.

Appendix I

PCR screening of ICE-1

Primers used in PCR screening of ICE-1

Catalogue No.	Name	Sequence (5' to 3')	Reference
RF101	Int_F	TGTTCATTCGCTCCAGTGA	This study
RF102	Int_R	GGGTTATGGTCGCCGGGGA	
RF103	fyuA_F	CCTTCCCTTCCGGTTCGT	
RF104	fyuA_R	GCTCTTACCCTGGTCGCC	
RF105	VirB1_F	ATGCTTTCCACCACAGC	
RF106	VirB1_R	TTATTCCTCCTCCTCACGG	
RF202	irp1_F	CAGAAACGTGGCTCGACAAC	
RF203	irp1_R	CTTCGATGACTGCCTGTTGC	

RF-Robeena Farzand

Primer pair used for identification of site of integration of ICE-1

Catalogue No.	Name	Sequence (5' to 3')	Reference
RF118	tasn_F	CGAGTCCAGTCAGAGGAGCCA	This study
RF102	Int_R	GGGTTATGGTCGCCGGGGA	

Primers used in PCR mapping of ICE-1

Catalogue No	Name	Sequence (5' to 3')	Reference
RF119	P1_F	CCGGGTTTCTGTCAGTTCG	This study
RF120	P2_R	GGACAGCTCAGGGAAATGG	
RF121	P3_F	AGCAATAGCGCCAGCATAC	
RF122	P4_R	GACCGGCTGAGCATTAACTG	
RF123	P5_F	TCGCTGTTACCGGACAACC	
RF124	P6_R	CTGGAGATCGAATACTGGCC	
RF125	P7_F	GTGATGGACAGCAACAGGTG	
RF126	P8_R	CAGATTATCGAGCGTGCGG	
RF127	P9_F	ATATCTCGGCGCTGTTCACC	
RF128	P10_R	CCAACCTCCAGAATCCGTTC	
RF129	P11_F	CCAGCGTCTGTCTGAATCG	
RF130	P12_R	CAGTTCAGGAGAACATCCGC	
RF131	P13_F	GCGGATGTTCTCCTGAACTG	
RF132	P14_R	GTGCGACCCATATTGACCTG	
RF133	P15_F	CGTGATTGATACGCGCTATG	
RF134	P16_R	CAGAAGCAACTCCAGTCGT	
RF135	P17_F	GCAATTTCAGTACCGGGCAAC	
RF136	P18_R	CATGAGGCTGCATTCCTTCC	
RF137	P19_F	GGCCTTAGCATTCGGTTGTC	
RF138	P20_R	GCGTGTACCTTGCCAAATCC	This study
RF139	P20'_F	GGATTTGGCAAGGTACACGC	
RF140	P21_F	TTACGTTCGTGGGCTTCTCC	
RF141	P21_R	GTGATTTCCGGGTTGTCCT	
RF142	P22_R	CAATCCGTACTGACCAAGCC	
RF143	P23_F	GGCTTGGTCAGTACGGATTG	
RF144	P24_R	ATCAATCTGCTCGACGATCC	
RF145	P25_F	GAATCGAGAATGCCAAGCAG	
RF146	P25_R	GACGATGCTTGGTGGAGATT	
RF147	P26_F	TCTGCTGCATCGTTCCTTC	
RF148	P26_R	GTCCTATCTCGGGTTCGTC	
RF149	ICE1-DR_R	TTGGCTCCTCTGACTGGG	
RF150	P21_2F	AGGACAACCCGGAAATCAC	

Appendix II

PCR screening of ICE-2

Primers used for screening of ICE-2

Catalogue No	Name	Sequence (5' to 3')	Reference
RF154	44710_F	CTCTGTTCCGCCATAAACC	This study
RF155	44710_R	GTTTCTTGCCGGGTATCGG	
RF156	Int2_F	CCACATATTCCAGCGTTGAC	
RF157	Int2_R	GTGAACATCAGGTGCCGATT	
RF158	DBP2_F	TTAGCCCTGCGTCCTTAAC	
RF159	DBP2_R	GAGCGTTATCAGGCCGTAT	
RF168	mob2_F	GAGGCTGATCGGTGTGTTG	
RF169	mob2_R	GTTCCTCGGTGCGCTATGA	
RF178	MCP_F	ATGGTCAGCAACATCCAGC	
RF179	MCP_R	GAAGCAACAGATGGCCGAT	
RF166	tRNA-phe		

Primers used for PCR mapping of ICE-2

Catalogue No	Name	Sequence (5' to 3')	Reference
RF209	A_F	GGCGAAATCAGATGTGAGG	This study
RF210	A_R	CTGCCCGAAAGGAACCACT	
RF211	B_F	ATGTAATAACGGTTCACTGGC	
RF212	B_R	ATGAAAGCCAGTGCTATGAGT	
RF213	C_F	TCACTCCTCAATGTTTCCTAATA	
RF214	C_R	ATGAGTGCCGACAGCTATC	
RF215	D_F	CGCTGCGTTCCTTATTGAAC	
RF216	D_R	TCGAGTGCCGATACATTGAT	
RF217	E_F	AAGAAGCGTCATCATAACCTGA	
RF218	E_R	CCTGCAACCCATGATAGCC	
RF219	F_F	GCATCCCGTACCTGAAGC	
RF220	F_R	CGATGATGCAGGTGAAGTCA	
RF221	G_F	TTGTCTCGATCCAGTTCGAC	
RF222	G_R	CTACACATGGCGCGAACAC	
RF223	H_F	TGCGTAATAAATGTGCATCGC	
RF224	H_R	GCATAGCCAGTCGGTAGAT	
RF225	I_F	GACAAACAGCGCCAGACG	
RF226	I_R	TGACTGAGGTTCTCTTGTTGT	
RF227	J_F	TTAGCAGCGAAGGACTTACC	
RF228	J_R	GCGAATTTATCTGACCAGACA	
RF229	K_F	GCACTCGTTACCTTTATCGCA	
RF230	K_R	CAACAGGTGACATTATGCAAG	
RF231	A_F	GGCGAAATCAGATGTGAGG	
RF232	A_R	CTGCCCGAAAGGAACCACT	
RF233	B_F	ATGTAATAACGGTTCACTGGC	

Appendix III

Primers used for the construction of ICE-1 marker plasmids

Catalogue No.	Name	Sequence (5' to 3')	Length of amplified fragment	Reference
RF107	oriT-HindIII_F	**GGCAAGCTT**CAAATAAAATGACAGTCATCATCCT	1760bp	This study
RF108	oriT956-HIII_F	**GGCAAGCTT**TATACACTCCCGCAATCAGG	956bp	
RF109	oriT568-HIII_F	**GGCAAGCTT**TGAAGTGGAACGTGGACAG	568bp	
RF110	oriT525-HIII_F	**GGCAAGCTT**ACAGGCTGACAGGCGGC	525bp	
RF111	oriT454-HIII_F	**GGCAAGCTT**GAAAAATAATGAAGTGGAACGTG	454bp	
RF112	oriT368-HIII_F	**GGCAAGCTT**CGCCCCAGCGAATTGAAG	368bp	
RF113	oriT-SalI_R	TAA**GTCGAC**GGCATCGCCCCATCAA	Reverse primer for 1760, 956, 568, 368 bp fragments	
RF114	oriTDR2-SalI_R	TAAGTCGACTGCGCCGGTACATGCGG	525bp and 454bp	
RF115	oriT608-SalI_R	TAAGTCGACAGACGGGGCGAGCGTATG	608	

Appendix IV

Primers used for the construction of ICE-2 marker plasmids

A. Primers used to amplify pACYC184 backbone

Catalogue No	Name	Sequence (5' to 3')	Reference
RF179	PU_F	ACTGGCCTCAGGCATTTGA	This study
RF180	PU_R	GTGCCTGACTGCGTTAGC	

B. Primers used to amplify various regions in ICE-2

Catalogue No	Name	Sequence (5' to 3')[a]	Reference
RF181	ICE2A_F	**ACGCAGTCAGGCAC**GGCGAAATCAGATGTGAGG	**This study**
RF182	ICE2A_R	**ATGCCTGAGGCCAGT**CTGCCCGAAAGGAACCACT	
RF183	ICE2B_F	ACGCAGTCAGGCACATGTAATAACGGTTCACTGGC	
RF184	ICE2B_R	ATGCCTGAGGCCAGTATGAAAGCCAGTGCTATGAGT	
RF185	ICE2C_F	ACGCAGTCAGGCACTCACTCCTCAATGTTTCCTAATA	
RF186	ICE2C_R	ATGCCTGAGGCCAGTATGAGTGCCGACAGCTATC	
RF187	ICE2D_F	ACGCAGTCAGGCACCGCTGCGTTCCTTATTGAAC	
RF188	ICE2D_R	ATGCCTGAGGCCAGTTCGAGTGCCGATACATTGAT	

RF189	ICE2E_F	ACGCAGTCAGGCACAAGAAGCGTCATCATAACCTGA	
RF190	ICE2E_R	ATGCCTGAGGCCAGTCCTGCAACCCATGATAGCC	
RF191	ICE2F_F	ACGCAGTCAGGCACGCATCCCGTACCTGAAGC	
RF191	ICE2F_R	ATGCCTGAGGCCAGTCGATGATGCAGGTGAAGTCA	
RF192	ICE2G_F	ACGCAGTCAGGCACTTGTCTCGATCCAGTTCGAC	
RF193	ICE2G_R	ATGCCTGAGGCCAGTCTACACATGGCGCGAACAC	This study
RF194	ICE2H_F	ACGCAGTCAGGCACTGCGTAATAAATGTGCATCGC	
RF195	ICE2H_R	ATGCCTGAGGCCAGTGCATAGCCAGTCGGTAGAT	
RF196	ICE2I_F	ACGCAGTCAGGCACGACAAACAGCGCCAGACG	
RF197	ICE2I_R	ATGCCTGAGGCCAGTTGACTGAGGTTCTCTTGTTGT	
RF198	ICE2J_F	ACGCAGTCAGGCACTTAGCAGCGAAGGACTTACC	
RF199	ICE2J_R	ATGCCTGAGGCCAGTGCGAATTTATCTGACCAGACA	
RF200	ICE2K_F	ACGCAGTCAGGCACGCACTCGTTACCTTTATCGCA	
RF201	ICE2K_R	ATGCCTGAGGCCAGTCAACAGGTGACATTATGCAAG	

a= Red colour indicates the complementary sequence of primers used to amplify pACYC184.

Appendix V

Primers used to construct various complementation plasmids

A. Pybt

Cat. No	Name	Sequence (5' to 3')[a]	Feature	Reference
RF205	ybt-F	**ACGCAGTCAGGCAC**GGACAGTCTGGTTGTGAGG	To amplify the *ybtXSPQA region using ICE-1 as template*	This study
RF206	ybt-R	**ATGCCTGAGGCCAGT**GTATCCGGGCCTCTGTCA		
RF207	PU_F	ACTGGCCTCAGGCATTTGA	To amplify backbone of pACYC184 (2232 bp) for infusion cloning	
RF208	PU_R	GTGCCTGACTGCGTTAGC		

a= Red colour indicates the complementary sequence of primers used to amplify pACYC184.

B. P-mob2 and P-traI

Cat. No	Name	Sequence (5' to 3')[a]	Feature	Reference
RF234	mob2_HindIII-F	**GGCAAGCTT**TCATTCTTCCTCTCCTTCTG	To mob-2 *using ICE-2 as template*	This study
RF235	mob2_NotI-R	ATAGTTTAGCGGCCGCGTGAGCGATCGCTATGTG		
RF236	traI_SalI-F	TAAGTCGACTTAGTTCAAAGAGCTAACTTC	To amplify traI using ICE-2 as template	
F237	traI_NotI-R	ATAGTTTAGCGGCCGCTATGCTCAATACTCTATTTTTCT		

a= Underline sequences represent the restriction digestion sites of the enzyme mentioned in primer name.

Appendix VI

Primers used for point mutations in *mob2*

Cat. No	Name	Sequence (5' to 3')	Features
RF238	MOBKE-F	GTGAGCGATCGCTATGTGATTG	Used to amplify SOE fragment of disrupted *mob*-2
RF239	$MOBK^{199}$-R	CAGGCGCGTTGCCCCTAC	Substitute lysine with alanine
RF240	$MOBK^{199}$-F	GTAGGGGCAACGCGCCTG	Substitute lysine with alanine
RF241	$MOBE^{507}$-F	CCACTGTGACGCATTCAGTGAA	Substitute glutamic acid with alanine
RF242	$MOBE^{507}$-R	TTCACTGAATGCGTCACAGTGG	Substitute glutamic acid with alanine
RF243	MOBKE-R	TCATTCTTCCTCTCCTTCTGCC	Used to amplify SOE fragment of disrupted *mob*-2

Primers used for plasmid construction for complementation experiment of point disrupted *mob*-2

Cat No	Name	Sequence (5' to 3')[a]	Features
RF244	PW_F	GGTCGACGGTATCGATAAGC	Inverse PCR to amplify the RFTool-1 plasmid
RF245	PW_R	CGGCCGCTCTAGAACTAGT	
RF246	MOBPW-F	**GTTCTAGAGCGGCCG**GTGAGCGATCGCTATGTGATTG	HD infusion cloning of $mob^{K199E507}$ and RFTool-1
RF247	MOBPW-R	**TCGATACCGTCGACC**TCATTCTTCCTCTCCTTCTGCC	

a= Red colour indicates the complementary sequence of primers used to amplify RFTool-1.

Appendix VII

Primers used to construct various mutant strains by lambda red recombination system

Primers used to amplify hygromycin gene cassette

Cat No	Name	Sequence (5' to 3')[a]	Features	reference
PR351	GM_F	CGAATTAGCTTCAAAAGCGCTCTGA	To amplify the hph cassette using pJTAG-Hyg as template DNA	Lab 212
PR2773	GM_R2	AATTGGGGATCTTGAAGTTCCT		

Primers used to construct ΔICE-1

Cat No	Name	Sequence (5' to 3')[a]	Features	Reference
RF-R01	ICE1_UF	TTTGCATTTCCTCGGCTGTC	Used to amplify upstream flank of ICE-1	This study
RF-R02	ICE1_UR	TCAGAGCGCTTTTGAAGCTAATTCGCGATGCGTAGGGTAAAATC		
RF-R03	ICE1_DF	AGGAACTTCAAGATCCCCAATTTCTGCCGGAAGGCGAATG	Used to amplify downstream flank of ICE-1	
RF-R04	ICE2_DR	GTATGGCTGTCGATGAAGCT		
RF-R05	ICE1-RF_F	GACGTTATTGACCGCCAGC	Screening primer for detection of ICE-1 deletion	
RF-R06	ICE1-RF_R	CTGCTTATCCCTTTCGCCG		

Primers used to construct ΔICE-2

Cat No	Name	Sequence (5' to 3')[a]	Features	Reference
RF-R07	ICE2_UF	TTGCCGTAGTGAATATGCTG	Used to amplify upstream flank of ICE-2	This study
RF-R08	ICE2_UR	TCAGAGCGCTTTTGAAGCTAATTCGAGATGGTGAAAAATGGCGC		
RF-R09	ICE2_DF	AGGAACTTCAAGATCCCCAATTCCGGCACCACTATTTAAAG	Used to amplify downstream flank of ICE-2	
RF-R10	ICE2_DR	GTACCCTCGCAATGGACATT		

Primers used to construct Δmob2

Cat No	Name	Sequence (5' to 3')[a]	Feature	Reference
RF-R11	mob2_UF	TTTGCATTTCCTCGGCTGTC	Used to amplify upstream region to *mob2*	This study
RF-R12	mob2_UR	TCAGAGCGCTTTTGAAGCTAATTCGGAAGAATGAAACGTTACCAGA		
RF-R13	mob2_DF	AGGAACTTCAAGATCCCCAATATCGCTCACCTGGTTGCC	Used to amplify downstream flank of *mob2*	
RF-R14	mob2_DR	GTTATTGCCGATTTGGGCG		
RF-R15	mob2-RF_F	CAACACTCTACCGTCACCA	Used to confirm precise excision of *mob2*	
RF-R16	mob2-RF_R	AGCTGGGTAGAGCCGAAGA		

Primers used to construct Δtral

Cat No	Name	Sequence (5' to 3')[a]	Feature	Reference
RF-R17	traI_UF	TGCTGCATAACCCGATAGAC	For amplification of upstream region to *traI*	This study
RF-R18	traI _UR	TCAGAGCGCTTTTGAAGCTAATTCGTTGAACTAATGGGACGAAATTGA		
RF-R19	traI _DF	AGGAACTTCAAGATCCCCAATTTTGAGCATAAATACCGCCGAT	For amplification of downstream region to *traI*	
RF-R20	traI _DR	CCATGCCAAACGGCTAAAC		
RF156	Int2_F	CCACATATTCCAGCGTTGAC	Used for the confirmation of precise deletion of *traI*	
RF-R21	traI -RF_R	CTGCCGTTCCTTTGTCGCA		

Primers used to construct Δmob-1

Cat No	Name	Sequence (5' to 3')[a]	Feature	Reference
RF-R22	mob1_UF	CCAGCGAGCAATAAGGCAC	For upstream flank of *mob1*	This study
RF-R23	mob1_UR	TCAGAGCGCTTTTGAAGCTAATTCGTAAAATCATGATACCTCCCTCG		
RF-R24	mob1_DF	AGGAACTTCAAGATCCCCAATTGATTTTTAAGGAGTGGTTATGCTG	For downstream flank of *mob1*	
RF-R25	mob1_DR	CGCTCGGTTTCAATGGCAAT		
RF143	mob1-RF_F (P23-F)	GGCTTGGTCAGTACGGATTG	For confirmation of deletion	
RF-R26	mob1-RF_R	GGTGGCTGGCGATAATCGA		

Primers used to construct ΔInt2a

Cat No	Name	Sequence (5' to 3')[a]	Feature	Reference
RF-R07	ICE2_UF	TTGCCGTAGTGAATATGCTG	For upstream flank of Int2a/ICE-2	This study
RF-R08	ICE2_UR	TCAGAGCGCTTTTGAAGCTAATTCGAGATGGTGAAAAATGGCGC		
RF-R27	Int2a_DF	AGGAACTTCAAGATCCCCAATTCATCCATAGTCAATTTCGTC	For downstream flank of Int2a/ICE-2	
RF-R28	Int2a_DR	CTTCTGAACCGGCATTGTG		
RF-R29	ICE2-RF_F	GATGTCAGCGAAAGGCAAG	Screening primers to confirm the deletion	
RF-155	44710_R	GTTTCTTGCCGGGTATCGG		

Primers used to construct ΔInt2b

Cat No	Name	Sequence (5' to 3')[a]	Feature	Reference
RF-R30	Int2b_UF	ATACAAAGGACGCGGAAGAC	Upstream flank of int2b	This study
RF-R31	Int2b _UR	TCAGAGCGCTTTTGAAGCTAATTCGCATGACGATTAGCCTTTTATAAAAT		
RF-R32	Int2b _DF	AGGAACTTCAAGATCCCCAATTTAGACATCAAGACCTCTGGT	Downstream flank of int2b	
RF-R32	Int2b _DR	CAACATCCTCTACGCTCTGA		
RF-R33	Int2b-RF_F	CGGCAATGGAAGGAAAGAAC	Screening primers to confirm the deletion	
RF-R34	Int2b-RF_R	GCTACCCGCGATTAAGGCA		

Appendix VIII

Primers used to confirm various plasmid and *E. coli*.

Cat No	Name	Sequence (5' to 3')[a]	Plasmid	Reference
PR1179	EBGNHe-F	CCCGCTAGCGAAAAGATGTTTCGTGAAGC	pKOBEG-Apra	Lab 212
PR1180	EBGh3-R	GGGAAGCTTATTATCGTGAGGATGCGTCA	pKOBEG-Apra	Lab 212
RF116	p184_F	ATCAGGCGGGCAAGAATGTG	pACYC184	This study
RF117	p184_R	GTAAGTTGGCAGCATCACCC	pACYC184	This study
PR139	M13-F	TGTAAAACGACGGCCAGT	Primers outside the multiple cloning site of pWSK29	Universal
PR140	M13 -R	CAGGAAACAGCTATGACC	Primers outside the multiple cloning site of pWSK29	Universal
PR1825	SacB – F	TAACAGCAGCGTGACAAGTGTAGGCCCGTAGTCTGCAAAT	Primers used to detect sacB on pflp2-Apra	Lab 212
PR1826	SacB – R	GCCCTATGGGATTCACCTTT	Primers used to detect sacB on pflp2-Apra	Lab 212
PR3006	EglmS-down	GATGACGGTTTGTCACATGG	Specific to *E. coli* genome	Lab 212
PR2001	EglmS-down	TTGTATGTCTTCGCCGATCAG	Specific to *E. coli* genome	Lab 212

Appendix IX

Primers used to detect the excised form of ICE-1 and ICE-2.

Cat no.	Name	Sequence (5' to 3')	Features	Source
RF160	ICE2-1-F	TGAATATGCTGCCTGCGCT	Binding upstream region (*attL*) of *int2a* of ICE-2	This study
RF161	ICE2-2-R	GTGAACATCAGGTGCCGATT	Binding within *int2a*	
RF162	ICE2-3-F	TCGCCGTCTATCAGCAAAG	Binding within 3´ end of ICE-2	
RF163	ICE2-4-R	GATGGGCATTTCTGAAGCC	Binding downstream to *attR* site of ICE-2	
RF170	ICE1-1-F	GGTTTTTATTTGCCCGGTAAGCAG	Binding upstream region (*attL*) of *int* of ICE-1	
RF171	ICE1-2-R	GACTCATCTGGCGTTCTACTGC	Binding within *int*	
RF172	ICE1-3-F	GGTGGTCATTCTGGTGGTCTTG	Binding within 3´ end of ICE-1	
RF173	ICE1-4-R	GCTTCGTCTGGGTATGGCTGT	Binding downstream to *attR* site of ICE-1	

Appendix X

Summary of ICE-1 associated integrase gene in different strains of *K. pneumoniae*

Klebsiella pneumoniae (Strains)	Designation of gene[a]	Nucleotides (Coordinates)[b]		Accession	Size (bp)	% of Identity[c]	Gene ID	E-value
		Start	End					
NTUH-K2044	*int-ICEKP1*	3395997	3397259	AP006725.1	1263	100	57158257	0
1084	*int-B1*	1849066	1847804	CP003785.1	1263	98	13529074	0
	int-B2	1883280	1882047	CP003785.1	1234	94	13526726	0
	int-B3	1885512	1886745	CP003785.1	1234	86	13526731	0
HS11286	*int-KPHS1*	3433717	3434978	CP003200.1	1262	98	11848489	0
SB3432	*int-KPR1*	3488220	3489453	FO203501.1	1234	94	499531263	0
	int-KPR2	3525734	3526490	FO203501.1	757	97	499531302	0
342	*int-KPK1*	1914098	1912865	CP000964.1	1235	87	6939205	0
	int-KPK2	1865920	1864722	CP000964.1	1201	85	6938556	0
	int-KPK3	1880735	1879539	CP000964.1	1205	75	6936748	0
1251 (P4-like integrase)	*int-P4KP1*	1	792	FJ212119.1	792	97	237847270	0
2523 (P4-like integrase)	*int-P4KP2*	1	791	FJ212118.1	791	97	237847268	0
KCTC 2242	*int-KPN1*	3160357	3161567	CP002910.1	1214	84	339762709	0

a annotation of genes found in GenBank database

b Coordinates of genes in genome sequences of different strain of *Klebsiella pneumoniae* in their GenBank accession numbers.

c DNA nucleotide sequence identity determined by Blastn

Appendix XI

RFTool-1

TCTGACGCTCAGTGGAACGAAAACTCACGTTAAGGGATTTTGGTCATGAGATTATCAAAAAGGATCT
TCACCTAGATCCTTTTAAATTAAAAATGAAGTTTTAAATCAATCTAAAGTATATATGAGTAAACTTGG
TCTGACAGGTGCAATACGAATGGCGAAAAGCCGAGCTCATCGGTCAGCTTCTCAACCTTGGGGTTAC
CCCCGGCGGTGTGCTGCTGGTCCACAGCTCCTTCCGTAGCGTCCGGCCCCTCGAAGATGGGCCACTT
GGACTGATCGAGGCCCTGCGTGCTGCGCTGGGTCCGGGAGGGACGCTCGTCATGCCCTCGTGGTCA
GGTCTGGACGACGAGCCGTTCGATCCTGCCACGTCGCCCGTTACACCGGACCTTGGAGTTGTCTCTG
ACACATTCTGGCGCCTGCCAAATGTAAAGCGCAGCGCCCATCCATTTGCCTTTGCGGCAGCGGGGCC
ACAGGCAGAGCAGATCATCTCTGATCCATTGCCCCTGCCACCTCACTCGCCTGCAAGCCCGGTCGCC
CGTGTCCATGAACTCGATGGGCAGGTACTTCTCCTCGGCGTGGGACACGATGCCAACACGACGCTG
CATCTTGCCGAGTTGATGGCAAAGGTTCCCTATGGGGTGCCGAGACACTGCACCATTCTTCAGGATG
GCAAGTTGGTACGCGTCGATTATCTCGAGAATGACCACTGCTGTGAGCGCTTTGCCTTGGCGGACAG
GTGGCTCAAGGAGAAGAGCCTTCAGAAGGAAGGTCCAGTCGGTCATGCCTTTGCTCGGTTGATCCG
CTCCCGCGACATTGTGGCGACAGCCCTGGGTCAACTGGGCCGAGATCCGTTGATCTTCCTGCATCCG
CCAGAGGGCGGGATGCGAAGAATGCGATGCCGCTCGCCAGTCGATTGGCTGAGCTCATAAACTCTT
CCTTTTTCAATATTATTGAAGCATTTATCAGGGTTATTGTCTCATGAGCGGATACATATTTGAATGTAT
TTAGAAAAATAAACAAATAGGGGTTCCGCGCACATTTCCCCGAAAAGTGCCACCTAAATTGTAAGCG
TTAATATTTTGTTAAAATTCGCGTTAAATTTTTGTTAAATCAGCTCATTTTTTAACCAATAGGCCGAAA
TCGGCAAAATCCCTTATAAATCAAAAGAATAGACCGAGATAGGGTTGAGTGTTGTTCCAGTTTGGAA
CAAGAGTCCACTATTAAAGAACGTGGACTCCAACGTCAAAGGGCGAAAAACCGTCTATCAGGGCGA
TGGCCCACTACGTGAACCATCACCCTAATCAAGTTTTTTGGGGTCSGAGGTGCCGTAAAGCACTAAA
TCGGAACCCTAAAGGGAGCCCCCGATTTAGAGCTTGACGGGGAAAGCCGGCGAACGTGGCGAGAA
AGGAAGGGAAGAAAGCGAAAGGAGCGGGCGCTAGGGCGCTGGCAAGTGTAGCGGTCACGCTGCG
CGTAACCACCACACCCGCCGCGCTTAATGCGCCGCTACAGGGCGCGTCCCATTCGCCATTCAGGCTG
CGCAACTGTTGGGAAGGGCGATCGGTGCGGGCCTCTTCGCTATTACGCCAGCTGGCGAAAGGGGG
ATGTGCTGCAAGGCGATTAAGTTGGGTAACGCCAGGGTTTTCCCAGTCACGACGTTGTAAAACGAC
GGCCAGTGAGCGCGCGTAATACGACTCACTATAGGGCGAATTGGGTACCGGGCCCCCCCTCGAGGT
CGACGGTATCGATAAGCTTGATATCGAATTCCTGCAGCCCGGGGGATCCACTAGTTCTAGAGCGGCC
GCCACCGCGGTGGAGCTCCAGCTTTTGTTCCCTTTAGTGAGGGTTAATTGCGCGCTTGGCGTAATCA
TGGTCATAGCTGTTTCCTGTGTGAAATTGTTATCCGCTCACAATTCCACACAACATACGAGCCGGAAG

CATAAAGTGTAAAGCCTGGGGTGCCTAATGAGTGAGCTAACTCACATTAATTGCGTTGCGCTCACTG
CCCGCTTTCCAGTCGGGAAACCTGTCGTGCCAGCTGCATTAATGAATCGGCCAACGCGCGGGGAGA
GGCGGTTTGCGTATTGGGCGCTCTTCCGCTTCCTCGCTCACTGACTCGCTGCGCTCGGTCGTTCGGCT
GCGGCGAGCGGTATCAGCTCACTCAAAGGCGGTAATACGGTTATCCACAGAATCAGGCACATGTTC
TTTCCTGTTATCCAGATCTCGCTACGGGTCGGATTTGAAGTCGTCTTGGTAGGAGGCAGCCTGAATG
GCGAATGCGGCATCAGAGCAGATTGTACTGAGAGTGCACCATACCTCTCAGGCGCCGCTGGTGCCG
CTGGTTGGACGCCAAGGGTGAATCCGCCTCGATACCCTGATTACTCGCTTCCTGCGCCCTCTCAGGC
GGCGATAGGGGACTGGTAAAACGGGGATTGCCCAGACGCCTCCCCCGCCCCTTCAGGGGCACAAAT
GCGGCCCCAACGGGGCCACGTAGTGGTGCGTTTTTTGCGTTTCCACCCTTTTCTTCCTTTTCCCTTTTA
AACCTTTTAGGACGTCTACAGGCCACGTAATCCGTGGCCTGTAGAGTTTAAAAAGGGACGGATTTGT
TGCCATTAAGGGACGGATTTGTTGTTAAGAAGGGACGGATTTGTTGTTGTAAAGGGACGGATTTGT
TGTATTGTGGGACGCAGATACAGTGTCCCCTTATACACAAGGAATGTCGAACGTGGCCTCACCCCCA
ATGGTTTACAAAAGCAATGCCCTGGTCGAGGCCGCGTATCGCCTCAGTGTTCAGGAACAGCGGATC
GTTCTGGCCTGTATTAGCCAGGTGAAGAGGAGCGAGCCTGTCACCGATGAAGTGATGTATTCAGTG
ACGGCGGAGGACATAGCGACGATGGCGGGTGTCCCTATCGAATCTTCCTACAACCAGCTCAAAGAA
GCGGCCCTGCGCCTGAAACGGCGGGAAGTCCGGTTAACCCAAGAGCCCAATGGCAAGGGGAAAAG
ACCGAGTGTGATGATTACCGGCTGGGTGCAAACAATCATCTACCGGGAGGGTGAGGGCCGTGTAG
AACTCAGGTTCACCAAAGACATGCTGCCGTACCTGACGGAACTCACCAAACAGTTCACCAAATACGC
CTTGGCTGACGTGGCCAAGATGGACAGCACCCACGCGATCAGGCTTTACGAGCTGCTCATGCAATG
GGACAGCATCGGCCAGCGCGAAATAGAAATTGACCAGCTGCGAAAGTGGTTTCAACTGGAAGGCC
GGTATCCCTCGATCAAGGACTTCAAGTTGCGAGTGCTTGATCCAGCCGTGACGCAGATCAACGAGC
ACAGCCCGCTACAGGTGGAGTGGGCGCAGCGAAAGACCGGGCGCAAGGTCACACATCTGTTGTTCA
GTTTTGGACCGAAGAAGCCCGCCAAGGCGGTGGGTAAGGCCCCAGCGAAGCGCAAGGCCGGGAA
GATTTCAGATGCTGAGATCGCGAAACAGGCTCGCCCTGGTGAGACATGGGAAGCGGCCCGCGCTCG
ACTAACCCAGATGCCGCTGGATCTGGCCTAGAGGCCGTGGCCACCACGGCCCGGCCTGCCTTTCAG
GCTGCGCAATCGCCCTTCCCAACAGTAGATTTCGGGTAAGTCTCCCCCGTAGCGGGTTGTGTTTTCA
GGCAATACGCACGCTTTCAGGCATACCTGCTTTCGTCATTTTGTTCAGCGCTCGTACCAGGGCCATAG
CCTCCGCAACCTGACCATCGTAGTCACGCAGCGTCAGTGAACCCCCGAACAGAGA

The underline sequences represents the BHROR region.

Appendix XII

Phase contrast microscopic examination of biofilm formed by WT and ICE mutant strains

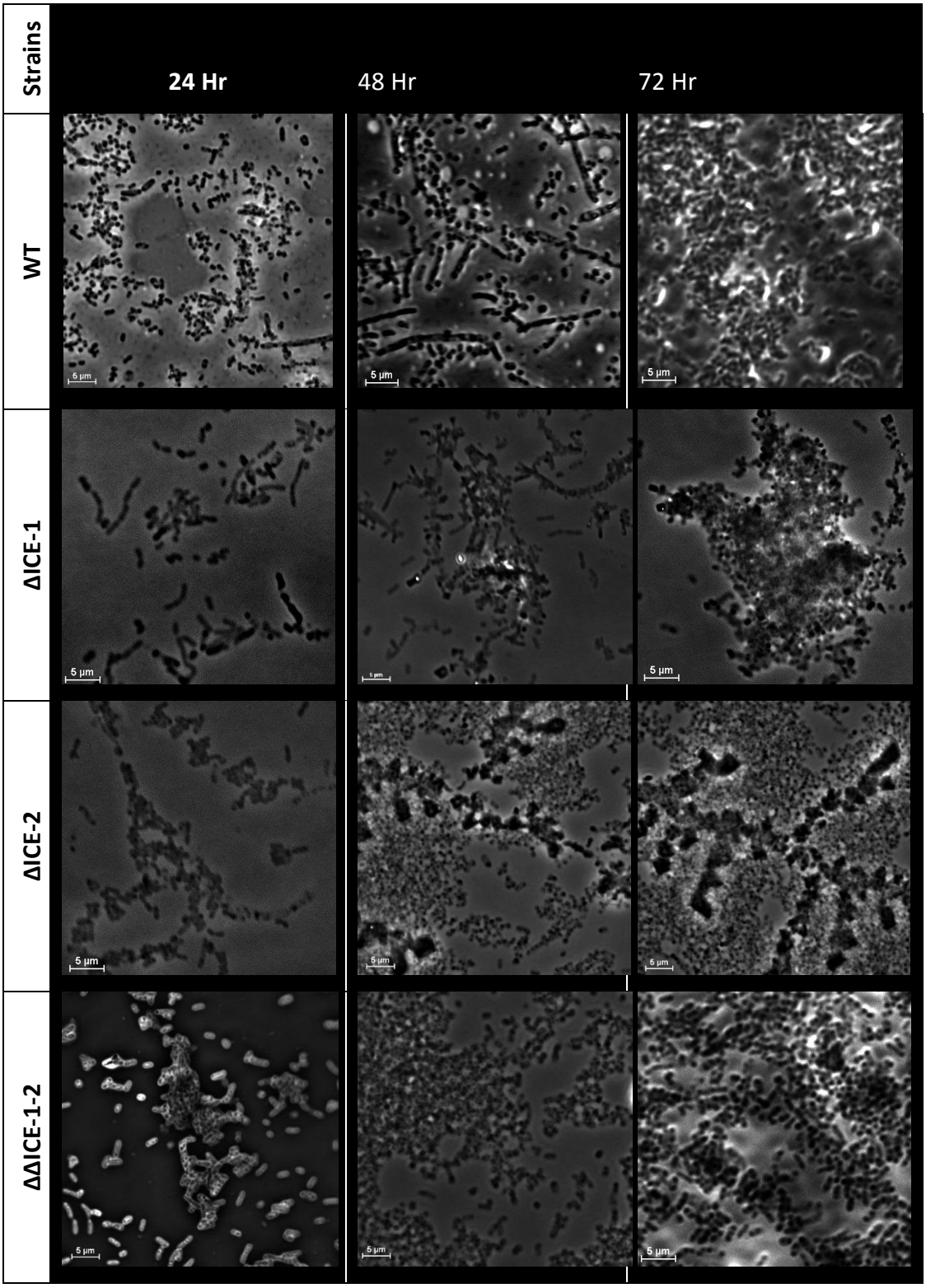

Figure S1. Phase contrast microscopy of biofilm formed by HS11286 and ICE mutants. The bacterial cells were grown in LB under static conditions at 37 ^{o}C for 24, 48 and 72 hr

Appendix XIII

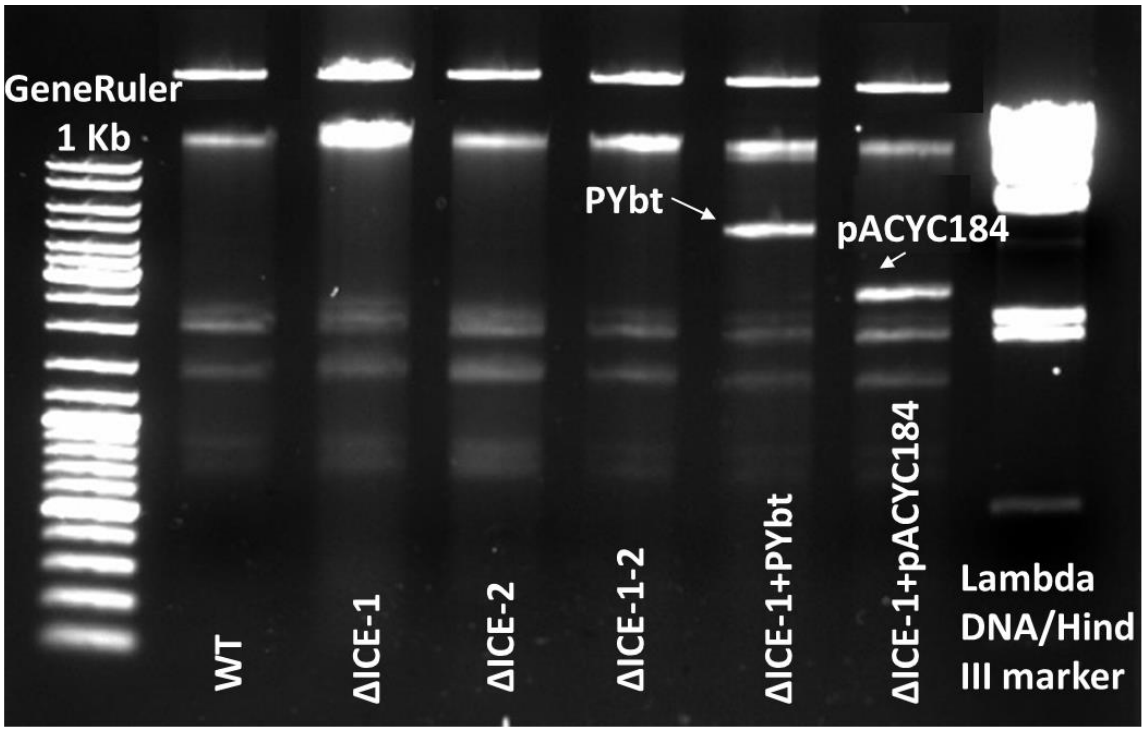

Figure S2. No natural plasmids loss.

Plasmid mini prep was performed from WT, ICE mutants and complemented mutant strains. Equal amount (300 ng) of plasmid DNA was loaded each well. No loss of natural plasmids were observed due to transformation of Pybt and pACYC184.

Appendix XIV

A. Oral presentation at "Departmental Postgraduate Conference 2015 at University of Leicester"

Title "Distributions and roles of integrative and conjugative elements (ICEs) in *Klebsiella pneumoniae*"

(Commended for good presentation)

B. Poster presented at various events.

1. Presented at "English Language Teaching Unit Postgraduate Festival 2016 at University of Leicester"

Title "Horizontal gene transfer by Type four secretion system in *Klebsiella pneumoniae* is repressed by nano weapon Type six secretion system"

2. Presented at " Microbiology Annual Conference 2016 in Liverpool"

Title "Evidence for Cross-talk in DNA mobilisation related to two integrative and conjugative elements in K. pneumoniae"

3. Presented at "Microbiology Annual conference 2017 in Edinburgh"

Title "MOB-2 an energy amplifier; for DNA mobilisation related to two integrative and conjugative elements in k. pneumoniae"

4. Presented at "Royal Society of Biology Poster-walks competition 2017 at Lincoln University"

Title "Fitness, Bugs and DNA"

(Received first prize for this poster)

1.

Horizontal gene transfer by "Type four secretion system" in *Klebsiella pneumoniae* is repressed by nano-weapon "Type six secretion system"

UNIVERSITY OF LEICESTER

COMMONWEALTH SCHOLARSHIPS

Robeena Farzand

Department of Infection, Immunity and Inflammation

Background

The genome of *Klebsiella pneumoniae* HS11286 carries two different types of type four secretion systems (T4SS) on two integrative and conjugative elements and also type six secretion systems (T6SS) on two different loci.

Aims

1. To determine the effect of type six secretion system on conjugation (horizontal gene transfer)
2. To construct a model mutant for mobilization assay.

Methods

1. Mutation

Deletion of respective cluster of gen were done by **Lambda-Red recombination system,** which is molecular biology technique based on homologous recombination

2. Conjugation

Conjugation was done by transforming marker plasmid in wild type and mutants of *K pneumoniae HS11286, which were then used as* donors and *E coli* HB101 as recipient.

3. Screening and Statistical Analysis

After conjugation screening was done for

1. Total *E. coli* Recovery
2. Transconjugants
3. Donors recovery
4. Efficiency of trans-conjugation was calculated by

$$= \frac{\text{nTransconjugants}}{nRecipient\ Recovered}\left(\frac{\text{CFU}}{\text{ml}}\right)$$

5. Student t-test was used for statistical analysis

Findings

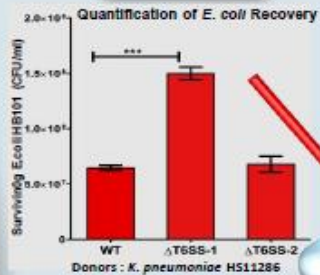

MORE

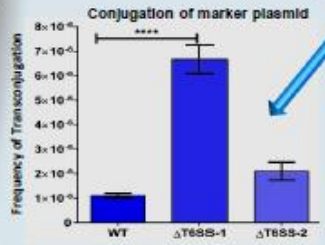

Inference

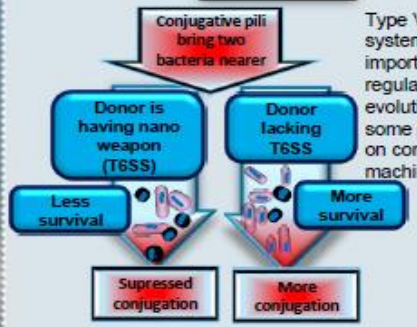

Type VI secretion system (T6SS) plays important role in regulation of bacterial evolution in terms of some presiding action on conjugation machinery.

Future Applicability

Further selective deletions of gene cluster responsible of capsule biosynthesis have been done and model mutant have been constructed to improve the dynamic range of the mobilization test system.

Reference

1. LIU, P., LI, P., JIANG, X., BI, D., XIE, Y., TAI, C., DENG, Z., RAJAKUMAR, K. & OU, H. Y. 2012. Complete genome sequence of *Klebsiella pneumoniae* subsp. pneumoniae HS11286, a multidrug-resistant strain isolated from human sputum. *J Bacteriol,* 194, 1841-2.

Supervisors: Prof. Mike Barer & Dr Kumar Rajakumar

2.

Evidence for cross-talk in DNA mobilisation related to two integrative and conjugative elements in *K. pneumoniae*

Robeena Farzand (rf130@le.ac.uk), Mike Barer, and Kumar Rajakumar

Department of Infection, Immunity and Inflammation, University of Leicester, Leicester, LE1 7RH

The genome of *Klebsiella pneumoniae* (Kpn) HS11286 carries 9 genomic islands, including two integrative and conjugative elements (ICEs), ICEKpnHS-1 and ICEKpnHS-2 [1]. Type IV secretion systems (T4SS) are one of the major modules of these ICEs and are responsible for conjugative transfer of nucleoprotein complexes. The objective of this work was to investigate the interaction between the two distinct T4SSs in DNA mobilisation.

A plasmid containing oriT of ICE-1 (pACYC184-oriT1) was constructed to facilitate conjugation assays. Initial work revealed that deletion of ICE2 led to a six-fold reduction in trans-conjugants with the ICE-1 marker plasmid. A capsule deletion mutant was used in the work outlined below as this gave a higher baseline transconjugants frequency.

HYPOTHESIS

Enhanced mobilisation of ICE-1 marker plasmid by the presence of ICE-2 is mediated by mob-2

Elements considered in this investigation

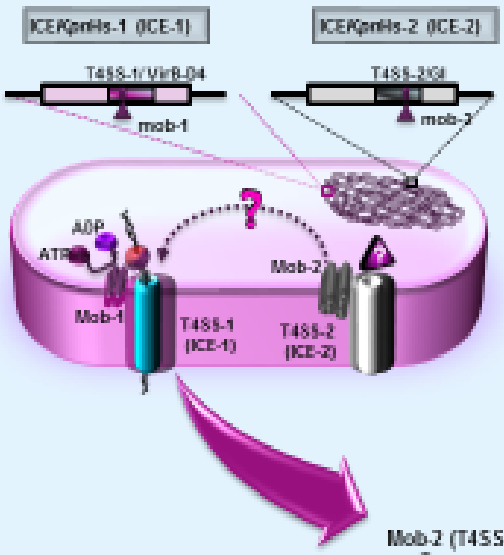

ICE-2 facilitates mobilization of the ICE-1 marker plasmid via mob-2

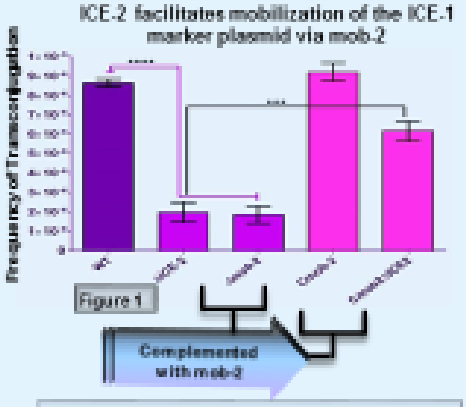

Fig1. *K.pn* HS11286 with the identified deletions were used as donors and *E.coli* HB101 as recipient. The deletion of ICE-2 and even the single gene mob-2 on ICE-2 leads to six-fold reduction in plasmid mobilization which is complemented in trans with mob-2 alone.

The T4SS, originally described in *Agrobacterium tumefaciens*, has three ATPase's: VirB4, VirB11 and VirD4 [2]. Mob-1 and Mob-2 are homologues of VirD4, which recruits the relaxosome and delivers it to the T4SS and is defined as the coupling protein (T4CP). Analysis of the mob-1 sequence indicates that it lacks an ATP-binding motif required for activity.

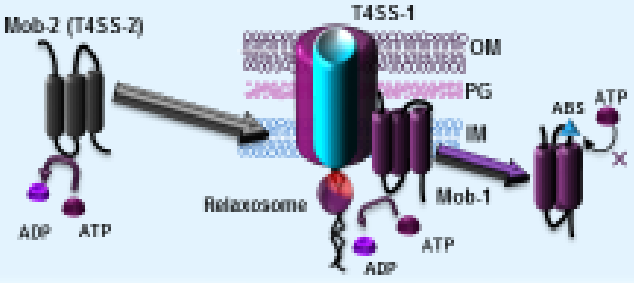

CONCLUSION

1. Mob-2 plays a significant role in mediating the cross talk between two non-homologous ICEs.
2. As mob-1 appears to lack its ATP binding sites, we propose that the enhanced mobilization of the ICE-1 marker plasmid attributable mob-2 may reflects its ATPase activity. Work to address this question is in progress.

Reference:

1. Liu, P. et al., 2013. J Bacteriol, 194, 1841-1843.
2. Cascales, E. et al., 2003. J Bacteriol, 185(11), 2681-2704.

3.

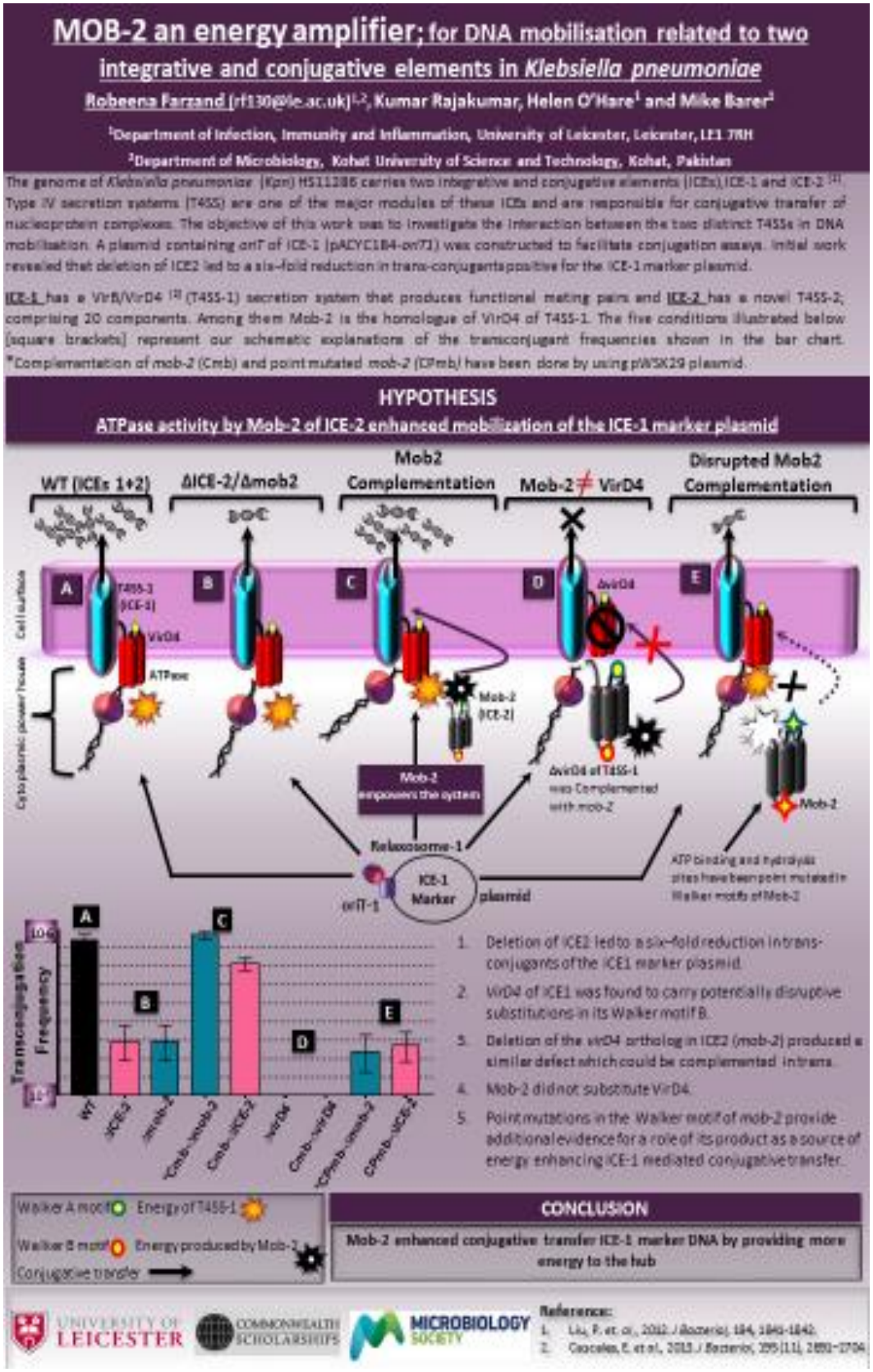
MOB-2 an energy amplifier; for DNA mobilisation related to two integrative and conjugative elements in Klebsiella pneumoniae
Robeena Farzand (rf130@le.ac.uk)[1,2], Kumar Rajakumar, Helen O'Hare[1] and Mike Barer[1]
[1]Department of Infection, Immunity and Inflammation, University of Leicester, Leicester, LE1 7RH
[2]Department of Microbiology, Kohat University of Science and Technology, Kohat, Pakistan
The genome of Klebsiella pneumoniae (Kpn) HS11286 carries two integrative and conjugative elements (ICEs) ICE-1 and ICE-2 [1]. Type IV secretion systems (T4SS) are one of the major modules of these ICEs and are responsible for conjugative transfer of nucleoprotein complexes. The objective of this work was to investigate the interaction between the two distinct T4SSs in DNA mobilisation. A plasmid containing oriT of ICE-1 (pACYC184-oriT1) was constructed to facilitate conjugation assays. Initial work revealed that deletion of ICE2 led to a six-fold reduction in trans-conjugants positive for the ICE-1 marker plasmid.
ICE-1 has a VirB/VirD4 [2] (T4SS-1) secretion system that produces functional mating pairs and ICE-2 has a novel T4SS-2, comprising 20 components. Among them Mob-2 is the homologue of VirD4 of T4SS-1. The five conditions illustrated below [square brackets] represent our schematic explanations of the transconjugant frequencies shown in the bar chart.
*Complementation of mob-2 (Cmb) and point mutated mob-2 (CPmb) have been done by using pWSK29 plasmid.
HYPOTHESIS
ATPase activity by Mob-2 of ICE-2 enhanced mobilization of the ICE-1 marker plasmid
WT (ICEs 1+2)
ΔICE-2/Δmob2
Mob2 Complementation
Mob-2 ≠ VirD4
Disrupted Mob2 Complementation
Cell surface
Cytoplasmic/ power house
A
B
C
D
E
T4SS-1 (ICE-1)
VirD4
ATPase
ΔvirD4
Mob-2 (ICE-2)
Mob-2 empowers the system
ΔvirD4 of T4SS-1 was Complemented with mob-2
Relaxosome-1
oriT-1
ICE-1 Marker plasmid
ATP binding and hydrolysis sites have been point mutated in Walker motifs of Mob-2
Transconjugation Frequency
WT
ΔICE-2
Δmob-2
CMob-ΔMob-2
CMob-ΔICE-2
virD4
CMob-virD4
CPmb-Δmob-2
CPmb-ΔICE-2
1. Deletion of ICE2 led to a six-fold reduction in trans-conjugants of the ICE1 marker plasmid.
2. VirD4 of ICE1 was found to carry potentially disruptive substitutions in its Walker motif B.
3. Deletion of the virD4 ortholog in ICE2 (mob-2) produced a similar defect which could be complemented in trans.
4. Mob-2 did not substitute VirD4.
5. Point mutations in the Walker motif of mob-2 provide additional evidence for a role of its product as a source of energy enhancing ICE-1 mediated conjugative transfer.
Walker A motif
Energy of T4SS-1
Walker B motif
Energy produced by Mob-2
Conjugative transfer
CONCLUSION
Mob-2 enhanced conjugative transfer ICE-1 marker DNA by providing more energy to the hub
UNIVERSITY OF LEICESTER
COMMONWEALTH SCHOLARSHIPS
MICROBIOLOGY SOCIETY
Reference:
1. Liu, P. et. al., 2012. J Bacteriol, 194, 1841-1842.
2. Cascales, E. et al., 2013. J Bacteriol, 195(11), 2393-2404.

4

Fitness, bugs and DNA

Roheena Farzand (rf130@le.ac.uk)[1,2], Kumar Rajakumar, Helen O'Hare[1] and Mike Barer[1]

[1]Department of Infection, Immunity and Inflammation, University of Leicester, Leicester, LE1 7RH

[2]Department of Microbiology, Kohat University of Science and Technology, Kohat, Pakistan

Did you know that even bugs, like bacteria and viruses, need to be fit? Fitness, in biological terms, relates to the ability to survive and produce the next generation of offspring. This is something that is crucial for bugs like *Klebsiella pneumoniae*, which can progress into diseases such a pneumonia. Improving our understanding of what affects fitness in bugs is important so we can create better treatments to fight them.

Mobile Genetic Elements

In this study impact of Integrative and Conjugative elements (ICE) on growth fitness, drug resistance, virulence were investigated.

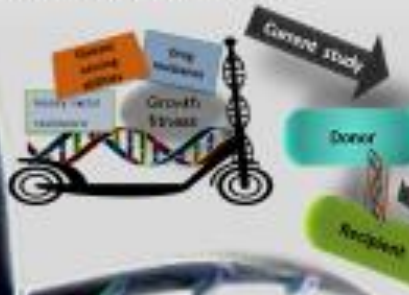

ICE can be transferred by cell-cell contact

RESEARCH FINDINGS

1. Growth fitness Assay

Presence of ICE-1 enhanced growth in both nutrient rich and iron restricted conditions

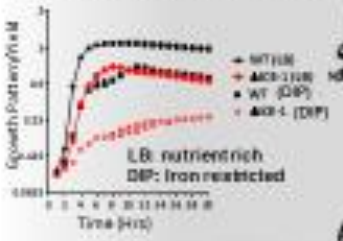

2. Severity of disease causing abilities

Deletion of ICE-2 showed decrease in the harmfulness of the bug

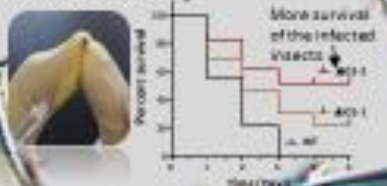

3. Antibiotic Resistance

Presence of ICE-1 enhanced resistance against various antibiotics specially associated to export channels/pumps.

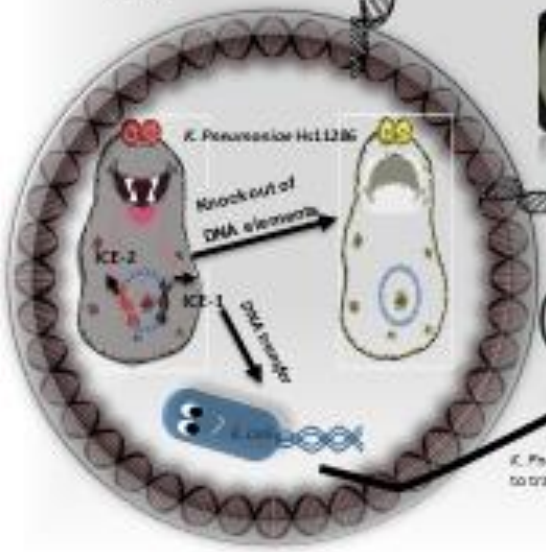

The recipient were confirmed for

a. Growth fitness
b. Antibiotic resistance

Future Recommendations

1. Help to understand the diversity of various bugs
2. Help to create better treatments
3. To investigate if the control of spread of mobile DNA fragments is possible?